SOME ASPECTS OF HUMAN PERFORMANCE IN A HUMAN ADAPTIVE MECHATRONICS (HAM) SYSTEM

by

Tussanai Parthornratt

A thesis submitted in partial fulfilment of the requirement for the award of

Doctor of Philosophy

Loughborough University

June 2011

ABSTRACT

An interest in developing the intelligent machine system that works in conjunction with human has been growing rapidly in recent years. A number of studies were conducted to shed light on how to design an interactive, adaptive and assistive machine system to serve a wide range of purposes including commonly seen ones like training, manufacturing and rehabilitation. In the year 2003, Human Adaptive Mechatronics (HAM) was proposed to resolve these issues. According to past research, the focus is predominantly on evaluation of human skill rather than human performance and that is the reason why intensive training and selection of suitable human subjects for those experiments were required. As a result, the pattern and state of control motion are of critical concern for these works.

In this research, a focus on human skill is shifted to human performance instead due to its proneness to negligence and lack of reflection on actual work quality. Human performance or Human Performance Index (HPI) is defined to consist of speed and accuracy characteristics according to a well-renowned *speed-accuracy trade-off* or *Fitts' Law*. Speed and accuracy characteristics are collectively referred to as speed and accuracy criteria with corresponding contributors referred to as speed and accuracy variables respectively. This research aims at proving a validity of the HPI concept for the systems with different architecture or the one with and without hardware elements.

A direct use of system output logged from the operating field is considered the main method of HPI computation, which is referred to as a *non-model approach* in this thesis. To ensure the validity of these results, they are compared against a *model-based approach* based on System Identification theory. Its name is due to being involved with a derivation of mathematical equation for human operator and extraction of performance variables. Certain steps are required to match the processing outlined in that of non-model approach. Some human operators with complicated output patterns are inaccurately derived and explained by the ARX models.

Keywords: human performance; Human Adaptive Mechatronics; HAM; manual control system; simple tracking operation; computer-based experiment; simple tracking task; point-to-point operation; human skill; helicopter test rig; hardware-based experiment; model-based approach; non-model approach

ACKNOWLEDGMENTS

The research work reported in this thesis was carried out at the Mechatronics research Centre, Wolfson School of Mechanical and Manufacturing Engineering, at Loughborough University, during the period 2007-2011. This work was supported by School scholarship of Loughborough University (United Kingdom) and Human Resource Development scholarship of Assumption University (Thailand).

First and foremost, I would like to express my heartfelt appreciation to Professor Robert Parkin and Professor Mike Jackson for their continuous advice, support and concern since day one of my Ph.D. life. Numerous discussions and suggestions have generated useful and practical ideas that overcame countless technical issues. These are all deemed invaluable for shaping and completing the work in this research.

Owing to his patronage on my education, the deepest gratitude goes to Rev. Bro. Dr. Prathip Martin Komolmas (President Emeritus of Assumption University of Thailand), whose lifelong kindness, continuous support and encouragement for my highest education since elementary level have motivated and remarkably created a strong ambition in my heart. My special thanks go to Rev. Bro. Dr. Bancha Saenghiran for giving me a great opportunity, Dr. Krisana Kitcharoen for always keeping me in touch with Bro. Martin, P'Kat for her moral support and P'Meow for always sorting things out for me.

For my family, I would like to express my utmost gratitude to my mother (Benjaporn Pundid) for being a fantastic listener and mentor no matter what and how terrible my pain is. She always listens and I know she always will. Without her lifelong dedication and continuous patience, I would never have overcome those impossible barriers throughout my whole life. Years we underwent hardship and crisis together have strengthened our bond and they will always reside in my deepest memory. My special thanks go to my beloved aunt and uncle (Na Aew and Na Mong) for their tireless

support and countless help when I stay in the UK and my mom suffers from her photosensitive symptoms.

Last but not least is for my colleagues. I would like to thank Sultan, Sedat, Nash, Brian, Vianney, Mathavan, Khurram, Najib, Niranjan, Hafis, Matthew, Phil, Luke and others in the Mechatronics Research Centre for their useful tips, discussions and uplifting conversations. In particular, I would like to thank Sultan for his great support and guidance since day one, Khurram for his great advice on research thinking, Mathavan for his continuous concern and support regardless of the issues I have, Matthew for his technical assistance and troublshooting on the helicopter test rig and Phil for a number of useful discussions. My thanks also go to David Liddell for sorting the helicopter test rig out and troubleshooting its practical issues.

Lastly, many thanks to Mary Treasure for proofreading my journal manuscript and many other helps, Jo Mason for her administration and security staff of Loughborough University for their care and concern when I stayed through out-of-hour time to complete some experimental works.

Table of Contents

LIST OF SYMBOLS

D	Distance
G	Gain
I_d	Index of Difficulty
ω	Angular velocity
α	Angular acceleration
M	Moment of force
J	Moment of inertia
θ_p	Pitch angle
θ_y	Yaw angle
x_i	Raw performance variable
$\hat{x}_i$	Average normalized performance variable (avg-norm)
$\hat{x}'_i$	Reflected performance variable (refl)
Y_i	Actual data
$\hat{Y}_i$	Fitted data
$\overline{Y}$	Average value of actual data
e_i	Error between a cursor position and target position
HPI	Human Performance Index
J_i	Performance criterion (J_1 = speed, J_2 = accuracy)
R^2_{av}	Average coefficient of determination
R_i^2	Coefficient of determination of segment i
$RMSE$	Root Mean Squared Error
SS_E	Sum of a squared error
SS_T	Sum of a squared total
T	Time taken
V_{av}	Average speed
V_i	Performance variable
V_{xx}	Resultant performance variable (after processing)
W_{Ji}	Weight of a performance criterion J_i
W_{Vk}	Weight of a performance variable V_k
a	Speed ratio

1-a	Accuracy ratio

LIST OF ABBREVIATIONS

ACT-R	Adaptive Control of Thought-Rational
ANFIS	Adaptive Network-based Fuzzy Inference System
ANN	Artificial Neural Network
ARMA	AutoRegression Moving Average
ARMAX	Autoregressive Moving Average with eXogenous inputs
ARX	AutoRegression with eXogenous inputs
CCW	Counter-ClockWise
CI	Confidence Interval
CW	ClockWise
D-OMAR	Distributed Operator Model ARchitecture
dpi	dot per inch
FOMOCM	Fixed-Order Optimal Control Model
GOMS	Goals, Operators, Methods and Selection rules
HAM	Human Adaptive Mechatronics
HMM	Hidden Markov Model
HOS	Human Operator Simulator
HPI	Human Performance Index
ILC	Iterative Learning Control
MAO	Meal Assistance Orthosis
MIDAS	Man-machine Integration Design and Analysis System
MOCM	Modified Optimal Control Model
OCM	Optimal Control Model
OMAR	Operator Model ARchitecture
OP	Optimal Projection
PCIO	Personal Computer Input-Output
PID	Proportional Integral and Derivative
ppi	point per inch
SOAR	State, Operate and Result
THERP	Technique for Human Error Rate Prediction

LIST OF FIGURES

LIST OF TABLES

Chapter - 1.

Introduction

1.1. Introduction

This chapter introduces the background, motivation, area and scope of the research work covered in this thesis. It aims to point out how system intelligence potentially increases productivity and overall performance of a conventional human-machine (man-machine) system. Human performance characteristics, featuring two entities - speed and accuracy - are proposed to represent performance level and to serve as human factor specifications for a man-machine system. The thesis structure then follows starting from the problem statement of one-way man-machine interaction to the solution of human performance realization.

1.2. Research background

Since the term *Mechatronics* was first used by Mr. Tetsuro Mori to describe a machine system or device with actuation and control mechanisms, Mechatronic technology and advancement have evolved and become common in many engineering disciplines (Auslander, 1996). Recent machine systems can be considered to be Mechatronic in some way. System designers are increasingly meeting various sophisticated challenges, including the need to understand the multidisciplinary nature of their work, the generation of interdisciplinary perspectives and the need to integrate system elements together (Wikander, Törngren et al., 2001). In addition to a mechatronic system design in general, a design to incorporate a human user into a control loop is equally important, as pointed out by Schweitzer (1996), particularly for a human-operated machine system or simply, a man-machine system. The term “man-machine system”, according to the literature, is used interchangeably with the term “human-machine system”.

One of the first studies of the interaction between human and machine was part of a defence research program in the 1940s (Tustin, 1947). A challenge to model a human as one element of a human-in-the-loop setup emerges when a prediction and simulation of human responses are essential for a system test and evaluation (Gaines, 1969). Researchers derived human models empirically from various experimental setups in the laboratory. As a result, these models are not universal and strictly valid only for specific setups and working conditions. Human modelling techniques and domains range from psychology and cognitive science to control engineering and statistics (Pew, 2008).

With an increasing trend to research human interaction with machine or mechatronic systems, Agah (2000) suggested that human-machine system research elements should consider the application, the research approach, system autonomy, interaction distance and interaction media. According to this broad outline, there is no clear pattern and dimension of interaction that can be considered fundamental for an intelligent human-machine system.

Research on man-machine systems evolved further and finally lead to the creation of Human Adaptive Mechatronics (HAM) in 2004 (Furuta, 2004). HAM is an intelligent man-machine system with an ultimate objective of building a symmetrical interaction between a human and a mechatronic system (Suzuki, Furuta et al., 2005). This symmetrical interaction means that the mechatronic system should be capable of adapting human performance, correcting control actions and then responding rather than simply responding to the human operator's commands like conventional man-machine systems.

In HAM systems, the importance of human existence is focused and a development of mechanisms to measure human performance level is therefore essential. This essentially forms the core for the research work in this thesis.

1.3. Research motivation

As mechatronic technologies prosper, a conventional machine system appears to be mechatronic and more interactive with a human in one way or another, as pointed out earlier. *Conventional man-machine systems* contain no mechanism to realize a human as a component in the loop. Therefore, this man-machine system can be viewed as a one-way system that only passively responds to commands sent by a human operator. A drawback of such a system is the lack of situational awareness or suitability of a human workload.

Consider the case of a complicated control situation like the flight controls of an aircraft; a human operator or pilot can introduce instability or oscillation into the system. This circumstance is referred to as a *Pilot-induced Oscillation* or PIO. Ashkenas, Jex et al., (1964) described PIO as "an inadvertent sustained oscillation of a pilot-vehicle system."

Past researches concluded that PIO could lead to handling problems, uncontrollable conditions, loss of control and, ultimately, crash landing (Dornheim, 1992, cited in Pachter and Miller, 1998; Furuta, Iwase *et al.,* 2005). Interestingly, a higher percentage of PIO occurred in a highly-advanced flight control system (Ashkenas, Jex et al., 1964). The study also suggested the cause of a PIO to be the pilot rather than the aircraft itself. One of the potential causes of PIO was actuator saturation, as reviewed by Pachter and Miller (1998).

One potential solution to avoid a catastrophe resulting from errors associated with human failure or deficiency is a measurement of the handling quality or control action characteristics of the operator and the provision of adaptive mechanisms accordingly. A man-machine system with this feature will effectively be adaptive and assistive to different individuals.

Apart from a vehicular system, recognition of human performance level can also be beneficial for the craft-based manufacturing systems (Cusumano, 1992). According to the MTC (Manufacturing Technology Centre: with Loughborough University being one of the research partners, 2010), one of the industrial needs is to achieve a constant quality of product regardless of human operators and this means a system-wide mechanism to differentiate individual human is increasingly important. It is worth noting that types and levels of automation have to be designed with extra care to minimize the complacency and negligence of human operators (Parasuraman, 1997).

In this regard, human characteristics or performance level realization on the machine's side can potentially serve as a fundamental for adaptive control mechanisms in intelligent man-machine or HAM systems. A scenario of unsymmetrical human-machine interaction is as depicted in Figure 1.1.

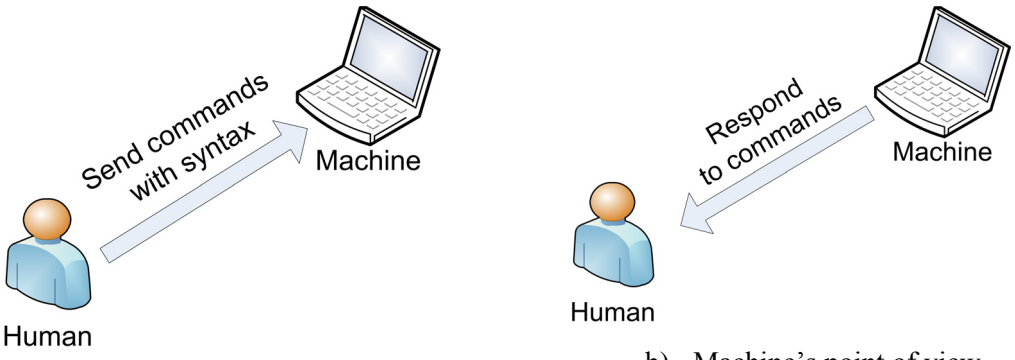

a) Human's point of view

b) Machine's point of view

Figure 1.1. Asymmetrical human-machine interaction (based on Suzuki, Furuta *et al.*, 2005)

From the human's point of view in Figure 1.1(a), a command or set of commands are sent to a machine via a user interface with the correct syntax, otherwise error messages will be returned for correction. Once the commands are all correct, the machine then recognizes the commands, interprets them as machine codes and performs a predefined operation accordingly. In short, the human operator has to learn the command syntax in order to receive a desired response from the machine.

For most of the cases of machine failure or errors, humans know where to review a set of commands or machine parts and correct them. Humans can also check the settings and investigate signs of failure. This is simply because a human built the machine,

created the command syntax and defined the instruction sets. In simple words, the human has or at least needs to have an insight into the machine system before he/she starts using it.

From the machine's point of view, as shown in Figure 1.1 (b), it blindly accepts the set of commands sent from the human, interprets them and responds according to the predefined instruction sets. A machine is not capable of analyzing the human operator's actions, making any prior changes and avoiding foreseeable failures, even if they are obvious. A human operator has to search for the sources of failures, correct them and re-run the machine. From this aspect on the machine's side, no mechanism exists to evaluate the human actions or performance level and respond adaptively.

In conclusion, the feature to recognize human performance is missing in a conventional man-machine system. The literature suggests a number of techniques and implementations in different human-operated systems but without formulating a rigid foundation and structure for the human performance level. Consequently, the knowledge contribution from the literature is truly system-specific and limited, as will be elaborated in the following chapter. This is where the main research work on which this thesis aims to build is to be found.

1.4. Area of research

Research work in this thesis focuses on a human-machine interaction by introducing theory and techniques to assess human performance in the aforementioned asymmetrical interaction scenario. A diagram illustrating the three main aspects of the area of research is found in Figure 1.2.

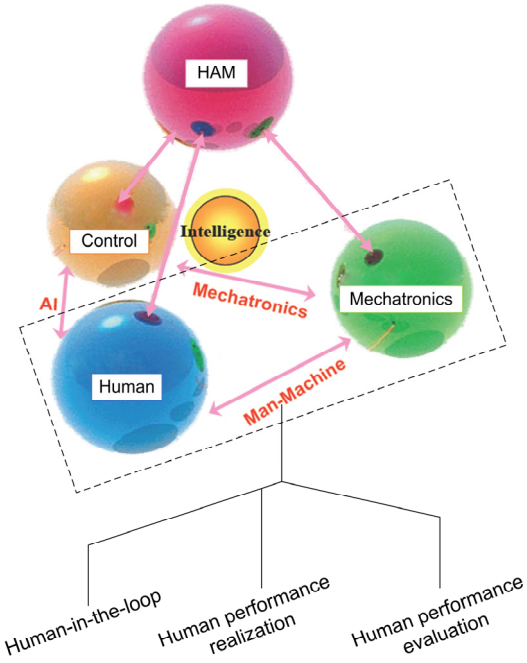

Figure 1.2. Area of research diagram (based on the Human Adaptive Mechatronics diagram by Suzuki, Furuta et al. (2005)

Consideration of a human's presence in a man-machine system is usually regarded as a human-in-the-loop environment. The addition of a human into the system affects the whole system directly and makes the overall performance subjective. Techniques to deal with a human-in-the-loop environment are therefore proposed to build up fundamentals for human performance realization.

To fulfil this, both non-model and model-based approaches are proposed. The non-model approach obtains human performance characteristics directly from a system response without needing a human model (mathematical equation) whereas the model-based approach obtains human performance characteristics from a governing human model. The resulting human performance values computed from both approaches are to be analysed with regard to consistency and control strategy involved in operating the system of interest. Full details of these two approaches will be provided in Chapter 3.

1.5. Research Novelty

This research work covers the following novel concepts and methodologies to quantify human performance:

- Novel formation of the concept called *Human Performance Index (HPI)* to quantify the speed and accuracy characteristics of human operator in a man-machine system based on a classical *speed-accuracy trade-off* or *Fitts' Law* (Chapter 3).
- The scalability of the HPI concept is considered allowing an expansion of a sample group as appropriate.
- Applying the proposed HPI concept to the systems with and without hardware elements to prove the concept's versatility.
- Analysing human performance directly from the system output with a separate axis treatment (*non-model approach* in Chapter 5).
- Novel use of System Identification theory to derive the human mathematical models and analyse their performance level (*model-based approach*). A comparison of these results with those of non-model approach is also conducted to illustrate the concept's validity (Chapter 6).
- The first complete representation of human control strategy in a form of speed and accuracy plus suggestions for human factor specifications in terms of a speed-accuracy ratio.

Figure 1.3 and Figure 1.4 show the block diagram of this research work and systems used for the experiments conducted in this thesis respectively.

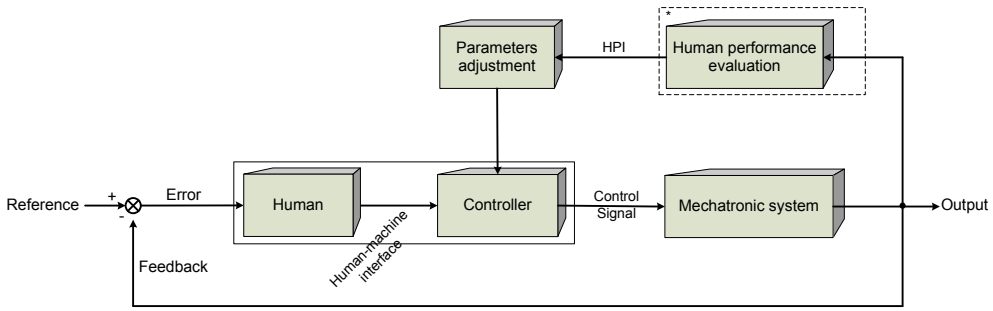

Figure 1.3. Intelligent man-machine system block diagram (Note: * represents the focus of this research.)

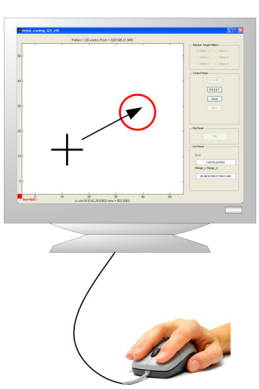

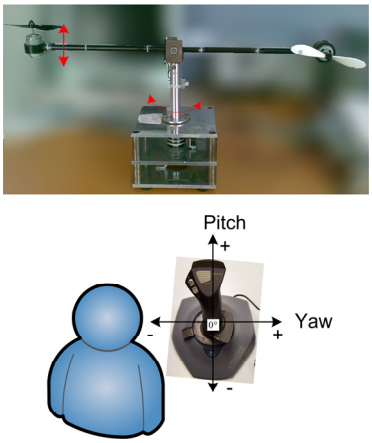

a) Computer-based system: computer-mouse setup **b) Hardware-based system: helicopter test rig**

Figure 1.4. Systems used in this research

This thesis continues with the literature review on the manual-control systems and its evolution towards the Human Adaptive Mechatronics (HAM) in Chapter 2. Chapter 3 covers the complete Human Performance Index (HPI) concept and research methodologies including the definitions on performance variables, performance criteria, data processing, presentation forms and detailed methodology for proving the concept. Chapter 4 explains the experimental setups for applying the concept to the computer-based and hardware-based systems followed by Chapter 5 and Chapter 6 that cover the implementation of non-model and model-based performance computation approaches respectively. Discussion on several issues on the present research together with conclusions and research directions can be found in the final chapter.

Chapter - 2.

Literature Review

2.1. Introduction

The objective of this chapter is to provide a background on Human Adaptive Mechatronics (HAM) starting from its predecessor, a conventional human-machine or man-machine system with a focus on human operator. This covers a number of studies about human models and characteristics that are parts of an evolution towards a HAM system. Other fields of study rather than engineering are also included for a complete understanding on human from different perspectives. This chapter concludes by addressing fundamental differences of this research from those works in the past and a shift of focus from human skill to human performance.

2.2. Research relevant to man-machine systems

It is true that a research on human as part of a machine system or human in the loop is not new. In fact, research on man-machine or human-machine systems emerged as early as the 1940s with a focus on manual control systems or a system requiring a human to operate and complete an operation with flexibility and intelligence like vehicle and weapon control (Elkind, 1956). At its early stage, the main interest was on a human pilot and then spanned across other vehicular systems (Tustin, 1947; Elkind, 1956; Dander, 1963; Ashkenas, Jex et al., 1964; Young and Meiry, 1965; Mcruer, 1967; Angel and Bekey, 1968; Kelley, 1968). The evolution path is as presented in Figure 2.1.

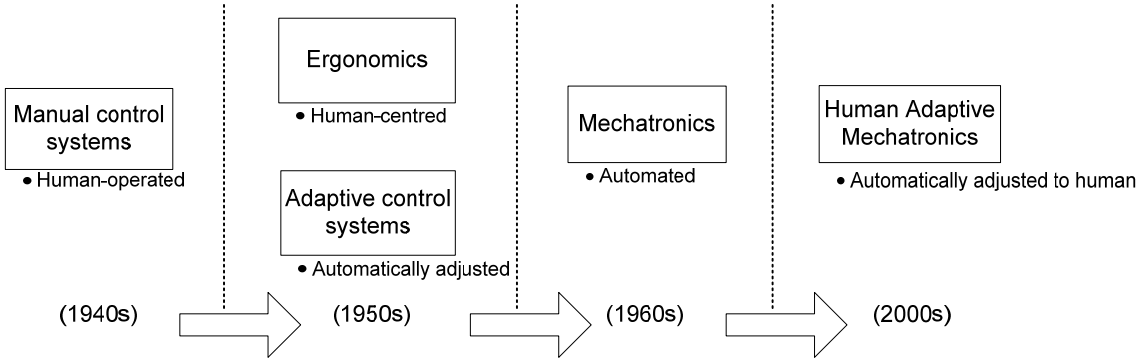

Figure 2.1. Evolution path of research relevant to man-machine systems

In 1950s, studies on man-machine systems were further developed and could be classified into two main directions based on their primary objectives (Aseltine, Mancini et al., 1958; Corlett and Stapleton, 2001). Such distinction is whether the focus is on human or machine as a driving force. From this viewpoint, a human-centred research is therefore collectively referred to as *Ergonomics* or *Human Factors* and a machine-centred research is collectively referred to as *Adaptive control system*. By definitions, ergonomics is a science of integrating understandings on a human in terms of his/her physical, cognitive and organisational characteristics into a design and usage of machines. Examples are a study on human concerning anatomical, anthropometric, physiological and biomechanical characteristics (physical), perception, memory, reasoning and motor response (cognitive) and optimization of sociotechnical systems or interactions between human and workplaces (organisational) .

For the machine-centred research, an adaptive control system was initiated with an effort to design and implement machines with abilities to work efficiently as conditions change and react to those changes automatically. This indeed reflects a focus on automation or operation requiring minimal human intervention to ensure system stability and productivity even though human appeared to be part of such control system like autopilots for aircrafts (Åström, 1983). Major adaptive control techniques include heuristic approach, self-tuning controllers (STC), model adaptive reference systems (MRAS) and self-organising systems (Bobál, Bohm et al., 2005).

To summarise, both Ergonomics and adaptive control systems have been continually developed, advanced and branched into several other areas sustaining a focus of its own depending on the context. A human-computer interaction research is a good example of a digital-age ergonomics (Card, Moran et al., 1983; Scott MacKenzie, 1992) whereas an intelligent controller based on adaptive-network-based fuzzy inference system (ANFIS) is a good example for an adaptive control system with learning capabilities (Jang, 1993).

Due to the fact that the work presented in this thesis is focused on how and in what manner human operator can be examined, only the literature contributing to human modeling and human characteristics will be presented. Before covering these areas in detail, descriptions of a manual control system comprising task, procedural, environmental and human-centred variables is presented in Figure 2.2 (Mcruer, 1967).

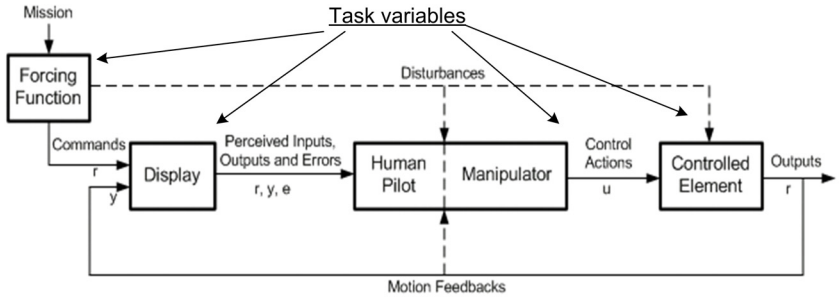

- Environmental variables:

In-flight VS fixed-base
Vibration
G-Level
Temperature
Atmospheric Conditions
Etc.

- Operator-centred variables:

Motivation
Stress
Workload
Training
Fatigue
Etc.

- Procedural variables:

Instructions
Practice
Experimental Design
Order of Presentation
Etc.

Figure 2.2. Manual control system variables with reference to a pilot-vehicle system (Mcruer, 1967) (Note: G-level means a gravitational acceleration level)

According to Figure 2.2, *Environmental variables* and *Operator-centred variables* are related to external and internal conditions respectively with reference to a human operator whereas *Task variables* are related to the operation and *Procedural variables* are related to scope and instructions of an experiment. Therefore, the first two variables are uncontrollable and are likely to cause system disruption.

Regarding types of operation, they are based on the pattern and availability of feedback signals provided to the operators or task variables. According to Mcruer and Krendel, 1959, these systems can be classified as compensatory (only a magnitude of error), pursuit (an input-output information), preview (interpreted output based on current input called quickened display) and precognitive systems (purely intuitive) as presented in Figure 2.3.

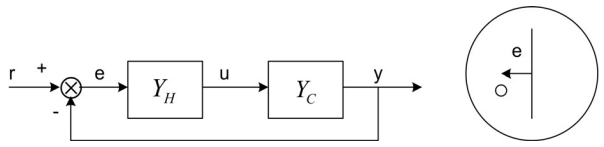

a. Compensatory system

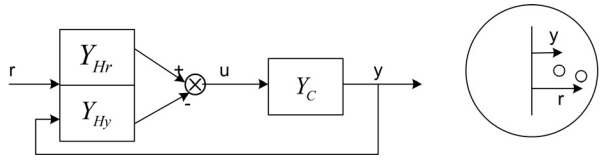

b. Pursuit system

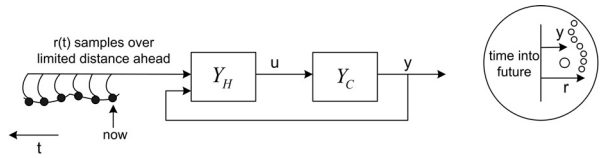

c. Preview system

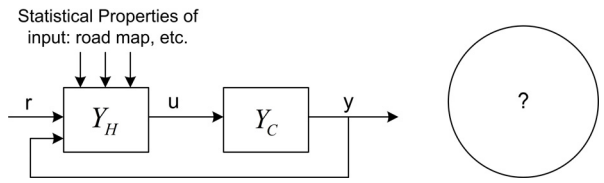

d. Precognitive system

Figure 2.3. Manual control system classifications (Sheridan and Ferrel, 1974)
[Note: Y_C, Y_H, Y, r, Y_{Hr} and Y_{Hy} are controlled element, human controller, output, target, human response to the target and output respectively.]

A *compensatory system* is similar to a *pursuit system* in the characteristics of the feedback signal shown on a display. These feedback signals are directly available to the system with only difference in the way they appear to a human operator. For a compensatory system, a display shows the magnitude of error directly proportional to the distance between a circle and a fixed vertical line whereas a complete picture on a mission consisting of both input and output signals are presented to a human operator

for a pursuit system. For a preview system, a quickened display allows a human operator to foresee an output pattern based on his/her current actions and characteristics, which is considered very useful for high-order control systems like those of helicopters, aircraft, submarines etc. to be used cooperatively with a real output (Birmingham and Taylor, 1954). The last manual control system or a *precognitive system* is a system without a display based on the fact that a human can interpret the first derivative quantity of the provided input signals (Kleinman, Baron et al., 1970; Kleinman, Baron et al., 1970). Therefore, based on familiar task variables, a skilled human operator can infer a target pattern mentally, make a prediction on the next position and act correspondingly.

Now human modelling will be presented and followed by human characteristics.

2.2.1. Human modeling

A *human modeling* was studied due to a motivation to understand and predict human responses from a man-machine system. The diverse structures and principles of human modelling involve a classification of a human model into a mathematical model, a reliability model and a cognitive model, as suggested by Pew (2008).

2.2.1.1. Mathematical model

Human mathematical model is analytically derived from collected data in an operation field. This was initiated in the 1940s by Tustin based on the operation of an electrically-controlled tank turret (Gaines, 1969). A human was concluded to possess a linear servomechanism behaviour (Tustin, 1947) but the resultant human models varied in different manual control systems (Suzuki and Harashima, 2005). Quasi-linear and optimal control models are among the most widely used human models in the field. Therefore, details of these two models are presented first and followed by a linear parametric model and intelligent model.

- **Quasi-linear model**

A *quasi-linear model* is based on the hypothesis that human response will be linear (Tustin, 1947; Mcruer and Krendel, 1959). Figure 2.4 presents a block diagram showing its components.

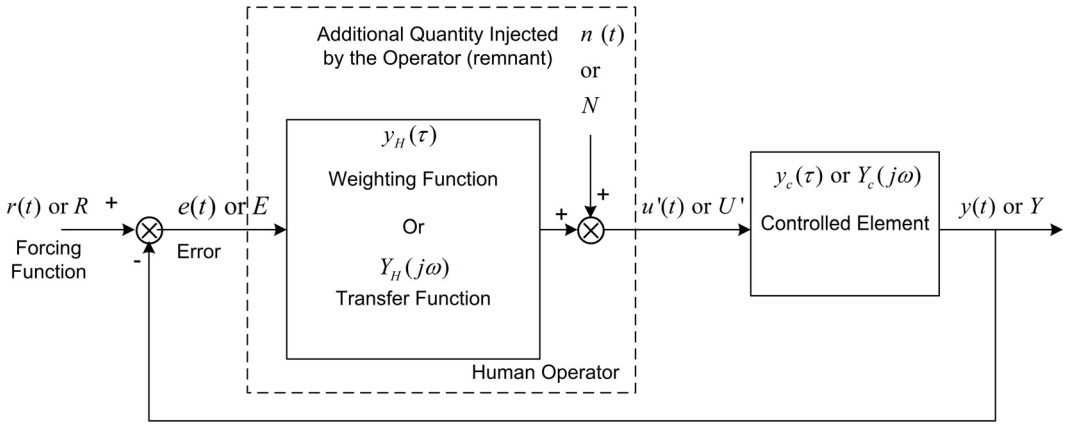

Figure 2.4. A block diagram of quasi-linear human model in a man-machine control loop (Mcruer and Krendel, 1959, with modifications on variables notation). Note: Capital letters with $j\omega$ represents a frequency-domain variable.

Mcruer and Krendel (1959) claimed that the human model consists of linear (Y_H) and non-linear (N) elements, hence the name of the model. A non-linear element is a representation of the noise and disturbance of human control action, collectively called a *remnant*.

A human transfer function ($Y_H(j\omega)$) appears in the following form.

$$Y_H(j\omega) = \frac{K \cdot e^{-j\omega\tau}}{j \cdot T_N \cdot \omega + 1}\left[\frac{j \cdot T_L \cdot \omega + 1}{j \cdot T_I \cdot \omega + 1}\right] \tag{2-1}$$

Where K is a proportional gain, τ is a reaction time delay, T_L is a lead time constant, T_I is a lag time constant and T_N is a neuromuscular lag.

Regarding the non-linear components of the model or remnants, their locations might differ from Figure 2.4 depending on a system perspective as studied in detail by Elkind, (1956). It is also interesting to see that there are a number of possible variants from this general quasi-linear model structure presented in Equation (2-1). Among the most commonly used forms, human can be regarded as a lead-lag compensator (Mcruer and

Krendel, 1959(a); Mcruer and Krendel, 1959(b)) or PID controller (Ragazzini, 1948 via Suzuki, Kurihara et al., 2006) with and without a time delay term. All of these forms are suitable for modelling a human performing a point-to-point tracking, which can be computed using a system identification theory and represented in a linear parametric form (Suzuki, Kurihara et al., 2006).

- **Optimal Control Model (OCM)**

Though the representation of human in a transfer function format is widely acceptable, a limitation on only a single input of the quasi-linear model leads to a development of the model in a state-space form called *Optimal Control Model (OCM)*. A human can now be modelled as a multiple-input multiple-output system with a structure as shown in Figure 2.5.

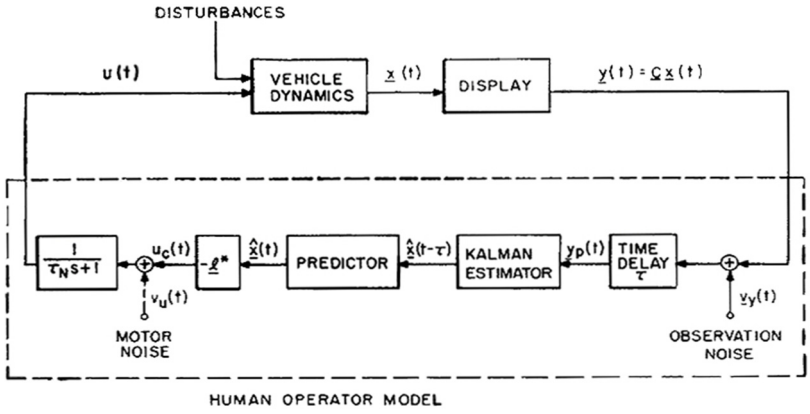

Figure 2.5. A block diagram of an Optimal Control Model (OCM) in a man-machine control loop (Kleinman, Baron et al., 1970)

An optimal control model estimates system states by using a Kalman filter in cascade with a linear predictor, as presented in Figure 2.5. The state-space equations for such an optimal control model are presented in steps as follows, starting from system equations (Kleinman, 1969).

$$\dot{\underline{x}}(t) = \boldsymbol{A}\underline{x}(t) + \boldsymbol{B}\underline{u}(t) + \underline{w}(t) \tag{2-2}$$

$$\underline{y}(t) = \boldsymbol{C} \cdot \underline{x}(t) \tag{2-3}$$

$$\underline{y_p}(t) = \boldsymbol{C} \cdot \underline{x}(t-\tau) + \underline{V_y}(t-\tau) \tag{2-4}$$

Where $\boldsymbol{A}$, $\boldsymbol{B}$ and $\boldsymbol{C}$ are state, input and output matrices respectively. $\underline{x}(t)$, $\underline{u}(t)$ and $\underline{w}(t)$

are the vectors of states, inputs and external disturbances respectively.

$\underline{y_p}(t)$, $\underline{x}(t-\tau)$ *and* $\underline{V_y}(t-\tau)$ are vectors of display output, states and observation noise respectively and τ is human's inherent time delay.

The estimated states resulting from the Kalman filter and predictor are:

$$\underline{\hat{x}}(t) = \underline{\xi}(t) + e^{A\tau}[\hat{x}(t-\tau) - \underline{\xi}(t-\tau)] \tag{2-5}$$

$$\dot{\underline{\xi}}(t) = A\underline{\xi}(t) + Bu^{*}(t) \tag{2-6}$$

A complete structure of this optimal control model based on variables from Equations (2-5) and (2-6) is presented in Figure 2.6.

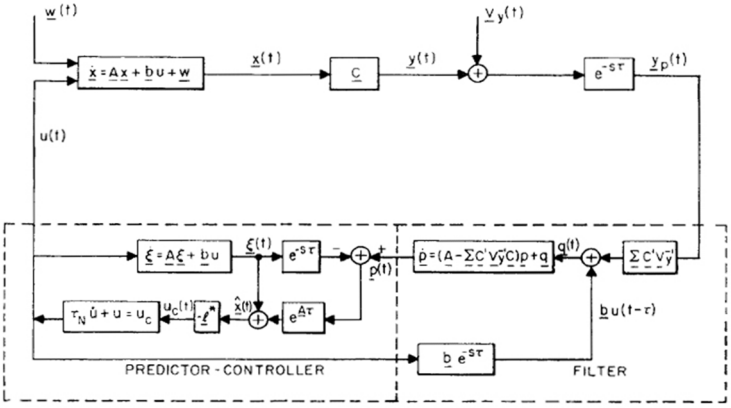

Figure 2.6. Structure of optimal controller with time delay and observation noise (Kleinman, Baron et al., 1970).

In summary, this type of model implies that a human operator must possess full expertise and motivation in performing an operation to comply with a state prediction based on Kalman estimator. Due to this fact, the model has been modified to suit a broader class of human and avoid overcomplicating a model like *Modified Optimal Control Model (MOCM)* and *Fixed-Order Modified Optimal Control Model (FOMOCM)*. The MOCM introduced extra features like attention allocation and thresholds into the OCM (Davidson, Schmidt et al., 1992) whereas FOMOCM applied the Optimal Projection (OP) method to form a compensator with a suitable order (Doman and Anderson, 2000). However, these OCM variants still retain the original feature of the OCM model thanks to their Kalman estimator. This also suggests an optimal control model is more suitable for complex machine dynamics or higher-order systems (Doman and Anderson, 2000).

- **Linear parametric model**

To add a degree of flexibility to the previous human model, a new human model structure is proposed. This type of human model applies a system identification theory to formulate mathematical models in the form of linear difference equations (Ljung, 1999). *AutoRegressive with eXogeneous inputs (ARX)*, *AutoRegressive Moving-Average (ARMA)*, *AutoRegressive Moving-Average with eXogeneous inputs (ARMAX)* are examples of the autoregressive model family. The major difference from other types of human model is that a linear parametric model is not a true and accurate model. It is rather the one best suited within a range of interest.

According to Ljung (1999), a generalized model structure with q (z-transform notation) is as shown below.

$$A(q)y(t) = \frac{B(q)}{F(q)}u(t) + \frac{C(q)}{D(q)}e(t) \tag{2-7}$$

Where *y(t), u(t)* and *e(t)* are output, input and error signals respectively. *B(q)* and *F(q)* are respectively the numerator and denominator of *G(q)*, a transfer function. *C(q)* and *D(q)* are respectively the numerator and denominator of *H(q)*, a disturbance function. All q-functions are of the form $1+?_1q^{-1}+...+?_{n?}q^{-n?}$ with ? representing A, B, C, D and F and the structure as presented in Table 2-1.

Table 2-1. Common Linear Parametric Models (Ljung, 1999)

Polynomials in Equation (2-7)	Name of model structure
B	FIR (Finite Impulse Response)
A B	ARX
A B C	ARMAX
A C	ARMA
A B D	ARARX
A B C D	ARARMAX
B F	OE (output error)
B F C D	BJ (Box-Jenkins)

The structures given in Table 2-1 allow different levels of flexibility for the disturbance characteristics to be best suited for different quality of the collected data. Trials on various structures are suggested as the algorithm recursively adjust its parameters to yield the least squared difference and this leads to the most reliable model (Ljung, 1999). System identification techniques have been successfully applied to different tasks and systems. To be specific, this type of model is suitable for human performing

point-to-point and *continuous tracking* operations. A point-to-point tracking assumes that human's control action is constant from one point to another point (Suzuki, Kurihara et al., 2006) whereas a continuous tracking requires the input pattern that is specifically designed to accommodate all necessary spectrums from a human response (Cooper, 1991; Gittleman, Dwan et al., 1992; Ljung, 1999; Ertugrul, 2008).

In this research, a point-to-point operation is of the focus and a linear parametric model is to be derived for each target segment for both computer-based and hardware-based systems. Further details on this will be covered in Chapter 6.

- **Intelligent model**

Due to the nature of a human being adaptive and time-variant, the higher capable human model was proposed to include these behaviours. This category of human model is usually referred to as an intelligent model or Artificial Intelligence (AI). Many man-machine systems were studied to extract fuzzy control rules due to the resemblance with human reasoning, which are sometimes inexplicable (Shaw, 1993; Zapata, Kawakami et al., 1999). An enhancement of a traditional Proportional Integral and Derivative (PID) controller with fuzzy logic to fine-tune the controller parameters was also proved to be very useful and pragmatic (Ollero and Garcia-cerezo, 1989; S.Tzafestas and Papanikolopoulos, 1990; Santos, Lopez et al., 2005). However, such system is not functional when no rules can be applied (Gingrich, Kuespert et al., 1992). The learning feature of Artificial Neural Network (ANN) complements this missing ability. One example of ANN can be found in Figure 2.7.

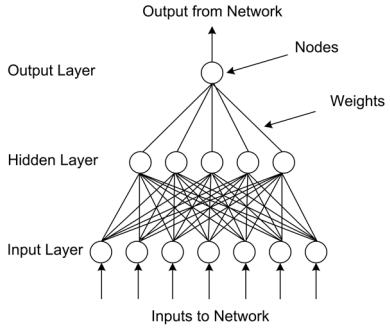

Figure 2.7. Back propagation neural network human model (Gingrich, Kuespert et al., 1992)

In order to combine both learning and reasoning abilities of a human operator, Adaptive Network Fuzzy Inference System (ANFIS) was introduced to allow an adjustment of

membership function's shape for each fuzzy rules (Jang, 1993). This kind of system is presented in Figure 2.8.

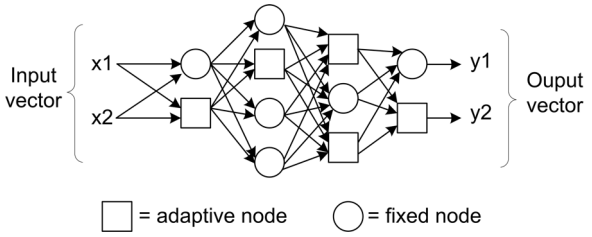

Figure 2.8. Adaptive Network Fuzzy Inference System (ANFIS) (Jang, 1993; Jang and Chuen-Tsai, 1995)

Similarly, there is another kind of learning algorithm called *Iterative Learning Control (ILC)* but it mainly deals with operations requiring a predetermined reference pattern to be followed (Cai, 2009; Wang, Gao et al., 2009). Therefore, this technique is more suitable for automated systems as the operation needs to be well-established and allows only a small degree of flexibility.

2.2.1.2. Reliability model

This class of model is derived from probability theory to compute system success rate (Miller and Swain, 1986 and Pew, 2008). Probabilities of *success* and *failure* are denoted as a small letter and capital letter respectively corresponding to the task variables A and B.

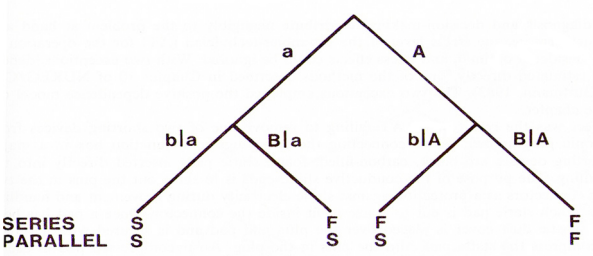

Figure 2.9. Technique for Human Error Rate Prediction (THERP), Human Reliability Analysis (HRA) (Miller and Swain, 1986) [Note: Series = AND, Parallel = OR]

According to Figure 2.9, the probability of success in the operation consisting of the first task (*A*) and the second task (*B*) is conditional depending upon processing types.

For the series system, the probabilities of success (*Pr[S]*) and failure (*Pr[F]*) are as follows:

$$\Pr[S] = a \cdot (b \mid a) \tag{2-8}$$

$$\Pr[F] = 1 - a \cdot (b \mid a) = a \cdot (B \mid a) + A \cdot (b \mid A) + A \cdot (B \mid A) \tag{2-9}$$

For the parallel system, the probabilities of success and failure are as follows:

$$\Pr[S] = 1 - A \cdot (B \mid A) = a \cdot (b \mid A) + a \cdot (B \mid a) + A \cdot (b \mid A) \tag{2-10}$$

$$\Pr[F] = A \cdot (B \mid A) \tag{2-11}$$

Other reliability models are the Siegel and Wolf Network Model, SAINT and Micro SAINT, the Human Operator Simulator (HOS), etc. (Pew, 2008). This class of human model is abstract and useful for an overall system analysis in terms of down time or failure percentage.

2.2.1.3. Cognitive model

In contrast to other human models from the engineering discipline, a *human cognitive model* is based on human sciences that integrate human cognition to cover the complete framework starting from perception to action. Important human cognitive models are given in detail below.

- **Rasmussen's model**

Rasmussen (1983) described the human response to stimuli as stacks of behaviour (Figure 2.10). Each stack represents a unique nature of response depending upon experiences and skills. Types of information in each stack require different levels of processing and these are referred to as *signals, signs* and *symbols* from the lowest to the highest layer respectively. That is, a human can interact instantly and naturally with signals using his/her skill. Hence, the shortest time is taken for this reaction. For signs and symbols, a longer time is required to process as recognition and interpretation processes are involved respectively. Due to its layered architecture of reaction, Rasmussen's model is also regarded as a *layered, sub-goal, cognitive model*.

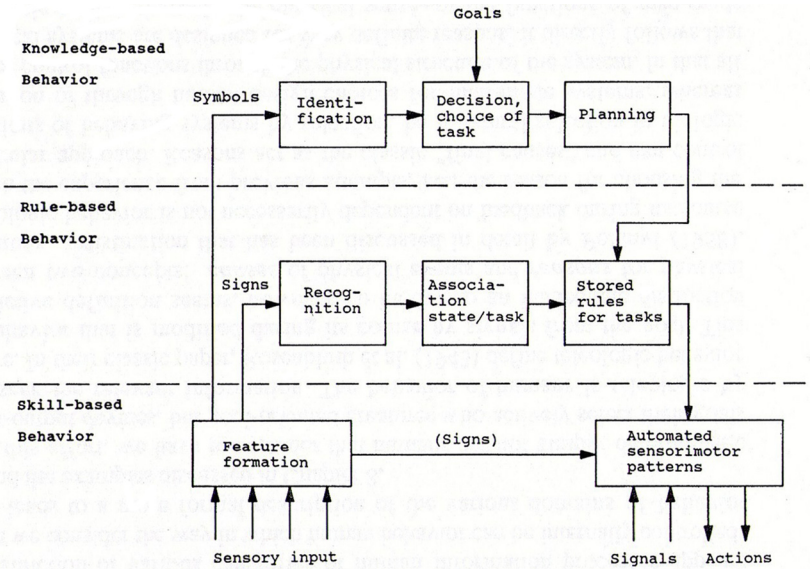

Figure 2.10. Rasmussen's model: Skill, rule and knowledge-based behaviour (Rasmussen, 1983; Rasmussen, 1986; Rasmussen, Pejtersen et al., 1994)

- **GOMS model**

Goals, Operators, Methods and Selection rules (GOMS) is a goal-oriented cognitive model introduced by Card, Moran et al. (1983). This type of model is comprised of sub-goals to achieve the ultimate goal in the operation of interest. Goals are what need to be achieved in an operation using a set of sub-goals (operators), instructions (methods) and criteria (selection rules). Selections rules help make a decision about which operator is to be used and which methods are suitable to go with the chosen operator(s). Therefore, information processing in the human brain keeps going until the ultimate goal is achieved. A strategy to select methods and selection rules relates directly to the skills and experiences of a human operator.

- **Kawato's model**

Kawato's model is a representation of human characteristics as a feedforward and feedback control system (Kawato, 1999). The emphasis of this human model is on the learning part, which effectively switches a feedback or compensatory behaviour to feedforward behaviour as shown in Figure 2.11. Kawato found that the feedback path of a human control system causes the adjustment of the inverse model as the learning

mechanism takes place in the cerebral cortex. An initial error is gradually reduced and fully compensated for by the end of the learning stage. Other cognitive models are SOAR (State, Operate And Result), ACT-R (Adaptive Control of Thought-Rational), MIDAS (Man-machine Integration Design and Analysis System), OMAR (Operator Model ARchitecture) and D-OMAR (Distributed Operator Model ARchitecture) (Pew, 2008).

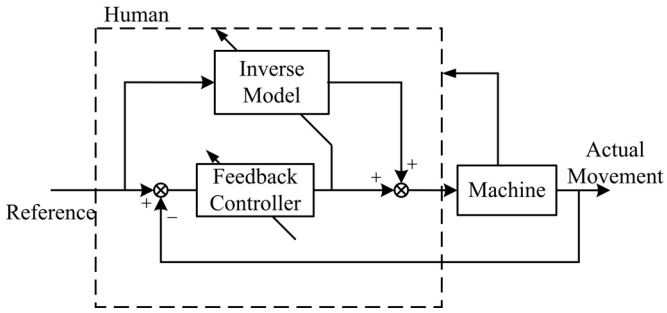

Figure 2.11. Kawato's human model (Kawato, 1999)

As a conclusion for human modelling, all the introduced techniques from different disciplines are based on different characteristics and hypotheses. To apply these models for different purposes, a selection needs to be made with care. A mathematical model is suitable for engineering design like optimizing and predicting system performance. A reliability model is also suitable for engineering applications but with a generality in predicting system failure rather than a system response. For the human cognitive model, it is important for a task such as system interface design, mental workload computation or one requiring an insight into human cognition and information processing.

With reference to the focus of research work reported in this thesis, only Rasmussen's and linear parametric model will be used for building up a human performance concept and computing model-based human performance respectively. Human models will be derived using System Identification theory (Chapter 6) and used for validating the results computed from that of the non-model approach (Chapter 5). Additionally, the parameters of a linear parametric model computed from the System Identification will be analysed with reference to the definitions of performance variables (Chapter 3).

2.2.2. Human characteristics

According to the literature, human characteristics are found to be another widely studied area next to human modelling thanks to its broadness and applicability. However, only those derived from or based on engineering context will be of main concern and they are *skill, adaptability, reaction time* and *speed-accuracy*. Among these characteristics, skill is so dynamic and subjective that it can be interpreted from different viewpoints. To provide a clear picture on what this means and on what basis the human performance index concept is built upon, it is reasonable to have a section dedicated just for human skill called *Related work on human skill evaluation* and then followed by the drawbacks before introducing the outline for the work reported in this thesis. Selected human characteristics from the literature along with their relationships are now presented in detail as follows.

2.2.2.1. Adaptability

Adaptability, adaptive capacity or equalization, in a man-machine system, means an ability of a human to maintain a level of performance under disturbances by adjusting his/her actions correspondingly. With reference to the quasi-linear human model, it can be visualised to contain alterable and unalterable characteristics, which are dependent upon and intrinsic to each and every human operator respectively as presented in Figure 2.12.

Even though the adaptive characteristics of humans are varied, there are consistent behaviours on the total forward tranfer function and the adaptive range of operation that mark a degree of predictability of human action.

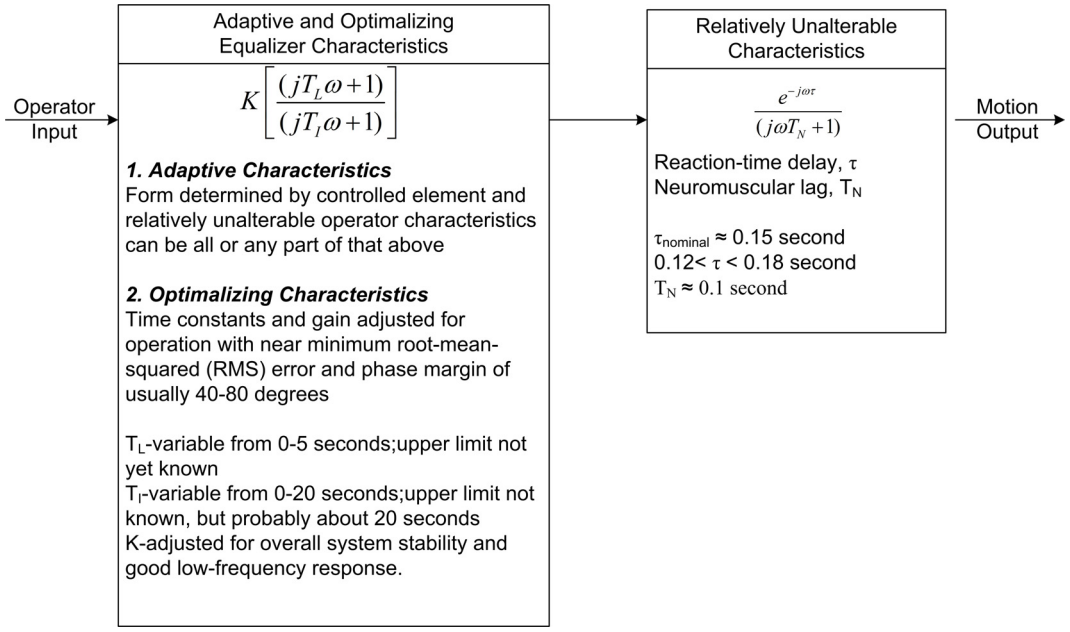

Figure 2.12. Condensed quasi-linear human model based on Equation (2-1) (Mcruer and Krendel, 1962)

Regarding the total forward transfer function, it characterizes the effort of a human operator to always maintain his/her characteristics as a good servo (Jagacinski and Flach, 2002). Observations on invariant forms of human response around the crossover region led to the formulation of a model called a *crossover model* (Mcruer and Krendel, 1959). This is as shown below.

$$Y_H(j\omega)\cdot Y_p(j\omega) = \frac{\omega_c \cdot e^{-j\omega\tau_e}}{j\omega} \tag{2-12}$$

Where Y_H and Y_P are the human and plant (controlled system) transfer functions respectively. τ_e is an effective time delay. ω_c is a crossover frequency.

Based on this equation, a human operator behaves like a crossover model if and only if a crossover frequency or its gain value can be kept nearly constant. This means that a human operator tends to compensate and stabilize a system around the crossover frequency throughout the operation. It is also found that a time delay is directly connected to the recursive delay identifier (Boer and Kenyon, 1998). Even though a human can act adaptively to maintain its total forward transfer function, there is an allowable *adaptive range of operation* or *adaptive range* suggesting the capability bounds of a human operator (Skolnick, 1966). Such range is in terms of T_L (lead time

constant), T_I (lag time constant) and T_N (neuromuscular constant) as shown in Figure 2.13.

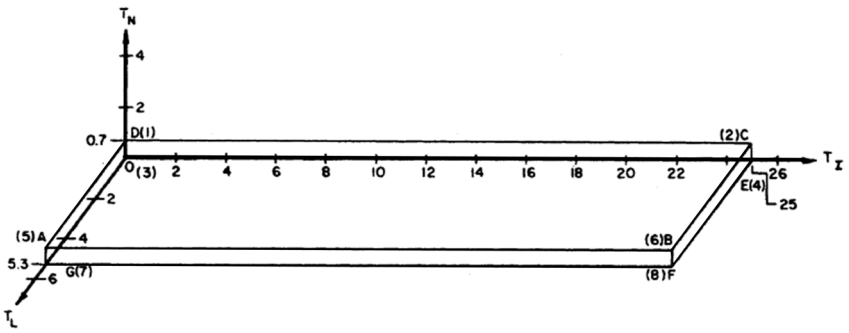

Figure 2.13. Human adaptive range (T_L: 0-5.3s, T_I: 0-25s., T_N: 0-0.7s) (Skolnick, 1966)

Regarding the nature of the parameter T_N, it directly relates to the reaction time that will be presented in the next topic. For other parameters, their values depend upon the conditions of an action leading to another interesting characteristic, speed and accuracy, which will follow the next topic.

2.2.2.2. Reaction time

Responding to and accomplishing an arbitrary task, in general, a human requires the reaction time and movement time (Fitts and Peterson, 1964). This is equivalent to the acquisition time and execution time (Card, Moran et al., 1980; Preyss and Meiry, 1968). It is found to be an inherent human response and widely regarded as an intrinsic characteristic with a magnitude varying from person to person. The research study carried out by Liao, Jagacinski et al. (1995) also suggested an increment of acquisition time with aging. The concept of a human's reaction time is found to comply with McRuer's quasi-linear model, which is termed the *reaction time delay*. The source of this time delay is due to human physiology, in particular, the neuromuscular and perceptual system (Miall, Weir et al., 1993). Reaction time serves as a preparation time prior to the actual motor actions. It can be best perceived as the pause duration before the response to a stimulus, with a typical value of 250 milliseconds (Birmingham and Taylor, 1954). By knowing this, it is important to allow a reaction time for a task completion in proportion to the complexity and nature of that task.

2.2.2.3. Speed and accuracy

Apart from adaptability, speed and accuracy serve as an inherent trade-off widely realized in other disciplines including computer science and experimental psychology. Concern about speed and accuracy usually arises when there is a need to compromise productivity over the level of accuracy. The most well-known and used speed-accuracy trade-off is called *Fitts' Law*, which was defined in a similar fashion to Shannon's theorem. That is, it holds the meaning of information capacity per one response of a human (Fitts, 1954; Fitts and Peterson, 1964). Fitts' law was based on experiment by tapping a stylus back and forth based on a pair of targets with varied width (W) and distance (A) (see Figure 2.14 with the corresponding parameters). The width and distance between a pair of targets forms a relationship defined as the *Index of Difficulty* (I_d or ID). *Fitts' La*w or *Fitts' model*, in the most common form, is presented as shown.

$$T = a + b \cdot I_d \quad \text{(second)} \tag{2-13}$$

$$I_d = \log_2\left(\frac{2A}{W}\right) \quad \text{(bits)} \tag{2-14}$$

Where T is a movement time, a is a margin of a movement time (second), b is a slope (seconds/bit) and I_d is an index of difficulty (bit). A reciprocal of b is the rate of information processing (bits/second).

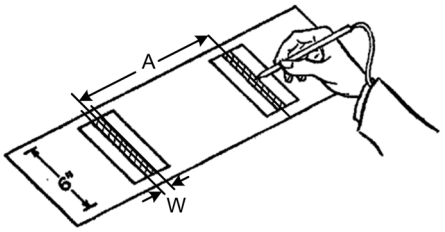

Figure 2.14. Fitts' reciprocal tapping task using a stylus and metal plates (apparatus dimensions added, (Fitts, 1954))

The concept on Fitts' law is valid for a general pointing operation and proven to be valid for other forms of operation like trajectory tracking in 2 dimensions (Scott MacKenzie and Buxton, 1992; Mottet, Bootsma et al., 1994; Accot and Zhai, 1997) and a 3-dimensional scenario (Murata and Iwase, 2001). In all setups, this means a longer time has to be spent on the target with larger I_d. A compromise between speed and

accuracy can be implied as slower movement is required to land on a distant and narrow target.

However, the action involved to achieve this is highly subjective and dependent on the selected control strategy. The definition of I_d can therefore be different due to the system point of view and governing assumptions: assuming a Gaussian distribution for the landing position, I_d is referred to as the effective I_d (Scott MacKenzie, 1992) whilst assuming a different I_d as perceived by a human operator, it is referred to as the actual/utilization I_d (Zhai, Kong et al., 2004).

Even though there are a number of researchers focusing on speed and accuracy in different engineering systems (Bradshaw and Sparrow, 2000; Marayong and Okamura, 2004; Sribunruangrit, Marque et al., 2004; Beamish, Scott MacKenzie et al., 2006; Schirner and Domer, 2008), there is no rigorous treatment and foundation to come up with a computational structure that can be used in any man-machine system. From this perspective, the research work in this thesis aims to formulate a novel structure to quantify speed and accuracy of a human as one of its novelties.

As a conclusion for the literature on human modelling and characteristics, a rigorous structure or platform to incorporate human characteristics variables or performance variables for a computation of overall performance has not yet been established. This deficiency inspired the idea to formulate an entity that can be used to indicate the performance level as being comprised of variables or criteria of the same properties. This consolidates the core of this research, which concerns human performance evaluation.

2.3. The background to HAM

2.3.1. Evolution of the manual control system

According to the literature, research work in the past was either machine-oriented or human-oriented. The focus started with the development and design of human-vehicle systems like aircraft, helicopters, tanks, submarines without consideration of human coordination on one hand. On the other hand, only pure studies on human behaviours in the systems with simple dynamics like object tracking and puzzle solving.

With reference to Figure 2.1, further development of technologies on manual control systems, ergonomics and adaptive control systems helped drive and consolidate machine systems into a multi-disciplinary engineering commonly referred to as *Mechatronics*. The term Mechatronics is used to describe a system or device that contains actuation and control mechanisms relying solely on its mechanical, electronic, software and control elements (Auslander, 1996; Wikander, Törngren et al., 2001). Following its inception in the 1960s, there has been continuous interest in improving the man–machine interface in these systems (Schweitzer, 1996). In this context, such man-machine systems are designed and operated according to the way they were programmed in response to human that only serves as an active control element to complete the loop. Therefore, system configurations and controller settings have to be pre-programmed causing a lack of adjustment based on the actual responses by a human. Research on human coordination was deemed minimal and evolved into a cooperative man-machine system. In other words, the trend of Mechatronics technology is going towards human-oriented man-machine systems (Schweitzer, 1996). The degree to which a humans' presence is treated differently is crucial for precision-required systems like surgical robotics (Cleary and Nguyen, 2001; Marayong and Okamura, 2004) and rehabilitation devices (Zhang and Nakamura, 2006).

In brief, the trend of man-machine system research started with a treatment of human and machine as separate blocks with minimal awareness. This awareness is based on the machine's point of view. The trend of development then goes to an increasing degree of

awareness including adaptive control mechanisms design. Man-machine systems with adaptive control in relation to a human's presence are then regarded as a two-way or symmetrical interaction system termed *Human Adaptive Mechatronics (HAM)*.

2.3.2. Human Adaptive Mechatronics (HAM) systems

HAM is defined as a mechanical system that is capable of adapting the characteristics of its own self optimally to the skill of a particular user or human operator (Suzuki *et al.*, 2005a). This kind of machine system can be considered as an advance on a conventional and cooperative man-machine system. A HAM system also aims to improve a human's skill and maximize overall performance of the human-machine system. Therefore, a HAM system is an intelligent machine featuring human characteristics recognition and the ability to react adaptively. A HAM system generally concentrates on how to make an interpretation of human characteristics and to design adaptive control mechanisms. To provide a proper background on HAM systems, a brief history and scope of HAM research will be included in Sections 2.3.2.1 and 2.3.2.2. A summary of the perspectives on conventional man-machine systems and HAM systems is tabulated below.

Table 2-2. Summary of human-machine and Human Adaptive Mechatronics (HAM) systems

System of interest	Goal
Man-machine system	To analyze a system response and design a stable system with a human in the control loop
Human Adaptive Mechatronics (HAM) system	To enable the adaptability of a machine to a human operator and improve the overall performance

2.3.2.1. Historical background

HAM originated in Japan with the main objective to advance Mechatronics technology in a more mutually understandable way among human and mechatronic systems (Tokyo Denki University, 2004; Furuta, 2004). HAM was one of the 21st Century Centre of Excellence (CoE) research projects in 2003 with Professor Katsuhisa Furuta as a research leader at Tokyo Denki University (TDU) in Japan. This research project was

sponsored by the Japanese Ministry of Education, Sports, Culture, Science and Technology (MEXT), from 2003 to 2007. At the end of the HAM project in Japan, research collaboration was established with the United Kingdom as an EPSRC-funded UK-Japan network on Human Adaptive Mechatronics (HAM) in 2007.

2.3.2.2. Scope of HAM research

HAM research was initially centralized at Tokyo Denki University (TDU) with three research groups. These groups were the human group, control group and mechatronic group (2004).

The *Human Group* focuses upon a brain wave and locates brain sections in response to different brain activities. The main objective of the human group is to generate a brain signal pattern for skilled human operators and to gain an insight into how to perform a skilled operation. Neurophysiology, experimental psychology and human science are the disciplines that lead to human skill quantification and human controller derivation (Suzuki *et al.*, 2005b, 2004b).

The *Control Group* is to study a global mathematical model of a man-machine system with a focus on a human-in-the-loop structure. The study on human hand motion also showed the relationship of skilled movement and a human operator's skill (Tokyo Denki University, 2004; Takeuchi *et al.*, 2006). The ultimate goal of the control group is to derive an optimal control strategy for the man-machine system of interest.

The *Mechatronics Group* deals with an implementation and interface of human and mechatronic devices. This includes system integration of a derived human controller into the system of interest. The target of a HAM system is to embed a skilled operator behaviour into a device. Examples of such implementations at Tokyo Denki University (TDU) are surgical robots (Masamune *et al.*, 2005) and a walking support device (Hirata *et al.*, 2005).

2.3.2.3. Structure of HAM system

By the original definition of HAM, as proposed by Japan's Tokyo Denki University (TDU) in the year 2003 as part of the Centre Of Excellence (COE) research programme (Furuta, 2003; Furuta, 2004), there are four essential features for HAM system implementation under the Section *Key items of HAM* as presented below (Suzuki, Tomomatsu *et al*., 2004).

" *... HAM must quantify human skill-level of the manipulation. HAM has to assist an operator by giving useful supports and by changing its own functions and structures. For the realization, the following items are needed.*

1. *Definition and quantification of human skill,*
2. *Cognition of a human model from the machine-side,*
3. *Assistance method for human by the machine,*
4. *Change of machine's function.* **"**

Based on the aforementioned features, HAM systems can be structured into modules as follows.

Module 1: Human skill quantification

This module serves as the very first step in implementing any HAM system. HAM is designed to support or assist a human operator in performing a task with higher efficiency in a symmetrical manner. The major concern in this module arises when considering which human characteristics are to be used to reflect such a human difference and according to the original definition, a quantification of human skill is of the focus. However, there are plenty of possibilities and the man-machine interaction pattern has to be taken into consideration. Human differences in other terms can therefore be perceived as a stepping-stone to enable the representation of a human in a quantitative manner.

Module 2: Human modelling

Considering the result on a selection of Module 1, a human has now been quantified in one aspect and has become distinguishable. The next step is how to make the human realizable from a machine's point of view. This module ensures that the human

difference from Module 1 is represented in a machine-understandable format. The usability of the human difference is as equally important as the human difference itself. Therefore, this has to be defined carefully.

Module 3: Assistance mechanism

With regard to the resulting design of human skill quantification and modelling platform, the next step is to consider possible supports for a human operator. Definitions of algorithms, structures and patterns of assistance are truly essential for this module. The requirements for an assistance mechanism must match the characteristics of the system to be implemented. The examples are signal availabilities and accessibilities, the human-machine interface, degrees of freedom and so on. A human-machine interface and pattern of assistance are the main elements to be considered when designing the assistance mechanism. Physical and visual assistance are the most common forms found in the HAM literature.

Module 4: Adaptive control mechanism

This element may need to be designed closely with the assistance mechanism to ensure compatibility. The degree of assistance marks a difference between an *assistance mechanism* and an *adaptive control mechanism*. A design of this mechanism is about selecting suitable adaptive control technologies such as heuristic adaptive controllers, self-tuning controllers (STC) and model adaptive reference systems (MARS) (Bobál, Bohm *et al*., 2005). Apart from the adaptive technologies, complications involving human learning and adaptability have to be taken into consideration to ensure that these issues are minimized to avoid machine domination. A change in the dynamics and/or control parameters for systems of interest has to directly relate to each individual human.

Based on the module descriptions, the fact that Modules 1 and 2 are essential to enable an implementation of Modules 3 and 4 can be inferred. That is, to supply a pattern and level of assistance from system to human operator correspondingly. A summary of the HAM modules can be found in Figure 2.15.

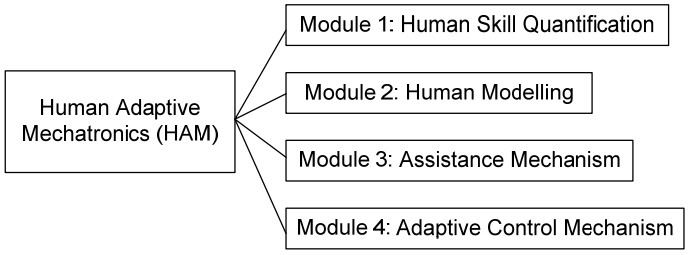

Figure 2.15. Human Adaptive Mechatronics (HAM) modules summary

As a result of the dependence of the development of **Modules 3 and 4** on **Modules 1 and 2,** most of Japanese HAM research focuses on the complete HAM system implementation leaving the development of **Modules 1** and **2** rather shallow and system-specific, as is to be discussed shortly. This observation is, however, understandable as a complete HAM system illustrates the potential of HAM systems in reality and serves as a technology showcase (Furuta, 2004; Kurihara, Suzuki *et al*., 2004; Suzuki, Furuta *et al*., 2005; Suzuki and Harashima, 2005).

Due to the fact that HAM is an emerging field, it is reasonable to illustrate the nature of available Japanese HAM literature in terms of **Modules** to form a basis for the problem in general, to concentrate on the missing elements or deficiencies demanding rigorous treatment and to ensure its essence. The focus is on the publications by TDU, as being an Institute of origin, to avoid ambiguity about the essence of HAM systems. The missing element(s) will subsequently be elaborated in Chapter 3. Details of the main Japanese HAM projects, which can be grouped as haptic device systems, robots and vehicles, will now be provided below.

1. **Haptic device systems**

Haptic devices are the most presented and frequently used system in HAM research at TDU. The same haptic device was reused for different operations in different systems. Because of this fact, an overview of all the articles will be firstly given and then followed by specific works along with the corresponding **Module** developments.

A haptic device is a man-machine interface, or can be regarded as a control device, that was developed and designed to measure a force magnitude via force sensors and supply

a force feedback to a human user. The advantage of this force feedback in HAM research is twofold, especially in a virtual environment or teleoperation, to provide a tactile feeling to a human operator and compensate for insufficient amplitude of force by that human operator (Kurihara, Suzuki *et al*., 2004; Katsura, Matsumoto *et al*., 2005). The latter can be perceived as a *guiding force* and it is therefore considered as a form of assistance or **Module 3**. Such assistance is possibly provided in visual forms depending on the applications. The scale of assistance (**Module 4)** varies with human characteristics and the most-used human characteristic in haptic device systems for **Module 1** is human skill. For a technique to realize the human skill (**Module 2)**, online system identification was applied to retrieve human parameters in terms of a Proportional-Derivative (PD) controller and a time delay. Parameters from an expert human operator are the key to an adaptive control mechanism. To obtain these parameters, a human operator who can pass a ten-hour-a-day training in two months with no further improvement is required (Suzuki, Kurihara *et al*., 2006). A block diagram of an overview of the haptic device system in HAM research is as shown in Figure 2.16(a). Two versions of these haptic devices up to the year 2006 are also given; one-handed and two-handed haptic devices are as shown in Figure 2.16(b) and (c) respectively.

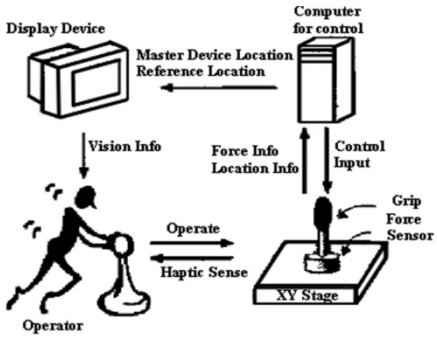

a) A block diagram of haptic device systems (Kurihara, Suzuki *et al*., 2004)

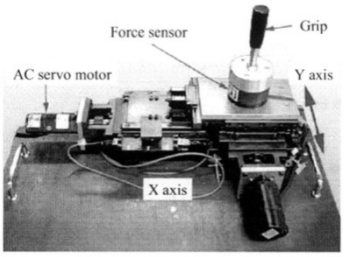

b) One-handed haptic device (Kado, Pan *et al*., 2006)

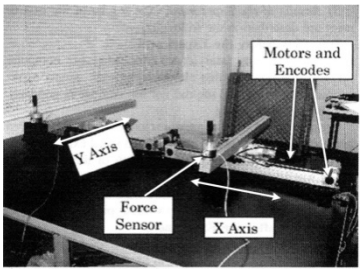

c) Two-handed haptic device (Suzuki, Pan *et al*., 2006)

Figure 2.16. Haptic device systems

According to the overview given above, the actual development of HAM modules based on a haptic device can be divided into a *complete* and *incomplete* (specific) research work for simplicity. Regarding a complete HAM development, there were two main systems, which are a point-to-point tracking task and a circle drawing task. In the study of a point-to-point task by Kurihara, Suzuki et al. (2004), an *assist-ratio* or assistive force function (**Module 4**) was proposed and defined as being directly proportional to the parameter differences between expert and individual human operators (**Module 2**), which is effectively a skill factor (**Module 1**). The assistive force is supplied via a haptic interface in this case (**Module 3**). Another research **project** on a point-to-point tracking **device**, conducted by Suzuki and Harashima, 2006(a); Suzuki, Kurihara et al., 2006(b), came up with a different assist-ratio definition. For a circle-drawing task conducted by Suzuki, Pan et al. (2004), visual assistance in terms of a guide marker was provided (**Module 3**) instead of a force, in proportion to the variance of radius and phase of a circle completed in the previous trial (**Module 4**). The radius and phase variance are defined as a human skill in this task (**Modules 1 and 2**).

For the case of incomplete HAM system developments, a simulated ball juggling and inverted pendulum were used by Furuta, Kado et al. (2006); Kado, Pan et al. (2006) respectively. These two works are different from the others since they introduce a *corrective force* rather than an *assistive force*. As the name implies, a corrective force is applied in relation to a difference between an optimal and actual force rather than a human skill, hence, missing the development for **Modules 1 and 2**. A human operator is expected to learn from the pattern of the corrective force or *teacher* referred to as the concept of *Skill Acquisition.*

Another two incomplete HAM systems, presented by Suzuki, Harashima et al. (2005); Suzuki, Kurihara et al. (2005), were regarding a brain signal pattern while controlling a virtual pendulum (**Module 1**) and a point-to-point task with variable haptic device dynamics respectively. The former studied a difference in brain signal between a high-skilled and low-skilled human. The latter changed the tuneable parameters of a haptic device in relation to a human's parameters (**Module 4**) extracted from an online identification process (**Module 2**). The objective is to enable a variation in the handling

properties of the haptic device itself (**Module 3**). Remarkably, there is no consideration on any human characteristics or **Module 1** in this work at all.

To sum up on the haptic device systems, the variety of the work shows the main interest is in developing an *adaptive control mechanism* (**Module 4**) using a *human skill* (**Module 1**). The assistance is in mainly visual and physical forms thanks to a display and force-feedback mechanism on the haptic device.

2. Robots

The studies on mobile robots were primarily targeted at surgery and mobile robot systems. In terms of HAM Modules, a complete system has not yet been realized for these two robot systems.

For the case of surgery robots, *human skill* is the key feature to be used for a *skill index* calculation as presented by Masamune, Takeda et al. (2004). This can be perceived as **Module 1 and 2** developments respectively. Masamune, Takeda et al. (2004) studied different types of control device (a joystick, footswitch and force sensor device) in a continuous line-tracking task on a provided display and the results suggested that the human operator performed best with a joystick. The essence for coordinating surgical equipment involves a displayed image in an image-guided surgery system. For another surgery robot, Scrub Nurse Robots (SNR) or surgeon's assistant was designed and developed to produce a HAM surgery robot system, initially for a laparoscopic operation (Masamune, Ohnuma et al., 2005; Yoshimitsu, Tanaka et al., 2005). A state-transition model is used to represent a surgeon, scrub nurse and patient interaction (**Module 2**) and this was the only focus in this research (Figure 2.17(a)). The result suggested a smooth transition between states in a non-repeated manner for an expert surgeon.

For mobile robot systems, the ones presented by Suzuki, Tomomatsu et al. (2004); Igarashi, Takeya et al. (2005) are teleoperated or remotely controlled. The system had a display showing the robot's conditions and its surrounding area from the installed camera(s). Visual effects of the display characteristics and contents on human

sensitivity were studied (Igarashi, Takeya *et al*., 2005). Human visual sensitivity, presented in terms of a regression coefficients matrix, is found to be useful for the design of an instant alert feed window onto the operator's display to gain attention and immediate action. This, in fact, serves as **Module 1 and 2** developments for this research work. Another work by Suzuki, Tomomatsu et al. (2004) for controlling a robot to reach three cans in a physical workspace, interprets the need for human skill for a **Module 1** development. A human's Line Of Sight (LOS) on a provided display was used to represent human skill in a state transition model form (**Module 2**). The result showed a correlation between a skilled operator and his/her LOS pattern and suggested that this pattern could provide visual assistance to a non-skilled or less-skilled operator. For the robot category, there is **no** actual development of **Modules 3 and 4.** The main emphasis was on definitions of *human skill* in different forms and aspects.

3. Vehicles

In this category, vehicles with complicated dynamics were studied with a focus on *human skill* (**Module 1**). Due to its uncommon dynamics, manipulation of a virtual hovercraft using a joystick was selected and carried out. Human skill in Suzuki, Watanabe et al., 2007) is defined by an LOS located on a provided display in a point-by-point task (similar to the use of LOS for a human skill in Suzuki, Tomomatsu et al.(2004) in the robot category). The time spent on gazing at the current target is decreasing as the time progresses comparing to the next target (**Module 2**). This indicates a skill development by a human operator. The snapshot of this experiment is shown in Figure 2.17(b).

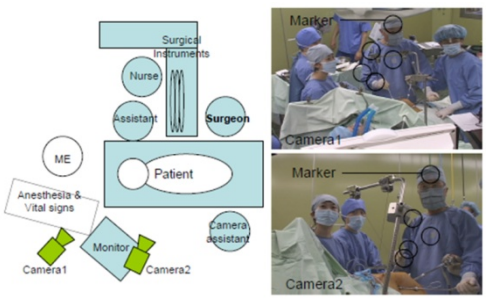

a) Robots: Experimental setup to generate a state-transition model (Masamune, Ohnuma *et al*., 2005)

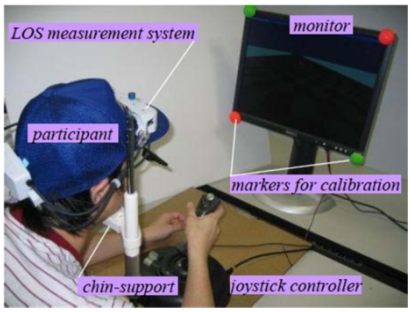

b) Vehicles: Virtual hovercraft with LOS measurements (Suzuki, Watanabe *et al*., 2007)

Figure 2.17: Examples of research on robot and vehicle HAM systems

In contrast to a human's LOS, Sasaki, Takeya et al. (2007) defined a *skill index* in terms of a distance deviation from the centre line and the time spent to complete a track (**Module 2**). Human operators were asked to complete a task by following a centre line of a rectangular track using a joystick. The result suggested a high skill in corner turning with a pattern reminiscent of a Gaussian or bell-shaped function. However, there was no development of **Modules 3** or **4** for each of these works.

All previous studies at TDU investigated numerous methods and techniques to represent human skill, compute it in a corresponding task or setup and use it as a designed assistance and adaptive control mechanism. It would be highly advantageous if these methods were universally applicable to any arbitrary man-machine system. This raises the question of whether it is suitable to merely quantify *human skill* and rely upon its *scenario-dependence property*. This also reflects a real concern about skill consistency in response to changes in system working conditions and environment. Consequently, human skill definition has to be changed correspondingly every time a skill of interest is shifted away from the original scenario and context. Consideration of an alternative to quantify human difference and generalize the quality of its control action underlies the main problem of this research.

2.3.3. Part of the problem that is addressed by this thesis

Based on an extensive literature survey in engineering and non-engineering fields, it can be observed that, although HAM research is emerging, it is still at an early stage. Confusion and hesitation in classifying the literature as HAM-related unquestionably arise. As pointed out, a wide coverage from human science to man-machine engineering forms the essential background to the creation of an evolutionary path leading to HAM systems. It is also obvious that HAM research is partially connected with an engineering field called *Human Factors* or *Ergonomics* (sometime used interchangeably), which is dedicated and centred around a human as part of a man-machine system including its surrounding issues such as safety, workspace design and so on. However, HAM

concentrates more on the design of a symmetrical man-machine interaction and the methodology to build an awareness of such interaction **for** both parties.

Considerable numbers of articles have been found outside of the HAM research community, which fit into the **Module** structure. This shows clearly the differences in terminologies and perspectives on the nature of intelligent and human adaptive man-machine systems. Good examples of these overlapping fields are collaborative/ cooperative robotics, rehabilitation and biomedical engineering. The concept of *flexible automation* is essential for such man-machine systems (Wickens and Hollands (1999) cited by Marayong and Okamura, (2004)). Research conducted by Marayong and Okamura (2004); Hirata, Jr.Oscar et al. (2005); Zhang and Nakamura (2006) are selected as examples of *non-HAM research* with HAM contributions. Marayong and Okamura (2004) aimed to study *human performance* (**Module 1**) in response to an admittance-control using a *Steady-hand Robot*. This human performance is in terms of execution time and errors (**Module 2**). Admittance ratio reflects a stiffness of virtual fixtures, which is a form of assistance to constrain a motion in a virtual workspace (**Module 3**). The picture can be found in Figure 2.18(a).

Another two examples from rehabilitation engineering are by Zhang and Nakamura, 2006 and Hirata, Jr.Oscar et al., 2005 on a food-feeding device (Figure 2.18(b)) and a walker-helping system (Figure 2.18(c)) respectively. Hirata, Jr.Oscar et al. (2005) developed a walking helper system with a varying degree of support and an adjustable centre of rotation. The centre of rotation is actively adjusted by forces imposed on the frame by human users to prevent a rotation. The magnitude and position of these forces reflect a difference between users that has to be treated adaptively. This implies human performance information for each user in terms of his/her associated weakness areas but no explicit definitions are derived.

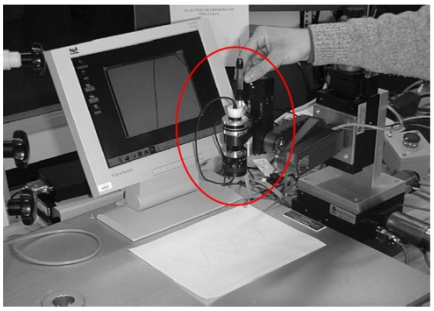

(a) The John Hopkins University Steady-hand robot with generated guidance virtual fixtures on the display by Marayong and Okamura, 2004 (**Modules 1, 2 and 3**)

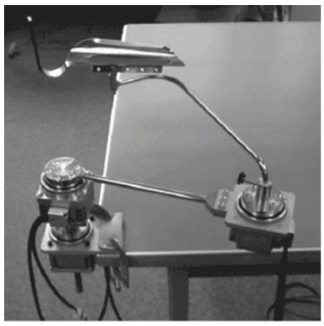

(b) Meal Assistance Orthosis (MAO) by Zhang and Nakamura, 2006 (**Modules 3 and 4**)

(c) Walking helper system by Hirata, Jr.Oscar *et al*., 2005 (**Module 4**)

Figure 2.18. Examples of non-HAM research with HAM contributions.

For the case of a food-feeding device, Zhang and Nakamura (2006) developed a device called *Meal Assistance Orthosis (MAO)* with a neural network-based controller for adaptive support for different humans. MAO also comes with a compensation or assistance force, which corresponds to a learned trajectory for each individual human user. Information on the trajectory from a plate to mouth for one human user is potentially a human difference that needs to be treated adaptively and this links to the arm's physical strength. Similar to the previous case, no explicit definitions are derived. In terms of the **Modules** structure, it is obvious that the MAO system contributed to **Modules** 3 **and 4** whereas the walking helper system contributes only to **Module 4** developments. Both of these two investigations *lacked Module 1 and 2* activities because of the fact that there were only a number of tests on different humans to validate the proposed adaptive mechanism and there was no explicit definition of any human characteristics.

With reference to *non-HAM literature* to date, as can also be observed from some of the selected works above, the focus has shifted from a conventional man-machine system to a human adaptive machine system with flexible automation and cooperative characteristics. This implies an increasing concern about a human's overreliance on a machine in a fully or partially automatic mode. In other words, the machine's response should be redesigned to be adaptive and in relation to the human's response in a suitable fashion. It can also be observed that, unlike in *HAM research,* human performance is used in *non-HAM research* to represent a human difference instead of a human skill.

As a conclusion for HAM and non-HAM field research, the lack of a rigid foundation for human difference and realization (**Modules 1 and 2)** results in a re-design of strategy and concept for every single man-machine system. So far, however, there has been no generalized platform to take a commonality of human characteristics into account. For this reason, the commonality of human characteristics is the focus of this research and it can potentially underline a common first step for every HAM system implementation. In addition, this thesis does **not** concentrate on the development of **Modules 3 and 4** but, rather, it seeks to make a contribution towards the application and implementation of these two modules. In particular, a rigorous structure of human performance (**Module 1)** and a proposed concept for human performance evaluation (**Module 2)** are the main concerns in this thesis. The ultimate objective aims to provide a widely applicable generalization of a human operator applicable to arbitrary HAM systems.

Figure 2.19 illustrates the summary of man-machine systems literature starting from manual control systems to Human Adaptive Mechatronics (HAM). Figure 2.19 also shows that human skill is the only main characteristic used in HAM and this research is targeted at resolving this to make it more generalised. Now the background about human skill will be discussed and followed by its drawback.

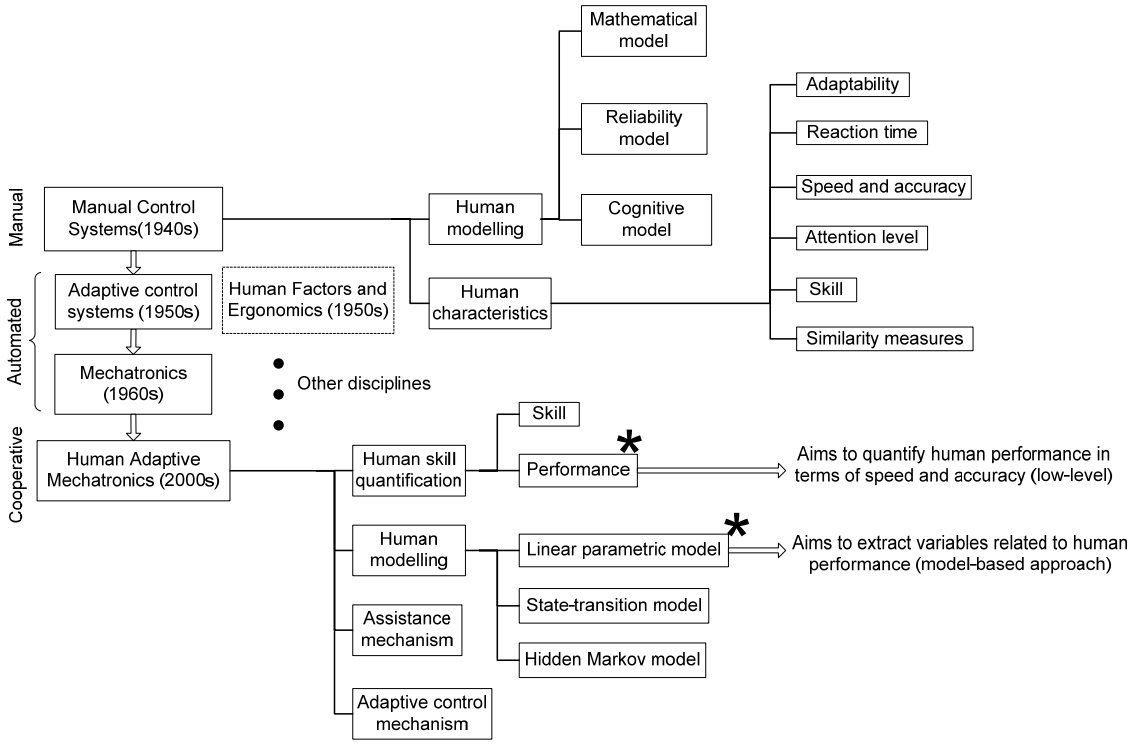

Figure 2.19. Literature review summary [Note: * represents the working areas and objectives of this research]

2.4. Related work on human skill evaluation

In the engineering field, skill is defined as the ability to perform a task with a fast speed, less error and a good problem-solving strategy (Suzuki, Furuta et al., 2005). These characteristics need to be repeatable to confirm its validity. According to the literature, characteristics that contribute to human skill can be classified into attention, similarity measurement and model-based analysis.

2.4.1. Attention

A concept of *minimum attention* for human control actions was introduced and concluded to link strongly to the skill of that individual by Brockett (1997). This seems similar to a term called *intermittency*, as stated by Birmingham and Taylor (1954); Mcruer and Krendel (1962); Mcruer (1980); Iwase, Hatakeyama et al. (2006), which connects to a human's concentration or level of attention to a stimulus. Even though the term *minimum attention* refers loosely to the manner in which the attention is spent on

an ongoing task, this implies an arbitrary fashion. In contrast, the term *intermittency* literally means a periodic alertness to operate and check on an ongoing task. Therefore, these two terms are closely related and can then be used to explain human behaviour once expertise and skill have been obtained in one particular task.

As noted, a human tends to initially have a shorter intermittent period or longer attention on a controlled element. The level of his/her concentration is getting lower as time progresses due to his/her peace of mind and non-erroneous operation. The level of attention is regained once abrupt changes are injected into the system (Mcruer, 1980). This type of human behaviour is also well described as a sudden shift of skill-based behaviour to knowledge-based behaviour in Rasmussen's human cognitive model (see Figure 2.10). Based on this intermittent behaviour, Iwase, Shoshiro et al. (2005) applied the concept to update a human's control strategy in an inverted pendulum system. This intermittent behaviour is represented by the example in Figure 2.20.

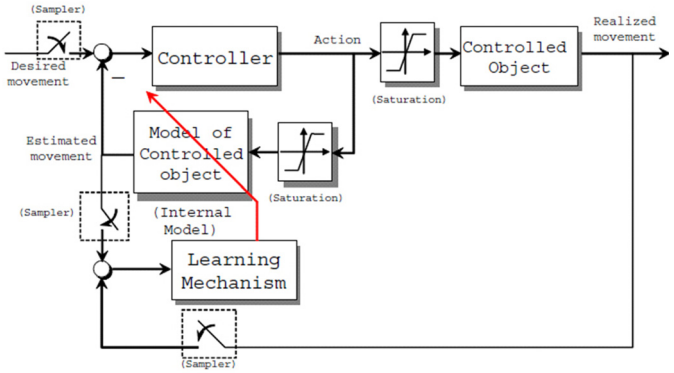

Figure 2.20. Intermittent control action of human (Iwase, Shoshiro et al., 2005)

Suzuki, Watanabe et al. (2007) extended the study on the human gaze to draw an interconnection with human skill. The result of reduced eye fixation, thanks to skill development, was consistent with the decreasing attention and intermittency interval concluded in past researches. Ueno and Uchikawa (2004); Ueno, Manabe et al. (2005) also concluded that there is a connection between an alertness level and eye movement.

As a result of past research, the adaptability of a human interconnects with the attention behaviour in some ways. To be specific, the stimuli that induce the change of the system dynamics cause the change in a human's attention and lead him/her to adaptive actions to maintain system stability.

2.4.2. Similarity measure

A number of researchers proposed the concept of a *similarity measure*, as inspired by expert control behaviours. The objective of this technique is to compare how close a normal human performs with reference to an expert human. Suzuki, Furuta et al. (2005) developed a reference model by using the ARX (AutoRegressive with eXogeneous inputs) technique. Human parameters from the ARX model in the PID controller form are used to calculate an error index with reference to the real expert human.

The similarity measure is based on a probability of observation given the corresponding model (P_1/P_2) as shown in Figure 2.21. The results suggested that a machine with a satisfactory similarity measure could perform closely to the human expert. This implies a skilled action resembling that of the original source of learning.

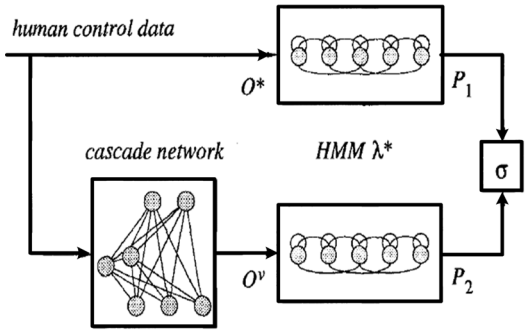

Figure 2.21. Summary of similarity measures using the Hidden Markov Model technique (Nechyba and Xu, 1996).

2.4.3. Model-based analysis

This technique relies on the sequence of a task execution with movement smoothness or dexterity which is regarded as a major characteristic of the human expert. A state-transition model or scenario model can also be used for the analysis. The concept of microslip, from cognitive science, as shown in Figure 2.22, is one example of the difference between a beginner and an expert human action (Suzuki, Tomomatsu et al., 2004). A microslip detection technique, carried out by Takeuchi, Suzuki et al. (2006), allows a jerky action to be spotted which is less probable for an expert human.

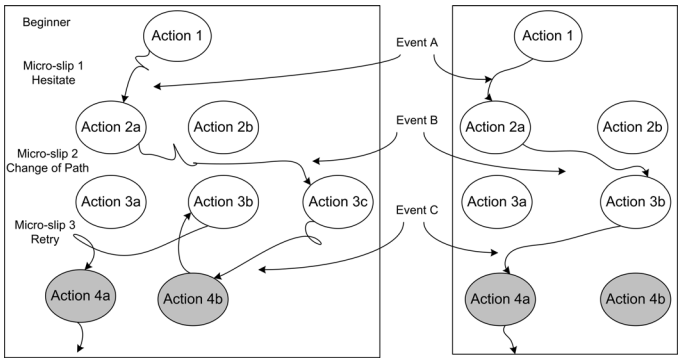

Figure 2.22. Motion flow diagram and microslip of human motion (Suzuki, Tomomatsu et al., 2004)

Another model that can be used to examine human motion is the *state-transition graph* as in Figure 2.23. Lee and Chen (1994) proposed to use this kind of graph to represent human skill, which effectively clusters the feasible state transition regions and interpolates the appropriate state transitions.

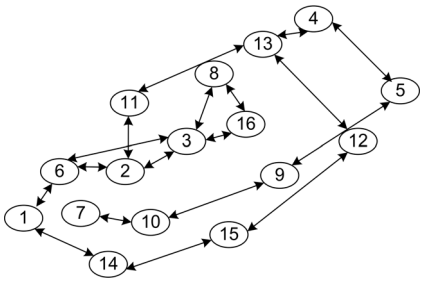

Figure 2.23. Example of a state transition graph for a skilled movement (Lee and Chen, 1994)

This technique is similar to Suzuki, Tomomatsu et al. (2004). For the case of Angel and Bekey (1968), the concept of a finite-state machine was applied. A use of statistical model like Hidden Markov Model (HMM) is also widely researched (Nechyba and Xu, 1995; Nechyba and Xu, 1996; Nechyba and Xu, 1997; Xu, Song et al., 2002; Palmroth, Tervo et al., 2009; Tervo, Palmroth et al., 2010). These are examples of model-based techniques that can be used to evaluate the skill of a human.

Apart from a physical man-machine environment, computer programmers are also keen to design their games at the difficulty level best-suited to players' skills (Hunicke and Chapman, 2004; Yannakakis and Hallam, 2004; Andrade, Ramalho et al., 2005; Hunicke, 2005). Such dynamic difficulty level concept is designed to make a routine check on players' conditions so that the game elements can be adjusted accordingly

depending on the game genres (Spronck, Sprinkhuizen-Kuyper et al., 2004). Due to this nature, the program is written to actually monitor a number of criteria at a fixed cycle to imply human skill rather than a genuine goodness of how the game is played. This consequently makes the concept applicable to only a closed and controlled environment, which may not be pragmatic.

2.5. Skill Versus Performance

Due to the fact that there has been a number of research conducted on the subjects of human skill and human performance, their differences are worth elaborating. The objective is to distinguish their resemblances and point out the directions of this research. According to the Oxford English Dictionary (1989), *performance* is defined as *the quality of execution of such an action, operation, or process* whereas *skill* is defined as *the capability of accomplishing something with precision and certainty*. Literally, skills can be acquired or learnt by practice and in effect, increases the performance. It is apparent that human performance is general and reliant on the output quality whereas human skill is specific to manner of completion. For example, the skill metrics consisting of task efficiency, complexity of the task sequence, ability to plan and make decisions and task difficulty have also been proposed and implemented in mobile machine operations (Hölttä and Koivo, 2009; Palmroth, Tervo et al., 2009; Tervo, Palmroth et al., 2009; Tervo and Koivo, 2010; Tervo, Palmroth et al., 2010).

In addition, all of the human skill evaluation techniques explained earlier are based on a flow of states in an operation and the model has to be trained to represent the skill level of a particular person. This implies that information on a posteriori probability or expert characteristics has to be readily available. Applying this technique to a newly invented or unseen machine system without the existence of a human expert would be a challenging task. Therefore, this is considered as a major drawback of human skill.

On the other hand, the advantage of relying on human performance instead of human skill is that a complacency or negligence in performing a task can be properly treated (Parasuraman, 1997; Parasuraman, Sheridan et al., 2000; Parasuraman, 2008). In other words, the overall productivity is of higher priority than the manner of completion. Therefore, the concept of Human Performance Index (HPI) is proposed based on human performance rather than human skill.

2.6. Summary

This chapter provides a literature review covering the evolution of manual control systems towards Human Machine Mechatronics (HAM) systems including human modelling and characteristics. The nature of the literature found in this field of research is broad and diverse making it totally multi-disciplinary and psychology-related. The depth and breadth of advancements in man-machine systems along with deficiencies suggest that the trend of machine development is more human-centred aiming to avoid overreliance on machines and lose competence in those of skill-demanding operations.

Chapter - 3.

Proposed Concept and Research Methodologies

3.1. Introduction

The literature review chapter covers a variety of disciplines ranging from human science to engineering thereby showing the multi-disciplinary nature of Human Adaptive Mechatronics (HAM) research. This chapter mainly describes a novel concept for human performance computation based on the deficiency identified and discussed in Chapter 2 along with structures and forms of the Human Performance Index (HPI). Information on research methodologies will also be discussed including performance variables and computation approaches.

3.2. Proposed concept overview

A generalized structure of human performance is proposed to represent human difference along with a platform for human realization on the machine's side. A rationale for using a human performance instead of a human skill is according to Rasmussen's model of human performance (Rasmussen, 1983; Rasmussen, 1986; Rasmussen, Pejtersen et al., 1994). Human action on a facing task can be classified, from the lowest to the highest reaction time, as *skill-based*, *rule-based* and *knowledge-based action* (Figure 3.1).

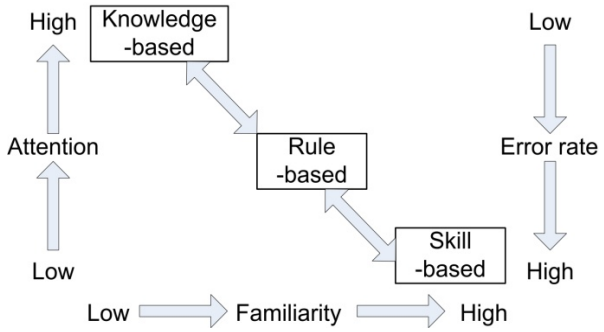

Figure 3.1. A human performance diagram summarized from Rasmussen's model (Rasmussen, 1983; Rasmussen, 1986; Rasmussen, Pejtersen et al., 1994)

A selection of one of these reactions is intuitive and highly dependent on the degree of training. It is not straightforward to determine the source of the reaction, as they are *inseparable, combinational* and *transformable* among one another. A change of working conditions, setup and/or environment turns a reaction by a skill into a rule or a rule into knowledge depending on the degree and manner of that change. Favourable changes can cause the shift in an opposite direction, that is, from knowledge to rule and rule to skill. In many cases, a combination of skill, rule and knowledge is preferable. The key is a *familiarity* with that task, which in turn reflects a level of human attention. *Negligence* arises once a reaction is purely based on a skill. Therefore, a minimum level of attention needs to be retained to minimize the error rate regardless of the skill level.

A key to determine a source of human action is an ability to explain how he/she gets things done. Intuitive and unconscious action involves *skill*, whereas an explicit know-how involves *rules* or logical thinking. A higher level of reaction, which requires a longer reaction time for analysis and critical thinking, is referred to as *knowledge*. There are boundaries between these three elements and they vary from person to person. Training and learning make such boundaries progressively seamless and promote a transformation of knowledge and rule into skill. Namely, the time to access knowledge and rules is remarkably less and equivalent to that of a skill after intensive and continuous training. However, a developed skill is repeatable or consistent if, and only if, the rule and knowledge has been properly formed in the human's brain during the training and learning process.

The point is, human skill is not the only element involved in a complete human performance model or the only element responsible when a human is performing a task. Moreover, skill consistency cannot be guaranteed due to the fact that it dynamically changes with situations and has become intuitive in many cases. That is why a redefinition of human skill is required for all the research done in the past, which can be considered as a deficiency.

With regard to Rasmussen's model, it is interesting to see that it complies with *Kawato's model* (Figure 2.11, cited and used in all Japanese HAM papers) in transforming a feedback to a feedforward response during a learning process. A feedback response can be perceived to be equivalent to knowledge-based and rule-based action. Similar to the case of Rasmussen's model, a degree of the transformation and a weighting on feedback-feedforward action are still inexplicable. This fact confirms the complications involved in trying to pinpoint the root of a human action, as it tends to be combinative of skill, rule and knowledge. Hence, the reason why human skill is non-universal is obvious.

In conclusion, it is hard to distinguish from a human's control action alone whether he/she is relying purely on his/her skill. Human performance, consisting of skill, rule and knowledge, is therefore a real representation of a human's versatility in task accomplishment. This thesis relies on this fact and the concept of using speed and accuracy as criteria for human performance.

3.3. Background

In addition to the fact that human performance covers every aspect of human action and can be varied by negligence (as pointed out earlier), human performance can also be varied by intention and the requirements/constraints imposed by an operation. Personal judgment of such requirements/constraints, either explicitly or implicitly given, results in different control strategies being used to perform the operation. The use of a process

to select a suitable control strategy is described by Higgins (Higgins, Shah et al., 1997) in *Regulatory Focus Theory*. The theory says that there are two types of regulatory focus, which are *promotion* and *prevention*, appearing mentally in both momentary and chronic (permanent) manners. The promotion focus aims at achieving the highest productivity or maximum output whereas the prevention focus aims at achieving the highest precision or minimum error rates. Figure 3.2 gives a list of features for the promotion and prevention foci.

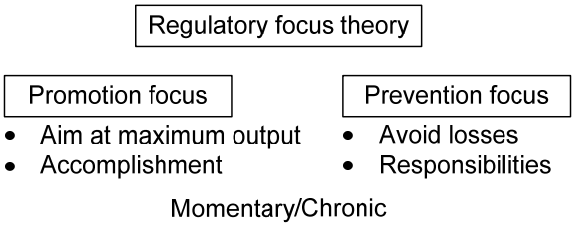

Figure 3.2. Regulatory focus theory (summarized from Higgins, 1997)

In short, the regulatory focus theory claims that a human operator can adjust his/her speed and accuracy characteristics while performing a task to fulfil system requirements. Hence, the use of speed and accuracy characteristics to form a structure of human performance, called the *Human Performance Index (HPI),* is proposed. The speed and accuracy characteristics are effectively a *control strategy* that a human operator selects to use on the facing operation. This thesis aims to quantify and standardize the HPI in terms of speed and accuracy so that it can be applied to arbitrary man-machine systems. Definitions and methodology for calculating the HPI from both computer-based and hardware-based systems using non-model and model-based approaches are the main targets. A structure for the HPI can be found in Figure 3.3.

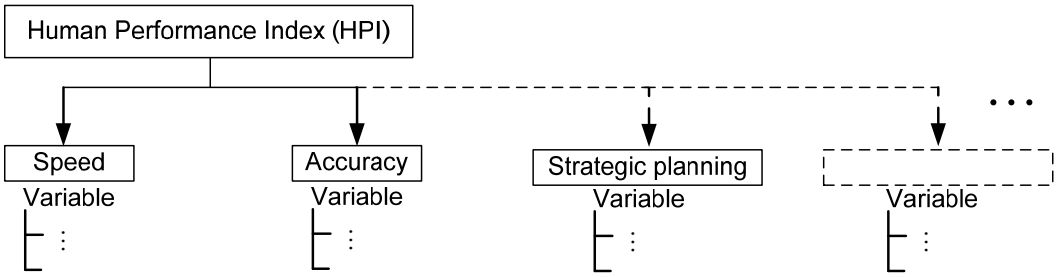

Figure 3.3. Proposed HPI structure containing speed and accuracy variables.

The proposed HPI concept is supported by the validity of the speed-accuracy trade-off based on Fitts' Law (Meyer, Abrams et al., 1988; Meyer, Smith et al., 1990; Förster, Higgins et al., 2003; Zhai, Kong et al., 2004). That is, the linearity of Fitts' law describes one control strategy selected by a human operator to perform a given task. A sacrifice of speed over accuracy and *vice versa* causes a change in his/her control strategy and consequently results in different slopes or different information-processing rates (Chapter 2). Förster, Higgins et al., 2003) also stressed that such a change was due to a control strategy chosen by a human operator for that operation. More importantly, this control strategy was imposed by the system requirements rather than purely by the nature of that particular human operator.

Despite awareness of the speed–accuracy trade-off, it is worth stressing that these implications are considered to exist in various man–machine operations but without rigorous methods for quantification. It is obvious from Fitts' law that only a movement time or speed characteristic is considered. That is, there is no explicit representation of the speed–accuracy relationship. The HPI concept is defined to resolve this issue by quantifying the speed and accuracy characteristics of a human and representing them numerically.

3.4. The Human Performance Index (HPI) concept

A Human Adaptive Mechatronics (HAM) system requires a feature to measure differences between human operators based on their control actions so that a machine can work adaptively without dominating them. To enable the aforementioned characteristics, human performance is proposed as the key to a symmetrical man-machine operation. A mechanism to realise human difference quantitatively and standardise it is the focus of this research featuring a novel structure of human performance called the *Human Performance Index (HPI)*. This concept is in contrast to the conventional idea of using human skill to represent human difference, as pointed out in Chapter 2. Further considerations of performance consistency and complication to define a system-dependent human skill are major concerns. This means that an

evaluation of human performance relies wholly on actual control actions rather than the mastery of the control operation. It is evident from the literature that human skill is inexplicable by nature and not completely transferable (Nechyba and Xu, 1995). A shift of focus to human performance can avoid such complications and consequently reduces error rates and system failures stemming from negligence and the abrupt performance decreases of an individual.

3.4.1. Structure

The HPI is proposed to consist of three levels of hierarchy as shown in Figure 3.4, which is similar to the Quality Index Framework (Hölttä and Koivo, 2009) but with only 2 layers and strictly based on man-machine system environment. HPI is essentially a weighted sum of criteria based on a number of variables that are attributed to a human performance classified as a *performance criterion* and a *performance variable*. The concept of representing a performance criterion based on a characteristic of interest is similar to Xu, Song et al. (2002). The only difference is in representing an overall performance value from a number of performance criteria rather than a single performance value on its own, as shown in Figure 3.5.

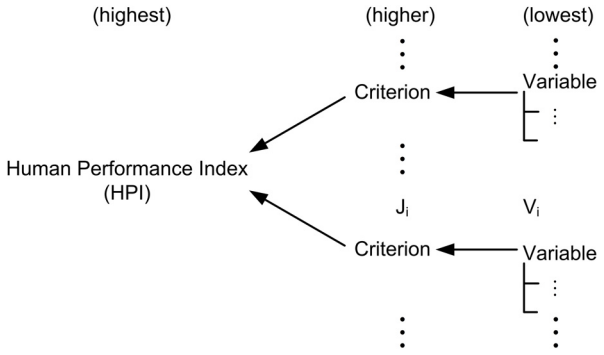

Figure 3.4. A proposed structure of Human Performance Index (HPI) – Lowest to highest hierarchy from right to left.

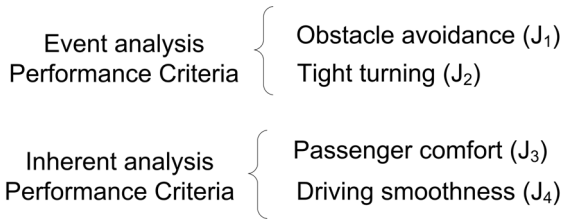

Figure 3.5. Performance criteria from a driving simulation (summarized from Xu, Song et al., 2002)

According to the proposed HPI structure in Figure 3.4, the lowest hierarchy consists of a number of physical quantities or *variables* that contribute to a cumulative quality of a higher hierarchy. The physical quantities classified into the lowest hierarchy are literally contributing factors that share or imply the same characteristic. These contributing factors are defined as *human performance variables* or simply *performance variables*. For the higher hierarchy, a group of physical quantities or *variables* sharing the same characteristic is cumulatively referred to as a *human performance criterion* or simply a *performance criterion*. Each criterion effectively represents a single characteristic of human performance. The weighted sum of these criteria is defined as a *Human Performance Index (HPI)*.

With reference to the proposed HPI structure, the definitions of performance criterion and performance variable are therefore arbitrary depending on the characteristics and the system of interest. A general view of the HPI concept will be given first along with definitions, forms and sample performance variables. To assure a wide applicability of the concept, it is necessary to carefully define and group the common characteristics practically retrieved or extracted from a system of interest. Fortunately, these common characteristics can be classified as speed and accuracy and this will be treated separately in the section that follows the general HPI concept.

3.4.2. Definitions

A *HPI* is proposed to be a *generic performance indicator* based on a sample group that can be visualised as a relative performance value of a human operator. A HPI is defined

to reflect a deviation of an individual human operator from an average human operator by having a HPI value higher or lower than 1. This can be simply done by normalising an HPI value by the average of a sample group of interest. Effectively, a person with a HPI value greater than 1 is considered *above average* whereas one with a value smaller than 1 is considered *below average*. Processing of the performance variables is obviously required prior to a HPI computation to yield this specified numerical meaning and format. Details on this topic will be described under the *Processing the performance variables* section.

Defining the HPI as a relative quantity is advantageous because it offers scalability and reasonableness. With regard to scalability, an expansion of a sample group is always possible and reflective of a wider range on human abilities and characteristics. Similarly, reasonableness implies that a computed HPI is realistic with reference to a sample group. Effectively, the larger and wider the range of a sample group, the less the subjectivity of the computed HPI will turn out to be.

The idea of introducing the concept of relative human performance is a different approach to that of many HAM researchers in that it emphasises intensive training to yield a human expert model from the selected potential human operators. Rather than using a human expert model as a reference, a suitable HPI value derived based on a sample group is proposed as a reference for assistance or adaptive control parameters instead. However, a development of the HPI concept in this thesis aims at forming a common first step for HAM system implementation rather than applying it in coordination with **Modules 3 and 4**. Definitions of performance variable and performance criterion according to Figure 3.4 are as follows:

A performance variable (V_i) is defined as a basic element of a HPI, which is literally a physical quantity extracted from a human operator's control action. Examples for this can be the total time taken for a task completion, the frequency of errors and so on. Performance variables implying the same characteristics can be classified into the same group. The group of these performance variables is defined as a performance criterion

(J_i). Each variable of the same criterion is associated with a performance variable weight (W_v) or degree of significance of the physical quantity it represents. In general, the conditions for equal weights for all variables can be safely assumed. For each performance criterion, its associated performance criterion weight (W_j) can also be safely assumed to be equal to other performance criteria but a variation of performance criterion weight interestingly connects to a human control strategy as will be discussed in a later section. The weighted sum of these performance criteria effectively represents an overall human performance based on a number of performance variables.

In brief, there are two weighted sums involved in a HPI computation, which are the *weighted sum of the performance variables (V_i) and the weighted sum of the performance criteria (J_i). The first weighted sum is defined as a performance criterion score or simply a criterion score and the latter weighted sum is defined as a Human Performance Index (HPI), which are both dimensionless. Basically, a performance criterion score reflects a performance in one particular characteristic whereas a HPI reflects the overall performance of a human operator. Hence a performance criterion score itself can be seen as a variable HPI and a HPI to be a fixed HPI. For simplicity, the term HPI is used instead of a fixed HPI unless otherwise stated. Further details on the forms of HPI are described following this section.* The above definitions can be illustrated as shown in Figure 3.6.

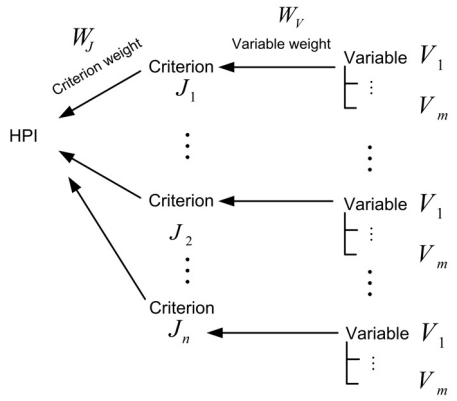

Figure 3.6. Detailed Human Performance Index (HPI) Structure (Note: 'n' = the number of performance criteria and 'm' = the number of performance variables.)

Equations for computing a performance criterion score (J_i) with m number of performance variables and a HPI with n number of performance criteria are as follows.

$$J_i = J_i(V_1, V_2, \ldots, V_k) = \frac{\sum_{k=1}^{m} W_{V_k} \bullet V_k}{\sum_{k=1}^{m} W_{V_k}} \tag{3-1}$$

$$HPI = HPI(J_1, J_2, \ldots, J_n) = \frac{\sum_{i=1}^{n} W_{J_i} \bullet J_i}{\sum_{i=1}^{n} W_{J_i}} \tag{3-2}$$

For the case of *equal significance* for the performance variables and performance criteria, the conditions of equal performance criterion weights ($W_{V1} = W_{V2} = \ldots = W_{Vm} = W_V$) and equal performance variable weights ($W_{J1} = W_{J2} = \ldots = W_{Jn} = W_J$) apply respectively. The values of W_V and W_J can be simply calculated by *1/m* and *1/n* respectively ($\sum W_V = \sum W_J = 1$). Equation (3-1) and (3-2) can then be simplified and expressed in the following forms.

$$J_i = J_i(V_1, V_2, \ldots, V_k) = \frac{1}{n} \bullet \sum_{k=1}^{m} V_K \tag{3-3}$$

$$HPI = HPI(J_1, J_2, \ldots, J_n) = \frac{1}{m} \bullet \sum_{i=1}^{n} J_i \tag{3-4}$$

Considering the conditions used for a HPI computation in this thesis, only equal significance for all performance variables or an equal variable weight (W_V) condition is assumed. A consideration to draw a connection between a human control strategy and his/her performance criterion weight is one of the main contributions of this research. A control strategy used in task completion or the operation of interest is to be proved to link strongly to a human performance.

To illustrate possible physical quantities contributing to a performance level of a human operator as defined above, an example of an HPI structure is presented in Figure 3.7.

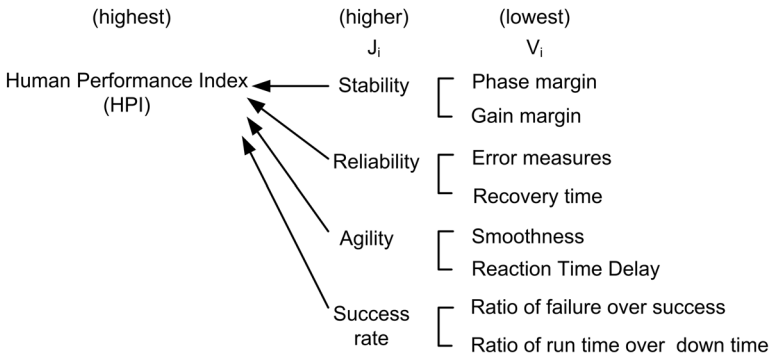

Figure 3.7. Human Performance Index (HPI) structure example.

With reference to Figure 3.7, stability, reliability, agility and success rate are chosen as examples of performance criteria in a man-machine system. Performance variables presented in Figure 3.7 under a corresponding performance criterion are also provided as an example. It is obvious that a stability criterion is an important parameter for control engineering, whereas other criteria are arbitrarily selected. These performance criteria can be calculated either directly from a human operator's control action or from a derived model, depending on the physical quantity of interest. Further explanation will be provided in a later section along with the processing of the performance variables to yield a ready format for HPI computation.

In summary, a HPI is a weighted sum of the performance criteria, whose particular performance criterion score is a weighted sum of the performance variables. A HPI can also be viewed as a *relative performance level* based on a sample group. Section 3.4.3 introduces two forms of HPI along with the definitions and usage of each form.

3.4.3. Forms of the Human Performance Index (HPI)

In order to use a HPI as a performance indicator, two forms of HPI are proposed for use in two different conditions. These conditions are based on the availability of the application requirements for particular human characteristics (effectively, the performance criterion weights (W_j)). The application requirements can serve as human factor requirements for a particular application. A suggestion about such requirements is

one of the main parts of this research and will be treated in the analysis. A HPI structure containing both variable and fixed HPI can be found in Figure 3.8.

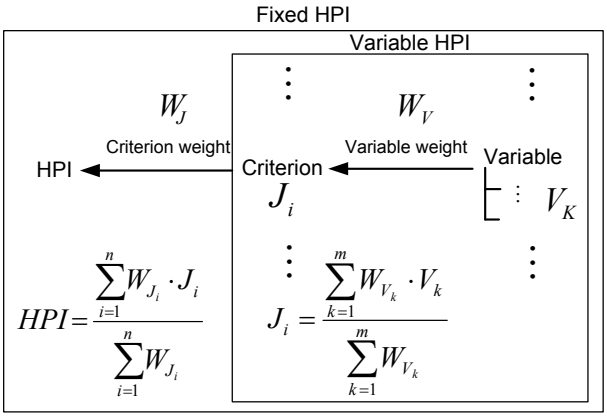

Figure 3.8. Human Performance Index (HPI) forms with reference to a full HPI structure in Figure 3.6.

3.4.3.1. Variable HPI

A *variable HPI* is a raw HPI consisting of only a set of performance criterion scores (J_i) based on each criterion. This form of HPI represents only one particular human characteristic and is open for multiplication with a corresponding performance criterion weight. As mentioned in the previous section, a variable HPI can be expressed as shown in Equation (3-4), which is effectively an individual performance criterion score. This variable HPI represents goodness on one particular performance criterion or a particular *J*.

Examples of a variable HPI, with reference to the HPI structure example in Figure 3.7, are stability score, reliability score, agility score and success rate score. With regard to the meaning of a variable HPI, it can be ambiguous, especially in cases where selected performance criteria are closely related to one another. A contribution of one performance criterion might overlap with other performance criteria. Therefore, a careful selection of performance criteria is crucial to preserve the generality of the HPI. That is, the performance criteria of interest should be as application-independent as possible. In this thesis, only two performance criteria are selected, which are the *speed*

criterion and the *accuracy criterion*. The definitions and usage of these two performance criteria will be described in a separate section. From the application point of view, the variable HPI serves as a performance indicator of a human operator in one particular characteristic. This can then be useful in a system design process to optimize a man-machine system performance affected by specific characteristics of a human operator.

3.4.3.2. Fixed HPI

A *fixed HPI* or simply an HPI is a summation of the product of all performance criterion scores and their associated performance criterion weightings. A fixed HPI literally reflects an overall human performance level. Considering a difference between a variable HPI and fixed HPI as an analogy to a Grade Point Average (GPA) grading system ensures a meaning of the HPI concept as follows.

In essence, a *variable HPI* can be viewed as a *grade* received upon an assessment of one particular subject among several enrolled subjects whereas a *fixed HPI* can be viewed as a *GPA*. The grade for each subject is based on coursework designed in line with the subject's objectives and deliverables. The performance for each assigned item of coursework is evaluated and used as part of an overall assessment for the associated subject. Each coursework item can then be regarded as a *performance variable* and the mark allocation for each coursework item can be regarded as a *performance variable weight*. For a number of enrolled subjects, the *credit hour* for each subject (the weight for each subject) is equivalent to a *performance criterion weight* (W_j) in a HPI computation. The analogy between HPI and GPA is as illustrated in Figure 3.9.

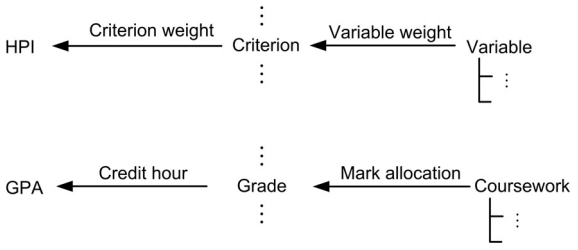

Figure 3.9. Analogy between HPI (Human Performance Index) and GPA (Grade Point Average)

Despite a clear similarity in representing an overall human performance in a form of HPI and GPA, there is a difference in the processing of the monotonicity of the performance variables. The main purpose is to make the performance variables compliant with the proposed definitions. That is, the HPI value higher than an integer value of one is generally regarded as a human operator with a *higher than average* performance whereas the HPI value lower than one means a lower than average performance. This is, in fact, the monotonicity characteristic of the performance variables. To deal with a mixture of performance variables with different monotonicity characteristics, extra processing is required for all performance variables and this will be described in a later section.

In terms of interpretation and usage, different man-machine system/applications are hypothesized to require different human performance levels for an efficient and safe operation. It is assumed that one particular man-machine system comprises one set of the *performance criterion weights* and this set varies from system to system. Such a performance criterion weight reflects the significance level of the corresponding performance criterion appropriate for the operation of interest. A set of performance criterion weights is proposed to be effectively used as *human factor requirements*, as part of man-machine system requirements. A human operator with a higher HPI value means he/she can *potentially* operate that man-machine system closer to the requirements. The word *potentially* is used to indicate a full motivation state at the experiment time being as close as possible to the trial runs during a HPI computation stage.

A *fixed HPI* is suitable for representing an overall performance level with particular man-machine system requirements. It is clear from the definition that a fixed HPI is meaningful only when the information on a variable HPI is available. Namely, details of performance criterion scores and associated weights are required to compute an overall performance level for a human operator.

Considering the benefits of the forms of HPI, a variable HPI can be useful for a system designer to consider critical human characteristics whereas a fixed HPI can be useful for a system auditor to design a fail-safe working environment. Overall, a variable HPI serves as the design metrics for a system designer that can be effectively used as parameters for an adaptive mechanism of a HAM system. For a fixed HPI, it is defined to target a holistic human performance. Figure 3.10 summarizes these two forms of HPI with suggested uses.

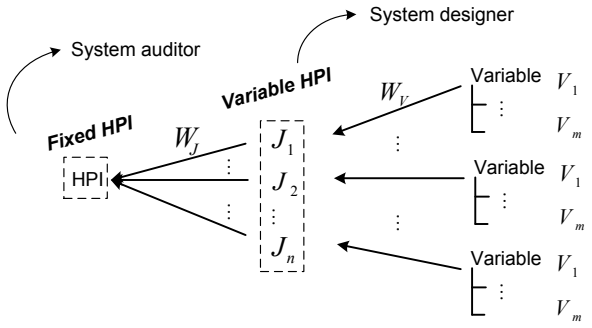

Figure 3.10. Human Performance Index (HPI) forms summary.

3.4.4. HPI based on only speed and accuracy criteria

In the previous sections, the definitions and structure of the Human Performance Index (HPI) concept were described in general alongside a sample structure and the forms of HPI. It is now worth taking a closer look into the sample structure presented in Figure 3.7 and considers a classification of the performance variables. In theory, excessive performance criteria can make a HPI structure system-specific and redundant, which is opposed to the HPI concept initially proposed, which was to be as generalized as possible. These redundant performance variables can lead to an over-emphasis on only one particular human characteristic or an overlap with other performance variables. However, a number of characteristics are always correlated and have effects on the others.

Regarding Figure 3.11, the diagram is based on Figure 3.10 that presents an example of an HPI structure containing stability, reliability, agility and success performance as the performance criteria. These performance criteria simply contain performance variables

with common characteristics that can effectively be classified into only two groups, which are speed and accuracy. A rationale for this is a tendency to decrease a speed in exchange for an increase in accuracy and *vice versa*, which accords with Fitts' Law (Fitts and Peterson, 1964). Even though Fitts' law was derived from hand movements in tapping a stylus between spaced plates, it is still well applicable to the case of hand movement on a computer mouse as pointed out in Scott MacKenzie (1992); Scott MacKenzie and Buxton (1992); Accot and Zhai, (1997). Moreover, the validity of a speed-accuracy trade off has been concluded in recent researches in experimental psychology (Förster, Higgins et al., 2003) and Human-Computer Interaction (HCI) fields (Zhai, Kong et al., 2004). Further details are as provided in Chapters 2. Hence, the HPI structure is then proposed to comprise only the speed accuracy criteria. A concise version of the HPI structure is as presented in the following figure.

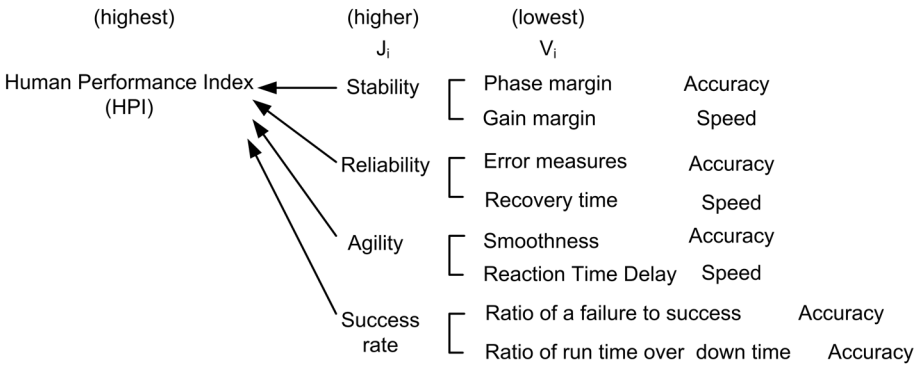

Figure 3.11. Human Performance Index (HPI) variables classified as either speed or accuracy

The detailed structure of HPI shown in Figure 3.6 can be simplified into Figure 3.12 with only two performance criteria (n=2). Performance variables for a speed criterion and accuracy criterion are arbitrarily chosen with a main concern being their generality. With speed and accuracy chosen to be the performance criteria of a HPI, a performance criterion score can be referred to as a *speed score* and *accuracy score* respectively. A numerical value of the speed score reflects the goodness of the *time-efficiency characteristics* whereas a numerical value of the accuracy score reflects the goodness of the *error-related characteristics*. Due to the fact that the focus of this thesis is on only two performance criteria, the relationship between the respective weights of these two performance criteria can therefore be easily viewed as a *ratio*. The ratio of the speed

criterion weight and the accuracy criterion weight is then referred to as the *speed-accuracy ratio.* Variation of this speed-accuracy ratio results in different HPI values and a degree of variation can, interestingly, lead to a degree of sophistication for a selected control strategy.

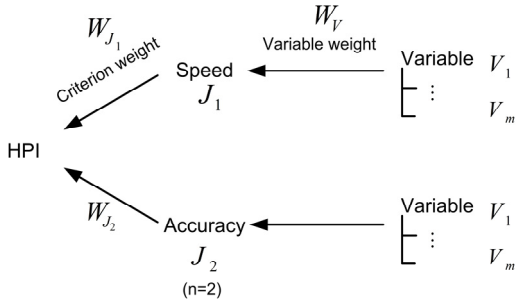

Figure 3.12. Human Performance Index (HPI) structure with only speed and accuracy criteria (J_1 and J_2 respectively)

From this aspect, a maximum HPI value resulting from a set of performance criterion weights connects to a human's *control strategy* used in completing an operation. The speed-accuracy ratio is therefore as equally important as the HPI value and needs to be defined accordingly.

3.5. Research Methodologies

3.5.1. Overview

With emphasis to create fundamentals for evaluating human performance, the methods used to serve this purpose consist of several elements to ensure validity and versatility of the concept. The first quality, *validity*, is to be achieved by applying two computation approaches to the experimental data collected from the operating field. The agreement of results from these two approaches suggests a validity of human control strategy based on speed and accuracy. The second quality, *versatility*, is to be achieved by using two sets of experimental setups containing and not containing hardware elements. The latter system is considered a second step to the computer-based system having more

complicated dynamics and interaction with physical elements. Interestingly, this does not only make it more difficult to operate but also serves as a real mechatronic system.

Experimental work on this thesis is based on computer-based and hardware-based man-machine systems. Computer-based experiments are designed to illustrate the existence of speed and accuracy characteristics for each human operator whereas the hardware-based experiments are targeted at applying the HPI concept in a real man-machine system. A point-to-point tracking, in which a human operator is asked to aim at a set of positions one-by-one in a two-dimensional domain, is selected for both computer-based and hardware-based systems. The manner of operation differs for the case of the hardware-based system.

For a computer-based system, a computer mouse is used to aim at a set of red circles displayed on a computer screen using a program written in MATrix LABoratory (MATLAB) programming language. For simplicity, this operation will be referred to as a *simple tracking task*. A real-time logging is written as a .m function to save useful program variables for every human subject for an offline HPI analysis. For a hardware-based system, a helicopter test rig is used with a joystick as a control device. The task is to move a metal bar to a set of horizontal angles one-by-one with the bar as horizontal as possible. The program for the helicopter test rig operation is written in Microsoft Visual Basic (VB) language. Similar to the simple tracking task, real-time logging is required for an offline analysis using MATLAB. Further detail on both systems will be explained in Chapter 4.

Research methodologies cover performance variables treatment, HPI computation approaches and important parameters used in computing goodness of performance values match between the two approaches.

3.5.2. Performance variables treatment

In order to comply with the definitions given in Section 3.4.2, an average-based method for HPI computation is proposed. An average value of the performance variables is used as a normalization factor instead of a maximum value, unlike the original definition of normalization. Resulting variables are therefore greater than, equal to or less than the average value. That is, these variables are now centred around the average value, hence the name of the proposed method. This consequently allows an enlargement of sample group making the concept scalable and less subjective.

An overview of how the average-based HPI computation method links to the HPI structure is presented in Figure 3.13. Note that the performance variable processing is applied to the data logged from a system output and control variables. This logged data is used as a source to extract raw performance variables.

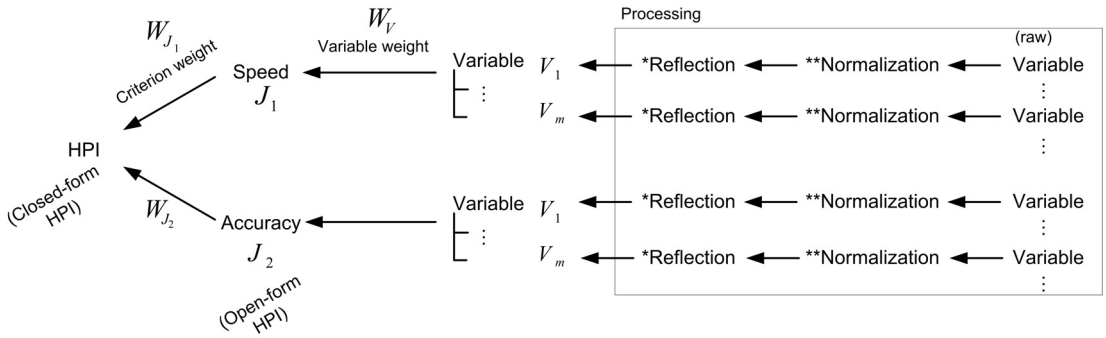

Figure 3.13. Average-based Human Performance Index (HPI) computation overview (Note: * denotes a reflection operation, ** denotes a normalisation by an average value)

With reference to Figure 3.12, the main processing blocks for raw performance variables, respectively called normalization and reflection, are added (labelled as *processing* in Figure 3.13). This is simply the processing of logged data to obtain a value appropriate for computing performance criterion scores V_1 and V_2. By referring to an appropriate format, V_1 and V_2 need to have a common monotonicity. In other words, a magnitude interpretation of V_1 and V_2 has to be consistent and therefore, appropriate

processing is required to achieve this. That is, to make these performance variables monotonically consistent.

3.5.2.1. Monotonicity of the performance variables

In order for performance variables to be monotonically consistent, the monotonicity of each performance variable has to comply with the monotonicity of the HPI. A monotonic function is mathematically defined as a *strictly increasing* (monotonically increasing) or *decreasing function* (monotonically decreasing), whose value either increases or decreases as the magnitude of an independent variable increases respectively (Pemberton and Rau, 2007). Figure 3.14 (a) and (b) show what it is meant by monotonicity in a mathematical context.

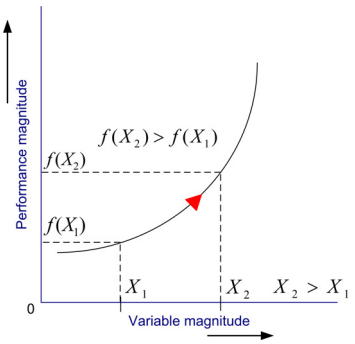

(a) Strictly increasing function

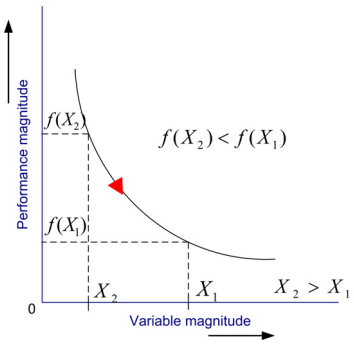

(b) Strictly decreasing function

Figure 3.14. Monotonic functions.

Respective conditions for a strictly increasing function and strictly decreasing function are as follows.

$$f(x_2) > f(x_1), \text{if } x_2 > x_1 \tag{3-5}$$

$$f(x_2) < f(x_1), \text{if } x_2 > x_1 \tag{3-6}$$

Monotonicity, or magnitude interpretation, is the main issue for HPI computation, as the performance variables may not have a common monotonicity. If these performance variables do not have a common monotonicity, the resulting HPI value is not considered to be reflective of an actual performance level. That is, strictly increasing performance

variables are mixed up with strictly decreasing performance variables causing unwanted compensation in the weighting.

An increment with a magnitude of one performance variable does not necessarily mean a higher performance level as a decrement may mean a higher performance level depending on the monotonicity of that performance variable. This means, a higher value of one performance variable can be interpreted as a higher performance level whereas a higher value of another performance variable can mean a lower performance level and *vice versa*. Therefore, a consideration of the monotonicity of these performance variables is vital and needs to be treated correctly.

The HPI itself, by definition, is a strictly increasing function. This means the greater the value, the higher the performance level. Every performance variable is therefore required to be strictly increasing to comply with the HPI value, which may require an extra processing of the strictly decreasing performance variables. The extra processing, called *reflection*, is required to convert strictly decreasing performance variables to strictly increasing performance variables without changing the meaning. The next section describes the performance variable processing in further detail.

3.5.2.2. Processing of the performance variables

According to the HPI definition in Section 3.4.2, an average normalization process is required for both strictly increasing and decreasing performance variables whereas a reflection process is required only for the strictly decreasing performance variables. The first step is to apply an average normalization and determine its monotonicity by referring to Equations (3-5) and (3-6). An interpretation of the incremented and decremented magnitude of the performance variable of interest in relation to the change of a performance level is the key for determining its monotonicity.

If the performance variable is strictly increasing, no further processing is required whereas if the performance variable is strictly decreasing, a reflection process is required to make it strictly increasing. This processing effectively converts a strictly decreasing performance variable into a strictly increasing performance variable while retaining its original meaning. A summary of the processing of the performance variables can be found in Figure 3.15.

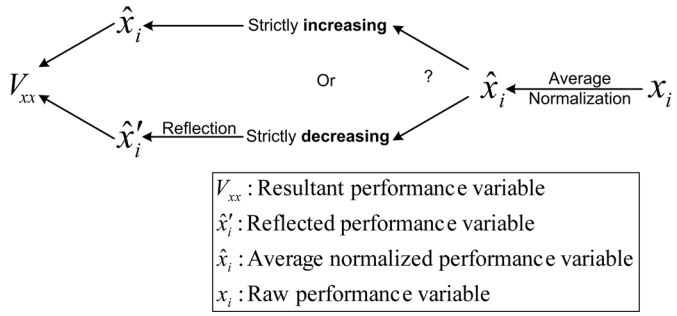

Figure 3.15. Processing of a raw performance variable (as shown in the processing block, Figure 3.14)

Detailed processing of the raw performance variables is as follows.

- *Average normalization*

An average normalization process is applied to all performance variables regardless of their monotonicity. Given $x_1, x_2 \ldots x_i \ldots x_N$ as a series of raw performance variables logged from *N* human operators in a sample group, i represents an i[th] human operator.

An average value and average normalized value of the performance variables are denoted as $\bar{x}$ and $\hat{x}_i$ respectively. Equation (3-7) shows an average normalization or normalization by an average value *of* x_i ($\bar{x}$). Equation (3-8) is based on a definition of average value and will be used thereafter.

$$\hat{x}_i = \frac{x_i}{\bar{x}} \tag{3-7}$$

$$Where \quad \bar{x} = \frac{\sum_{i=1}^{N} x_i}{N}$$

$$\sum_{i=1}^{N} x_i = \bar{x} \cdot N \tag{3-8}$$

Regarding the statistical properties of the performance variables after average normalization, the average and variance value of that performance variable are changed by this process. The average of the average normalized performance variable has become an integer value of one and the variance has been scaled by the average value squared. This means that the average normalized performance variables are now centred around 1, as required by the definition. A proof for the calculation of an average and variance of the average normalized performance variable is as follows.

With reference to the normalized performance variable given in Equation (3-7), the average value of $\hat{x}$ (denoted as $\bar{\hat{x}}$) can be calculated as follows.

$$\bar{\hat{x}} = \frac{\sum_{i=1}^{N} \hat{x}}{N} = \frac{\sum_{i=1}^{N} \frac{x_i}{\bar{x}}}{N} = \frac{\frac{1}{\bar{x}} \cdot \sum_{i=1}^{N} x_i}{N} \tag{3-9}$$

Substituting $\sum_{i=1}^{N} x_i$ from Equation (3-8) into Equation (3-9) results in an average value of the normalized performance variable being an integer of one ($\bar{\hat{x}} = 1$).

For a variance, a definition is as shown in Equation (3-10).

$$VAR_x = SD_x^2 = \sum_{i=1}^{N} \frac{(x_i - \bar{x})^2}{N} \tag{3-10}$$

To calculate the variance for an average normalized performance variable ($\hat{x}_i$), a raw performance variable (x_i) and its average value ($\bar{x}$) in Equation (3-10) are replaced by $\hat{x}_i$ and $\bar{\hat{x}}$ respectively. The variance of the average normalized performance variable can then be calculated as:

$$VAR_{\hat{x}} = \sum_{i=1}^{N} \frac{(\hat{x}_i - \bar{\hat{x}})^2}{N} = \sum_{i=1}^{N} \frac{(\frac{x_i}{\bar{x}} - \bar{\hat{x}})^2}{N} \tag{3-11}$$

Knowing that the average value of the average normalized performance variable is an integer of one ($\bar{\hat{x}} = 1$) leads Equation (3-11) to:

$$VAR_{\hat{x}} = \frac{VAR_x}{\bar{x}^2} \tag{3-12}$$

According to Equation (3-12), the variance of $\hat{x}$ equals the old variance over $\bar{x}$ squared. Now, an average normalized performance variable resulting from average normalization can be used for the HPI computation if that performance variable is of the strictly increasing type. However, a strictly decreasing performance variable needs a reflection process to convert it to a suitable form for HPI computation. Figure 3.16 presents a summary of the variables involved in the average normalization process together with statistical properties.

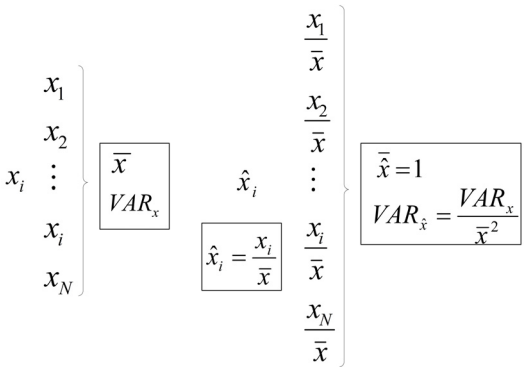

Figure 3.16. A summary of the statistical properties of raw performance variables and average normalization performance variables.

- *Reflection*

As mentioned in the previous section, a reflection is a process required for only a strictly decreasing performance variable. This is due to its interpretation as decay in performance level as a performance variable value grows.

According to Coxeter and Greitzer (1967), a reflection is defined as an operation to translate a point on one side to the opposite side of a mirror or an axis of reflection by preserving its distance. This translation results in an image point or reflected version of the original point, as depicted in Figure 3.17.

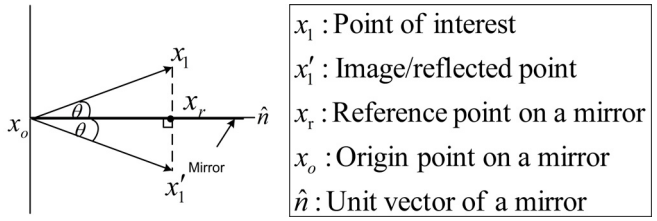

Figure 3.17. A reflection from point x_1 to point x_1' with reference to a mirror (2009)

Based on the above figure, the projection of a vector x_1 onto a mirror axis x_r can be mathematically expressed as Equation (3-13) (Coxeter and Greitzer, 1967; 2009).

$$proj_{x_r} x_1 = \left|\vec{x}_1\right| \cdot \cos\theta \cdot \frac{\vec{x}_r}{\left|\vec{x}_r\right|} \tag{3-13}$$

$$x_r = x_o + \hat{n}[(x_1 - x_o) \cdot \hat{n}] \quad \text{where} \quad \hat{n} = \frac{\vec{x}_r}{\left|\vec{x}_r\right|} \text{ is a unit vecto r of x}_r \tag{3-14}$$

Note that the resultant projected vector x_r equals zero when the angle between the mirror and the point of interest is $90°$.

The following equation is a property of the mirror where the point x_r on the mirror is equidistant from the point of interest x_1 and its image.

$$x_r = \frac{x_1 + x_1'}{2} \tag{3-15}$$

After arranging Equation (3-14) by a mirror property as in Equation (3-15), a reflected point (x_1') can then be calculated as follows.

$$x_1' = -x_1 + 2x_0 + 2\hat{n} \cdot (x_1 - x_o) \cdot \hat{n} \tag{3-16}$$

$$x_1' = -x_1 + 2x_0 + 2 \cdot proj_{x_r} x_1 \tag{3-17}$$

For simplicity, a reflection condition of $\theta = 90°$ is assumed and shifts the original point x_1 onto a vertical axis. This condition causes a projection term in Equation (3-17) to disappear and this can be depicted as shown in Figure 3.18.

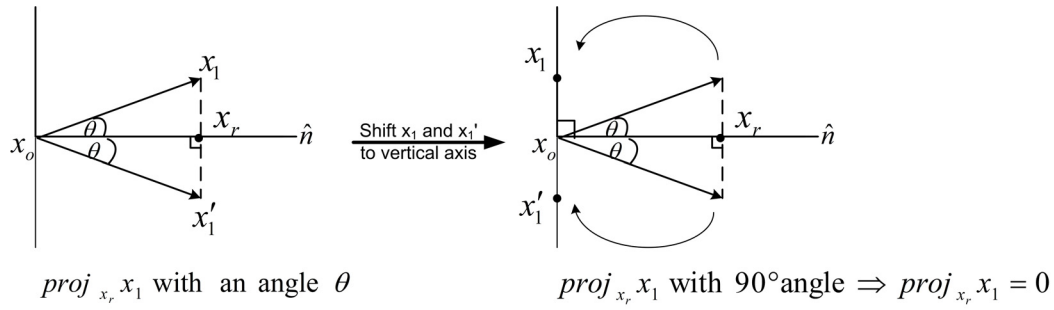

Figure 3.18. Reflection process on a strictly decreasing variable

Equation (3-17) is finally reduced to

$$x_1' = -x_1 + 2x_0 \tag{3-18}$$

To apply reflection in a HPI context, the variables x_o, x_1 and x_1' will now be replaced by $\bar{\hat{x}}$, $\hat{x}$ and $\hat{x}'$ respectively. A relationship of a reflected version of the average normalized performance variable can then be expressed as the following:

$$\hat{x}' = -\hat{x} + 2 \cdot \bar{\hat{x}} \tag{3-19}$$

Where

$\hat{x}'$ is a reflected version of the average normalized performance variable (x_{refl}).

$\hat{x}$ is an average normalized performance variable (x_{avg}).

$\bar{\hat{x}}$ is an average value of the average normalized performance variable ($x_{avg\text{-}norm}$).

Due to a property of reflection, a point of interest retains its distance from a mirror resulting in the magnitude of that point being preserved, as shown in Figure 3.17. This implies that a reflection process effectively performs a reverse monotonicity of a strictly decreasing average performance variable by making a larger value of that performance variable have a smaller performance value and *vice versa*. As a result, all strictly decreasing performance variables are now strictly increasing and are in a suitable form for HPI computation with their original interpretations preserved.

In conclusion, raw performance variables used in this proposed average-based HPI computation method are based on the data collected from experiments conducted on a sample group. The average value of the raw performance variables is used as a normalization factor. Following the average normalization process, strictly decreasing performance variables are processed further by a reflection operation whereas those of strictly increasing variables can be used directly for HPI computation. By the end of the processing, all performance variables are then strictly increasing and average normalized.

3.5.3. HPI computation approaches

In order to retrieve raw performance variables mentioned earlier, two methods are proposed to serve this purpose. HPI computation approaches are designed to prove the HPI concept rather than testing its statistical significance. This, therefore, scopes the research down to only a small sample group. According to the outline, two techniques to compute the HPI are proposed, namely the non-model and model-based approaches.

In general, both approaches rely on a logging of man-machine system output, computing a HPI based on performance variables classified into a speed criterion and an accuracy criterion (non-model approach), validation of a computed HPI with a model derived by system identification theory (model-based approach). Comparison and remarks on applying a HPI concept on both computer-based and hardware-based man-machine systems are to be drawn for these two systems. With regard to the way of retrieving and extracting human performance variables from a system output, two approaches are proposed in this thesis, which are the non-model and model-based approaches with further details as follows.

3.5.3.1. Non-model approach

A non-model approach, as the name implies, is proposed to directly operate on the logged data, retrieve raw performance variables, process these performance variables and compute a HPI. The only resource for HPI computation is the logged or experimental data, which serves as a direct performance measurement. This approach is therefore straightforward and requires no mathematical equations of any form. However, a real-time logging feature needs to be carefully designed when a computer program is written. MATLAB® and Microsoft® Visual Basic are used for computer-based and hardware-based man-machine systems respectively. A real-time sampling behavior to enable data logging differs from language-to-language and it is very important to deal with this accordingly. This part of a computer code complements the primary operation of the program.

Regarding the computation of the performance variables and HPI, the focus is upon the performance variables defined and classified as the speed criterion and the accuracy criterion. For the non-model approach, the comparison of their values between Trials 1 and 2 is presented but the real concern of this research is the comparison between non-model and model-based approaches (referred to as the trial-level (Step 1) and approach-level (Step 2) comparisons respectively, see Section 3.5.4. for explanations). It is straightforward to do a direct analysis on raw experimental data using a non-model approach because it is according to the way the performance variables are defined. On the contrary, extracting the quality represented by these variables from human mathematical models raises the issue about the goodness of match. Therefore, the approach-level comparison on each and every candidate variable is the key depending on the nature of the performance criterion of interest. This will become clearer when the definitions for speed and accuracy criteria are fully covered in Section 5.4, Chapter 5. From this perspective, the fact that no mathematical functions are required for HPI computation obviously makes the non-model approach less computationally complex compared to a model-based approach.

3.5.3.2. Model-based approach

For the second approach, it is proposed to primarily validate a result from the non-model approach and at the same time, to offer an alternative for HPI computation. Performance variables of interest are to be drawn from the resultant human mathematical model, which is derived by system identification theory. Under circumstances that a system is not easily modelled or having adaptive characteristics, this technique is preferable. The objective is to derive system parameters based on a set of data measured from the field of operation (Ljung, 1999). As originally pointed out by Tustin (1947), a human usually acts as a servomechanism in man-machine systems to reduce errors during the operation. The human literally acts as a controller and adjusts his/her response according to the magnitude of errors. From a control engineering aspect, human can also be regarded as a lead/lag compensator (Mcruer and Krendel, 1959; Mcruer and Krendel, 1959) or PID controller (Ragazzini, 1948 via Suzuki, Kurihara et al., 2006).

In addition, the values of each parameter or even the structure vary with test conditions from trial to trial regardless of human subjects. It is also suggested that human operator in a *Point-To-Point* task or a target tracking operation can be represented as a Proportional Derivative (PD) controller, which suffices for describing skill and expertise of that human operator (Suzuki, Furuta et al., 2005; Suzuki and Harashima, 2005; Suzuki, Harashima et al., 2005; Suzuki, Kurihara et al., 2005; Suzuki and Harashima, 2006; Suzuki, Kurihara et al., 2006). The assumption of relatively small time interval used between targets or a time spent on each segment is made so that a control action can be regarded constant in that interval (Suzuki, Kurihara et al., 2006).

In order to apply system identification theory, the MATLAB® toolbox is used and the process needs to be done iteratively to obtain the best-described model. It is therefore apparent from this fact that a model-based approach is more computationally complex and requires more resources for HPI computation. Despite this complication, a human

parametric model allows a simulation and prediction of the system output. A summary for both non-model and model-based approaches can be found in Figure 3.19.

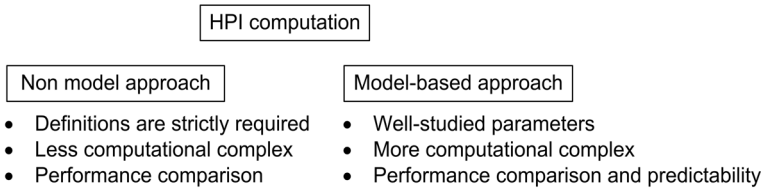

Figure 3.19. Features of the proposed Human Performance Index (HPI) computation approaches

With regard to applying the model-based approach, a segment connecting between target positions is used as a source for computing human ARX models (full details on the target sequence will be given in Sections 4.3.2 and 4.4.2, Chapter 4). Differences in system characteristics cause two major concerns on data processing and axes of motion for each segment (The first issue will be covered in Section 6.3.2, Chapter 6). The second issue is directly related to the modelling of human as two single-input single-output (SISO) systems. Even though the simulations confirm that this method is reasonable for the computer-based system, it is not the case for the hardware-based system. The reason for this is a failure to satisfy the *persistently exciting* condition of an input based on his/her vertical motions and the observations on lack of control actions. To fulfill the requirements of an output trajectory for computing accuracy characteristics, a fixed pitch-axis model is used instead (full details and proof will be presented in Sections 6.4.1.2)

3.5.4. Important parameters

Following the performance variables obtained from both the non-model and the model-based approaches, the next step is to determine goodness of these values. The aim is to compare the results from these two approaches and examine their agreement. Apart from ensuring a validity of the HPI concept, two trials on computer-based and hardware-based systems are conducted to examine consistency and reliability of human performance. This section covers only important parameters pertinent to such quality on both trial-level (results from Trials 1 and 2) and approach-level basis (results from non-

model and model-based approaches). A full analysis concerning patterns of motion and considerations on specific experimental setups dedicated for non-model and model-based approaches will be presented in Chapters 5 and 6 respectively.

Regarding the comparison basis, it is very important to stress that only a trial-level comparison on performance variables obtained by that of non-model approach is presented in this thesis. This is because the main objective is to compare the results from two approaches. Figure 3.20 illustrates what it means by this results comparison scheme.

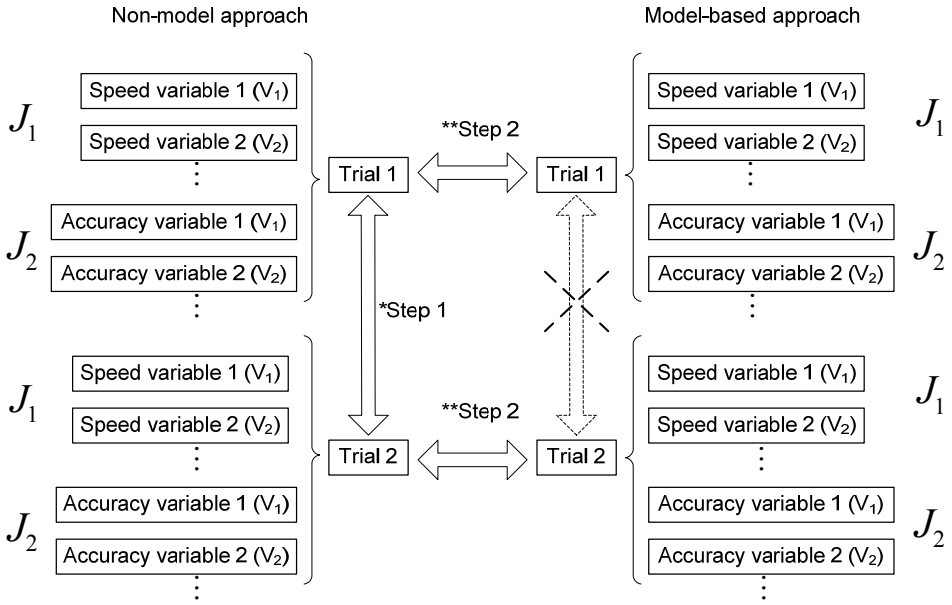

Figure 3.20. Results comparison diagram based on one human operator [Note: * and ** refer to the trial-level and approach-level comparisons respectively]

According to Figure 3.20, there are two sets of variables involved in this comparison scheme, which are performance variables (*V*) and performance criteria (*J*). V_1, V_2 ... V_m represents performance variables 1 up to m along with J_1, J_2 ... J_n for performance criterion 1 up to n. The performance criteria will be used for comparison in Step 1 whereas the performance variables will be used in Step 2. As pointed out earlier, the values for m and n are restricted to only 2 and that means J_1 and J_2 can simply refer to speed score and accuracy score respectively. The **trial-level calculations** or Step 1 comparison according to Figure 3.20 based on the results from that of non-model approach involves the following variables.

$$Average\ speed\ score:\ J_{1av} = \frac{\sum_{i=1}^{N} J_{1,i}}{N} \tag{3-20}$$

$$Average\ accuracy\ score:\ J_{2av} = \frac{\sum_{i=1}^{N} J_{2,i}}{N} \tag{3-21}$$

$$Absolute\ speed\ score\ difference: \Delta J_1 = \left| J_{1,i=1} - J_{1,i=2} \right| \tag{3-22}$$

$$Absolute\ accuracy\ score\ difference: \Delta J_2 = \left| J_{2,i=1} - J_{2,i=2} \right| \tag{3-23}$$

$$Average\ HPI: HPI_{av} = \frac{\sum_{j=1}^{R} HPI_j}{R} \tag{3-24}$$

$$Absolute\ HPI\ difference\ for\ ratio\ j: \Delta HPI_j = \left| HPI_{i=1} - HPI_{i=2} \right| \quad (HPI\ difference) \tag{3-25}$$

$$Average\ HPI\ difference: \Delta HPI_{av} = \frac{\sum_{j=1}^{R} \Delta HPI_j}{R} \tag{3-26}$$

Where

i = index of trial, N = Number of trials (N = 2 in this thesis)

j = index of speed - accuracy ratio, R = Number of speed - accuracy ratios (R = 5 in this thesis)

$HPI_j = HPI_{30:70}, HPI_{40:60}, HPI_{50:50}, HPI_{60:40}$ and $HPI_{70:30}$ calculated according to Equation (3 - 2)

Notes: Subscripts for linear, squared, sequence, speed-accuracy ratios will be used according to the context particularly to the system settings of hardware-based experiment. HPIs in these representations represent the fixed HPI value resulting from a specified speed-accuracy ratio.

Now once a model-based approach is applied to the same set of experimental data, the resultant sets of variables obtained are due for a Step 2 comparison. Unlike the previous case, the absolute differences of performance variables between non-model and model-based approaches are emphasised (approach-level instead of trial-level) assuming the consistency of human operators is preserved. Additionally, another major difference is a flexible pairing with the average values based on a whole set of human subjects rather than the average values based on trials. This is apparently due to the fact that a set of performance variables from non-model and model-based approaches are not the same and their differences need to be examined collectively to ensure conformity. Therefore,

the pair of performance variables yielding a minimum difference will be selected to represent the associated performance criterion as appropriate. To serve this purpose, the general performance variable denoted as X is used to represent an arbitrary variable in a difference calculation as follows.

$$Absolute\ variable\ difference: \Delta X_i X_j = \left| X_{i,model} - X_{j,non-model} \right| \tag{3-27}$$

$$Average\ variable\ difference: \Delta X_i X_{j,av} = \frac{\sum_{k=1}^{S} (\Delta X_i X_j)_k}{S} = \frac{\sum_{k=1}^{S} \left| X_{i,model} - X_{j,non-model} \right|_k}{S} \tag{3-28}$$

Where

i = index of performance variables from a model-based approach, j = index of performance variables from a non-model approach, k = index of human subjects and S = total number of human subjects participated in an experiment.

$X_{i,model} = V_{i,model}, V_{i,model}\ or\ J_{i,model}$ (performance variables or performance criterion with subscripts $_{model}$ and $_{non\text{-}model}$ for model-based and non-model approaches respectively)

Figure 3.21 shows a summary of Equations (3-27) and (3-28) based on a single performance criterion with 2 performance variables. A pair of performance variables from the model-based approach and that of non-model approach is defined as an *entry*. Each entry may comprise the same or different variables and is denoted as X_1-X_2 or $\Delta X_1 X_2$, where X_1 and X_2 are defined in an order of model-based variable and non-model variable respectively.

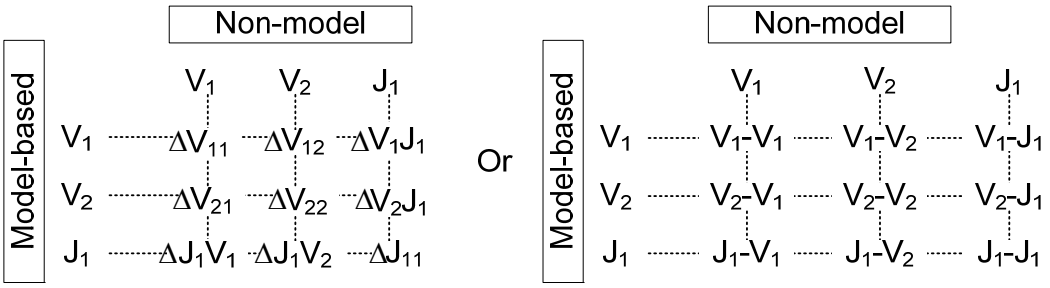

Figure 3.21. Summary of a distributive variable difference calculation (approach-level): subscripts *av* may be used to represent the average difference.

According to the definitions above, those variables obtained from the two approaches are used for a distributive comparison. Equation (3-28) suggests that a pair of variables used in calculating the average difference literally refers to both performance variables

and performance criteria. By calculating the performance criteria, the equally weighted performance variables are assumed and this will become clearer when the experimental data are analysed using the model-based approach under *performance variables* in Chapter 6.

3.6. Summary

This chapter describes the novel concept of the Human Performance Index (HPI) with general structure and forms with a focus on using speed and accuracy as the performance criteria. Details of the concept cover structures, forms and methodologies with regard to the performance variables extraction and proposed methods of extraction. Chapter 4 will then introduce the experimental works for use in analysing human performance by means of the non-model approach in Chapter 5 and the model-based approach in Chapter 6.

Chapter - 4.

Experiments on the computer-based and hardware-based systems

4.1. Introduction

This chapter introduces two experimental setups used as a framework for applying the Human Performance Index (HPI) concept. The key difference between these setups is based on the characteristic of a controlled object being inside a physical or virtual world. Characteristics and parameters of elements involved in the corresponding system are covered. Target sequence design, system settings, experimental procedures and results are also explained.

4.2. Outline for the experimental works

Following the proposed HPI concept and research methodologies described in Chapter 3, the focus is now shifted to applying the concept to two human-machine systems with different architectures and characteristics. The two selected human-machine systems are computer-based and hardware-based systems with the main objective being to verify the concept in both the virtual and physical domains/environments. In this aspect, the control action of a human relates directly to the selected control strategy in accordance with the task specifications, instructions, and his/her own abilities. The system response also marks the major difference between systems with different architectures, which, in turn, define the restrictions and nature of the human-machine systems.

Considering the resource for human performance computation, the data logged from the operating field are directly used in both non-model and model-based approaches

(covered in Chapter 5 and 6 respectively). The non-model approach involves an extraction of the performance variables without needing mathematical equations whereas the model-based approach uses model parameters from the derived mathematical equations as the performance variables. Computationally speaking, the latter approach is more complex and time-consuming yet essential to fulfil the proposed human performance concept. That is, the model-based approach serves as a validation of the results from the non-model approach. Consistency among the results might lead to a preference for the non-model approach over the model-based approach due to its simplicity and level of accuracy.

Regarding the nature of operation in both computer-based and hardware-based experiments, a *point-to-point* or *point-by-point operation* is selected as an example of a common task in many human-machine operations. For instance, the moving of an object from one position to another using a robot manipulator or a crane with certain types of control device illustrates the nature of such a task (Yoneda, Arai et al., 1997; Yoneda, Arai et al., 1999; Suzuki, Kurihara et al., 2006). Therefore, both computer-based and hardware-based experiments in this research are designed in compliance with this observation to ensure practicality.

For the computer-based experiment, a set of positions is defined to allow a human operator (the terms *a human user*, *a human subject*, *a participant* may be used interchangeably) to track a cursor on a computer display by using a computer mouse. Similarly, for the hardware-based experiment, a joystick is used to control a helicopter test rig, which has two degrees of freedom in rotating horizontally and vertically, to move along a set of targets in the azimuth/horizontal plane while keeping it as balanced as possible.

It is worth noting that these two independent experiments are proposed to complement or apply the HPI concept to the physical system (hardware-based system) in addition to the virtual system (computer-based system). In addition, the human operators in these experiments are not the same group of people, although there is one human operator

who took part in both experiments. However, the correlation of his/her performance in a computer-based and hardware-based system is not the focus of this research.

In fact, the computer-based experiment is considered the first step to implement the HPI concept due to its simple dynamics and operation familiar to the human operators in their daily lives. The hardware-based experiment is a step up on the previous system with more complicated dynamics involving unfamiliar operation that require more effort to complete the task. The increased dimensions on hardware dynamics and control elements complicate the application of the HPI concept comparing to the simple computer-based experiment and it will be become clearer when hardware characteristics are introduced. This consequently allows an extension of the HPI concept on a simple system to a more complicated system.

In summary, the computer-based and hardware-based experiments are conducted on human operators with the main objective to illustrate a human performance computation concept using the non-model approach and to validate the resultant HPIs using the model-based approach. The experiments from two different working environments suggest the potential application of the HPI concept in different scenarios. A comparison of these issues is the key.

Figure 4.1 presents the summary of the outline for the experiments along with the associated chapters in this thesis. According to Figure 4.1, this chapter describes and outlines the computer-based and hardware-based experiments in detail regarding the experimental design along with the experimental results. Chapters 5 and 6 are dedicated to the analysis of the experimental results presented in Chapter 4 using the non-model and model-based approaches respectively. The consistency of the HPIs from these two approaches reflects limitations and complications on deriving accurate mathematical equations of human.

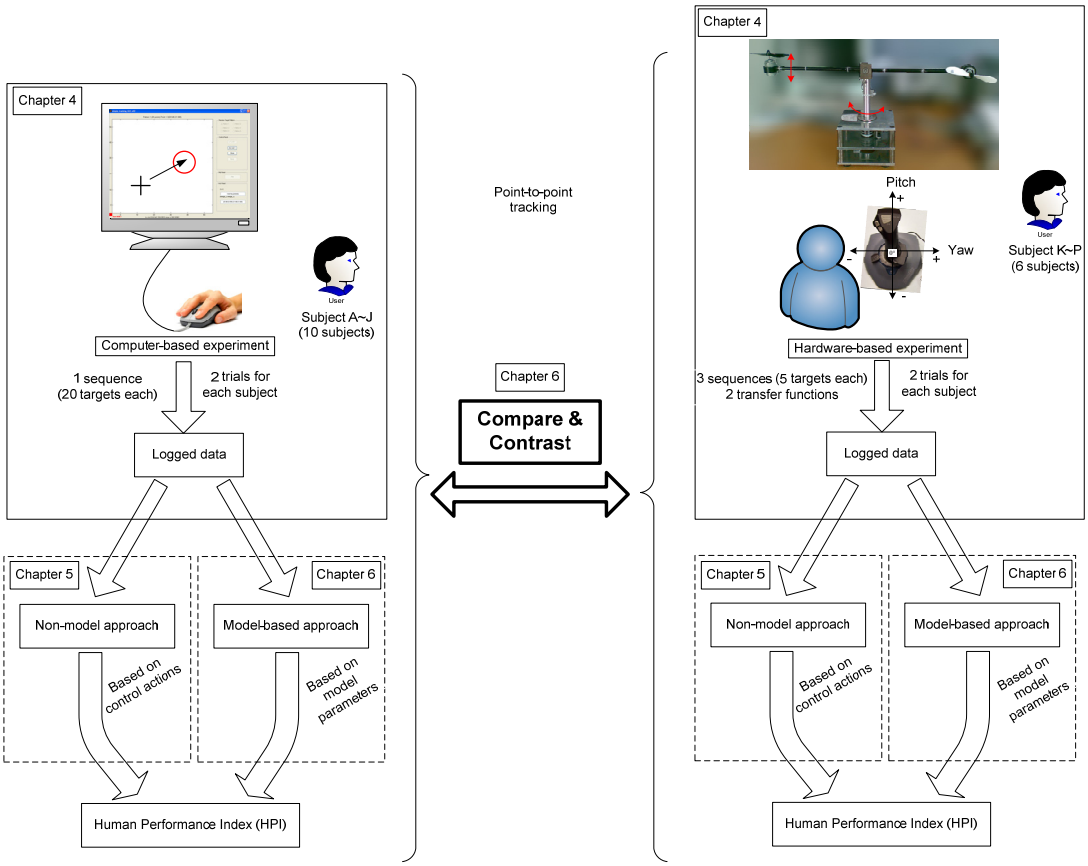

Figure 4.1. Structure of the thesis linked to the experimental works

4.3. Computer-based Experiment

The first experiment was based on a computer system with a computer mouse as a control device. The major aim of the experiment is to evaluate human performance using a simple human-machine system by applying the HPI concept. This experiment involved 10 people (1 female, 9 males) aged between 24 and 35 at the Mechatronics Research Centre (MRC) of Loughborough University who are daily computer users and familiar with a computer mouse.

Regarding the way the experiment was conducted, no extra training was imposed on any participant since the best performance and expertise of each individual are not the main concern of this research. Prior to the experiment, a two-minute session was provided for every participant as a warm up. The experiment was conducted at an arbitrary timeslot according to each participant's availability on the specified date. According to this arrangement, 3 days were used to complete 10 participants, of which

6 people participated on one day and 2 people on each of the other two other days. The amount of time spent with each participant was no longer than 5 minutes in total. These participants will be referred to as Subjects A to J.

4.3.1. Descriptions

The *point-to-point operation*, which is also referred to as a *simple tracking or target acquisition task* (Rao, Seliktar et al., 2000), is the focus. Since a computer mouse is a fundamental control device for a Human-Computer Interface (HCI), the operator's control action in terms of cursor coordinates and timestamp logged from the running program can be connected to their level of performance. A physical movement of a computer mouse corresponds to a graphical movement of a cursor on a computer display. This relationship is a *gain* of the system and can be adjusted via the display sensitivity settings. A computer mouse basically serves as a *position controller* in a human-computer system and *the cursor position* is a controlled system in this scenario. A block diagram of a computer-based system can be found in Figure 4.2. This block diagram contains a human controller, whose functionalities are to interpret a target distance according to a Euclidean distance and to convert a graphical distance to a physical distance. The equation for the Euclidean distance or a norm of a desired (target) position (y_d,x_d) and a current cursor position (y_c,x_c) is as follows.

$$d = \sqrt{(x_d - x_c)^2 + (y_d - y_c)^2} \tag{4-1}$$

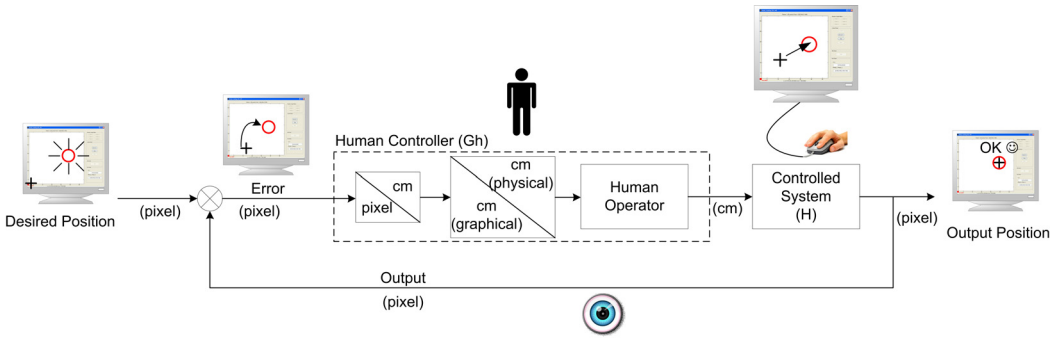

Figure 4.2. Computer-based experiment block diagram

Humans respond to a visual feedback with the aim of reducing the distance between the current cursor position and target position. It is worth noting that the human operates purely on the visual information provided on the computer display. This internal processing, which is relevant to object handling and hand movement, takes place inside the human brain and interrelates with several of its regions (Walpert and M.~Kawato, 1998; Kawato, 1999; Imamizu, Miyauchi et al., 2000.) Therefore, the human controller block includes a pixel (*pix*ture *el*ement) to centimetre conversion or a mapping of a graphical to a physical environment. This conversion allows a human operator to move a computer mouse correspondingly to the distance perceived and estimated. The internal model, which is derived mentally and involved in initiating motion, is therefore subjective and entirely based on perceptual sensitivity. The delay in associating muscular actions with the perception is referred to as the *reaction-time delay* (Mcruer and Krendel, 1962). The delay that follows the muscular actions to reach the destination is referred to as *neuromuscular time constant* (*ibid.*).

From a control system point of view, the controlled system is a cursor position on a computer display and a computer mouse acts as the control device for the cursor position. As mentioned earlier, the system can be considered as a *position control/ zero-order system* with a gain of the system being a scaling of graphical to physical movement (Jagacinski and Flach, 2002). Before calculating the value of the system gain, the equipment will be first described. A 12.1'' ATEC® laptop computer with Windows XP operating system was used with the screen setting of 1024 × 768 pixels (Width × Height). The resolutions of the computer display and DELL's optical mouse are 96 and 800 dots per inch (dpi) respectively.

Considering the system gain as a scaling of the mouse to the cursor movement and that this is related to the dpi values in both the physical and graphical domains, the ratio of a physical *dpi* (dpi_{mouse}) over a graphical *dpi* (dpi_{screen}) represents how the magnitude of movement in the physical domain relates to the cursor movement in the graphical domain (computer display). This ratio is denoted as the *gain* of the mouse as shown in Figure 4.3 (G_{mouse}).

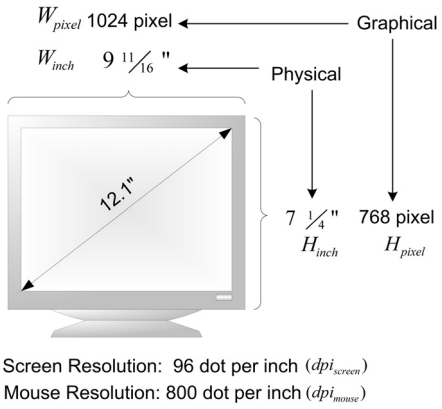

Figure 4.3. Graphical and physical domain in the computer-mouse setup

$$G_{mouse} = \frac{dpi_{mouse}}{dpi_{screen}} \tag{4-2}$$

It is worth noting that G_{mouse} is dimensionless and therefore, can be calculated from the *dpi* values in arbitrary units. However, G_{mouse} in units of pixels per inch ($G_{mouse\text{-}ppi}$) may be directly usable as a graphical unit (pixel) and is usually used in a graphical domain rather than a physical unit (inch or centimetre). In order to calculate this, the pixels per inch as a scaling of the graphical to physical settings is required. Physical settings here are according to the physical dimension of the laptop screen, as shown in Figure 4.3. Assuming the horizontal and vertical *ppi* are equal, $G_{mouse\text{-}ppi}$ can then be calculated as a product of *ppi* and G_{mouse} as shown below and the summary can be found in Figure 4.4.

$$ppi = \sqrt{\frac{W_{pixel} \cdot H_{pixel}}{W_{inch} \cdot H_{inch}}} \tag{4-3}$$

$$G_{mouse-ppi} = ppi \cdot G_{mouse} \tag{4-4}$$

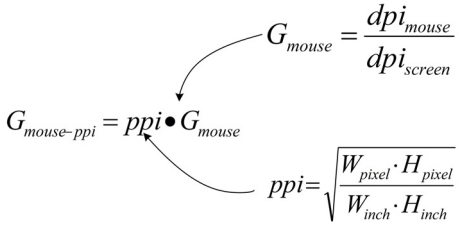

Figure 4.4. Summary of G_{mouse} calculation

The values of *ppi*, G_{mouse} and $G_{mouse\text{-}ppi}$, according to the settings, are *105.8 pixels/inch, 8.33* and *881.8 pixels/inch* respectively. Dividing $G_{mouse\text{-}ppi}$ by 2.54 simply converts a unit of G_{mouse} to pixels per centimeter, which is denoted as $G_{mouse\text{-}ppcm}$. With reference to

Figure 4.2, *H* is therefore a control system with the gain value of 881.8 or 347.2 (H_{ppi} = 881.8 or H_{ppcm} = 347.2). The general equation of the system gain is as follows:

4.3.2. Experimental design

The computer-based experiment used in this thesis is designed in accordance with the manual control system variables (Chapter 2). It is worth stressing that only task and procedural variables can be designed. Hence, the following table only contains the descriptions of only these two variables.

Table 4-1. Task and procedural variables for the computer-based experiment

Task variables	• Forcing/input function: random-appearing target sequence • Display: 12.1" LCD display, screen resolution • Control device: a computer mouse, mouse resolution • Controlled system: a computer cursor • Interface: MATLAB GUI with data logging algorithm • Logged quantities: x and y-coordinates, timestamp
Procedural variables	• Procedures: o Tracking a set of red circle targets on a computer display by a cursor using a computer mouse o Aligning a cursor at the centre before proceeding o Repeating the same target pattern for every participant for fairness • Instructions: o Tracking the target as quickly as possible o 2-minute practice trial before start o 2 trials, 20 targets for each trial

In this section, the Graphical User Interface (GUI) design of the program will be presented first and then followed by the target pattern design.

4.3.2.1. Graphical User Interface (GUI) design

The MATLAB®'s Graphical User Interface Design Environment (GUIDE) toolbox is used for the GUI design of a simple tracking operation in this research. This software is used as a platform for developing an interface with a human user for logging the user's data and analyzing the user's control actions in the simple tracking operation. The main components of the program are the area for tracking- *the operating area* - target pattern

selection and information display. The operating or tracking area is located at the centre of the program in the form of x-y axes with a target pattern selection located in the right pane. The information display includes the cursor's current x-y coordinates, timestamp, target number and the program's status located in the right panel next to the operating area. Figure 4.5 shows a screenshot of the simple tracking program designed using the MATLAB®'s GUIDE toolbox.

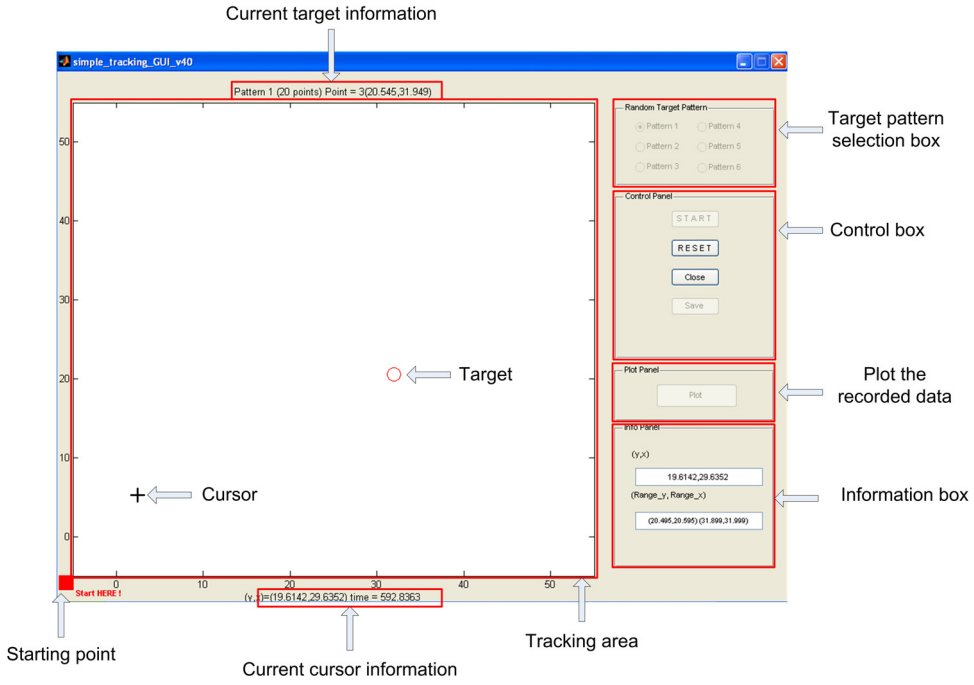

Figure 4.5. Screenshot of the simple tracking operation

With reference to the task descriptions, a random target pattern is selected by default for every participant, which is pattern 1 in this case, as shown in Figure 4.6(a). Some of these panels' elements are disabled once the operation commences, which is by pressing the start button, as in Figure 4.6(c), to avoid system crashes and feeding irrelevant information to the human operators. The status information, as of Figure 4.6(c), prints the status "Done" once a particular target tracking is accomplished, which lies within the range, as shown in Figure 4.6(d). The next target position is displayed instantly. At the end of the 20th target, the experiment supervisor saves the experimental result by clicking the "Save" button and resets the program ready for the next trial. The "Plot" button (Figure 4.6(b)) is enabled upon a trial completion for a quick check on the results. From the human operators' point of view, they are instructed to focus only on the operating area and the tracking status to ensure a successful tracking without

distraction leaving the supervisors with all the duties to save and check the experimental results. Further details on the right panel are as follows:

a) Target pattern selection panel

b) Plot command on the logged user's data

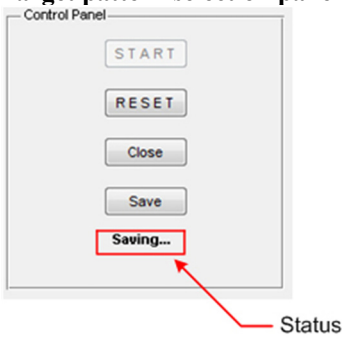

c) Control panel with status information

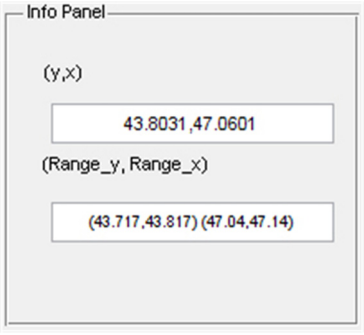

d) Information panel for the current target position

Figure 4.6. Right panel of the GUI based on Figure 4.5

Apart from the primary feature of the program to be used as an interface for the human users, a data logging mechanism also needs to be running in the background. The main purpose is to read the current x-y coordinates of the cursor and store them for further analysis of his/her control action. The MATLAB® GUIDE's standard function called *WindowButtonMotionFcn* is primarily used along with the *ptrack* function to read in the current cursor position (*currentpoint* variable) in the x-y coordinate system from the *axes* object's area, which is located inside the *figure* object (Figure 4.7). The axes' area is also used for plotting the target positions, which are generated offline prior to the experiment. It is worth noting that the current cursor and target positions are with respect to the *axes'* range rather than the computer screen. The *axes*' range is not readily in pixel units and therefore, a conversion factor for the axes' value to pixels is required.

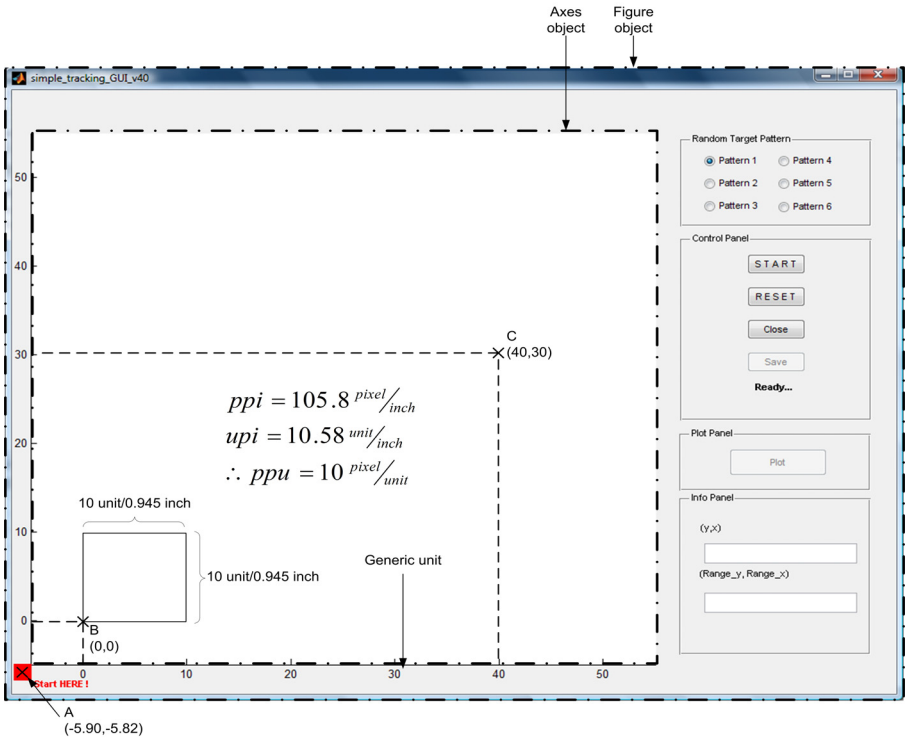

Figure 4.7. A GUI created on the ATEC® 12.1'' screen along with the graphical and physical dimensions [Note: Position A shows the start position, Position B shows the origin and Position C shows the sample position.]

To convert the x-y coordinates of the axes' object in Figure 4.7 to pixels, a pixel per axis unit (*ppu*) value based on the device settings and screen resolution is the key. This can be easily calculated from the ratio of pixels per inch (*ppi*) and units per inch (*upi*), as shown in Equation (4-5).

$$pixel/unit = \frac{pixel/inch}{unit/inch} \text{ or } ppu = \frac{ppi}{upi} \tag{4-5}$$

The ppi value that was obtained earlier from Equation (4-3) (= 105.8) can be used directly along with the *upi* value calculated as $\sqrt{\frac{10 \cdot 10}{0.945 \cdot 0.945}} = 10.58\, upi$. The *ppu* value is therefore found to be $\frac{105.8\, ppi}{10.58\, upi} = 10$ pixels/unit. As a result, the value of the x-y coordinates multiplied by 10 is the coordinate in pixels. Based on this conversion factor, a 200-pixel distance or 20-unit distance is arbitrarily chosen as a minimum distance to be travelled in the range of 0 and 50 on both x and y-axes. This is to ensure that the distance from target to target is sufficiently great.

In terms of a physical distance based on the chosen 200-pixel graphical distance, a conversion factor $G_{mouse\text{-}ppi}$, which is obtained earlier, can be used for calculation as shown below:

$$D_{graphical-pixel} = 200\,pixel \Rightarrow D_{physical-inch} = \frac{D_{graphical-pixel}}{G_{mouse-ppi}} = \frac{200}{881.8} = 0.227in / 0.58cm$$

From the value of 0.58cm for $D_{physical}$, it can be interpreted that the minimum physical distance (hand movement) of 0.58cm is required to achieve a 200-pixel graphical distance on a computer display. According to the setup in this experiment, the hand movement distance of 0.58cm distance is large enough not to be caused by any accidental or jerky movements. However, this value is dependent on the computer display settings, including the relationship of the screen size (physical dimension) and screen resolution (graphical dimension), which is effectively the *ppi* value of the screen.

4.3.2.2. Target pattern design

A random target sequence is selected for this experiment to avoid pattern recognition in predicting the upcoming position. One target position is shown on the computer display at a time until the cursor is correctly aligned at the target's centre. The target pattern is generated offline prior to the experiment and repeated for all participants. The distance of 200 pixels was chosen for the pair of targets, which is effectively mapped to a value of 20.

The target pattern is randomised with a standard uniform distribution of a floating-point number ranging from 0 to 50 with the condition that of Euclidean distance between target positions is at least 20, according to $d_{segment}$ in equation (4-6).

$$d_{segment_i} = \sqrt{(x_i - x_{i-1})^2 + (y_i - y_{i-1})^2} \tag{4-6}$$

Where (x_i,y_i) = the x-y coordinates of the current target i, (x_{i-1},y_{i-1}) = the x-y coordinates of the previous target and i starts from 1 to 20. (x_0=-5.82, y_0=-5.90, as shown by the red box in Figure 4.7).

The random values of 0 and 50 and a distance of 20 on the axes object are equivalent to 0 and 500 pixels and a distance of 200 pixels respectively. The resulting target pattern used in the experiment can be found in Figure 4.8 with the sample distances of targets number 1-2, 3-4 and 5-6 illustrated.

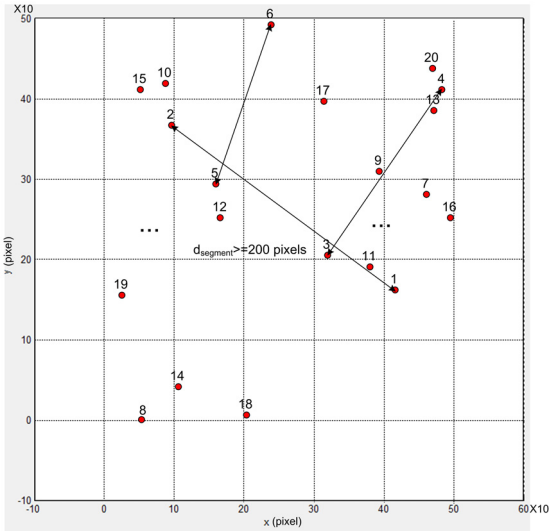

Figure 4.8. Target pattern for the computer-based experiment

In order to determine how difficult one target segment is in comparison to another target segment, the concept of *Index of Difficulty* (I_d) or the amount of information processed by a human to implement a tracking task is applied. With reference to the original Fitts' Law, the Index of Difficulty (I_d) is defined in terms of a travelled distance between a pair of targets (A) and the size of these targets (W) along the same axis (Fitts, 1954, see Figure 4.9(a)). That is, I_d is defined in a one-dimensional domain and its value represents the information processed by the human brain according to the following equation:

$$I_d = \log_2(\frac{2A}{W}) \tag{4-7}$$

The extension of Fitts' Law to a two-dimensional domain was therefore needed and the studies conducted by MacKenzie showed that the direction of approach and the target dimensions are the key. The scenario is as illustrated in Figure 4.9(b) and (c).

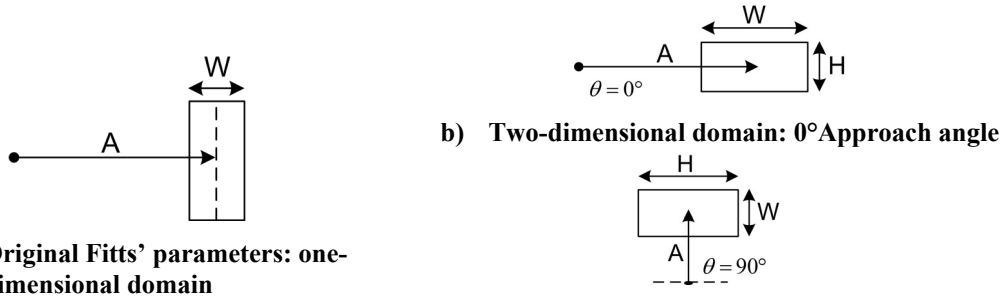

a) **Original Fitts' parameters: one-dimensional domain**

b) **Two-dimensional domain: 0°Approach angle**

c) **Two-dimensional domain: 90°Approach angle**

Figure 4.9. Fitts' Law in one-dimensional and two-dimensional scenarios (According to Scott MacKenzie, 1992; Scott MacKenzie and Buxton, 1992)

The approach direction is the angle of approach based on the centre of the rectangular target. With reference to the target of width W and height H, as shown in Figure 4.9(b) and (c), the roles of width and height are interchanged according to the approach angle. That is, the width of the target has to align with the approach angle. Therefore, W for the approach angle of 0° is now represented by *H* for the approach angle of 90° and vice *versa*. It can be seen that the dimensions of the target effectively cause a difference in the target width (*W*) used for the index of difficulty (I_d) calculation (Equation (4-7)). Therefore, this implies that the effect of approach angle can be reduced by using a target shape with equal dimensions, such as squares and circle. Figure 4.10 shows a circular target with 0° and 90° approach angles to illustrate this idea.

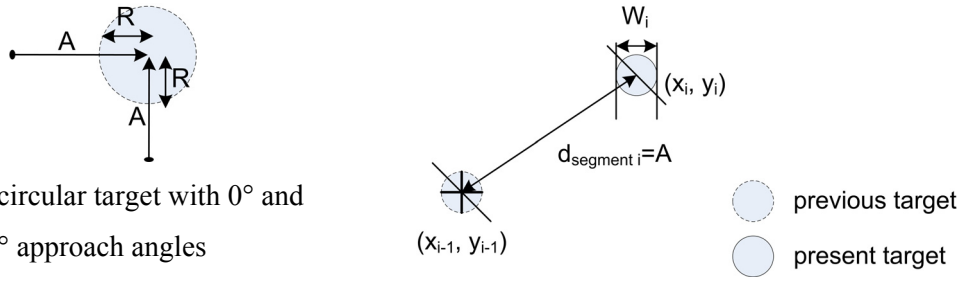

a) A circular target with 0° and 90° approach angles

b) *W* and *A* for a simple tracking experiment

Figure 4.10. A circular target with *A* as a travelled distance and W (2xRadius) as a target width

In order to calculate I_d for the computer-based experiment, *A* is effectively the distance between targets or $d_{segment}$ as described earlier and *W* is fixed at 14 pts ($^{14}/_{72}$ ″ or 20.61 pixels). The resultant target pattern along with $d_{segment}$ and the associated I_d are shown in Table 4-2 and plotted in Figure 4.11.

Table 4-2. Target positions table (* represents the dimensionless x-y coordinates)

Segment	y*	x*	d (pixel)	Id (bit)
1	16.14	41.65	523.32	5.67
2	36.70	9.59	380.87	5.21
3	20.55	31.95	275.82	4.74
4	41.11	48.34	262.91	4.67
5	29.38	15.89	345.00	5.07
6	49.19	23.83	213.34	4.37
7	28.06	46.12	307.09	4.90
8	0.05	5.31	494.94	5.59
9	30.93	39.36	459.62	5.48
10	41.84	8.80	324.48	4.98
11	19.04	37.93	369.95	5.17
12	25.20	16.56	222.45	4.43
13	38.51	47.13	333.39	5.02
14	4.13	10.66	501.14	5.60
15	41.04	5.17	373.11	5.18
16	25.20	49.55	471.17	5.51
17	39.63	31.45	231.45	4.49
18	0.65	20.39	405.23	5.30
19	15.44	2.63	231.06	4.49
20	43.77	47.09	527.16	5.68

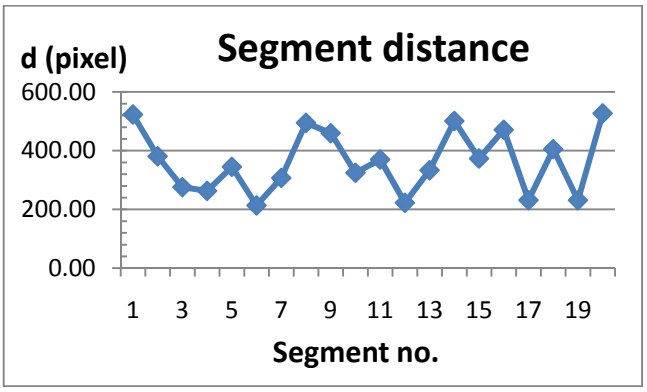

Figure 4.11. Distance of segment 1 to 20 based on the generated target pattern

The cursor used in the program is chosen to be of the crosshair shape with the same width as the circular target to ensure a careful alignment of the cursor onto the target and to minimize a slippage or accidental movement (Figure 4.10(b)). Next section describes the experimental procedures for the computer-based experiment.

4.3.3. Experimental procedures

With the use of the designed GUI discussed in the previous section, a point-to-point target tracking is performed according to the procedures shown in the flowchart (Figure 4.12).

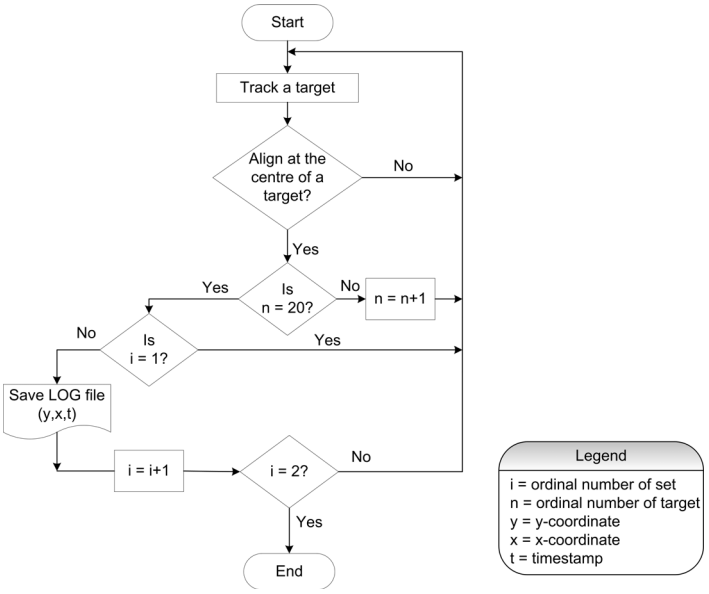

Figure 4.12. Flowchart of the simple tracking operation

Ten human subjects (A-J) were asked to track a common target pattern *as quickly as possible*. To start the experiment, a cursor has to be initially placed inside the red box (as shown in Figure 4.7). Any failure to do so is not counted and the trial needs to be restarted. A minimum warm-up trial of 5 minutes was provided for every human subject and he/she was asked to complete a set of 20 targets tracking twice following that. The total that each human subject has to complete is a tracking of 40 targets.

4.3.4. Experimental results

With the set of experiments conducted according to the designed program and experimental procedures, the results in terms of the control action or the path taken by the human operator in following the target pattern in a segment-by-segment format are presented. Human subjects A to J performed the action in his/her own way to complete the task as soon as possible. As a result, the variety of strategies followed by each individual shows the performance diversity. The characteristics of such performance in terms of speed and accuracy are the focus in this research. Reasons for selecting the use of a mouse as a controller are twofold, the reaction time is almost instantaneous from the user's point of view and the correlation between the hand and the cursor movement is familiar to any day-to-day computer user.

In the computer-based experiments, two trials of each human operator were conducted but only one will be presented. Using the pattern as described earlier, the snapshot of the result is presented in Figure 4.13.

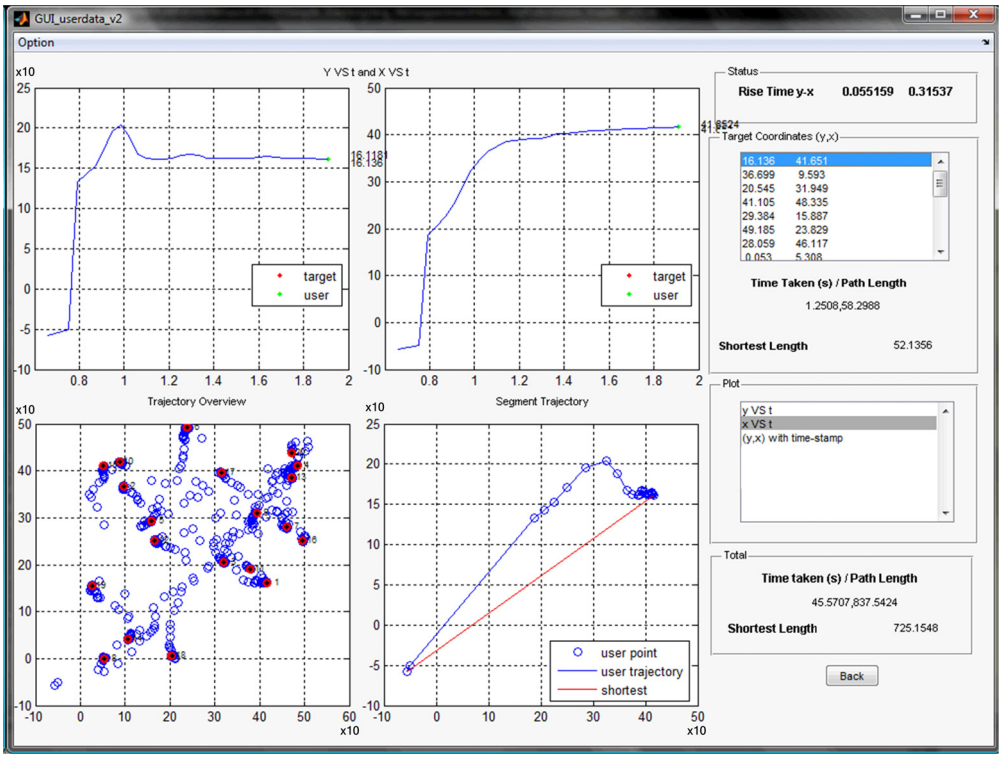

Figure 4.13. A snapshot of segment 1 from one human subject

As highlighted in the "*target coordinates (y, x) box*", only segment 1 is mainly plotted in this figure. The logged data are taken from one human subject with the snapshot of an overall target-tracking path from target number 1 to 20 and this is as shown at the lower left corner. In addition, because the MATLAB's *WindowButtonMotionFcn* sampling is *event-triggered*, a series of circles can then be observed from the figure. Therefore, the sampling frequency is reciprocal to the speed of the movement. That is, the slower the cursor moves, the more samples can be recorded and *vice versa*. For this reason, the resultant x-y coordinates and timestamp series need to be re-sampled prior to the analysis by the non-model and model-based approaches.

For further details on Figure 4.13, the y-t and x-t graphs for segment 1 are also plotted in the top row of the figure from left to right respectively. These two graphs are, in fact, based on the y-x graph as shown to the right of the overall snapshot. The y-x graph

shows the motion trajectory taken by subject A in order to track target number 1 as rapidly as possible. It can be seen that there is a degree of variation between the user's line and the ideal or straight line, which is the shortest path directly connecting a pair of targets. Figure 4.14 and Figure 4.15 show the graphs of all targets based on Figure 4.13.

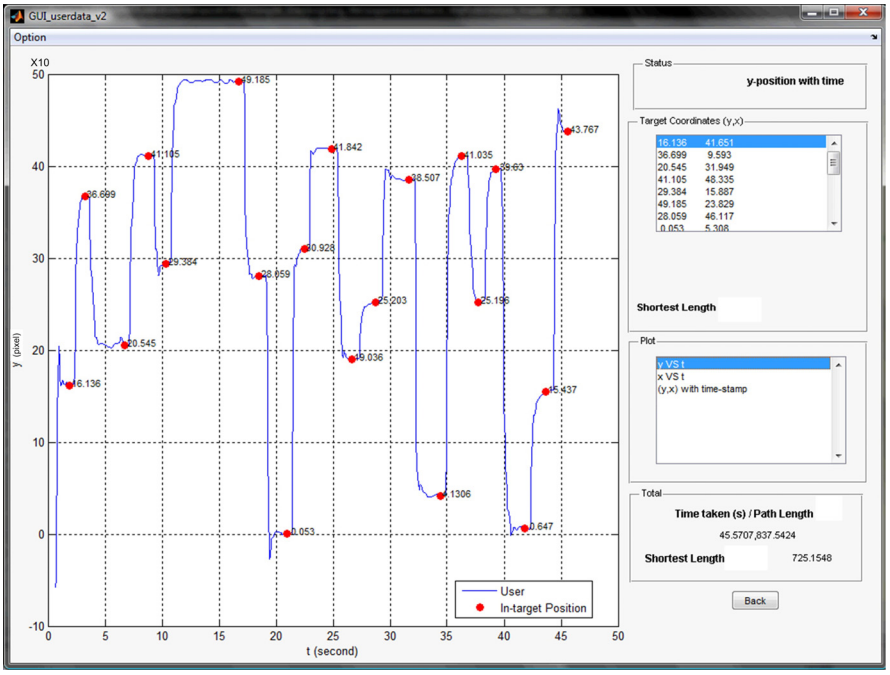

Figure 4.14. User's cursor positions along y-axis Vs time

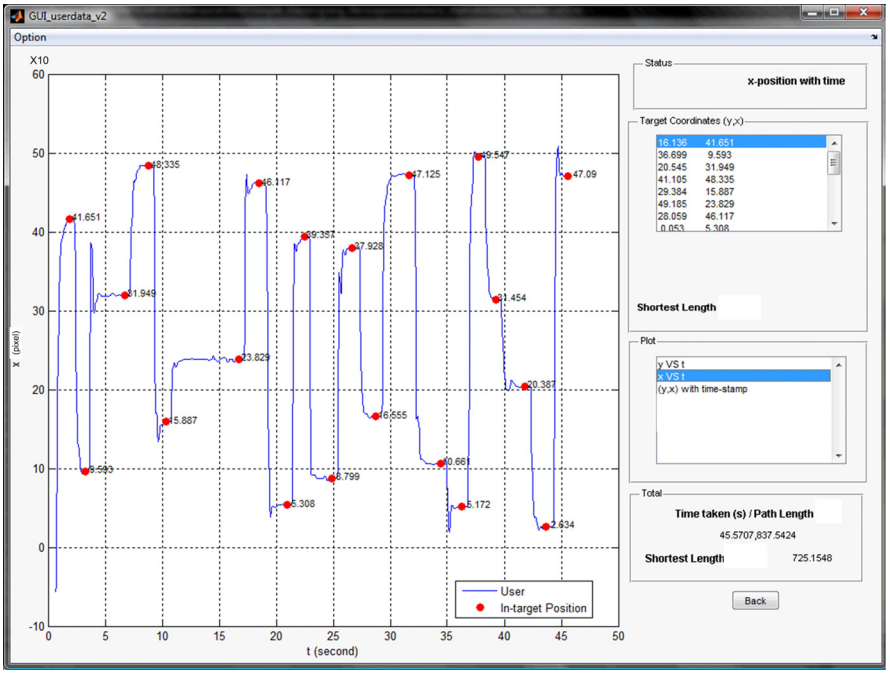

Figure 4.15. User's cursor positions along x-axis Vs time

To illustrate what the control action of a human operator looks like, the piecewise representation on the pair of targets or segments can be found in Figure 4.16 and Figure 4.17 (see page 102 and 103). The tracking pattern in this two-dimensional operation changes from one target position to another, presumably due to the order of the contiguous target positions and the context of the movement. That is, the movement towards the extreme may cause a concern not to move outside the operating field.

The relationship between the previous and current target positions can also affect the decision on the movement and this can be observed in Figure 4.16 and Figure 4.17 with regard to the motion of each segment. The trajectories taken by subject *A* are presented on a segment-by-segment basis giving a variation in achieving a tracking of one target position after another. The graphs contain the x-y coordinates of Trials 1 and 2 taken by subject *A*. These response shapes are in one of these two forms: a loophole or a zigzag.

It is worth noting that even for segment 6, which is the segment with the *lowest* Index of Difficulty (I_d) or shortest length, subject A still shows a large error in his/her first trial. According to these figures, the pattern of the control action is context-variant and dependent on the set of target positions. The mixture of loophole and zigzag patterns was due to the effort to compensate or optimize the operation time for completing the task and it is apparent that no fixed strategy is used for all target positions.

To proceed with these experimental results, the overall performance will be computed based on the average of all 20-target segments and this will therefore reflect his/her performance value for that particular trial. Chapter 5 will take and analyse these data directly whereas Chapter 6 will use them as an input to a System Identification algorithms specifically designed for the computer-based experiment. This means data processing and input/output pair treatment are specific to the computer-based experiment setup. Next, an overview on the hardware-based experiment and experimental results will be given.

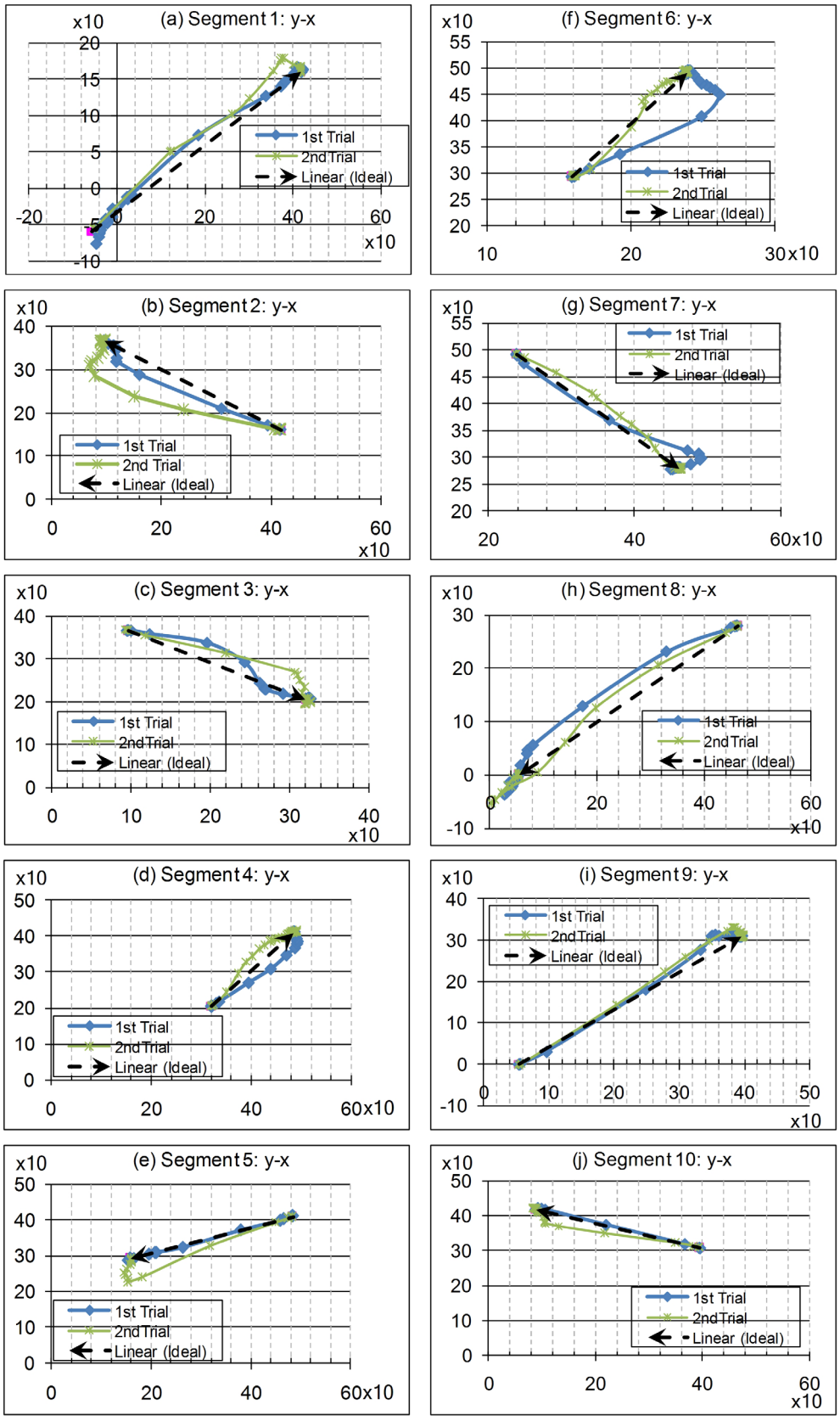

Figure 4.16. Control action of human subject A: target 1 to target 10 (in pixels)

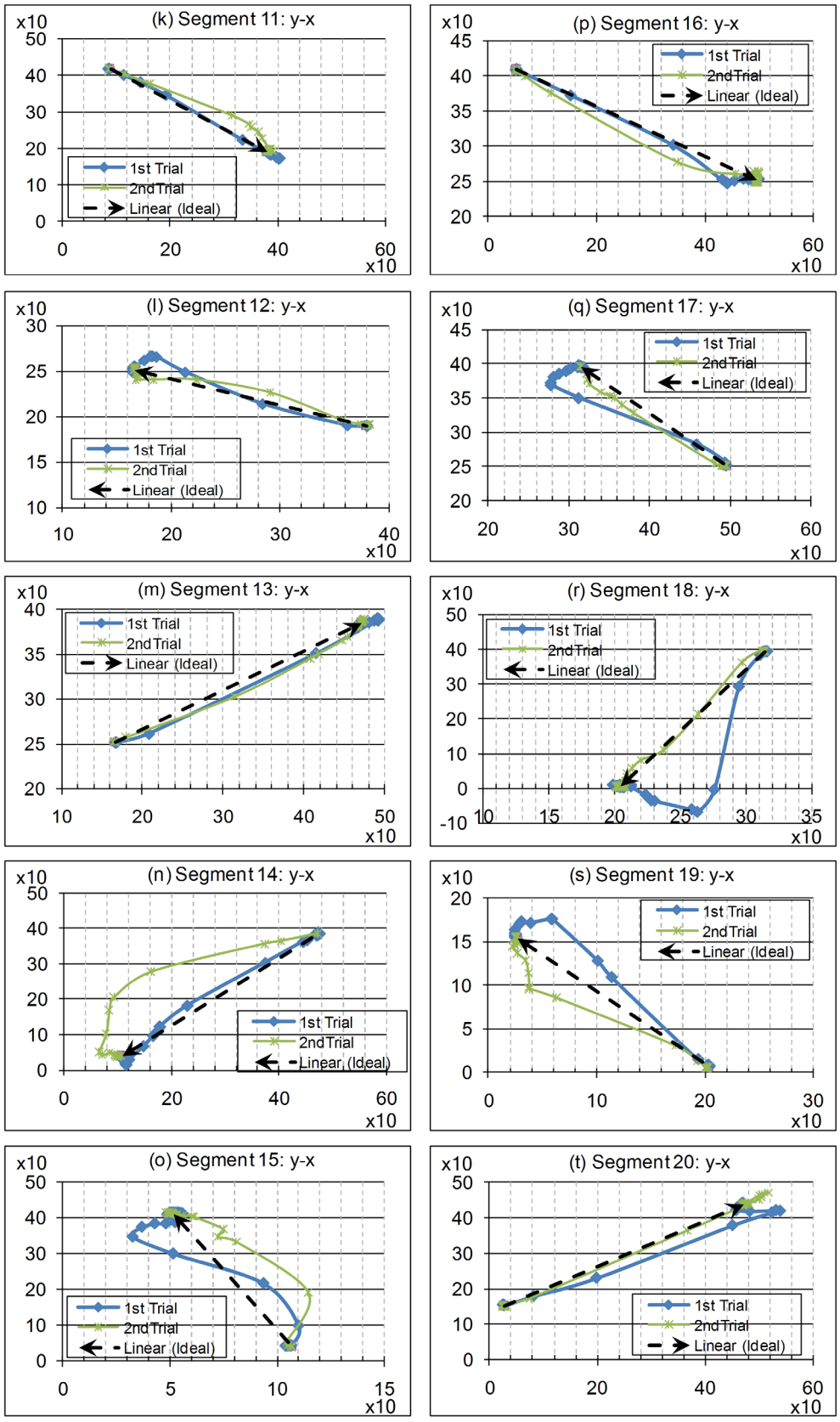

Figure 4.17. Control action of human subject A: target 11 to target 20 (in pixels)

4.4. Hardware-based Experiments

The main objective of the hardware-based experiment is to apply the Human Performance Index (HPI) concept to a real mechatronic system and to demonstrate that the concept is equally useful for systems with hardware elements as well. A variation of performance from one human operator to another relates to their familiarity with using a joystick. However, a correlation of experience in using a game joystick or the ability to fly a radio-frequency controlled helicopter with a control of a helicopter test rig is outside the scope of this research. Collected data from the experiments are to be analyzed in an offline manner according to the HPI concept proposed in Chapter 3.

Regarding an overview of the experiments, 6 human operators were asked to use a joystick to manoeuvre the metal bar of the helicopter test rig from one position to another according to the three predefined target sequences while keeping it as balanced (horizontal) as possible. These three sets of target sequences have different levels of difficulty and participants were asked to finish each sequence successfully. In addition, two control functions were designed to provide different patterns of response based on the joystick voltages to allow the comparison of overall performance and control action. Training sessions were also provided for familiarisation purposes prior to the experiment for each transfer function.

4.4.1. Descriptions

4.4.1.1. Hardware

For the hardware-based experiment in this thesis, the helicopter test rig, which was designed and built by 2 undergraduate students as part of their final year projects at the Wolfson School of Mechanical and Manufacturing Engineering of Loughborough University is used to apply and illustrate the application of the HPI concept on a real mechatronic system. The mechanical components of the helicopter rig included two

carbon-brush motors, two 6''x 4'' (diameter by pitch distance or a distance travelled for one complete revolution) propellers, a rotational bearing and slip rings, see Figure 4.18.

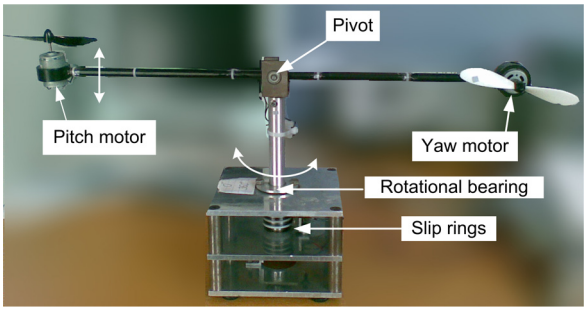

Figure 4.18. Mechanical components of the helicopter test rig

Regarding the aerodynamic component, two propellers that are attached to pitch and yaw motors serve as thrust generators for motion in the vertical and horizontal directions respectively. The magnitude of thrust is in proportion to the voltages supplied to the motors. To allow the generated thrust to create a rotation, a rotational bearing and slip rings allow the continuous rotation of a black metal bar.

Another main component of the helicopter test rig, a PCIO (Personal Computer Input/Output)/DAQ (Data AcQuisition) card, is used to process a set of commands based on a Visual Basic (VB) computer program and pass them to a PC (Personal Computer) adapter board/circuit board, which is connected directly to the mechanical parts, as shown in Figure 4.18, for control. A spring-centred or games joystick is used to control the speed of the pitch and yaw propellers according to a deflection angle sent for processing by the PCIO card. Four position sensors or potentiometers, which are located on the helicopter test rig and joystick, can be read and recorded by a computer program. Two potentiometers on the helicopter test rig are used to measure the yaw and pitch angle and two potentiometers inside the joystick are used to measure the deflection angle along the horizontal and vertical axes. The connection of these components can be found in a schematic diagram in Figure 4.19.

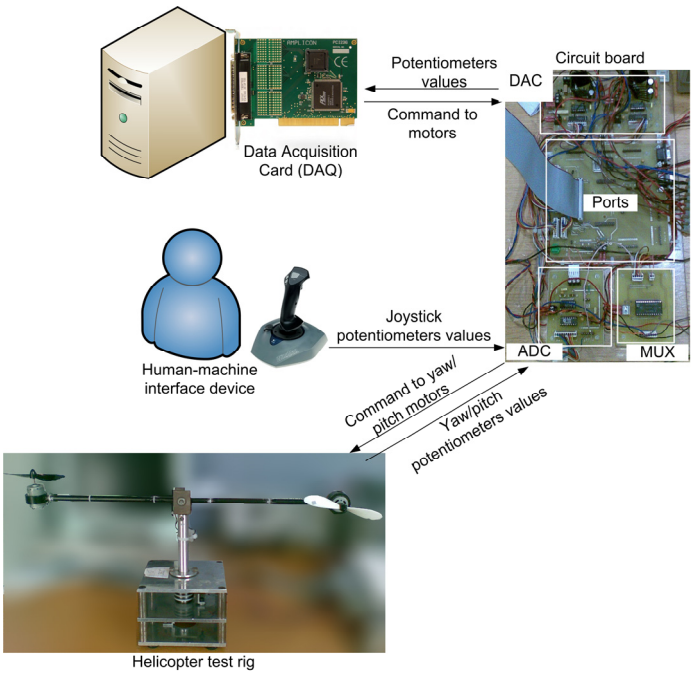

Figure 4.19. Schematic diagram of the helicopter test rig (please see Appendix B for full hardware details)

Regarding access to the potentiometers, a 16-channel multiplexer is used as a hub for a central connection to the helicopter test rig and joystick potentiometers. Each channel is dedicated for a particular potentiometer and in this setup, channels 4, 5, 6 and 7 are assigned to yaw and pitch potentiometers of the helicopter test rig and the yaw and pitch of the joystick respectively. A channel needs to be selected prior to the reading operation and, to avoid collision, only one channel is read at a time during the sampling interval. As a result, **four sampling intervals** are required to retrieve the whole set of these potentiometer readings. This also, effectively, means that each reading of the same channel or potentiometer consists of 4 samples separated from one another. Moreover, the moving average filter is applied to all the readings to mitigate the noisy voltages of the potentiometers.

In order to control this test rig efficiently, a human operator needs to have the ability to manoeuvre a metal bar (of length l = 50cm) by using suitable motor speeds according to the joystick's deflection angle. This is, in fact, in relation to the aerodynamics of the two propellers and the system dynamics. Cross-coupling of a motion from one axis to another axis due to the generated thrusts complicates an operation even further.

With regard to the direction of rotation, it is bi-directional according to the motor voltage polarity ±7.19V (a rotational speed graph of the motor operating in this voltage range can be found in Appendix A). As a result, the propellers' thrusts are generated with the directions as presented in Figure 4.20. CW and CCW denote the clockwise and counter-clockwise rotation, where the motors' and the metal bar's rotation are in reverse direction according to the generated thrusts.

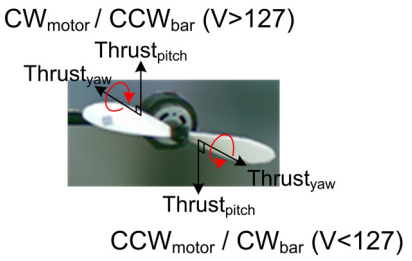

a) Thrust in yaw direction

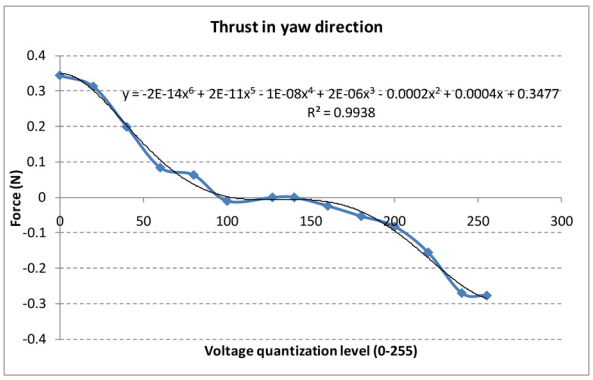

b) Thrust characteristics in yaw direction

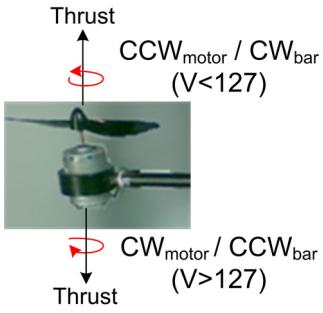

c) Thrust in pitch direction

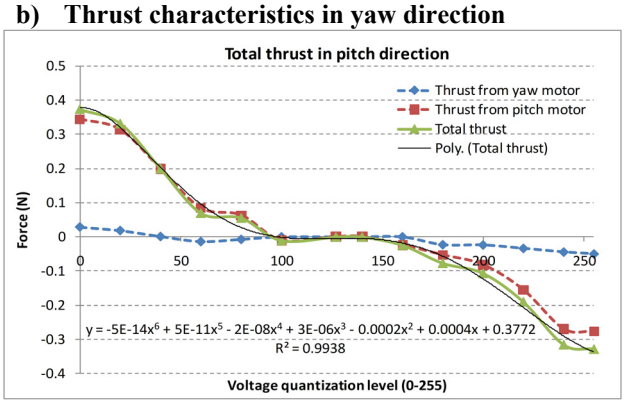

d) Thrust characteristics in pitch direction

Figure 4.20.Thrust characteristics in yaw and pitch directions

It can be observed that the thrusts from the yaw propeller lie along both yaw and pitch axes whereas the thrust from the pitch propeller lies only along the pitch axis. The cross-coupling effect of the yaw propeller thrust in the pitch direction causes a slight difference between the resultant thrust in the pitch direction and the resultant thrust in the yaw direction (as presented in Figure 4.20(b) and (d)).

The thrust/propeller's force in the yaw direction, which is generated only by the yaw motor, is denoted as $F_y(u_y)$ with u_y as the input motor voltage. In the pitch direction, the

thrust generated by the pitch motor is denoted as $F_p(u_p)$ and the thrust generated by the yaw motor is denoted as $F_p(u_y)$. These thrusts are directly in proportion to the supplied voltage and the motor's rotational speed. To make a measurement of these propellers' forces, a known mass was used to balance the metal bar at the corresponding supplied voltage. The values of this force together with effective mass for motor and propeller along pitch and yaw axes can be found in Appendix A.

Since the same model motor was used for both the yaw and pitch propellers, the generated thrust in yaw direction ($F_y(u_y)$) is therefore assumed to be equal to the generated thrust of the pitch motor in the pitch direction ($F_p(u_p)$). The friction located at the rotational bearing is usually small, however, extra force to overcome the static friction is initially required. In addition, the black metal bar is not naturally balanced (slightly unbalanced with its pitch elements being lower than that of yaw elements) due to different centre of gravity locations. As a result, a compensation force is also required but the magnitude will be lower. The signs of the moments involved were **positive in a clockwise direction** and **negative in a counter-clockwise direction**. Figure 4.21 and Figure 4.22 show the main moments that cause the rotation in the corresponding direction.

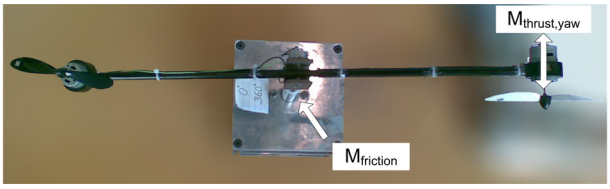

Figure 4.21. Moments for the motion in the yaw direction

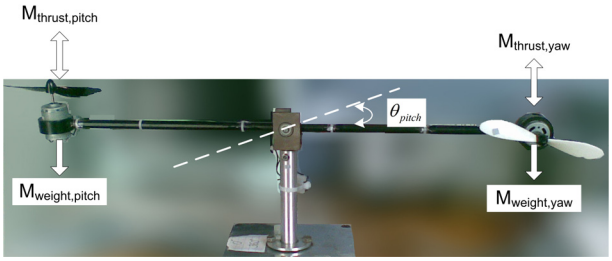

Figure 4.22. Moments for the motion in the pitch direction

According to the moments (*M*) shown in Figure 4.21 and Figure 4.22, the mathematical equations associated with the helicopter test rig characteristics can be presented according to Newton's first law for a rotational motion, $\sum_{i=1}^{n} M_i = \sum_{i=1}^{n} J_i \cdot \alpha$. Where M_i is the moment of the force, J_i is the moment of inertia and α is the rotational acceleration. The mass of the motors used in the following equations refers to the effective mass rather than the actual mass because of the centre of gravity difference. The orientation of the different motors causes the metal bar to be naturally unbalanced, i.e. $\theta_p \approx -16°$.

The moments along the yaw axis are as follows:

$$M_{yaw} - M_{friction} = (J_{pitch} + J_{yaw} + J_{bar}) \cdot \alpha_{yaw} \tag{4-8}$$

$$Where\ M_{yaw} = F_y(U_y) \cdot \frac{l}{2} \cdot \cos\theta_p\ ,\ J_{pitch} = J_{yaw} = m_{motor} \cdot (\frac{l}{2} \cdot \cos\theta_p)^2,$$

$$J_{bar} = \frac{1}{12} \cdot m_{bar} \cdot (\frac{l}{2} \cdot \cos\theta_p)^2$$

From Equation (4-8), the term $M_{friction}$ is the moment due to the friction at the rotational bearing (as shown in Figure 4.18). It has been found that the **minimum U_y values** to initiate motion along the yaw axis are **48 and 217 in the clockwise and counter-clockwise directions respectively**. Based on the thrust characteristics given before, the values of the voltage quantized level correspond to minimum forces of 0.161N and -0.159N respectively. Therefore, the force magnitude of approximately ±0.16N is needed to overcome the friction and initiate motion, which can be regarded as the static friction of the rotational bearing. The rolling friction torque of the standard ball-bearing, in terms of the bore diameter (d_m), the radial load (F) and the coefficient of friction ($\mu_s = 0.003, \mu_k = 0.0015$ for the deep groove bearings with d_m = 30mm installed on the helicopter test rig) can be calculated as follows Beardmore, 2010):

$$M_{friction} = \mu \cdot F \cdot \frac{d_m}{2} \tag{4-9}$$

It can be seen from Equation (4-8) that the moment of inertia is dependent on the pitch angle or, effectively, the metal bar alignment. Hence, the equation contains the $\cos\theta_p$ term.

As mentioned earlier, the cross-coupling of the yaw propeller's thrust in the pitch direction takes place in combination with the additional effect of the heavier pitch motor weight that causes the moment of weight as follows:

The moments along the pitch axis:

$$M_{weight} + M_{pitch} + M_{yaw} = (J_{pitch} + J_{yaw} + J_{bar}) \cdot \alpha_{pitch} \tag{4-10}$$

$$Where\ M_{weight} = (W_{pitch} - W_{yaw}) \cdot \frac{l}{2} \cdot \cos\theta_p\ ,\ M_{pitch} = F_p(u_p) \cdot \frac{l}{2},$$

$$M_{yaw} = F_y(u_y) \cdot \frac{l}{2} \cdot \cos\theta_p, J_{pitch} = J_{yaw} = m_{motor}(\frac{l}{2})^2, J_{bar} = \frac{1}{12} \cdot m_{bar} \cdot l^2$$

Considering the static forces of the helicopter test rig along the pitch axis, the compensation force in the vertical direction can be calculated as 0.008N in addition to the 0.16N compensation force in the horizontal direction to initiate a yaw motion.

Having outlined all of the main elements for the helicopter test rig or system of interest together with their essential characteristics, the following section discusses the step response of the helicopter test rig based on the varied quantized voltage in both the yaw and pitch axes. Step response characteristics are very important and need to be properly treated because of their effect on human's control action. A separation of step response from actual human response is required to allow the analysis of pure human data. Further details on this will be covered in Chapter 5 under the *rise-time effect* section.

4.4.1.2. Step responses

Unlike the computer-based system where a computer mouse movement is reflected instantly on the display, a certain amount of time is required for the helicopter test rig to move according to the supplied voltage at particular deflection angle of a joystick. According to the operating range of the motor voltage or input signal (u_x) from the previous section, the step responses of the helicopter test rig or the output angle along the yaw and pitch axes are observed. These responses are directly in proportion to the rotational speed of the yaw and pitch motors or, equivalently, the generated thrusts in the corresponding directions.

With reference to the physical structure and design of the helicopter test rig, the pitch angles are restricted to move in the range of ±45° in an elevation plane ($-45° \leq \theta_{pitch} \leq 45°$). However, no restrictions are applied to the yaw angle. That is, the metal bar is allowed to rotate freely with a yaw angle sweeping from 0° to 360° continuously thanks to the rotational bearing and slip rings. Effectively, a yaw angle for a rotation beyond 1 revolution is a multiple of 360° once the metal bar moves beyond the potentiometer's dead zone or the end of the coil ($0° \leq \theta_{yaw} \leq 360°$).

Regarding the initial conditions for the step responses along the yaw and pitch axes, the helicopter test rig is set to equilibrium throughout all measurements, by which the metal bar is stationary and the pitch angle of approximately -19° to -26° is marked depending on the resting position and friction at the pivot. The motor voltage is supplied to either the yaw or the pitch motor one at a time and the motion is observed separately. The step response in the yaw axis will now be presented and followed by the step response in the pitch axis.

a) Yaw step response

For a yaw axis motion, the incremental step of 5 quantization levels are used until a slight push on the metal rod is required to initiate movement, which means the generated thrust is insufficient to overcome the static friction at the rotational bearings. The same condition is applied to both the clockwise and counter-clockwise directions and to both the clockwise and counter-clockwise motions. It can also be observed that the amplitude of static friction is directly affected by the pitch angle and this will be shown in Figure 4.25(c) shortly. That is, the steeper the pitch angle, the higher the static friction. In addition, the cross-coupling effect of the yaw propeller's thrust in the pitch direction makes the pitch angle uncontrollable during the measurements (Figure 4.20 (b) and (d)). It would be ideal to install an axis lock or fixture on the pivot to restrain the motion only along the direction of interest. According to the aforementioned conditions, the step response is collected from the helicopter test rig and can be observed to have a repetitive pattern with some notes on the response shape as follows. It is worth noting that the sampling period of 0.03 seconds is used throughout the experiments.

Figure 4.23 shows the snapshot of the step response of $U_{yaw} = 0$ or the positive maximum of 7.19V from 0 to 10 seconds. It can be observed from a drop in the yaw angle of 360° that the helicopter test rig travels more than one revolution or beyond the dead-zone of the yaw potentiometer. In theory, the angle should drop from 360° to 0° instantly but because the potentiometers are quite noisy, a moving-average filter with a 5-sample window size is used to smooth out the readings. As a result, there is a lag of up to 5 samples occurring at the boundary between 360° and 0°.

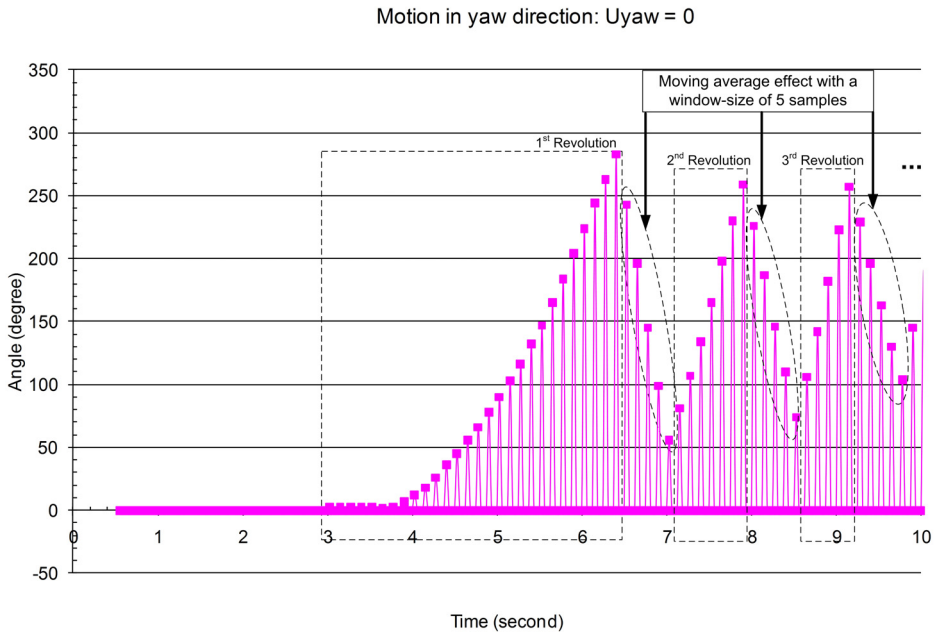

Figure 4.23. Step response in the yaw direction for $U_{yaw} = 0$

The width or time duration of each revolution also decreases as the rotation continues because the angular velocity increases (Figure 4.24(a)) and the angular acceleration is developed over time (Figure 4.24(b)). Figure 4.24 shows the corresponding angular velocity and acceleration containing the same number of revolutions in the same timeframe as that of Figure 4.23.

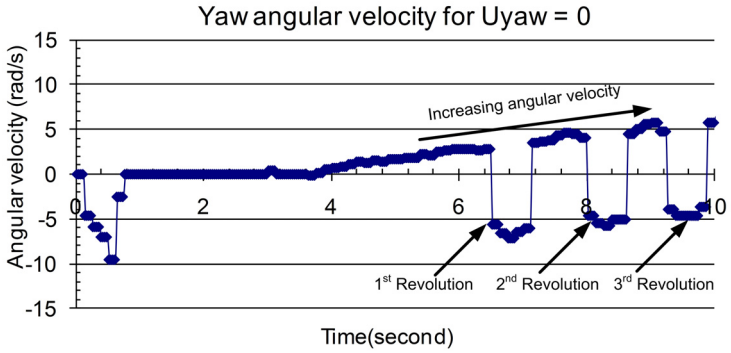

a) Increasing angular velocity

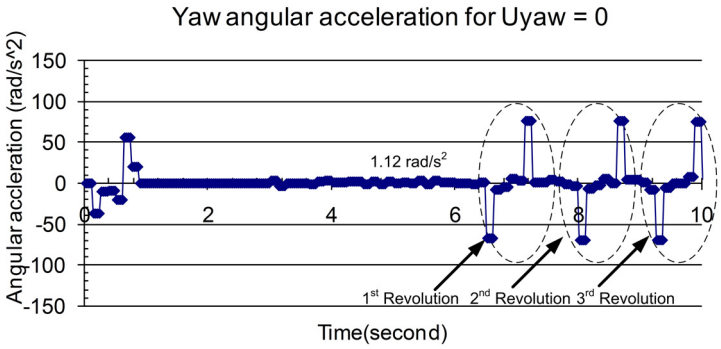

b) Constant angular acceleration

Figure 4.24. Angular velocity and acceleration for U_{yaw} = 0 for t = 0-10 s

Although Figure 4.24(a) and (b) are similar to Figure 4.23 in terms of the boundary crossings from one revolution to another, the shapes are quite different and noticeably affected by the moving-average filter, which is used to smooth out the noisy readings of the potentiometers. For the angular velocity, a greater number of samples is used for correcting the sharp turn at the 360° and 0° boundary as a result of the moving-average value of the yaw angle. It can be observed that 2 turns of the angular velocity can be spotted on Figure 4.24(a) where the first turn corresponds to the 0° to 360° crossover and the second turn corresponds to the recovery from the crossover. The values of angular velocity remain negative until the moving-average filter catches up with the fresh readings or 5 latest samples of the yaw angle where the values turn positive. Moreover, due to the fact that a particular channel or reading is retrieved once in every 4 sampling intervals, the readings are 4 samples apart and propagate through the other readings. The correct angular velocity, therefore, returns after 20 samples (4 $^{samples}/_{cycle}$ x 5 cycles).

In the case of the angular acceleration, two sign changes (turns) on the angular velocity cause a surge or spike on the angular acceleration graph in negative and positive regions, as illustrated in Figure 4.24(b). Once the angular velocities turns correct, the corresponding derivative quantity or the angular acceleration can be obtained in the next cycle or after 24 samples. The formula used for the calculation of angular velocity and angular acceleration for both yaw and pitch axes are as follows:

$$\text{Angular velocity } \omega: \quad \omega = \frac{\theta_i - \theta_{i-1}}{4 \cdot T_s} \tag{4-11}$$

$$\text{Angular velocity } \alpha: \quad \alpha = \frac{\omega_i - \omega_{i-1}}{4 \cdot T_s} \tag{4-12}$$

In the real situation, the main objective is to move from one yaw angle to another, of which a crossing between revolutions is not the case. Hence, it is reasonable to focus on the step response for only the first revolution. The summary for the yaw axis is as presented in Figure 4.25 (All graphs of step responses can be found in Appendix B).

It can be observed that the response in the clockwise direction (Figure 4.25(a)) is not purely symmetrical with the counter-clockwise direction (Figure 4.25(b)) due to the pitch angle effect on the static friction, as pointed out earlier. The rise time used in this calculation is the time taken to go from 10% to 90% of the maximum reached angle, whose value is not necessarily consistent across all the supplied voltages. This is due to the fact that the sampling frequency cannot catch up with the developed rotational speed of the metal bar and leads to a slippage of the angle in the dead zone.

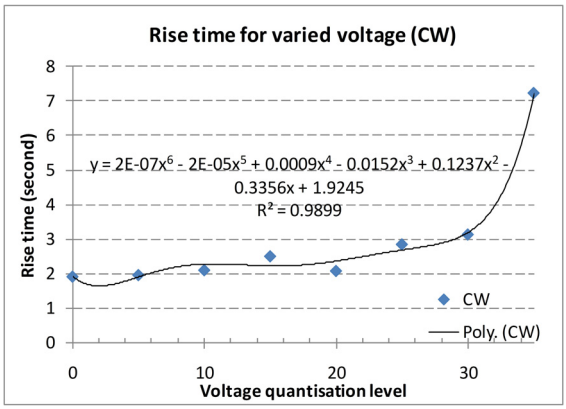

a) Yaw step response in a clockwise direction

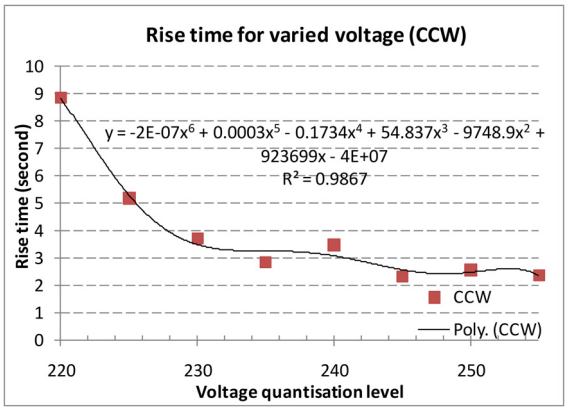

b) Yaw step response in a counter-clockwise direction

Figure 4.25. Yaw step response summary

b) Pitch step response

To determine the step response in the pitch direction, the metal bar is kept constant at the yaw angle of 270° for consistency and the motion starts moving from the pitch angle of approximately -26°, which is at the equilibrium of the metal bar, to a maximum angle of ±45°. However, the initial angle might vary slightly due to the pivot friction.

Because the maximum pitch angle is restricted, the pattern of the step response is saturated rather than repeated like those of yaw angles'. For high values of the supplied voltage, there might also be a bouncing of the metal bar once it strikes the top or bottom end since angles larger than 45° can also be spotted on the graphs.

According to the focus on balancing the metal bar, only the step responses for a lifting or positive angle are measured. The rationale for this is due to the fact that the thrust generated in a downward direction only accelerates or corrects the overshoot as the metal bar is naturally unbalanced with the negative pitch angle by default. Only the thrust in the upward direction is apparently required in normal circumstances. Figure 4.26 shows the step response for the voltage quantization level of 0 from the initial to the maximum allowable angle.

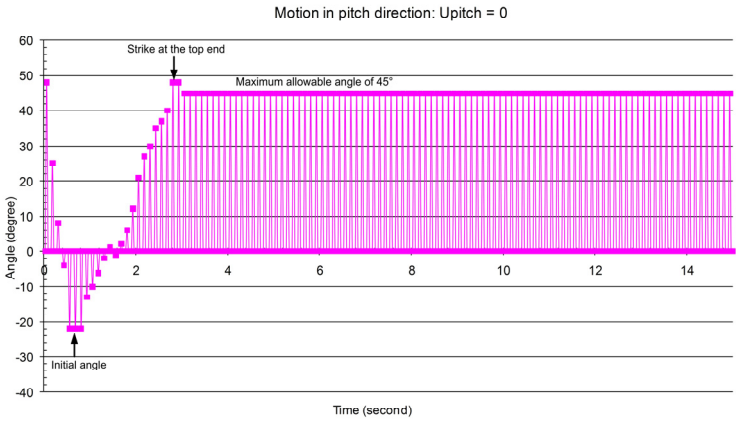

Figure 4.26. Step response in the pitch direction for $U_{pitch} = 0$

It is worth noting that the step responses are measured with the step increment of 5 up to the supplied voltage, at which the generated thrust moment cannot overcome the

motor's weight moment. The value of this quantized voltage level is found to be 85 and all other step responses can be found in Appendix B.

Figure 4.27 shows the summary of step responses in the pitch direction. It can be observed from the graph that a longer time is needed to reach the maximum angle when the supplied voltage is lower. In this experiment, only U_{pitch} in the range of 0-85 and the step response from initial to 0° pitch angle are practical. Therefore, the rise time in Figure 4.27 gives a general idea of how fast the output angle in the pitch direction responds to the variations in voltage.

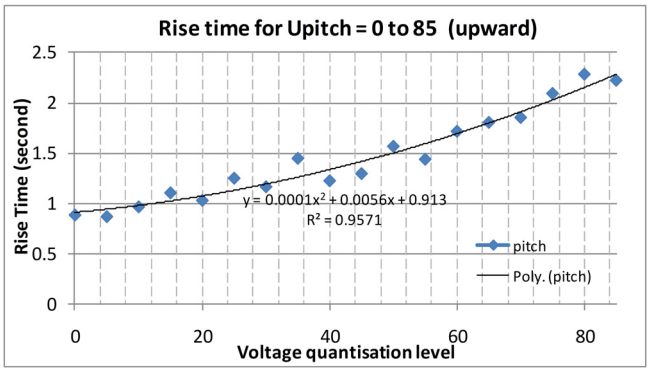

Figure 4.27. Pitch step response summary

4.4.1.3. Control device

In order to generate motor voltages that cause the metal bar's motion in the desired directions, a control device is needed. The helicopter test rig is designed to be controlled by a joystick or a control stick with two major control functions. The type of joystick used in this research is classified as a position or spring-centred joystick (Perry and Birmingham, 1968), which is appropriate for use in a *velocity* or *rate-control mode* (Mehr, 1973; Greenstein and Arnaut, 1987; Won, Tendick et al., 1987; Cooper, Jones et al., 2000). That is, a position or deflection angle of a joystick is mapped to one particular velocity rather than a position. This rationale is apparent because the spring force always seeks to move the stick towards the centre and it will lead to a bouncing of position back to its initial or centre position upon every release if it is programmed to

operate in a position control mode. Retaining the position of the controlled object by constantly holding the joystick is impractical and this can also lead to operator fatigue.

In order to implement the velocity control using a joystick, the process to read or retrieve the voltage of the joystick potentiometer and to write or send the output voltage to the corresponding motor are important. This input-output mapping can be referred to as a *transfer function* and the shape of this transfer function results in different motion profiles in terms of velocity and acceleration. Therefore, the transfer function for velocity control is simply a mapping of the joystick potentiometer voltage to the corresponding motor voltage.

With regard to the axes of the joystick, the horizontal axis is mapped to the motion along the yaw axis and the vertical axis is mapped to the motion along the pitch axis with the sign convention as shown in Figure 4.28. This is in accordance with the thrust direction shown in Figure 4.20, where the upward and clockwise rotation is denoted as positive and the downward and counter-clockwise rotation is denoted as negative. Two separate transfer functions for each axis are required and the operating range of the joystick along each axis is essential for the design process.

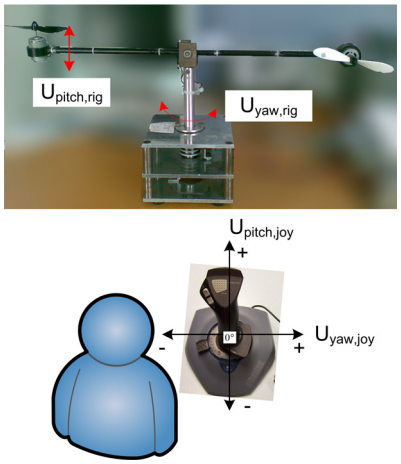

Figure 4.28. Axes mapping of joystick and helicopter test rig

The first step to design the transfer functions is to define the *stationary zones* of the helicopter test rig and define the operating range of the joystick in order to avoid undefined responses. As the name implies, the *stationary zone* is the area where the motor is stationary and it is also the area upon which the rest position of the joystick is centred. The centre of the stationary zone is observed to be at 120 for both yaw and pitch motors whereas the operation of the joystick varies from axis to axis. The stationary zones of the motors are found to be in the range of 100-140.

To determine the operating range of the joystick, the extreme positions and the centre of the joystick are measured. The transfer functions are then placed to fit the upper and lower segments of the operating range and leave the gap on the stationary zone. Two transfer functions are used in this research, which are of *linear and parabolic shapes*, with the objectives to illustrating and comparing the performance of different human operators.

For the linear transfer function (Figure 4.29), the output voltage increases or decreases constantly whereas the parabolic or squared transfer function (Figure 4.30) increases or decreases more towards the extreme of the operating range. The operating range of the joystick is measured as 185-199-225 for the pitch axis and 141-172-222 for the yaw axis, where 199 and 165 are the rest positions of the joystick.

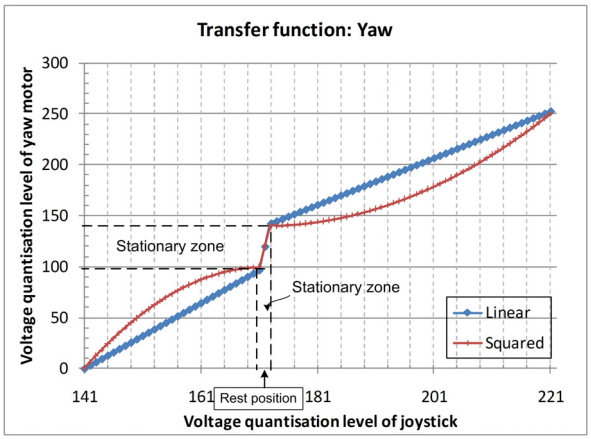

Figure 4.29. Linear transfer function for the yaw axis

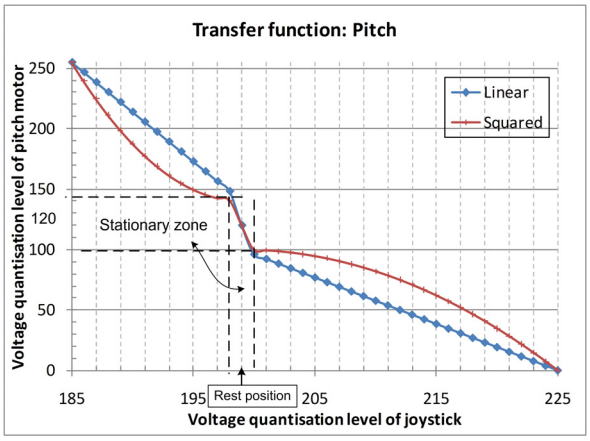

Figure 4.30. Transfer function for the pitch axis

Regarding the assignment of the motor voltage range to the axis direction as shown in Figure 4.28, user-friendliness is the main concern and this mainly affects the performance of a human operator. In order to allow a user to control the helicopter test rig with minimal difficulty, a direct connection of the physical domain from the controller point-of-view is important. The direction of the helicopter test rig in response to a manoeuvre of the hand motion on the joystick makes the control operation as spontaneous as possible.

The equations of the transfer functions are derived in a piecewise manner according to the direction of motion, where positive and negative directions of motion are treated separately. The standard equations in the forms of $y=mx+c$ and $y=ax^2+bx+c$ are used for the linear and squared transfer functions respectively.

4.4.2. Experimental design

With the use of two transfer functions of the joystick, the hardware-based experiment is designed and the summary can be found in Table 4-3.

Table 4-3. Task and procedural variables for the hardware-based experiment

Task variables	• Forcing/input function: 3 sets of target positions sequence • Display: own vision (no visual aids) • Control device: a spring-centred joystick • Controlled system: the helicopter test rig • Interface: VB program with data-logging algorithms • Logged quantities: yaw and pitch angles, timestamp, angular velocities, angular accelerations
Procedural variables	• Procedures: o Tracking 3 sets of target positions using a joystick o Aligning a metal bar onto the physical markers based on only visual perception o Following the sequence of the target positions one by one • Instructions: o Tracking the targets as quickly as possible o Keeping the metal bar as balanced as possible o Needing approval on each target position before proceeding o 2-minute practice trial before start o 2 trials on 2 transfer functions, 5 targets for each trial

Figure 4.31(a) shows the physical markers on the base of the helicopter test rig used in the tracking operation and Figure 4.31(b) shows the parameters for the Index of Difficulty (I_d) calculation, where A is the arc length and W is the width of the metal bar. Table 4-4 shows the height of high chair and human subjects A to F in this experiment.

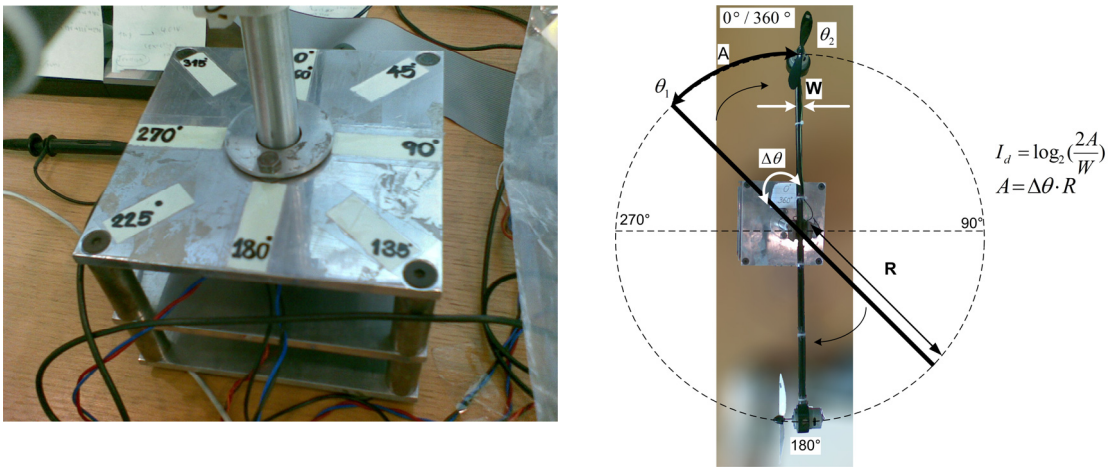

a) Markers for 45° and 90° degree angles **b) Top view of the helicopter test rig**

Figure 4.31. Illustrations of the physical markers and Index of Difficulty (I_d) parameters

Table 4-4. Height of high chair, human subjects A to F and average height o f subjects

Chair	Subject A	Subject B	Subject C	Subject D	Subject E	Subject F	Average
88cm	175cm	175cm	172cm	180cm	183cm	165cm	175cm

According to Fitts (Fitts, 1954; Fitts and Peterson, 1964), the characteristics of the target positions sequence can be calculated using the width and distance of the target in terms of I_d, as illustrated in Figure 4.31(b), with the results shown in Figure 4.32. Sequences 1, 2 and 3 are the sets of 180°, 90° and 45° angles respectively. Every sequence is designed to avoid a motion between the angle ranging between 315° and 360°, which resides in the potentiometer's dead zone. To fulfill this, the sets of 180° and 90° angles (Sequence 1 and 2) are designed to start at 90° whereas the set of 45° angles (sequence 3) is designed to starts at 45°. It is worth noting that the pitch motor is used as a reference throughout the experiment.

$$Sequence\#1: 90° \Rightarrow 270° \Rightarrow 90° \Rightarrow 270° \Rightarrow 90° \Rightarrow 270°$$
$$Sequence\#2: 90° \Rightarrow 180° \Rightarrow 270° \Rightarrow 180° \Rightarrow 90° \Rightarrow 180°$$
$$Sequence\#3: 45° \Rightarrow 90° \Rightarrow 135° \Rightarrow 180° \Rightarrow 225° \Rightarrow 270°$$

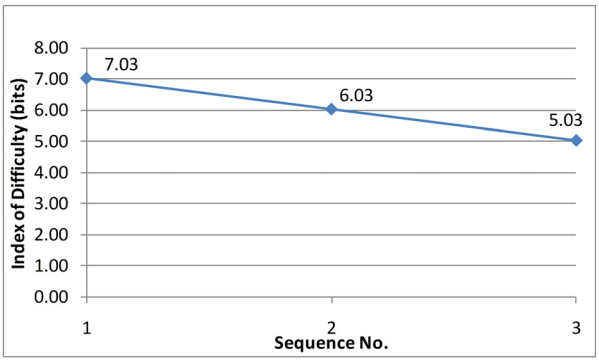

Figure 4.32. Target position sets and their Index of difficulty (I_d)

Based on the I_d values of the sequence, it can be observed that the experiment is started from the most difficult sequence and proceeds to the least difficult. However, the visual difficulty was also considered during the design of the target sequence. That is, the angles at the corner, i.e. 45°, 135°, 225° and 315°, might be trickier and more difficult to reach. In effect, the metal bar has to be controlled by a joystick and forced to land on the angle of interest to complete the tracking of that position. It is apparent from the operation point of view that the operator's eyesight plays an important role in the performance of each particular person.

4.4.3. Experimental procedures

Six participants aged between 24 and 40 (5 males and 1 female) were invited to participate in the hardware-based experiment at Mechatronics Research Centre (MRC) of Loughborough University. The orientation of the helicopter test rig is as shown in Figure 4.31(a) with a human operator directly facing the 180° marker. Because of the fact that there is no provision of any visual aids, a high chair is used instead of a normal chair for a clearer top view on the helicopter test rig. Moreover, an art board is provided for placing on the operator's lap in order to provide a flat and stable surface for operating the joystick while sitting on the high chair.

Each participant was asked to follow three sequences of the target positions using the pitch motor as a reference. A minimum period of 5 minutes was provided for familiarization with a particular transfer function prior to the real experiment. No intensive or extra training was provided so as to avoid the influence of skill on the genuine performance of each individual. Moreover, only one transfer function was used for a completion of three sequences at a time to avoid confusion and serve the purpose of familiarization. For performance comparison purposes, two trials on each sequence were conducted for every participant. In total, each participant had to complete 12 trials and, for convenience and performance reliability, the experiment was completed within a day. In fact, the time spent for each trial was 3-5 minutes depending on the human subjects, totalling approximately 1 hour.

4.4.4. Experimental results

Based on the index of difficulty values of the pre-defined target positions set as shown in Figure 4.32, the values suggest that sequence 1 requires the longest time to finish whereas the target sequences 2 and 3 require a time to finish in a descending order. In case of the computer-based system or the system without complicated dynamics, the consideration on how the system responds to the commands or control signals is seamless and therefore, considered trivial. However, this is not the case for the system

where a computer is connected to real hardware. The complexity of the system with hardware is not only dependent on the set of target positions but, in addition, there is the combination of the helicopter test rig dynamics and the hand-eye coordination required to control the joystick. The ability to move the helicopter from one position to another position while keeping it balanced apparently requires an overall understanding of the system and good eyesight. Human performance in terms of a degree of variation from the horizontal axis and overshoot are also important. Moreover, the perceptual errors of each individual can lead to the steady-state errors and these cannot be corrected for obvious reasons. This behaviour might vary and become worse over time as the eye stress develops.

Regarding the human control action on the helicopter test rig, the set of figures containing a yaw angular position, yaw angular velocity and pitch angular position are presented. Figure 4.33 and Figure 4.34 show the pattern of one human subject on target sequence 1 using the linear and squared (parabolic) transfer functions respectively.

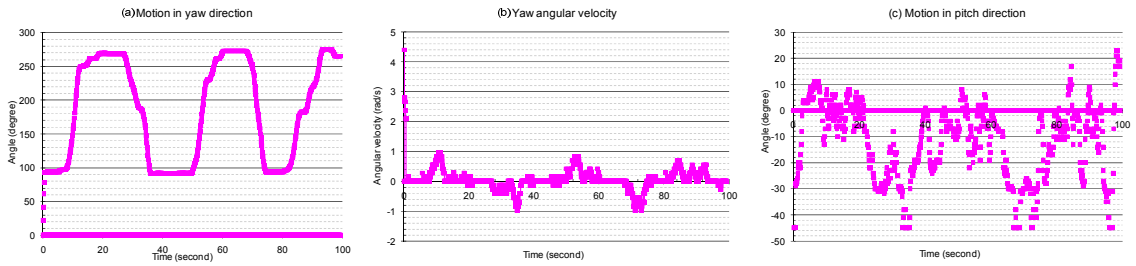

Figure 4.33. Results: sequence 1, linear transfer function

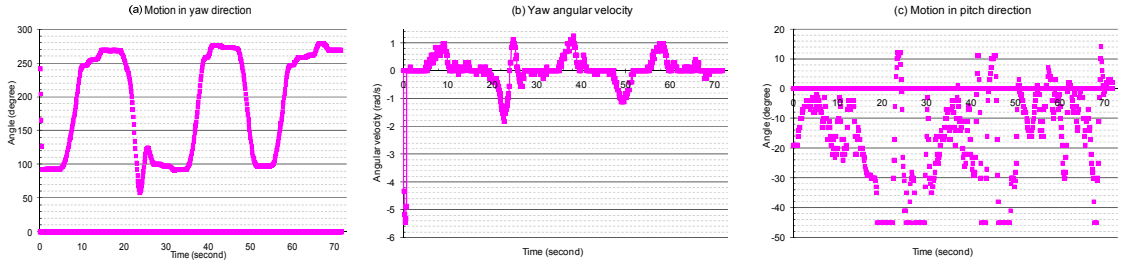

Figure 4.34. Results: sequence 1, squared/parabolic transfer function

It is worth noting that there is a short trail at the beginning of every yaw angle graph in the experiment due to the moving-average filter effect on the potentiometer readings. Consequently, this affects the corresponding characteristics like the angular velocity and

angular acceleration. Sequence 1 requires a human operator to move from a yaw angle of 90° to and from 270° and Figure 4.33(a) and (b) shows that this human operator can move in a clockwise direction rather smoothly but not in a counter-clockwise direction. This is mainly due to the difference in the static friction at the rotational bearing, which is caused by a shifting of the pitch angle up or down in accordance with the propellers' thrust characteristics (Figure 4.20(b) and (d)). Such a difference leads to an overreaction by a human operator on the control joystick, which requires a certain amount of time to get used to.

Moreover, the actions to land or to stop on the target positions can easily cause an undershoot or overshoot and require a correction. In particular, the overshoot can be spotted in Figure 4.34(a) at t≈20 seconds in a counter-clockwise direction on the way back from 270° to 90°. Literally, a spot-on action can be achieved once the familiarity with the helicopter characteristics is established. In addition, with the faster response of the joystick with the squared transfer function, which can be observed in terms of a developed angular velocity in Figure 4.34(b), the action to control with least overshoot can be more difficult.

With reference to the yaw angular velocity shown in Figure 4.33(a) and (b), the values are increased almost constantly while approaching the target positions (90° to 270°) and the drop of velocity is caused by the release of the joystick to stop at the target position. Apart from a consideration of the motion along the yaw axis, the motion along the pitch axis is found to be fluctuating around 0° pitch angle as shown in Figure 4.33(c) and Figure 4.34(c) due to the number of parameters required for the operation. In all cases, the resulting angular velocity in yaw direction lies within the range of ±1 rad/s, except Figure 4.34(b) where the counter-clockwise angular velocity goes up to almost -2 rad/s.

The following set of figures shows the yaw angular positions, angular velocity and pitch angular position for the target positions in sequence 2 and 3 using both the linear and squared transfer functions of the joystick.

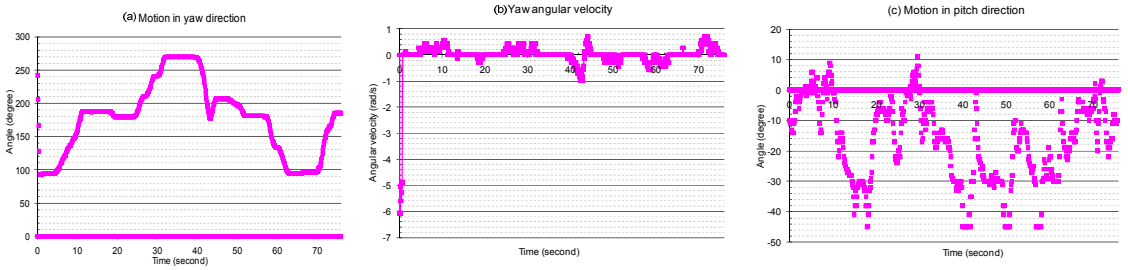

Figure 4.35. Results: sequence 2, linear transfer function

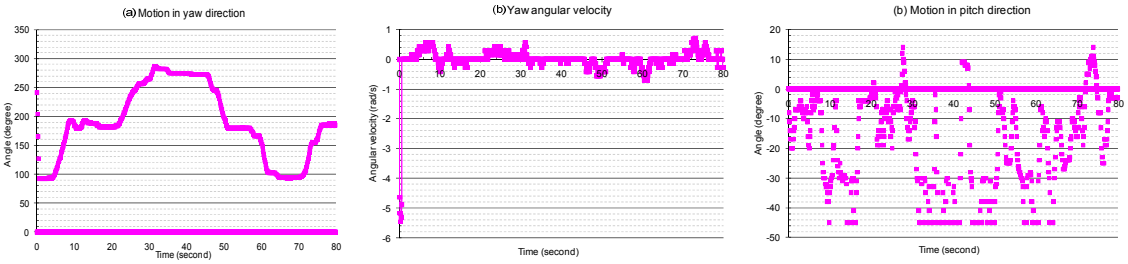

Figure 4.36. Results: sequence 2, squared/parabolic transfer function

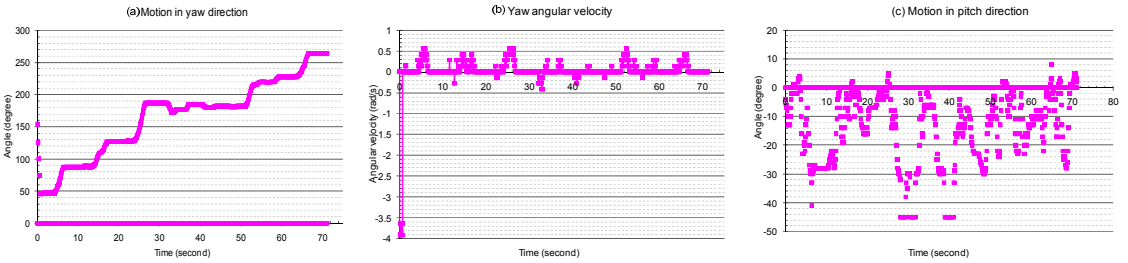

Figure 4.37. Results: sequence 3, linear transfer function

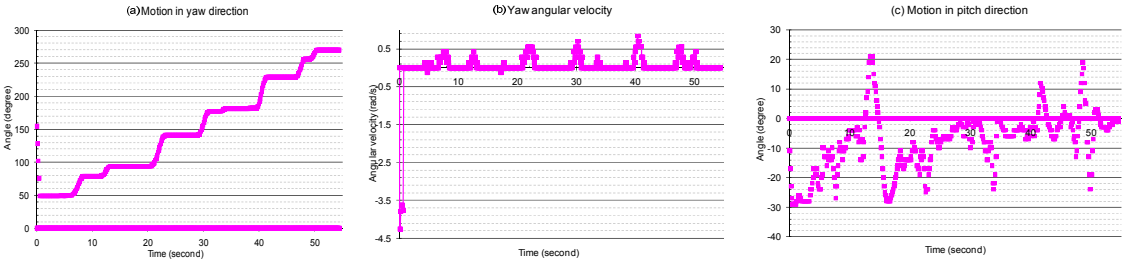

Figure 4.38. Results: sequence 3, squared/parabolic transfer function

For the target sequences 1 and 2, the target positions require the motion in both clockwise and counter-clockwise directions and the cross-coupling issue can be tricky for a human operator to cope with, especially in the case of a shorter distance (as in the target sequence 2). It is, therefore, difficult to track the target position as quickly as possible and at the same time, keep the rig balanced throughout the operation.

The single direction of motion, which can be seen in target sequence 3 (Figure 4.37 and Figure 4.38), marks a staircase shape of response and requires an understanding of only a single thrust characteristic in a clockwise direction, unless an overshoot takes place. This implies that the working conditions are easier from the operator's point of view. However, the fluctuation of angular position in the pitch axis can still be spotted but with a lower degree of reaching or striking the extreme end of the metal bar (Figure 4.37(c) and Figure 4.38(c)).

To be able to control the helicopter test rig effectively, one has to deal with an estimation of the suitable point of hand release in accordance with the angular velocity and the opposing friction in order to minimize overshooting and undershooting. It can also be observed that this human operator found the linear transfer function easier to control. Further analyses on the human performance based on the response graphs obtained from the experiments will be discussed in Chapter 6.

4.5. Summary

With reference to all experimental results presented in this chapter, the performance values associated with varied output patterns strongly reflect the accuracy characteristic of that person, which will become clearer in Chapters 5 and 6. This is true not only for a performance computation by the non-model approach (Chapter 5) but also for the model-based approach (Chapter 6) as they are essentially based on the same definitions. Hardware characteristics covered in this chapter also provide the essence for human performance analysis for both approaches.

Chapter - 5.

Analysis of the Human Performance using a Non-model Approach

5.1. Introduction

As pointed out earlier in Chapter 3 on the concept to represent a human performance in terms of speed and accuracy characteristics, this chapter introduces the way to retrieve human performance variables using the logged data directly from the operating field or a *non-model approach* for both computer and hardware-based systems. The way to present them in terms of speed and accuracy according to the Human Performance Index (HPI) concept will also be covered. This chapter starts by considering Fitts' Law and then applies the proposed average-based computation method on performance variables. Two forms of the HPI, which are of open-form and closed-form, are discussed. The results from the non-model approach provide fundamental information of human characteristics, which can lead to a validation using a model-based approach in the following chapter.

5.2. Outline for a non-model approach

In order to determine human performance in a direct manner, a control action or input-output relationship is used as the main resource for the *non-model approach*. Performance variables, which are defined to represent human characteristics in terms of speed and accuracy, will be extracted. This direct measurement can quickly, provided that proper algorithms and computer programs are optimized, measure the ratio of characteristics in terms of speed and accuracy. Ultimately, the HPI values for a particular man-machine system can be potentially used as a standard performance level for the operation of interest or as a reference for an adaptive control mechanism.

For both computer-based and hardware-based systems, the analyses will be started with an examination on the movement time of a human operator in completing the tracking task. The objective is to validate Fitts' Law on the systems with higher degree of complexity than the one-dimensional scenario of the original definition. That is, the computer-based system is based on a 2-dimensional tracking and the hardware-based system contains elements with dynamics and interactions among them. In order to apply Fitts' Law to these two systems, the output has to be analysed on a segment-by-segment basis or as a pair of targets with parameters treated according to the experimental setups and system characteristics. Further details will be discussed under Fitts' Law validation section. It is worth noting that the size of targets is fixed in both computer-based and hardware-based systems for simplicity.

Following the validation of Fitts' Law is the extraction of human performance variables with a direct use of system output. A pre-processing on the performance variables allows a mixture of variables with different monotonicity to be treated prior to the HPI computation, which effectively converts all variables to strictly increasing variables.

5.3. Fitts' Law Validation

To observe the existence of speed and accuracy tradeoff, which is fundamental to the proposed Human Performance Index (HPI) concept, Fitts' Law is primarily applied. With the focus on patterns of interaction, the computer-based system using a computer mouse as a control device involves an eye-hand coordination and interrelation between graphical-physical domain capabilities whereas the hardware-based system involves a manoeuvre of control device in relation to the aerodynamics and electrical characteristics of the helicopter test rig (as described in Chapter 4).

It is apparent from the pattern of interaction that systems of interest in this research are more complicated than the conventional stylus-based equipment, which was used as the

experimental platform for the original Fitts' Law invention (Fitts, 1954; Fitts and Peterson, 1964). The consideration on computer-based and hardware-based systems are discussed as follows.

5.3.1. Computer-based system

According to the setup of a computer-based system, a user's motion path or trajectory of a cursor in the Cartesian coordinate systems is used. This means 20 segments from 20 target positions are examined. Time responses of ten human subjects (A-J) based on two trials are presented Figure 5.1(A) to (J) correspondingly. The purpose is to illustrate a variation of time spent (movement time or *MT*) on the operation in relation to the Index of Difficulty (I_d), which is associated with the target size and location. With a consideration on 2 trials of the experiment (Trial 1 in solid lines, Trial 2 in dotted lines), the results show inconsistency of the same human subject and unsurprisingly, among other subjects. The complete set of data in Figure 5.1 are as tabulated in Table 5-1.

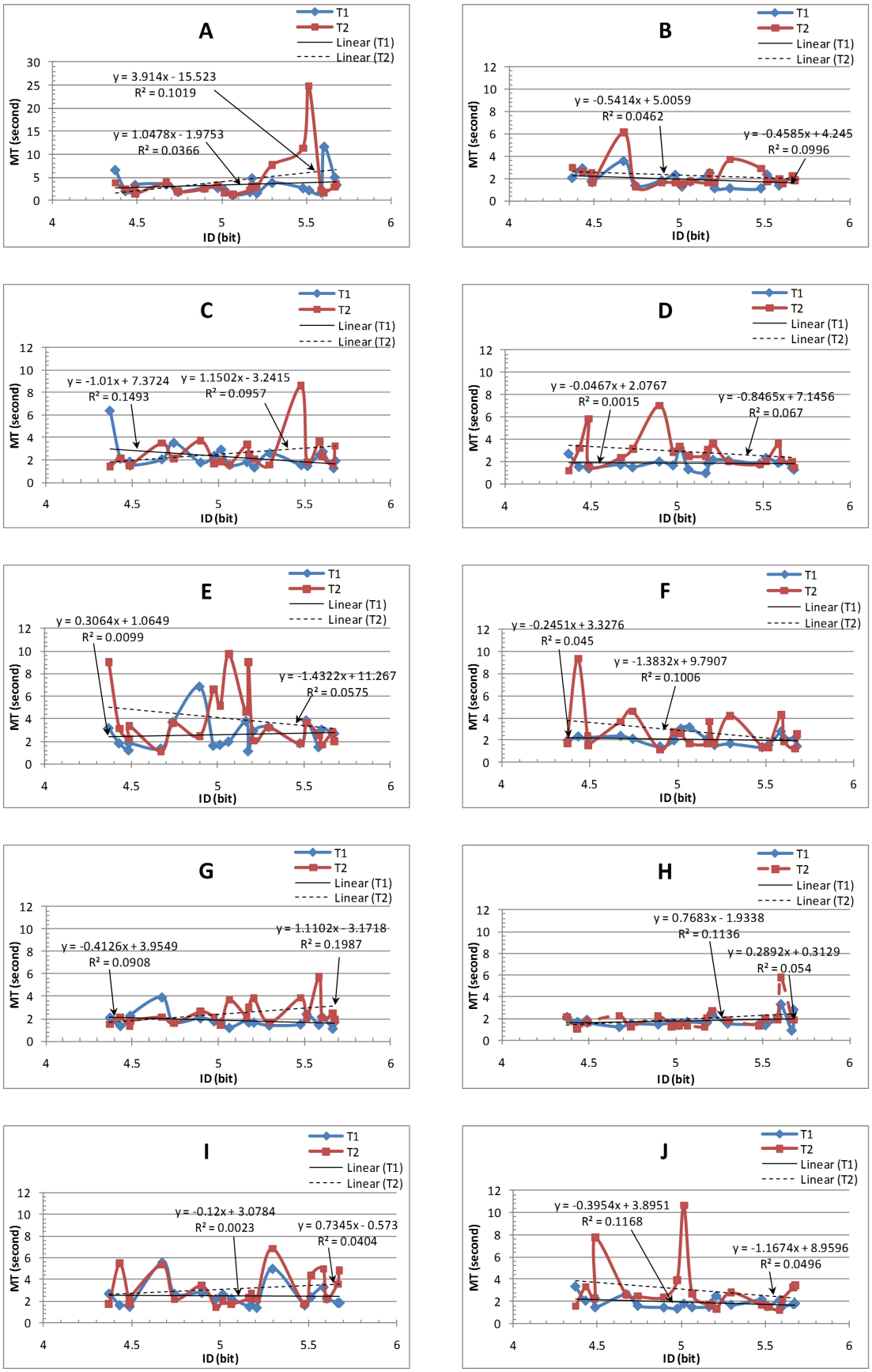

Figure 5.1. Movement time (*MT*) Vs Index of Difficulty (I_d) for the computer-based experiment (subject A-J)

Table 5-1. Movement time of target 1 to 20 for subject A to J

Segment	ID (bit)	Movement time (second)																			
		A		B		C		D		E		F		G		H		I		J	
		Trial 1	Trial 2	Trial 1	Trial 2	Trial 1	Trial 2	Trial 1	Trial 2	Trial 1	Trial 2	Trial 1	Trial 2	Trial 1	Trial 2	Trial 1	Trial 2	Trial 1	Trial 2	Trial 1	Trial 2
1	5.67	5.03	2.91	2.03	2.25	1.25	1.63	1.44	1.98	2.79	2.83	2.16	1.21	1.14	2.49	0.94	2.17	1.87	3.57	1.73	3.27
2	5.21	1.60	2.95	1.14	1.62	1.32	2.08	2.18	3.60	2.93	2.07	1.56	1.68	1.68	3.83	2.40	2.71	1.42	2.20	2.49	1.34
3	4.74	1.84	1.87	1.40	1.28	3.52	2.16	1.50	3.15	3.72	3.62	2.11	4.59	1.74	1.60	1.54	1.29	2.70	2.20	1.59	2.47
4	4.67	3.49	3.85	3.59	6.11	2.05	3.50	1.74	2.35	1.38	1.12	2.38	3.68	3.93	2.15	1.25	2.25	5.60	5.34	2.65	2.62
5	5.07	1.11	1.24	1.74	1.72	1.54	1.57	1.32	2.52	2.00	9.74	3.16	1.69	1.20	3.69	1.69	1.33	2.25	1.75	1.46	2.73
6	4.37	6.63	3.80	2.07	2.96	6.39	1.40	2.72	1.18	3.19	9.01	1.98	1.74	2.11	1.51	2.13	2.18	2.72	1.74	3.35	1.58
7	4.90	2.72	2.44	1.85	1.64	1.76	3.74	2.01	7.01	6.87	2.47	1.42	1.13	2.07	2.62	1.49	2.19	2.80	3.43	1.43	2.39
8	5.59	1.70	2.27	1.40	1.93	2.44	3.65	1.90	3.56	1.51	2.50	2.78	4.28	1.48	5.75	2.13	1.94	3.32	4.98	2.11	1.26
9	5.48	2.68	11.34	1.14	2.89	1.53	8.61	1.82	1.71	1.85	1.81	1.36	1.36	1.52	3.85	1.48	1.37	1.65	1.75	2.16	1.68
10	4.98	2.71	3.30	2.35	1.63	2.37	1.67	1.68	2.85	1.64	6.60	1.98	2.72	1.79	2.15	1.61	1.28	2.21	1.40	1.33	3.93
11	5.17	1.83	2.23	2.22	1.64	1.80	3.40	0.97	2.52	3.80	4.62	2.10	1.73	1.88	2.20	1.62	1.21	1.52	2.28	1.50	1.75
12	4.43	2.05	2.30	2.94	2.57	2.10	2.15	1.54	3.19	1.85	3.14	2.33	9.34	1.38	2.13	1.68	1.06	1.66	5.47	2.06	3.32
13	5.02	2.32	1.70	1.29	1.46	2.92	1.85	3.24	3.34	1.71	5.14	3.02	2.61	1.69	1.42	1.43	1.39	2.67	1.99	1.78	10.65
14	5.60	11.68	1.67	1.72	1.58	2.74	2.30	2.07	2.12	3.06	1.70	2.18	1.86	2.19	2.05	3.29	5.76	2.28	2.21	1.58	2.22
15	5.18	4.82	2.95	2.51	2.50	1.89	2.55	1.87	3.02	1.15	9.03	2.10	3.68	1.69	2.97	1.64	2.01	2.25	2.69	1.80	1.69
16	5.51	2.20	24.76	2.38	1.74	1.45	1.83	2.34	2.00	3.88	3.64	1.56	1.38	2.43	2.12	1.41	2.02	2.39	4.33	1.55	1.53
17	4.49	3.37	1.42	1.69	1.60	1.49	1.53	1.38	1.60	1.85	3.39	2.24	1.55	2.29	1.80	1.64	1.66	1.51	2.33	1.45	7.74
18	5.30	3.83	7.65	1.14	3.71	2.58	1.57	2.13	1.99	3.28	3.22	1.69	4.21	1.41	1.67	1.57	1.85	5.01	6.85	1.68	2.82
19	4.49	1.88	2.81	1.81	2.45	1.84	1.55	1.67	5.84	1.23	2.25	2.13	2.39	1.87	1.34	1.88	1.76	1.69	1.77	2.30	2.25
20	5.68	3.38	3.44	1.93	1.86	1.91	3.23	1.29	1.44	2.72	2.04	1.44	2.55	1.72	1.94	2.80	1.89	1.88	4.83	1.80	3.43

With regard to the alignment of the *MT*-I_d graphs, the response lines appear to have both positive and negative slope regardless of the subjects and trials. Clearer view on the validity of Fitts' law in the computer-based experiment can be drawn with reference to the summary of Fitts' parameters in Table 5-2.

Table 5-2. Summary of Fitts' Law parameters

Subject	Trial	Slope	Y-Intercept	Processing Rate (bit/s)	R^2
A	1*	1.05	-1.98	0.95	0.04
	2*	3.91	-15.52	0.26	0.10
B	1	-0.46	4.24	-2.18	0.10
	2	-0.54	5.01	-1.85	0.05
C	1	-1.01	7.37	-0.99	0.15
	2*	1.15	-3.24	0.87	0.10
D	1	-0.05	2.08	-21.40	0.00
	2	-0.85	7.15	-1.18	0.07
E	1*	0.31	1.06	3.26	0.01
	2	-1.43	11.27	-0.70	0.06
F	1	-0.25	3.33	-4.08	0.05
	2	-1.38	9.79	-0.72	0.10
G	1	-0.41	3.95	-2.42	0.09
	2*	1.11	-3.17	0.90	0.20
H	1*	0.29	0.31	3.46	0.05
	2*	0.77	-1.93	1.30	0.11
I	1	-0.12	3.08	-8.33	0.00
	2*	0.73	-0.57	1.36	0.04
J	1	-0.40	3.90	-2.53	0.12
	2	-1.17	8.96	-0.86	0.05

(Note: * means the trial with a positive slope. The processing rate is the reciprocal of this slope.)

The results in Table 5-2 show that there are variations of the sign of slopes with relatively small values of the coefficients of determination, which are only in the range of 0 and 0.2 in all cases. These results also show that the y-intercepts or margins of the movement time turn out to be both positive and negative, where the negative time margins are not as meaningful as the negative slopes.

However, according to Fitts' Law, the time response or movement time (*MT*) increases as the Index of Difficulty (I_d) increases and this effectively means a positive slope of the resultant linear regression. Based on this observation, there are only 8 out of 20 trials, from which belong to the subject A, C, E, G, H and I, that obey Fitts' Law. It turns out that both trials come from subject A and H and none of the trials from subject B, D, F and J is according to Fitts' Law. That is, the *MT* for the segments with lower I_d is larger

for the negative slopes instead of being smaller like those with positive slopes. The less steeper the slopes, the higher processing rate he/she is working at and the purpose is effectively to smooth out the response on the target position with higher I_d.

Apart from the human control strategy characteristic, it can be observed that the coefficients of determination (R^2) are relatively low in the range of 0 and 0.2, which means these experimental results loosely obey Fitts' Law. The reason for that is based on the difference between the instructions given to the human subjects in the original Fitts' experiments and the ones in this experiment. That is, human subjects were explicitly instructed to either emphasize accuracy rather than speed or perform without errors at all in the original Fitts' experiments (Fitts, 1954; Fitts and Peterson, 1964) whereas human subjects were explicitly instructed to emphasize speed rather than speed in this experiment. Such instructions directly affect human control actions in the original Fitts' experiments by forcing human subjects to spend more time as the index of difficulty increases in order to avoid error. Therefore, the low R^2 values are not surprising because human subjects are free to choose their control strategies accordingly.

5.3.2. Hardware-based system

With reference to the index of difficulty for the hardware-based experiment explained in Chapter 4, the I_d values of three target sequences are calculated to be 5.03, 6.03 and 7.03. Unlike the computer-based system, these I_d values are designed to be constant for all target positions of the same sequence and this mark the difference from the computer-based experiments. The reasons are due to lack of visual aids to the human operators and difficulties in locating an arbitrary angle in the physical domain. Therefore, a set of physical markers at distinct angles are pasted on the base of the helicopter test rig as shown in Figure 4.31(a), Chapter 4. The overview of average movement time (MT) based on the three target sequences against Index of Difficulty (I_d) for both trials can be found in Figure 5.2.

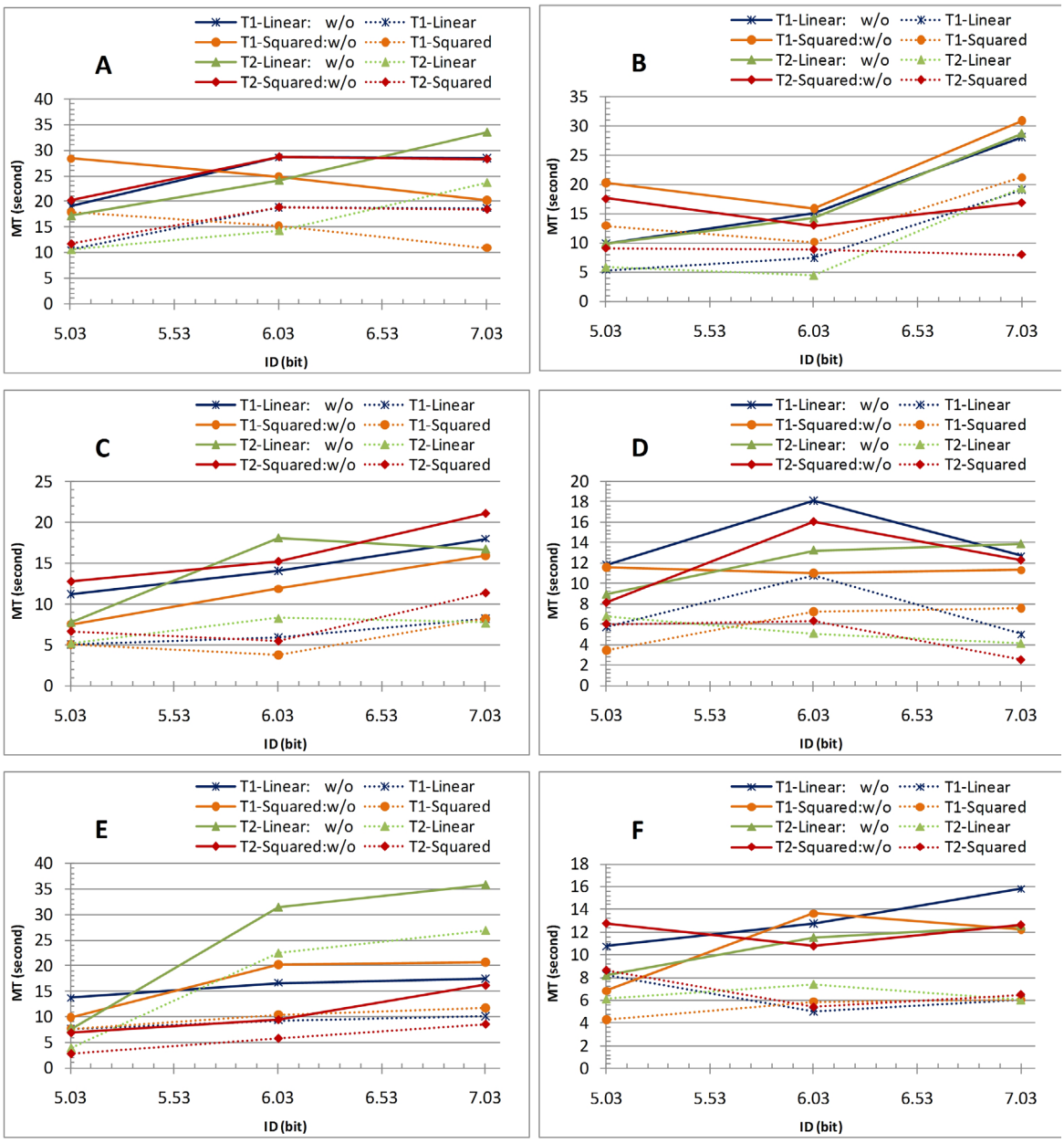

Figure 5.2. Average movement time (MT) Vs Index of Difficulty (I_d) for the helicopter test rig experiment (Subject A to F) with and without rise-time effect (dotted lines and solid lines respectively).

Based on Figure 5.2, it can be observed that there are variations of the average movement time in response to the increasing I_d across all 6 human subjects (A-F) in both trials based on two transfer functions of the joystick: linear and squared (please see the control device section in Chapter 5 for further details). Not only a variation, but also a reverse relationship to Fitts' Law can be observed in a number of trials. That is, the movement time increases as the I_d value decreases rather than decreases and *vice versa*. This is the average time spent in tracking five target positions in a particular sequence and each sequence is of the same Index of Difficulty (I_d). Interestingly, further analysis

into these graphs leads to different results if the rise time in yaw axis is considered. The term *rise-time effect* is used in this thesis to represent hardware characteristics on overall human performance, in particular, a rise-time characteristic of the helicopter test rig in yaw axis. Further details on how to determine the rise time and the algorithm involved in this calculation can be found in later section. The objective of including this rise-time effect is to separate hardware characteristic from a genuine human performance. Table 5-3 shows a summary of the linear regression equations derived from all subjects based on Figure 5.2.

Table 5-3. Linear regression equations for subject A~F with and without rise-time effect (denoted as w and w/o respectively)

Subject	Trial	Transfer Function	Slope		Y-Intercept		Processing Rate (Bit/S)		R^2	
			w/o	w	w/o	w	w/o	w	w/o	w
A	T1	Linear	4.10	4.71	-8.70	-3.07	0.24	0.21	0.74	0.74
		Squared	**-3.47**	**-4.05**	35.56	48.94	-0.29	-0.25	0.98	0.99
	T2	Linear	6.55	8.16	-23.23	-24.31	0.15	0.12	0.94	0.99
		Squared	3.37	3.99	-3.97	1.65	0.30	0.25	0.70	0.71
B	T1	Linear	6.86	9.09	-30.76	-37.14	0.15	0.11	0.86	0.95
		Squared	4.12	5.31	-10.09	-9.69	0.24	0.19	0.51	0.47
	T2	Linear	6.78	9.40	-31.03	-39.08	0.15	0.11	0.67	0.91
		Squared	-0.56	-0.34	12.00	17.83	-1.78	-2.98	0.90	0.02
C	T1	Linear	1.60	3.41	-3.25	-6.17	0.62	0.29	0.94	0.99
		Squared	1.57	4.19	-3.81	-13.48	0.64	0.24	0.47	1.00
	T2	Linear	1.26	4.49	-0.49	-12.91	0.80	0.22	0.59	0.64
		Squared	2.33	4.14	-6.19	-8.57	0.43	0.24	0.57	0.95
D	T1	Linear	-0.36	0.41	9.35	11.73	-2.75	2.44	0.01	0.01
		Squared	**2.06**	**-0.14**	-6.35	12.10	0.49	-7.36	0.81	0.20
	T2	Linear	-1.34	2.48	13.39	-2.96	-0.75	0.40	0.98	0.84
		Squared	-1.74	2.08	15.39	-0.41	-0.58	0.48	0.69	0.27
E	T1	Linear	1.26	1.87	1.41	4.65	0.80	0.53	0.96	0.90
		Squared	2.01	5.44	-2.17	-15.89	0.50	0.18	0.96	0.78
	T2	Linear	11.41	14.02	-51.09	-59.66	0.09	0.07	0.89	0.86
		Squared	2.84	4.65	-11.47	-17.19	0.35	0.22	1.00	0.94
F	T1	Linear	-1.09	2.52	13.03	-2.14	-0.91	0.40	0.43	0.98
		Squared	0.88	2.69	0.13	-5.34	1.14	0.37	0.83	0.56
	T2	Linear	-0.04	2.16	6.73	-2.28	-28.50	0.46	0.00	0.92
		Squared	-1.06	-0.06	13.26	12.42	-0.94	-16.01	0.42	0.00

(Note: The boldface letter represents the trial with no improvement.)

With regard to the parameters presented in Figure 5.2, the negative slopes now, interestingly, turn into positive slopes upon an inclusion of a rise-time effect except the rows with boldface numbers, as presented in Table 5-3. A shift of negative to positive slopes and a decrease of negative slope values are collectively referred to as an *improvement* on Fitts' Law validity. This means 22 out of 24 data sets (rather than 14 before including a rise-time effect) are now according to Fitts' Law. According to this

result, the effective movement time or the movement time with rise-time effect can then be reasonably used in place of the original movement time or time spent in the operation.

For the interaction between human and hardware systems, it is obvious that a genuine human performance can be suppressed or influenced by hardware characteristics and the degree of influence is subjective. In the helicopter test rig, pitch and yaw motors together with propellers play vital roles in affecting human performance. The outcome from one control signal or joystick angle is delayed by a mechanism to produce the aerodynamic forces to overcome the rotational friction at the bearings. Each step requires a certain amount of time for the hardware to respond and this should not be accountable for the time human spends to complete a task whereas a computer response can be reasonably assumed instantaneous or simultaneous with human action due to its high-speed microprocessor. Therefore, this is a major difference between the analyses on hardware-based system and computer-based system.

To summarize, a rise-time effect of the helicopter test rig plays important role in affecting human performance and the validity of the original Fitts' Law. The ability to estimate helicopter's rise time in relation to the control input can potentially reduce the percentage of overshoot and undershoot of the system as a whole. Therefore, a consideration of rise-time effect is reasonable and needs to be included in human performance computation.

5.4. Performance Variables

According to the proposed HPI concept in Chapter 4, the use of speed and accuracy criteria in human performance evaluation will now be implemented. Two forms of HPI, which are open and closed forms, will be presented with a set of performance variables pertinent to these two performance criteria.

Steps to evaluate human performance level using a non-model approach start from selecting physical quantities or performance variables of interest, defining how these selected quantities can be retrieved or calculated and classifying them into either speed or accuracy variables. The HPI structure used in this thesis can be found in Figure 5.3.

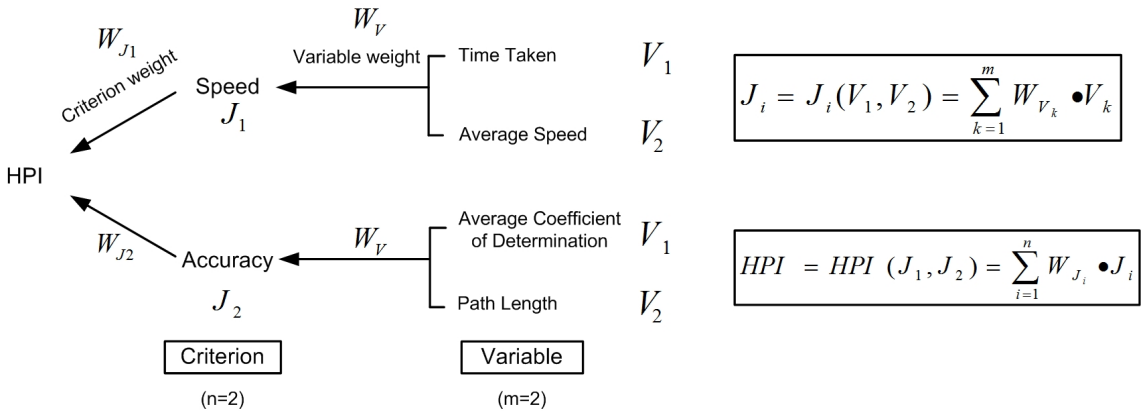

Figure 5.3. Human Performance Index (HPI) structure with speed and accuracy as the main contributors of human performance

In general, a HPI structure is comprised of two *performance criteria* and each criterion is comprised of several *performance criterion variables* or *performance variables*. For an implementation of HPI concept in this thesis, the performance criteria are chosen to be speed and accuracy, as described in Chapter 3. Each performance variable is classified as either speed or accuracy criterion based on its contribution and effect on the overall performance. Increment or decrement of the selected variables helps in determining its importance as the affecting factor to the performance as a whole. It is obvious that these performance criteria may not have common monotonicity. A processing is, therefore, required prior to a performance computation.

For simplicity, two performance variables are selected for each performance criterion and applied in both computer-based and hardware-based experiments. That is, a time taken and average speed are used as speed variables and a coefficient of determination and Root Mean Squared Errors (RMSE) are used as accuracy variables. The coefficient of determination in this thesis is redefined such that its value represents a closeness of a linear regression of user's trajectory to the ideal path rather than the user's actual path.

An overview on these performance variables based on a computer-based system can be found in Figure 5.4.

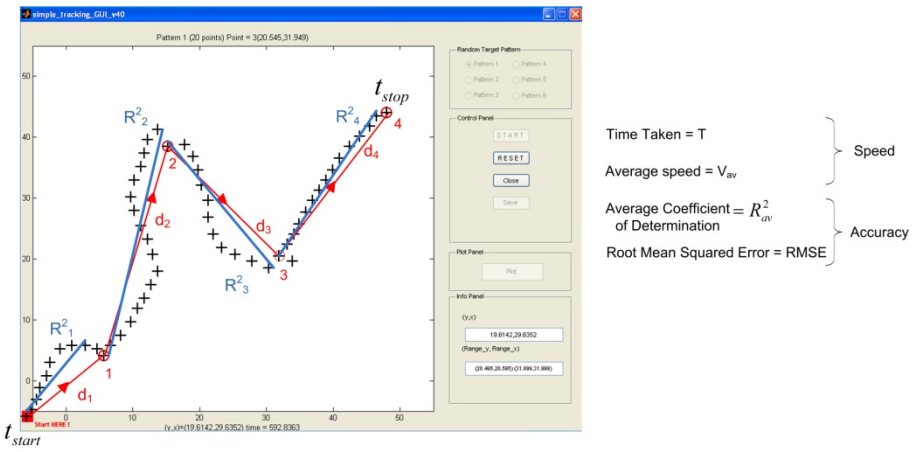

Figure 5.4. Control action of one human subject (target number 1 to 4): + represents actual user's cursor position and O represents target positions (1-4, in this figure). The straight lines with arrows connect between targets and the plain straight lines represent a linear regression line based on user's trajectory.

In order to retrieve or calculate the performance variables as defined above, it is apparent that user's trajectory needs to be treated as a set of segments, where each segment or a pair of previous and current target positions is examined one by one. A model-based analysis is also implemented in this fashion and its content will be covered in Chapter 6. Definitions on speed and accuracy variables are explained as follows, starting from a speed criterion.

5.4.1. Speed criterion

The speed criterion, as one of the performance criteria used in this thesis, is categorised based on a condition whether the variables contributes to a rate of completion. In other words, the candidate variables need to have a characteristic of time efficiency to be classified as a speed criterion. Such justification is solely with reference to the control action of a human operator and this seems to be straightforward for the non-model approach as an observation can be made directly. In this thesis, a time taken and average speed are chosen as two physical quantities for the speed criterion. The computer-based

and hardware-based systems are treated separately to clarify the accountability of hardware characteristics and the experimental setup.

5.4.1.1. Computer-based system

Figure 5.5 illustrates two speed variables based on the snapshot of a MATLAB GUI (as explained in Chapter 4).

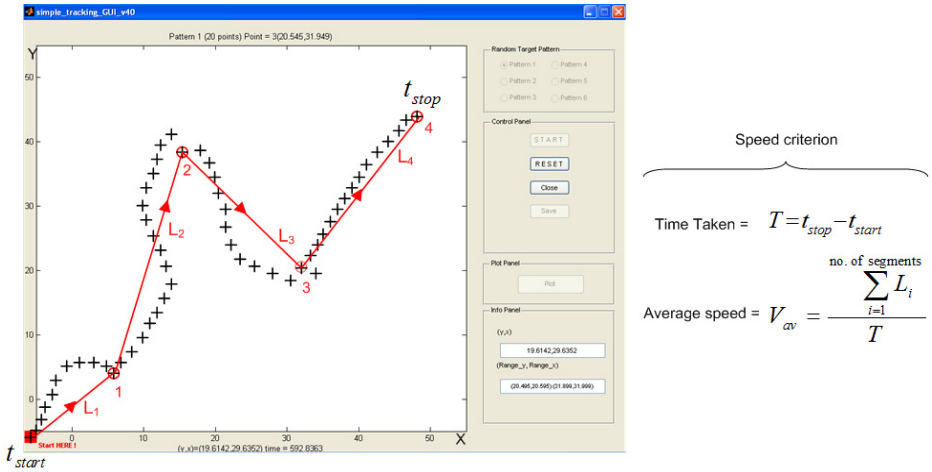

Figure 5.5. Speed variables

Time taken (T) is defined as a time stamp at the beginning (T_{start}) subtracted from a time stamp at the final target position (T_{stop}) as shown in Equation (5-1).

$$T = T_{stop} - T_{start} \tag{5-1}$$

For an *average speed (V_{av}),* a calculation refers to an ideal or shortest path between a pair of target positions. It is defined as a summation of linear segments distance between a pair of target positions divided by a time taken (T) from Equation (5-1). These two physical quantities effectively reflect how fast a human operator performs and therefore, both of these variables can be reasonably classified as a speed criterion.

$$V_{av} = \frac{\sum_{i=1}^{\text{no. of segments}} L_i}{T} \tag{5-2}$$

Where L_i is a segment length or a length of a piecewise linear equation (L_i) between a pair of targets.

Now that these speed variables have been defined, an interpretation of these two variables is straightforward despite the difference in monotonicity. That is, less time spent by a human operator means a higher performance in terms of speed characteristic whereas the opposite interpretation is required for the average velocity. It is worth noting that there is no accountability of any hardware characteristics into the definitions of the speed variables for the computer-based system. Hence, the following section introduces an effective time taken to represent a speed criterion for a use in the hardware-based system.

5.4.1.2. Hardware-based system

In contrast to a computer-based system where a computer responds at a fraction of second, it is definitely not the case for a hardware-based system (as described in Section 4.4.1.2, Chapter 4). A decent amount of time in the range of 2-7 seconds is required to trigger a yaw motion depending on the control input from the joystick. In this experiment, a rise time for pitch axis can be safely neglected because the mission is only to keep the metal bar closest to its balanced state while moving along the yaw axis. Moreover, thrust characteristics (as presented in Figure 4.20, Chapter 4) show that the aerodynamic forces from a yaw propeller alone can cause a pitch axis motion in both upward and downward directions. Therefore, only a compensation for excessive thrust is required from time to time to fulfill this operation. The issues regarding a control of the helicopter test rig are as summarized in Figure 5.6.

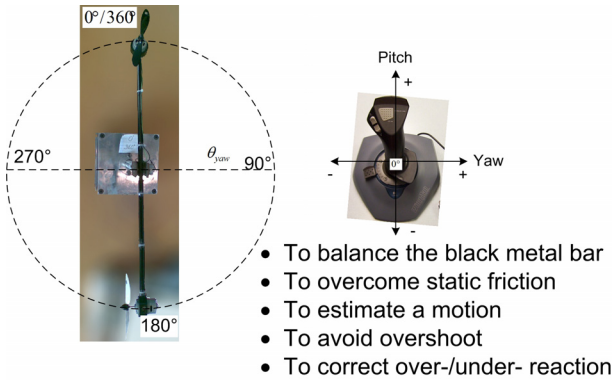

Figure 5.6. Issues about controlling a helicopter test rig from human operator's point of view

- **Rise-time effect**

Based on hardware characteristics in yaw axis, it is unreasonable to use a time taken directly as a speed variable unless it is deducted by a yaw rise-time. The resultant movement time then represents only a human response with minimal hardware effect. Figure 5.7(a) shows how human performance is affected by a rise time of the helicopter test rig based on the control signals in Figure 5.7(b). Figure 5.7 is based on one trial of a human subject in completing a target sequence 1 using a joystick.

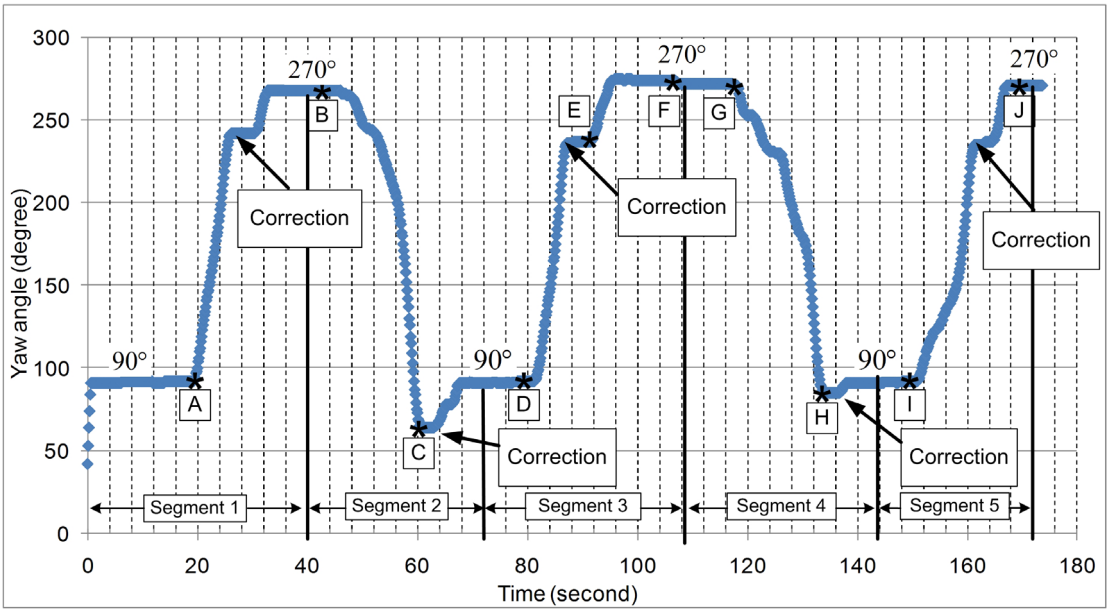

a) Time response in the yaw axis (θ_{yaw} Vs Time)

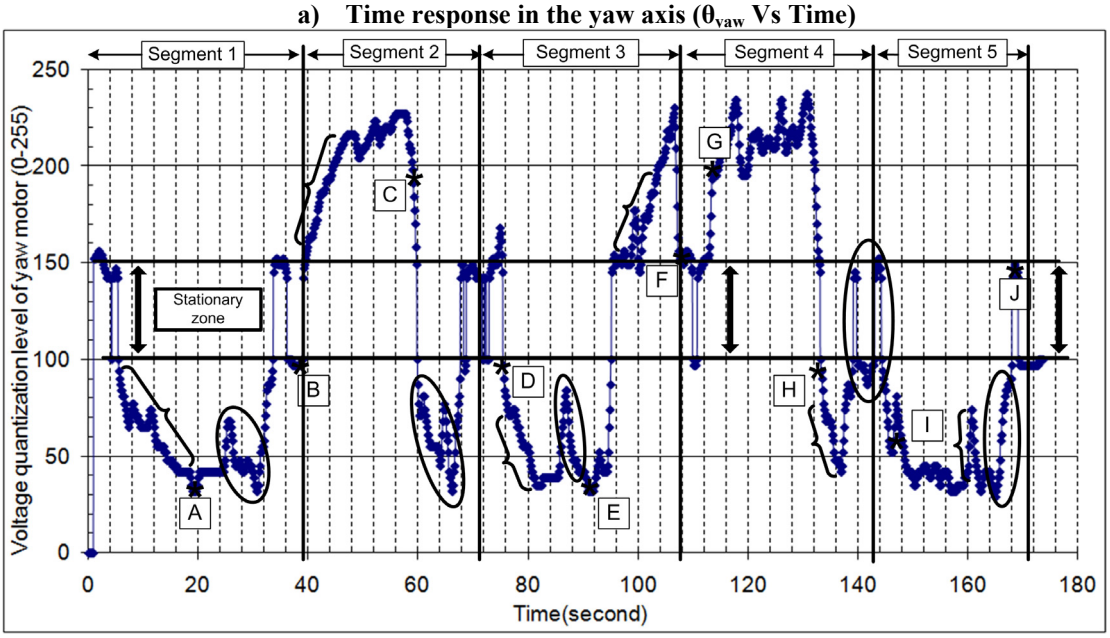

b) Control signal of the yaw motor (U_{yaw} Vs Time)

Figure 5.7. Rise-time effect of a helicopter test rig on human performance: linear transfer function (an open-loop controller), target sequence 1 (90°►270°►90°►270°►90°►270°)

Based on Figure 5.7, each segment of the target sequence is analysed side by side with its associated control signals to examine the response pattern due to an overshoot and undershoot of a human operator. The action following any overshoot and undershoot is referred to as *correction,* as shown in Figure 5.7(a). A number of set points, from A to J, are presented on the graphs to mark important occurrences related to the rise-time effect. Starting from points A, B, D, F, I and J: these points are the start and stop positions according to the timeline segmentation. For the first segment, Point A is the start position and point B is the stop position. For the second segment, Point B is the start position and Point D is the stop position, and so on. Basically, these segments can be regarded as a pair of target sequence from the first target position to the last one.

To initiate a motion, a minimum voltage is required and the action to keep increasing the voltage is very common for every human subject to sense the magnitude of friction. That means a human operator needs to apply the voltage outside of the *stationary zone*, as presented by the area inside the black double-headed arrows in Figure 5.7(b)). Before the motion takes place, pre-movements can be observed and they are shown by curly brackets. Human's action to overcome a static friction tends to last relatively too long and often end up in over-doing it. Moreover, a stationary zone or a range of control signal from 100 to 150 is included in Figure 5.7(b) to help determining undershoot or overshoot in accordance with Figure 5.7(a). For instance, there is a sudden drop of yaw velocity to zero in segment 1 or the motion from point A to point B. The corresponding time segment in Figure 5.7(b) shows a fluctuation of control signals and this indicates a correction of control action in terms of undershoot or overshoot by a human operator.

To look further into this, it can be observed that the control signal residing within a stationary zone and the yaw angle stays constant at approximately t=40 seconds. This means a correction is classified as *undershoot* when there is no reversal of the control signal or the control signal stays either below 100 or above 150 throughout the segment of interest (below 100 in this example). Same analysis can be made on other segments and it turns out that segment 5 also contains the undershoot too.

In case of an overshoot, the control signals wanders across the stationary zone from one side to the opposite side. That is, the control signals fall from above 150 to below 100 or rise from below 100 to above 150. Therefore, this behavior of control signals can be simply referred to as a control signal *crossover*. For instance, a swing of control signal from above 150 to below 100 can be spotted in segment 2 and segment 4 whereas a swing from below 100 to above 150 can be spotted in segment 3. These examples fall into the same category of control action correction by a human operator.

- **Average control signal calculation**

It can be seen in the previous section that a rise-time effect is related to the yaw motor control signal. To estimate the rise-time effect, there are two ways to calculate an average control signal of the motor for undershoot overshoot cases to represent an effective rise-time. Steps of calculation differ due to the response pattern. Figure 5.8 shows a summary of undershoot and overshoot with reference to Figure 5.7(b). The blocks with solid lines mark the range of control signal to be averaged over a segment, which will then be used for a rise-time calculation.

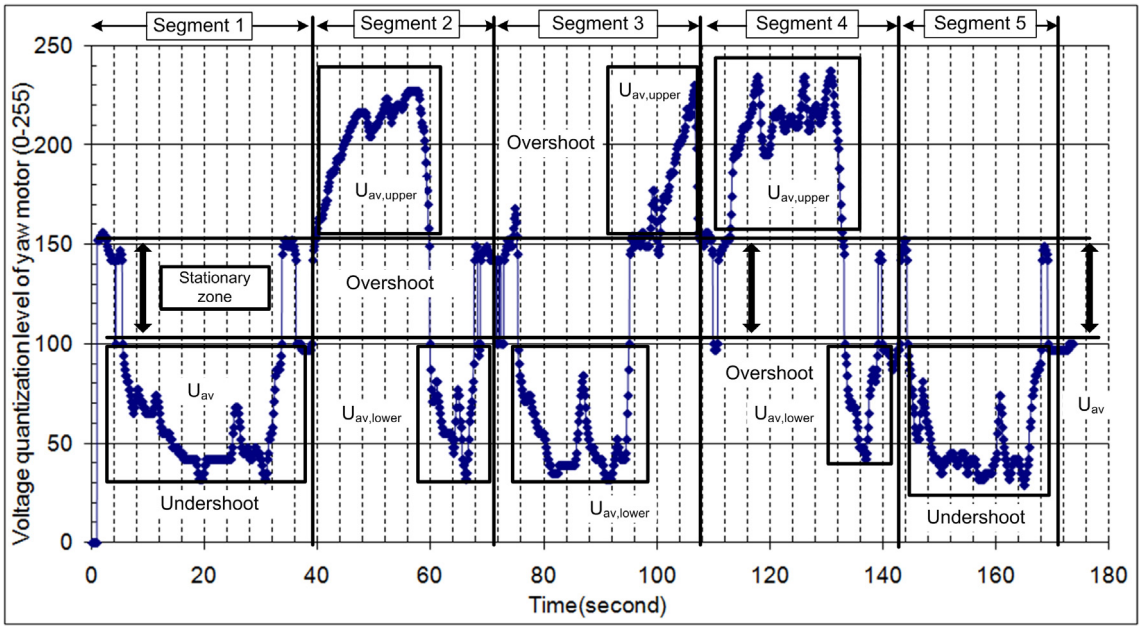

Figure 5.8. Summary on undershoots and overshoots along with the range for U_{av} calculation

Figure 5.8 also shows that, in case of an undershoot, the control signal residing in the stationary zone has to be dropped to avoid an unreasonably large rise time resulted from the polynomial equations in Equation (5-5). A split of control signal into two parts to exclude this stationary zone is also essential in case of an overshoot for the same reason. An average is then calculated over each part of the control signal and its sum is used to represent a rise-time for the whole time segment.

Undershoot:

$$U_{av} = \sum_{i=n}^{m} U_i \tag{5-3}$$

Where n and m are the first and last sample at the boundary of the stationary zone

Overshoot:

$$U_{av} = U_{av,upper} + U_{av,lower} = \sum_{i=n}^{m} U_i + \sum_{j=o}^{p} U_j \tag{5-4}$$

Where n, m and o, p are the first and last sample at the boundary of the stationary zone for the upper and lower parts of the stationary zone respectively

Yaw Rise time (RT) =

$$-5\times10^{-11}x^6 + 4\times10^{-8}x^5 - 1\times10^{-5}x^4 + 0.0011x^3 - 0.0315x^2 + 0.2735x + 1.6879 \tag{5-5}$$

Where x = U_{av} from either (5-3) or (5-4)

Effective time taken: $T_{eff} = T - RT$ (5-6)

Where T is the raw time taken

Ideally, an understanding on system dynamics allows a correct adjustment on the system response and this can in turn minimize the hardware effects. As shown in Figure 5.6, human users need to overcome the static friction at the rotational bearings, estimate the motion together with the direction of rotation and correct his/her over-reaction after realizing an undershoot/overshoot has taken place. Even though the best strategy to avoid any undershoot or overshoot is to release the joystick at the appropriate helicopter's speed, this is hard to achieve and requires time for familiarisation with the helicopter test rig.

In conclusion, a rise-time effect from the helicopter test rig appears in the forms of undershoot and overshoot. A calculation of an average control signal for these two cases

is according to Equations (5-3) or (5-4) respectively. T_{eff} can now be used in place of the original time taken (T) and be used for further performance computation.

5.4.2. Accuracy criterion

Accuracy criterion is another performance criterion proposed as part of HPI structure for a man-machine system in this thesis. The criterion itself is defined to reflect a variation of an output of a human operator from an ideal control action. That is, a trajectory followed by a human operator is compared against an ideal trajectory on a segment-by-segment basis and the accuracy variables are to be calculated accordingly.

Regarding the accuracy variables in this thesis, a coefficient of determination (R^2_{av}) and Root Mean Squared Error (RMSE) were selected and the definitions differ from system to system due to settings and experimental setups. Further detail on how the context of the experiment can affect the definitions will be given shortly.

It is worth noting that the coefficient of determination is redefined in such a way that the closeness between the linear regression line and the ideal line or a straight line connecting a pair of target positions is obtained instead of the original goodness of fit. In order to do this, a 2-dimensional trajectory is used and this will be explained separately for the computer and hardware-based systems.

5.4.2.1. Computer-based system

With reference to the logged data from a computer-based system, an example of a 2-dimensional trajectory from target 1 to 4 of one human subject is presented in Figure 5.9. The straight line connected between target positions (with arrows) represents an ideal path for that particular segment and the difference from this line is considered an error. For the plain straight lines, they represent the linear regression lines based on

user's path and they are used for a calculation of the redefined coefficient of determination.

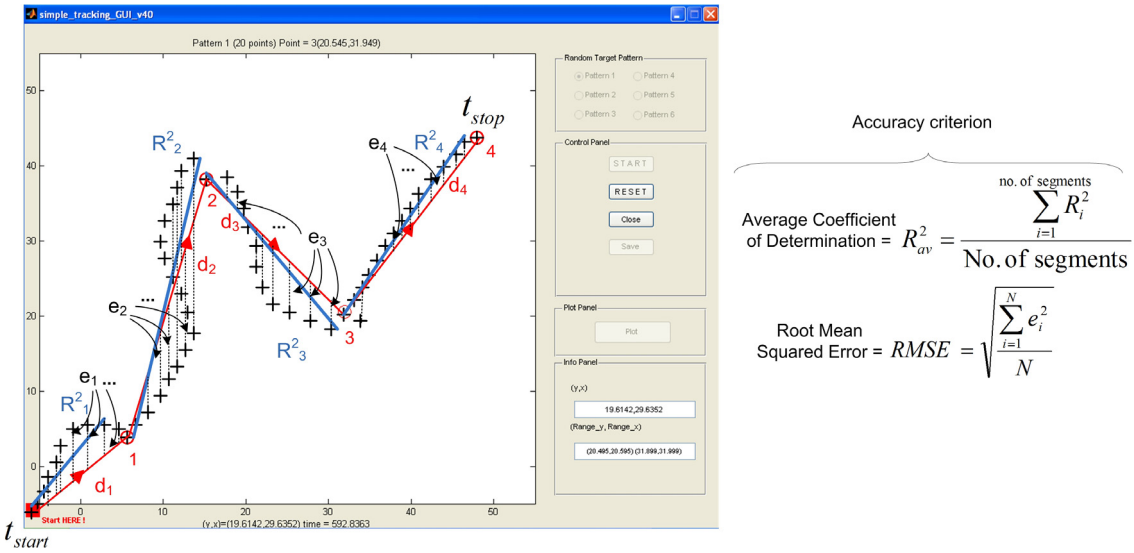

Figure 5.9. A 2-dimensional trajectory based on a computer-based system

Average coefficient of determination (R^2_{av}) is defined as a quantity to represent an average *goodness of fit* across all target-to-target segments. This variable aims to quantify the closeness of a straight-line path based on user's data to an ideal path (a straight line connecting between target positions). Such quantity is based on a linear regression concept with a coefficient of determination (R^2) value being a magnitude of closeness between actual data and its resulting linear regression equation. Therefore, the variables involved needs to be redefined, but firstly, the original coefficient of determination is as follows: (Montgomery , Runger et al., 2003).

$$R^2 = 1 - \frac{SS_E}{SS_T} \tag{5-7}$$

$$SS_E = \sum_{i=1}^{n} (y_i - \hat{y}_i)^2 \text{ = Sum of a Squared Error } (y_i \text{ = actual data, } \hat{y}_i \text{ = fitted data}) \tag{5-8}$$

$$SS_T = \sum_{i=1}^{n} (\hat{y}_i - \bar{y})^2 \text{ = Sum of a Squared Total } (\bar{y} \text{ = average value of actual data}) \tag{5-9}$$

To quantify *a closeness of user's straight-line path to the ideal path* instead of *a closeness of user's path and its associated linear regression equation* (original definition), the steps to complete this operation are as presented in Figure 5.10.

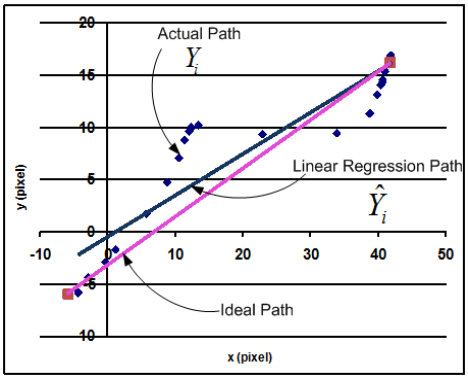

(a) Original: Y_i for actual data and $\hat{Y}_i$ for fitted data on a regression line

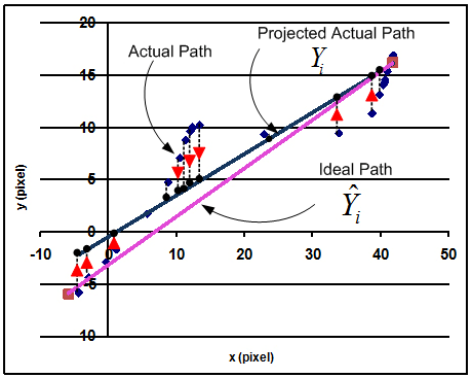

(b) Redefined: Y_i for projected actual data and $\hat{Y}_i$ for fitted ideal data

Figure 5.10. Comparison of the original and redefined coefficient of determination parameters based on one target segment

In effect, y_i is redefined as the *projected actual data* and $\hat{Y}_i$ *is* redefined as the *fitted ideal data* as illustrated in Figure 5.10(b). A redefined coefficient of determination can now be calculated directly from Equation (5-7) with a substitution of the original variables by those of redefined variables. To determine goodness for all segments, a redefined coefficient of determination is to be averaged over a number of segments as follows.

$$R_{av}^2 = \frac{\sum_{i=1}^{\text{no. of segments}} R_i^2}{\text{No. of segments}} \tag{5-10}$$

For a Root Mean Squared Error or RMSE, it is defined as an error between a cursor position (x_{cursor},y_{cursor}) and a target or ideal position (x_{target},y_{target}) on an ideal straight line connected between a pair of targets.

$$e = \sqrt{(x_{target} - x_{cursor})^2 + (y_{target} - y_{cursor})^2} \tag{5-11}$$

$$RMSE = \sqrt{\frac{\sum_{i=1}^{N} e_i^2}{N}} \tag{5-12}$$

Where N = total number of samples in the corresponding segment.

The result from Equation (5-12) averaged by a number of segments together with other raw performance variables obtained earlier are now ready for further processing for HPI computation.

5.4.2.2. Hardware-based system

In order to calculate accuracy variables from a helicopter test rig, there is a slight difference from a computer-based system regarding an ideal path or trajectory. Due to the objective to focus on yaw axis motion and keep the metal bar balanced, it is safe to assume that the ideal trajectory is purely based on a yaw angle with a pitch angle set to zero degree throughout all target segments. In other words, a helicopter motion can be assumed to strictly move only in Azimuth or horizontal plane. Now the ideal trajectory can be simply viewed as a horizontal line, whose y-axis is a pitch angle and x-axis is a yaw angle (Figure 5.11).

From human operator's point of view, he/she has to rotate the helicopter test rig around horizontally, stop to locate the target position and keep the metal bar horizontal at all times. Angle orientation in yaw and pitch directions are according to Figure 5.11(a) and (b). Figure 5.11(c) also shows a sample of target tracking from a yaw angle 90° to 270° with all user's positions presented as dots, user's linear regression presented as the solid line and the ideal trajectory presented as the dotted line.

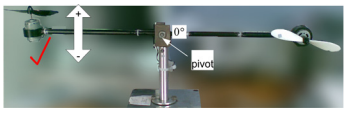

(a) Pitch angle orientation

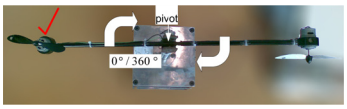

(b) Yaw angle orientation

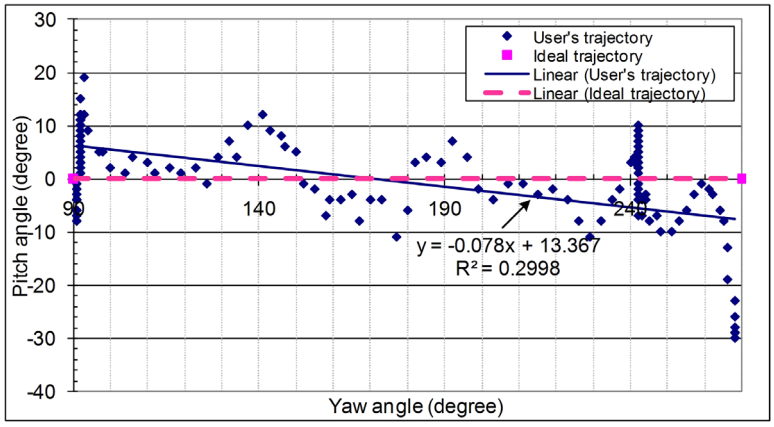

(c) Motion trajectory from 90° to 270° in yaw direction

Figure 5.11. A 2-dimensional trajectory based on a hardware-based system

Now the accuracy variables can be calculated with a horizontal line connected between yaw angles of interest as a reference or ideal path. Steps of calculation remain the same as the computer-based system and no other changes are required for parameters in the given formula.

To conclude, the same set of performance variables as part of speed and accuracy criteria for the computer-based system are also used in the hardware-based system. The only remark before usage is when retrieving these performance variables from a system with hardware and dynamics, that is, issues on how to incorporate hardware effects and in what manner it should be applied are to be carefully defined. Therefore, it is the matter of modifying the existing set of performance variables rather than defining a set of performance variables for hardware systems.

5.5. Human Performance Index (HPI) Forms

A HPI computation starts from retrieving performance variables from user's data (considered as raw), applying average normalization and then deciding if a reflection process is required. This depends on a monotonicity property of the performance variable of interest as a reflection process is only required for strictly decreasing variables. The steps to process raw performance variables can be found in Figure 5.12 and Figure 5.13.

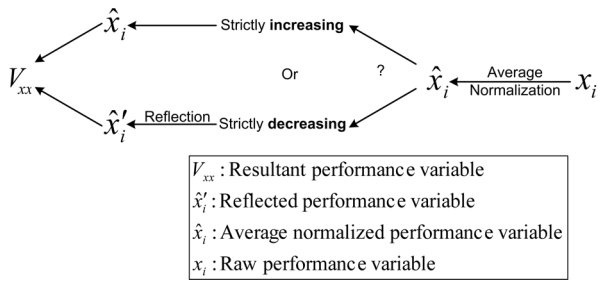

Figure 5.12. Processing of a raw performance variable

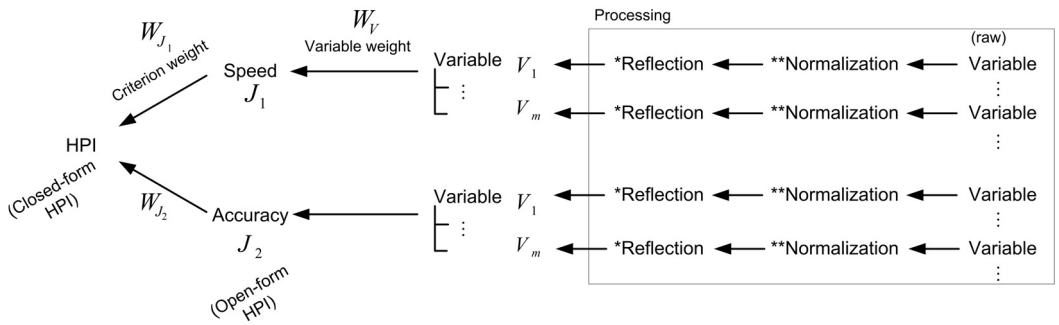

Figure 5.13. Steps for an Average-based Human Performance Index (HPI) computation

With regard to the speed and accuracy variables obtained from the previous section, V_{av} and R^2_{av} are strictly increasing whereas *T* and *RMSE* are strictly decreasing. Therefore, a reflection process is required for both *T* and *RMSE*, as an extra stage following the average normalization. For the abbreviations used in the tables and this point onwards, *avg* is for an average value, *avg-norm* is for normalization by an average value and *refl* is for a reflected value for the performance variable of interest. After applying average normalization and reflection to the performance variables, speed and accuracy scores are now centred around their average, which is that of 1.00, and they are also strictly increasing. These performance variables are ready to be used for a closed-form HPI computation, where the set of weightings are applied to the performance scores.

Up to this point (according to Figure 5.13), all the performance variables are strictly increasing and ready to be presented in either an open or closed-form. An open form HPI will be presented first and then followed by a closed-form HPI for both computer and hardware-based systems correspondingly.

5.5.1. Open-form HPI

Based on the definition of an open-form HPI given in Chapter 3, the performance variables of the same criterion are used to represent a HPI in an open form. The fully processed performance variables with equal weightings for *speed and accuracy criteria* are referred to as *speed and accuracy scores* respectively or simply *performance scores*. Regarding the performance variable weight, it is assumed that each variable is equally significant throughout all experiments. Therefore, for the system with 2 performance variables, the value of W_{VK} is simply equal to 0.5. A criterion score can then be regarded as a summation of those terms as shown below:

$$J_i = \sum_{k=1}^{m} W_{V_k} \cdot V_k \tag{5-13}$$

Where *i*=1 for a speed score and *i*=2 for an accuracy score. m is equal to a number of raw performance variables (in this case, m = 2 for both speed and accuracy scores). The

open-form HPI starting from the computer-based system will now be presented as follows.

5.5.1.1. Computer-based system

For the computer-based experiment, there are 2 sets of data based on 10 human subjects performing on the same target sequence, namely Trial 1 and 2. These 2 trials are used in the analysis for comparison purposes and to show a variation of human performance based on the HPI concept.

- *Speed score*

Speed variables consisting of raw and processed speed variables V_{av} and T from Trial 1 and 2 are presented in Table 5-4 and Table 5-5 respectively. V_{av} is a speed variable with strictly increasing monotonicity, therefore only average normalisation is required whereas T requires both average normalisation and reflection to convert its monotonicity to that of an increasing one. It can be observed from both tables that the average value of any speed variables is 1.00, which is according to the definition proposed in Chapter 3. The results indicate that a person with a speed score higher than 1.00 can be considered above average whereas a person with a speed score lower than 1.00 can be considered below average. Moreover, the standard deviation from these two trials can be observed to be very close to each other and that reflects a constant emphasis on speed in completing the operation.

Table 5-4. Trial 1: Speed score table (J_1) – computer-based system

Subject	V_{av} (cm/s)	$\mathbf{V_{avg\text{-}norm}}$	T(s)	$T_{avg\text{-}norm}$	$\mathbf{T_{refl}}$	Speed score
A	0.31	0.60	67.19	1.50	**0.50**	0.55
B	0.58	1.10	39.53	0.88	**1.12**	1.11
C	0.44	0.84	45.57	1.02	**0.98**	0.91
D	0.61	1.17	37.47	0.84	**1.16**	1.17
E	0.52	0.99	52.70	1.17	**0.83**	0.91
F	0.60	1.16	42.40	0.95	**1.05**	1.11
G	0.60	1.15	37.50	0.84	**1.16**	1.15
H	0.57	1.10	36.23	0.81	**1.19**	1.14
I	0.40	0.76	51.85	1.16	**0.84**	0.80
J	0.60	1.15	38.11	0.85	**1.15**	1.15
Average	0.52	**1.00**	44.85	1.00	**1.00**	1.00
SD	0.10	**0.20**	9.85	0.22	**0.22**	0.20

Table 5-5. Trial 2: Speed score table (J_1) – computer-based system

Subject	V_{av} (cm/s)	$\mathbf{V_{avg\text{-}norm}}$	T(s)	$T_{avg\text{-}norm}$	$\mathbf{T_{refl}}$	Speed score
A	0.24	0.60	86.91	1.48	**0.52**	0.56
B	0.51	1.26	45.15	0.77	**1.23**	1.24
C	0.39	0.96	51.94	0.88	**1.12**	1.04
D	0.40	1.00	56.97	0.97	**1.03**	1.02
E	0.34	0.85	79.94	1.36	**0.64**	0.74
F	0.46	1.15	55.39	0.94	**1.06**	1.10
G	0.46	1.13	49.28	0.84	**1.16**	1.15
H	0.53	1.31	39.33	0.67	**1.33**	1.32
I	0.33	0.81	63.11	1.07	**0.93**	0.87
J	0.38	0.94	60.67	1.03	**0.97**	0.95
Average	0.40	**1.00**	58.87	1.00	**1.00**	1.00
SD	0.09	**0.22**	14.82	0.25	**0.25**	0.23

From the tabulated speed scores given above, Figure 5.14 shows two graphs of speed scores for subject A up to subject J based on Trials 1 and 2. Noticeable difference between these two trials can be spotted across all subjects except subject A and F where the difference is only 0.01. However, it is interesting to see that there is no difference at all for subject G and that reflects his/her reliability as part of a control loop.

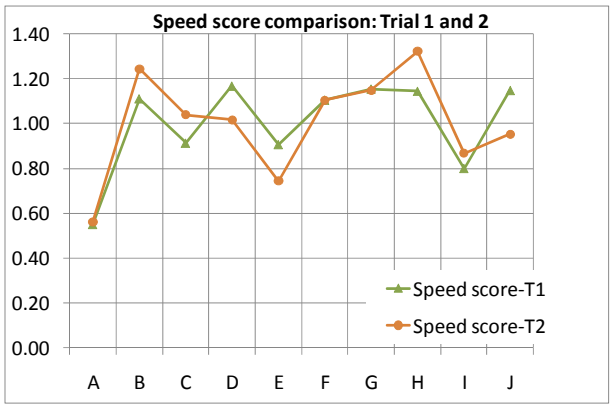

Subject	ΔJ1
A	0.01
B	0.13
C	0.13
D	0.15
E	0.16
F	0.00
G	0.01
H	0.18
I	0.07
J	0.20
Average	0.10
SD	0.08

Figure 5.14. Speed score graphs of subjects A to J: Trials 1 and 2 (computer-based system)

- *Accuracy score*

The values of R^2 and *RMSE* before and after processing are as tabulated in Table 5-6 and Table 5-7.

Table 5-6. Trial 1: Accuracy score table (J_2) – computer-based system

Subject	R^2	$\mathbf{R^2_{avg\text{-}norm}}$	RMSE (cm)	$RMSE_{avg\text{-}norm}$	$\mathbf{RMSE_{refl}}$	Accuracy score
A	0.98	1.03	0.44	0.57	**1.43**	1.23
B	0.98	1.02	0.48	0.62	**1.38**	1.20
C	0.97	1.02	0.46	0.59	**1.41**	1.22
D	0.98	1.02	0.64	0.82	**1.18**	1.10
E	0.97	1.01	0.69	0.88	**1.12**	1.07
F	0.88	0.92	2.07	2.67	**-0.67**	0.13
G	0.97	1.01	0.71	0.91	**1.09**	1.05
H	0.94	0.98	0.70	0.90	**1.10**	1.04
I	0.93	0.98	0.87	1.12	**0.88**	0.93
J	0.96	1.00	0.72	0.92	**1.08**	1.04
Average	0.96	1.00	0.78	1.00	1.00	1.00
SD	0.03	0.03	0.48	0.61	0.61	0.32

Table 5-7. Trial 2: Accuracy score table (J_2) – computer-based system

Subject	R^2	$R^2_{avg\text{-}norm}$	RMSE (cm)	$RMSE_{avg\text{-}norm}$	$RMSE_{refl}$	Accuracy score
A	0.98	1.05	0.34	0.31	**1.69**	1.37
B	0.97	1.04	0.56	0.51	**1.49**	1.26
C	0.95	1.02	0.59	0.53	**1.47**	1.24
D	0.95	1.02	0.89	0.81	**1.19**	1.10
E	0.97	1.04	0.85	0.77	**1.23**	1.13
F	0.79	0.85	3.87	3.53	**-1.53**	-0.34
G	0.97	1.04	0.47	0.43	**1.57**	1.30
H	0.88	0.94	1.62	1.48	**0.52**	0.73
I	0.92	0.99	1.01	0.92	**1.08**	1.03
J	0.95	1.01	0.76	0.70	**1.30**	1.16
Average	0.93	1.00	1.10	1.00	1.00	1.00
SD	0.06	0.06	1.04	0.95	0.95	0.50

It can be observed from Table 5-7 that subject F earned a negative accuracy score and it is interesting how this result shows up. Based on the values of accuracy variables, it turns out that *RMSE* value of subject F is too high or larger than twice of the average value. Therefore, the reflection process returns a negative *RMSE* value. As a result, the accuracy score turns negative for that particular subject. In terms of the accuracy scores for trials 1 and 2, Figure 5.15 shows that subject D performed with no difference at all whereas subject C earned the second lowest difference with a value of 0.02.

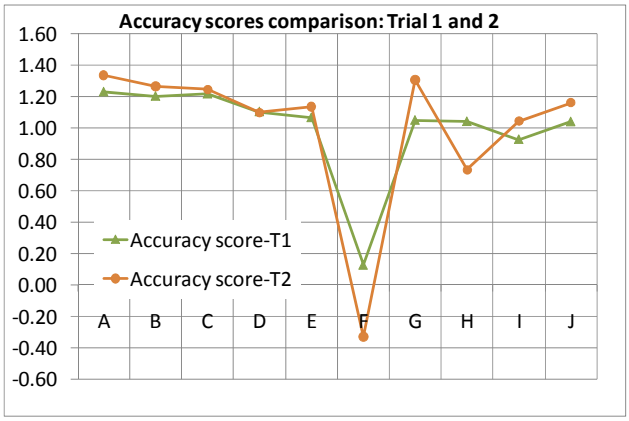

Subject	ΔJ2
A	0.11
B	0.06
C	0.03
D	0.00
E	0.07
F	0.46
G	0.26
H	0.31
I	0.12
J	0.12
Average	0.15
SD	0.14

Figure 5.15. Accuracy score graphs of subjects A to J: Trials 1 and 2 (computer-based system)

Based on speed and accuracy scores obtained from the computer-based system, a control action varies from subject to subject due to his/her control strategy in terms of a focus or interpretation of the statement *"completing the task as soon as possible"*. In the following section, an open-form HPI based on the hardware-based system will be discussed.

5.5.1.2. Hardware-based system

Similar to the computer-based system, two sets of experiment were conducted and used for human performance analysis. The only differences are in terms of a number of participants (6 rather than 10), transfer functions (2 rather than fixed) and sets of the target sequence (3 rather than fixed). Therefore, a number of graphs to be discussed will be more. The corresponding speed and accuracy scores graphs will be presented separately along with a table of summary on the performance difference and average performance scores between 2 trials. Moreover, the average performance scores are found to be at 1.00 in all cases, which is consistent with the definition, whereas the standard deviation (SD) values are found to be varying in response to the transfer functions.

With reference to the experimental procedures described in Chapter 5 (section 5.4.3), each human subject was asked to practice on each transfer function of the test rig briefly before starting any experiment and 3 sets of target sequence was completed in order starting from sequence 1 (denoted as seq1). Each target sequence was completed twice before moving to the next sequence. The experiment started with a linear transfer function, which is less complicated in its response shape, and then followed by a squared transfer function. It is worth noting that the experiment on the linear transfer function was completed before proceeding to the squared transfer function to avoid losing a feel of control and to avoid user's confusion because a response difference is relatively noticeable.

In summary, the experiment starts from a linear transfer function: T1-seq1-linear, T2-seq1-linear, T1-seq2-linear, T2-seq2-linear, T1-seq3-linear and T2-seq3-linear, to a squared transfer function: T1-seq1-squared, T2-seq1-squared, T1-seq2-squared, T2-seq2-squared, T1-seq3-squared and T2-seq3-squared.

- *Speed score*

For simplicity, Trials 1 and 2 of the same sequence and transfer function are plotted in the same graph to emphasize performance variation of each subject. These graphs are presented according to a chronological order of the experiments from left-hand column to the right-hand column. Following this set of graphs, a summary on speed score differences between 2 transfer functions along with associated average values are presented Table 5-8. Figure 5.16 shows the graphs of speed scores from all subjects. For convenience in comparing the scores from 2 sets of data, a summary of the speed score differences and average scores are calculated and included in Table 5-8.

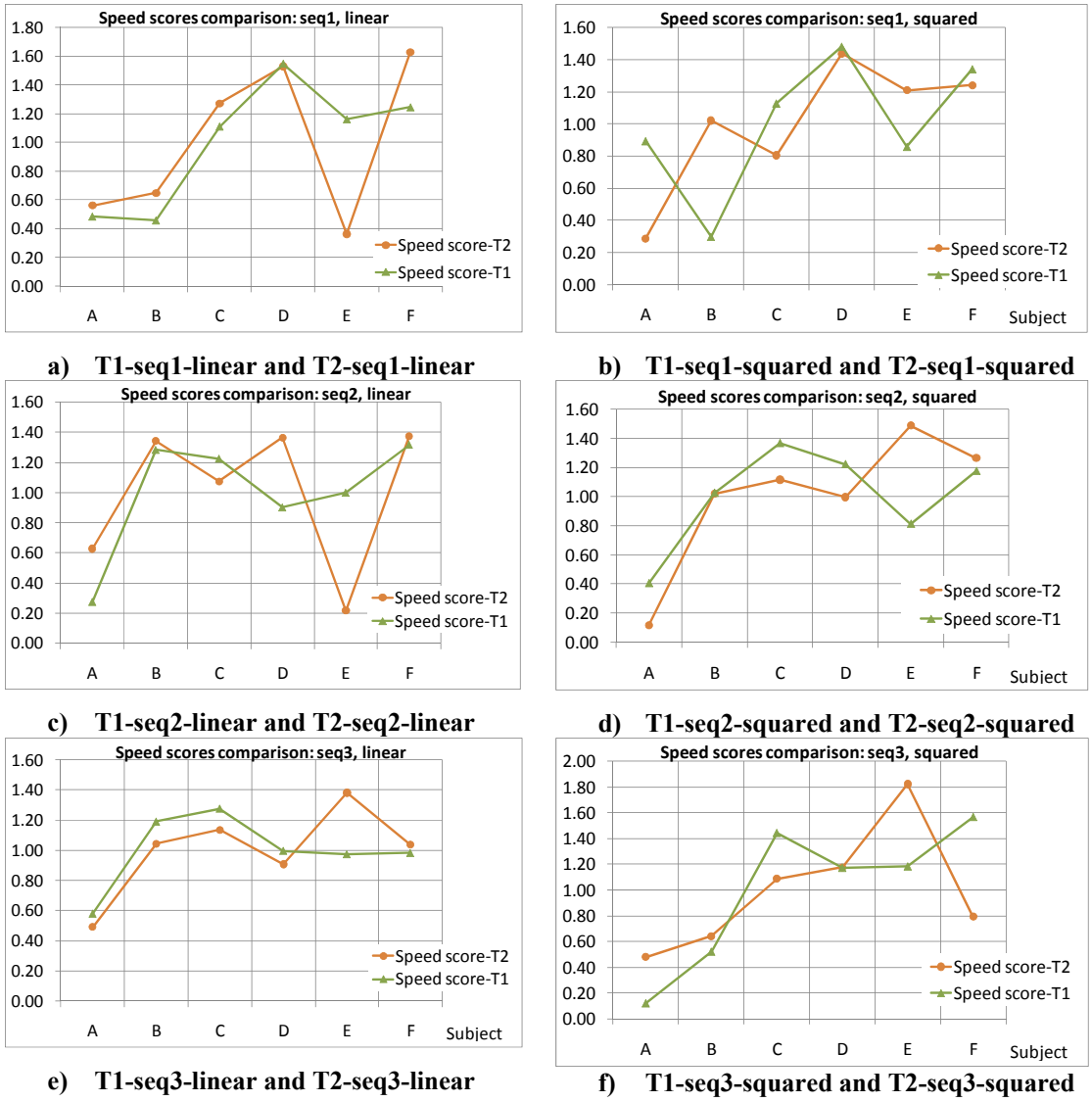

Figure 5.16. Speed scores (J_1) from different helicopter test rig trials and settings

Regarding the results based on target sequence 1 (Figure 5.16(a) and (b)), subject D has remarkably achieved the highest average speed score ($J_{av,linear}$ and $J_{av,squared}$) and the lowest speed score difference (ΔJ_{linear} and $\Delta J_{squared}$) for both transfer functions. This result implies that subject D can use both transfer functions rather equally well despite a slight decrease in the average score. It can also be observed that subject A, B and C, have their scores deviated more in the squared transfer function trials comparing to the linear ones (0.61, 0.72 and 0.32 Vs 0.08, 0.19 and 0.16), which is in contrast to subject E and F (0.35 and 0.10 Vs 0.80 and 0.38).

Table 5-8. Speed score summary for sequence 1, 2 and 3: hardware-based experiment

(a) Speed score: Seq1

Subject	$J_{1,T1\text{-}linear}$	$J_{1,T2\text{-}linear}$	$J_{1,T1\text{-}squared}$	$J_{1,T2\text{-}squared}$	ΔJ_{linear}	$\Delta J_{squared}$	$J_{av,linear}$	$J_{av,squared}$
A	0.48	0.56	0.89	0.29	0.08	0.61	0.52	0.59
B	0.46	0.65	0.30	1.02	0.19	0.72	0.55	0.66
C	1.11	1.27	1.13	0.81	0.16	0.32	1.19	0.97
D	1.55	1.53	1.48	1.44	**0.02**	**0.04**	**1.54**	**1.46**
E	1.16	0.36	0.86	1.21	0.80	0.35	0.76	1.03
F	1.24	1.63	1.34	1.24	0.38	0.10	1.44	1.29
Average	1.00	1.00	1.00	1.00	0.27	0.36	1.00	1.00
SD	0.44	0.54	0.42	0.41	0.29	0.27	0.45	0.34

(b) Speed score: Seq2

Subject	$J_{1,T1\text{-}linear}$	$J_{1,T2\text{-}linear}$	$J_{1,T1\text{-}squared}$	$J_{1,T2\text{-}squared}$	ΔJ_{linear}	$\Delta J_{squared}$	$J_{av,linear}$	$J_{av,squared}$
A	0.28	0.63	0.40	0.11	0.35	0.29	0.45	0.26
B	1.28	1.34	1.02	1.02	0.06	0.00	1.31	1.02
C	1.22	1.08	1.37	1.12	0.15	0.25	1.15	1.24
D	0.90	1.36	1.22	1.00	0.46	0.22	1.13	1.11
E	1.00	0.22	0.81	1.49	0.78	0.68	0.61	1.15
F	1.32	1.37	1.17	1.26	0.06	0.09	1.35	1.22
Average	1.00	1.00	1.00	1.00	0.31	0.26	1.00	1.00
SD	0.39	0.48	0.35	0.47	0.28	0.23	0.38	0.37

(c) Speed score: Seq3

Subject	$J_{1,T1\text{-}linear}$	$J_{1,T2\text{-}linear}$	$J_{1,T1\text{-}squared}$	$J_{1,T2\text{-}squared}$	ΔJ_{linear}	$\Delta J_{squared}$	$J_{av,linear}$	$J_{av,squared}$
A	0.58	0.49	0.12	0.48	0.09	0.36	0.54	0.30
B	1.19	1.04	0.52	0.64	0.15	0.12	1.12	0.58
C	1.28	1.14	1.44	1.09	0.14	0.36	1.21	1.26
D	1.00	0.91	1.17	1.18	0.09	0.01	0.95	1.17
E	0.97	1.38	1.18	1.82	0.41	0.64	1.18	1.50
F	0.98	1.04	1.57	0.79	0.06	0.77	1.01	1.18
Average	1.00	1.00	1.00	1.00	0.15	0.38	1.00	1.00
SD	0.24	0.29	0.56	0.48	0.13	0.29	0.25	0.46

For target sequence 2, subject B is found to perform with lowest ΔJ_{linear} , which ties with subject F for the lowest $\Delta J_{squared}$. The average speed scores of subject F is found to be the highest for linear transfer function whereas subject C's is the highest for squared transfer function. Similar to target sequence 2, subject is found to earn the lowest ΔJ_{linear} but the smallest $\Delta J_{squared}$ goes to subject D. In terms of average speed score, subject C and E earned the highest for linear and squared transfer functions respectively. Overall, it can be observed that the speed score differences (ΔJ) are of lower values for the squared transfer functions in all target sequences except target sequence 3 and so are average speed scores (J_{av}). This result implies that a speed performance deviation is generally lower for the squared transfer function.

- *Accuracy score*

Similar to speed score calculation, the results are plotted in Figure 5.17 and then followed by a table of summary for each target sequence.

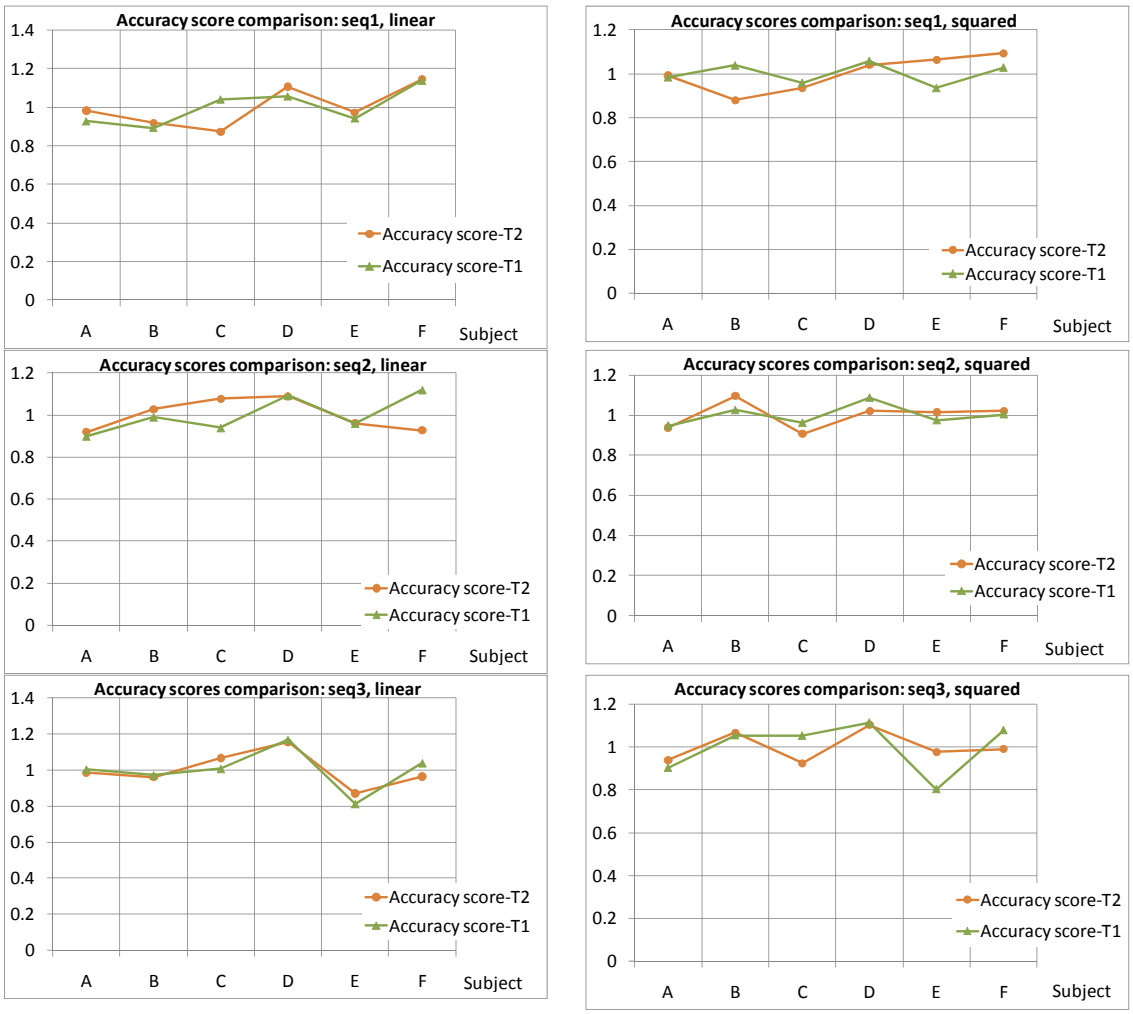

Figure 5.17. Accuracy scores (J_2) from different helicopter test rig trials and settings

At a glance on Figure 5.17, the degree of accuracy scores deviation is certainly less than those of speed scores and this really is the case. The highest standard deviation based on accuracy scores difference is only 0.08 comparing to 0.29 from the speed accuracy scores (see Table 5-9).

Table 5-9. Accuracy score summary for sequence 1, 2 and 3: hardware-based experiment

(a) Accuracy score: Seq1

Subject	$J_{2,T1\text{-}linear}$	$J_{2,T2\text{-}linear}$	$J_{2,T1\text{-}squared}$	$J_{2,T2\text{-}squared}$	ΔJ_{linear}	$\Delta J_{squared}$	$J_{av,linear}$	$J_{av,squared}$
A	0.93	0.98	0.98	0.99	0.06	0.01	0.95	0.99
B	0.89	0.92	1.04	0.88	0.03	0.16	0.91	0.96
C	1.04	0.87	0.96	0.93	0.17	0.02	0.96	0.95
D	1.06	1.11	1.06	1.04	0.05	0.02	1.08	1.05
E	0.94	0.97	0.93	1.06	0.03	0.13	0.96	1.00
F	1.14	1.14	1.03	1.09	0.01	0.06	1.14	1.06
Average	1.00	1.00	1.00	1.00	0.06	0.07	1.00	1.00
SD	0.09	0.11	0.05	0.08	0.06	0.06	0.09	0.05

(b) Accuracy score: Seq2

Subject	$J_{2,T1\text{-}linear}$	$J_{2,T2\text{-}linear}$	$J_{2,T1\text{-}squared}$	$J_{2,T2\text{-}squared}$	ΔJ_{linear}	$\Delta J_{squared}$	$J_{av,linear}$	$J_{av,squared}$
A	0.90	0.92	0.95	0.94	0.02	0.01	0.91	0.94
B	0.99	1.03	1.02	1.10	0.04	0.07	1.01	1.06
C	0.94	1.08	0.96	0.91	0.14	0.05	1.01	0.93
D	1.09	1.09	1.09	1.02	0.00	0.07	1.09	1.05
E	0.96	0.96	0.97	1.02	0.00	0.04	0.96	0.99
F	1.12	0.93	1.00	1.02	0.19	0.02	1.02	1.01
Average	1.00	1.00	1.00	1.00	0.07	0.04	1.00	1.00
SD	0.09	0.07	0.05	0.07	0.08	0.03	0.06	0.05

(c) Accuracy score: Seq3

Subject	$J_{2,T1\text{-}linear}$	$J_{2,T2\text{-}linear}$	$J_{2,T1\text{-}squared}$	$J_{2,T2\text{-}squared}$	ΔJ_{linear}	$\Delta J_{squared}$	$J_{av,linear}$	$J_{av,squared}$
A	1.00	0.99	0.90	0.94	0.02	0.04	0.99	0.92
B	0.97	0.96	1.05	1.07	0.01	0.01	0.97	1.06
C	1.01	1.07	1.05	0.92	0.06	0.13	1.04	0.99
D	1.17	1.15	1.11	1.10	0.01	0.01	1.16	1.11
E	0.81	0.87	0.80	0.98	0.06	0.17	0.84	0.89
F	1.04	0.96	1.08	0.99	0.07	0.09	1.00	1.03
Average	1.00	1.00	1.00	1.00	0.04	0.07	1.00	1.00
SD	0.11	0.10	0.12	0.07	0.03	0.07	0.10	0.08

Referring to target sequence 1, the lowest accuracy score differences based on linear and squared transfer functions go to subject F and A respectively (at the value of 0.01). Moreover, subject F also earned the highest accuracy scores from both linear and squared transfer functions. Subject D and E earned the lowest accuracy score ΔJ_{linear} for target sequence 2 whereas the lowest accuracy score $\Delta J_{squared}$ goes to subject A. The highest accuracy scores go to subject B and D for squared and linear transfer functions

respectively. For target sequence 3, subject B and D both earned the lowest ΔJ_{linear} *and* $\Delta J_{squared}$ whereas the highest scores go to subject D for both transfer functions.

Considering the issue on human performance consistency, it seems that some subjects are noticeably consistent or capable of adapting his/her ability very proactively to the change in transfer functions and target sequences comparing to others. It can also be observed that the accuracy scores are more consistent on average comparing the speed accuracy scores and this indicates a more emphasis on speed characteristics for all the subjects in the operation a whole. The following section discusses about the closed-form HPI for both systems with a use of performance scores obtained from this section for in the calculation.

5.5.2. Closed-form HPI

Now that all performance scores have been calculated, an overall human performance based on these scores can be proceeded. A closed-form HPI, which can be visualized as a general performance value comprising a number of performance variables, is similar to a Grade Point Average (GPA), whereas an open-form HPI or simply a *performance score* is similar to a letter grade for one particular module or subject. Therefore, a closed-form HPI or simply HPI is an overall performance value of a human operator in the system of interest in relation to the sample group. Equation (4-2) is revisited for convenience.

$$HPI = \left(\sum_{i=1}^{N} W_{J_i} \cdot J_i\right) \Big/ \sum_{i=1}^{N} W_{J_i} \tag{5-14}$$

Similar to the performance variables weighting in an open-form HPI discussed earlier, the weight of speed and accuracy is required to calculate a HPI. The set of speed-accuracy weightings, which can also be regarded as speed-accuracy ratios, mark a trend of HPI and in effect, quantify the control strategy adopted by a human operator. This control strategy is actually in accordance with Higgins Higgins, Shah et al., 1997) to confirm that human can adjust his/her control strategy to suite task requirements.

As we will see, each individual control strategy is truly subjective and its value is varied with different degree of deviation on the speed-accuracy ratios. In other words, it is the matter of interpretation of the given instructions and physical abilities that define the manner a control action are performed. From this point of view, several speed-accuracy ratios are chosen to illustrate the HPI value trend and identify how his/her control strategy is weighted or formulated in terms of speed and accuracy. That is, the weighting of speed over accuracy scores are primarily set at fixed values of 30:70, 40:60, 50:50, 60:40 and 70:30 in this thesis. The HPI values at these fixed ratios are denoted as $HPI_{30:70}$, $HPI_{40:60}$, $HPI_{50:50,}$ $HPI_{60:40}$ and $HPI_{70:30}$ respectively. In practice, it would be ideal if a system designer can determine a suitable speed-accuracy ratio and this can then be regarded as a human factor requirement.

Similar to the previous section on the open-form HPI analysis, a discussion will be started from a computer-based system and then followed by a hardware-based system. A table of summary will also be presented for comparison purposes.

5.5.2.1. Computer-based system

Similar to the open-form HPI calculation, 2 trials will be presented to illustrate performance variation. The presentations are in 3-dimensional and 2-dimensional formats to show the trend of HPI values *ratio-wise* and *subject-wise* respectively. The difference between ratio-wise and subject-wise HPIs is the presentation of HPI values with one particular speed-accuracy ratio on all subjects rather than one particular subject on varied speed-accuracy ratios. Figure 5.18, Figure 5.19, Figure 5.20 and Figure 5.21 show all the HPI graphs and then followed by a summary table (Table 5-10).

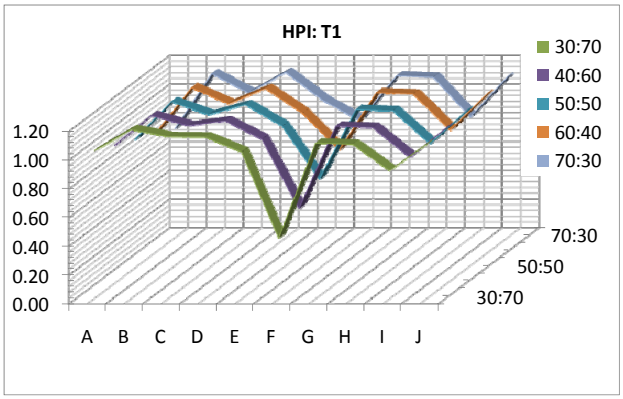

Figure 5.18. Trial 1: 3-dimensional closed-form HPI graphs for human subjects A to J (computer-based system)

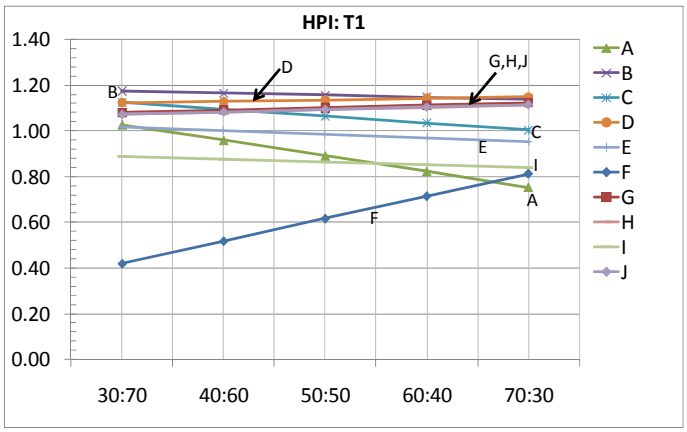

Figure 5.19. Trial 1: HPI with varied speed-accuracy ratio for human subjects A to J (computer-based system)

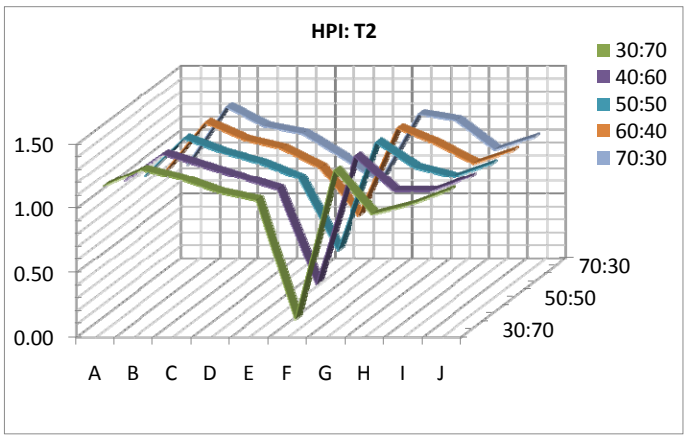

Figure 5.20. Trial 2: 3-dimensional closed-form HPI graphs for human subjects A to J (computer-based system)

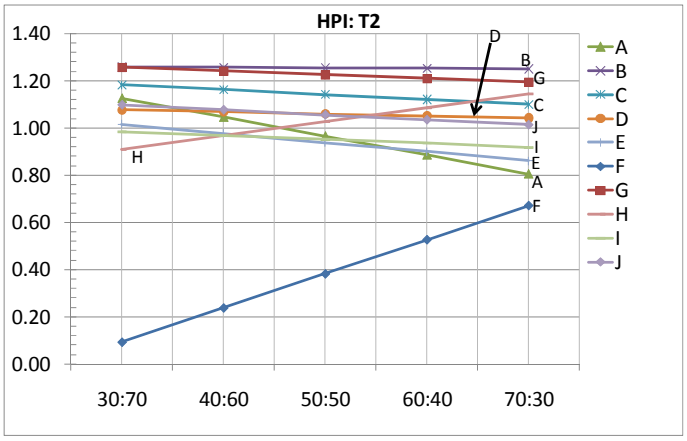

Figure 5.21. Trial 2: HPI with varied speed-accuracy ratio for human subjects A to J (computer-based system)

Table 5-10. Summary table (computer-based system)

Subject	J_{1av}	J_{2av}	HPI_{av}	$\Delta HPI_{30:70}$	$\Delta HPI_{40:60}$	$\Delta HPI_{50:50}$	$\Delta HPI_{60:40}$	$\Delta HPI_{70:30}$	ΔHPI_{av}
A	0.56	1.30	0.93	0.10	0.09	0.08	0.06	0.05	0.08
B	1.18	1.23	**1.21**	0.08	0.09	0.10	0.10	0.11	0.10
C	0.98	1.23	1.10	0.06	0.07	0.08	0.09	0.10	0.08
D	1.09	1.10	1.10	0.05	0.06	0.08	0.09	0.11	0.08
E	0.83	1.10	0.96	0.00	0.02	0.05	0.07	0.09	0.05
F	1.10	-0.11	0.50	0.33	0.28	0.23	0.19	0.14	**0.23**
G	1.15	1.18	1.16	0.18	0.15	0.12	0.10	0.07	0.12
H	1.23	0.89	1.06	0.16	0.11	0.07	0.02	0.03	0.08
I	0.83	0.98	0.91	0.10	0.09	0.09	0.08	0.08	0.09
J	1.05	1.10	1.07	0.02	0.01	0.04	0.07	0.10	0.05
Average	1.00	1.00	1.00	0.11	0.10	0.09	0.09	0.09	
SD	0.21	0.41	0.20	0.10	0.08	0.06	0.04	0.03	

With reference to Table 5-10, an absolute difference between HPI values from Trials 1 and 2 is denoted as ΔHPI whereas an average ΔHPI value for each subject based on all speed-accuracy ratios is denoted as ΔHPI_{av}. These calculations are according to the research methodologies presented in Section 3.5.4, Chapter 3. The slope of HPI against speed-accuracy ratio graphs reveals a relationship between speed and accuracy over a control action. Positive slope indicates a dominance of accuracy over speed and *vice versa* for a negative slope. The larger the slope, the larger a drop (for negative slopes) or rise of an associated HPI value from one speed-accuracy ratio to another. The slope of HPI against speed-accuracy ratio is also indicative of a degree of adaptability considering those speed-accuracy ratios as a human factor requirement for a system of interest.

Regarding the issue on speed and accuracy scores, it can be observed that the larger the difference between speed and accuracy scores, the steeper their HPI values. Subject F, as seen in Figure 5.19 and Figure 5.21, is a good example of a large speed score over accuracy score with the largest ΔHPI_{av} of 0.23. The unbalanced speed and accuracy scores, effectively, cause an increase of his/her HPI as the speed-accuracy ratio increases. On a contrary, subjects E and J, whose results appear to have the smallest ΔHPI_{av}, have a nearly flat response to the increasing speed-accuracy ratios.

For an interpretation point of view, subject B, who obtains the highest average HPI values across the whole range, are least affected by the speed-accuracy ratios on the one hand. On the other hand, this reflects a consistent performance value of subject B across the range of speed-accuracy ratios of that man-machine system, which is presumably to be determined and tested before manufacturing.

5.5.2.2. Hardware-based system

In this hardware-based system, all 12 graphs with the same conditions as the open-form HPIs calculation will be presented starting from target sequence 1, 2 and 3 using both linear and squared transfer functions (Figure 5.22, Figure 5.23 and Figure 5.24 respectively). These graphs are presented with reference to the same speed-accuracy ratios as specified in the computer-based system.

It is interesting to see that, among these 3 target sequences, HPI graphs of the target sequence 1 (Figure 5.22) appear to have almost unique lines with no crossings among other lines comparing those of other target sequences. The summary on these HPI graphs for target sequence 1, 2 and 3 are given in Table 6-11, Table 6-12 and Table 6-13 respectively.

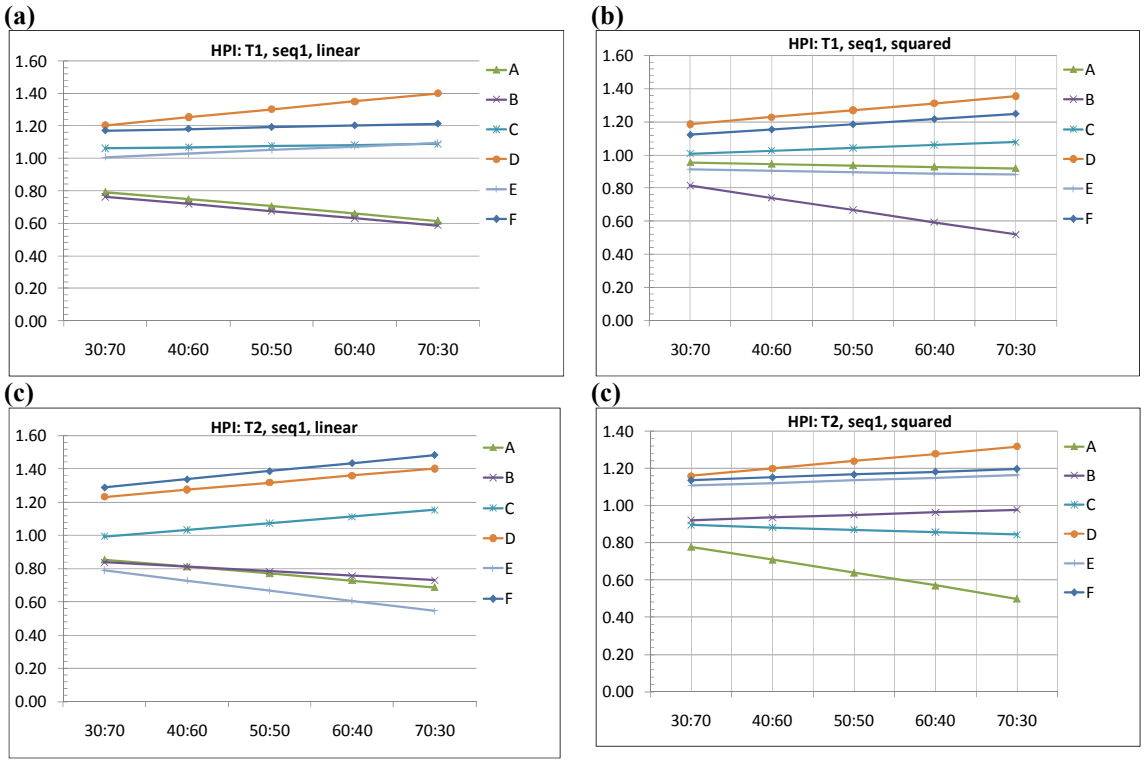

Figure 5.22. HPI sequence 1: hardware-based system (HPI vs. speed-accuracy ratio)

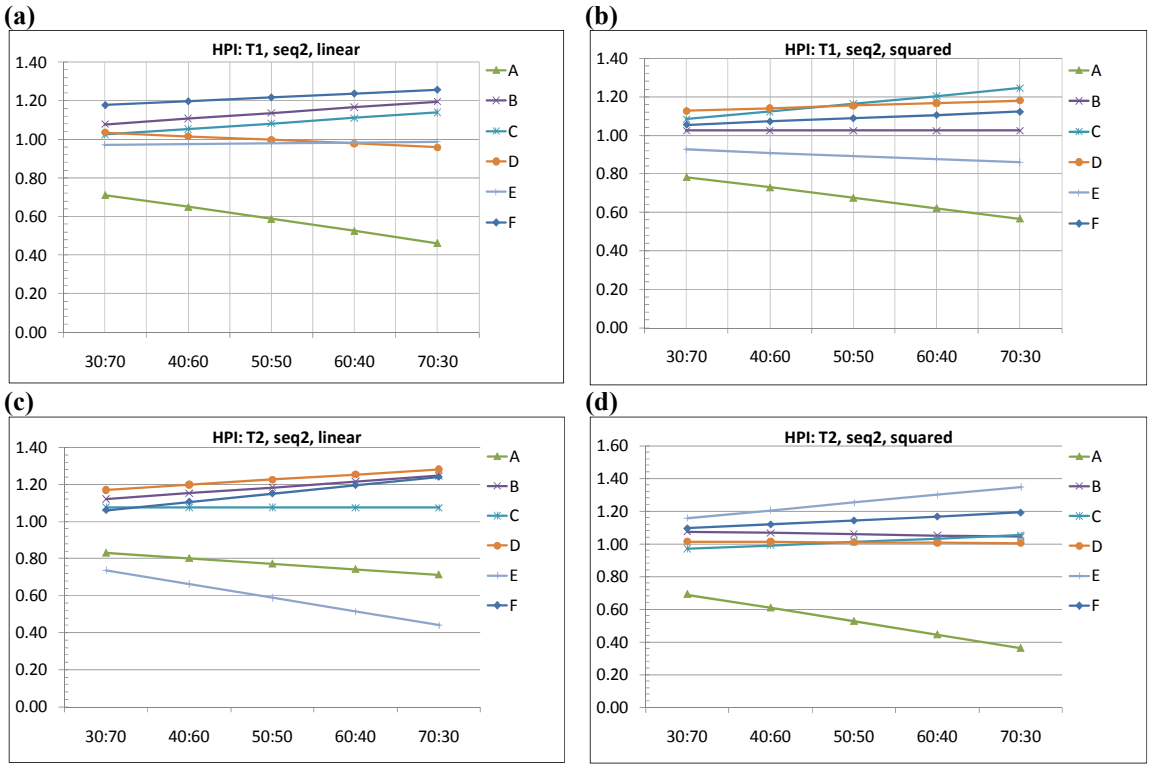

Figure 5.23. HPI sequence 2: hardware-based system (HPI vs. speed-accuracy ratio)

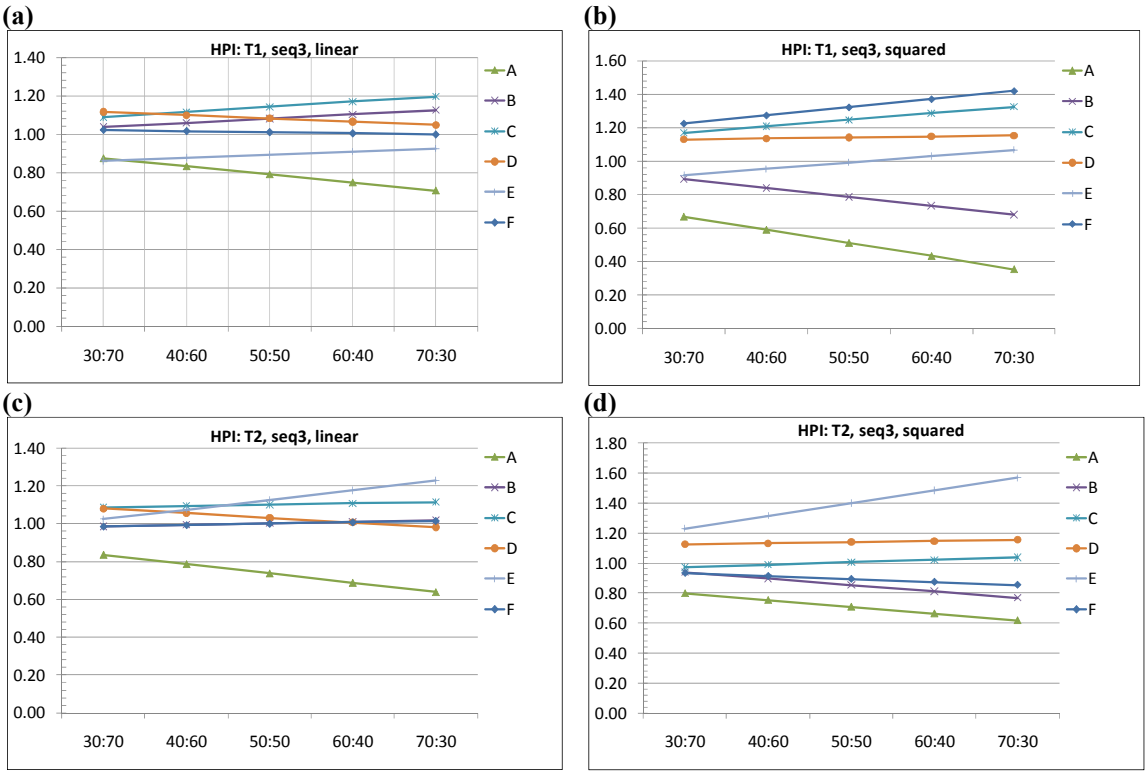

Figure 5.24. HPI sequence 3: hardware-based system (HPI vs. speed-accuracy ratio)

From Figure 5.22, Figure 5.23 and Figure 5.24, both increasing and decreasing trends of the HPI graphs can still be observed as before but a HPI increase at the already high HPI values can be spotted in all target sequences and transfer functions but not from the same subjects. For target sequence 1, subject D appears to have this behavior in Figure 5.22(a), (b) and (d), whereas subject F can be spotted in Figure 5.22(c). For target sequence 2 and 3, subjects F, C, D and E (Figure 5.23(a), (b), (c) and (d)) and C, F and E (Figure 5.24(a), (b), (c)* and (d)*: *E in both figures) can also be spotted respectively.

Moreover, the deviation of $HPI_{70:30}$ are observed to be the largest in all figures among other speed-accuracy ratios, which is totally opposite to the case of the computer-based system discussed earlier. In that system, the highest deviation is found to be at $HPI_{30:70}$ (Table 5-10). From the graphs presented above, statistical information based on trials 1 and 2 for all target sequences and transfer functions are summarised in Table 5-11, Table 5-12 and Table 5-13 respectively.

Table 5-11. Target sequence 1: summary table (hardware-based experiment)

Seq1	Linear				Squared			
Subject	J_{1av}	J_{2av}	HPI_{av}	ΔHPI_{av}	J_{1av}	J_{2av}	HPI_{av}	ΔHPI_{av}
A	0.52	0.95	0.74	0.07	0.59	0.99	0.79	0.30
B	0.55	0.91	0.73	0.11	0.66	0.96	0.81	0.28
C	1.19	0.96	1.07	0.04	0.97	0.95	0.96	0.17
D	1.54	1.08	**1.31**	0.02	1.46	1.05	**1.25**	0.03
E	0.76	0.96	0.86	0.38	1.03	1.00	1.02	0.24
F	1.44	1.14	1.29	0.20	1.29	1.06	1.18	0.02
Average	1.00	1.00	1.00	0.14	1.00	1.00	1.00	0.17
SD	0.45	0.09	0.26	0.14	0.34	0.05	0.19	0.12

Table 5-12. Target sequence 2: summary table (hardware-based experiment)

Seq2	Linear				Squared			
Subject	J_{1av}	J_{2av}	HPI_{av}	ΔHPI_{av}	J_{1av}	J_{2av}	HPI_{av}	ΔHPI_{av}
A	0.45	0.91	0.68	0.19	0.26	0.94	0.60	0.15
B	1.31	1.01	1.16	0.05	1.02	1.06	1.04	0.03
C	1.15	1.01	1.08	0.04	1.24	0.93	1.09	0.15
D	1.13	1.09	1.11	0.23	1.11	1.05	1.08	0.14
E	0.61	0.96	0.78	0.39	1.15	0.99	1.07	0.36
F	1.35	1.02	**1.18**	0.07	1.22	1.01	**1.12**	0.05
Average	1.00	1.00	1.00	0.16	1.00	1.00	1.00	0.15
SD	0.38	0.06	0.21	0.14	0.37	0.05	0.20	0.12

Table 5-13. Target sequence 3: summary table (hardware-based experiment)

Seq3	Linear				Squared			
Subject	J_{1av}	J_{2av}	HPI_{av}	ΔHPI_{av}	J_{1av}	J_{2av}	HPI_{av}	ΔHPI_{av}
A	0.54	0.99	0.76	0.05	0.30	0.92	0.61	0.20
B	1.12	0.97	1.04	0.08	0.58	1.06	0.82	0.07
C	1.21	1.04	**1.12**	0.04	1.26	0.99	1.13	0.24
D	0.95	1.16	1.06	0.05	1.17	1.11	1.14	0.00
E	1.18	0.84	1.01	0.23	1.50	0.89	**1.20**	0.41
F	1.01	1.00	1.01	0.02	1.18	1.03	1.11	0.43
Average	1.00	1.00	1.00	0.08	1.00	1.00	1.00	0.22
SD	0.25	0.10	0.12	0.08	0.46	0.08	0.23	0.17

According to the information given in the summary table above, subject D and F obtained the highest average HPI (HPI_{av}) in target sequence 1 and 2 for both transfer functions respectively. For target sequence 3, subject C and E obtained the highest HPI_{av} from linear and squared transfer functions respectively. The values of standard deviation for HPI_{av} on all subjects start from target sequence 3, 2 and 1 in an ascending order for the linear transfer function whereas the results are the opposite for those based on the squared transfer function.

The results reflect that an average standard deviation is larger for a use of squared transfer function in completing a target sequence with smaller *Index of Difficulty* (I_d) or distance between targets. On a contrary, it is found that an average standard deviation is lower for a use of linear transfer function in closer targets.

5.6. Summary

This chapter has covered all the details on the non-model approach to compute Human Performance Index (HPI). This approach directly uses the control action and output results from the experiment as the resource for calculation. Human characteristics are found to be directly proportional to the instructions but rather subjective due to physical limitation and personal abilities. It is interesting to see that Fitts' Law is not much obeyed due to a varied control strategy to complete the task as quickly as possible. A trial-level comparison also suggests that participants tried to maintain their control strategies even though the results varied. The experiments on a computer-based and hardware-based system were conducted and the analysis on both open-form and closed-forms HPI were completed. Chapter 6 will try to achieve the same set of analyses with reference to human mathematical models and the focus will be shifted from the trial-level comparison to the approach-level comparison.

Chapter - 6.

Analysis of the Human Performance using a Model-based Approach

6.1. Introduction

In addition to the non-model Human Performance Index (HPI) computation presented in Chapter 5, this chapter introduces a model-based approach and applies it to both computer-based and hardware-based systems. The model-based approach serves as an alternative to HPI computation, which will be potentially used for validating the results from the non-model approach that is solely based on the control action of a human operator. In order to achieve this, a theory of system identification is applied on a segment-by-segment basis with reference to the input-output data. For simplicity, the models derived in this thesis are restricted to a single-input single-output structure, which will then be used for human performance computation. The objective of this chapter is to verify human performance index results from a model-based approach with a non-model approach in Chapter 5. The use of variables from human ARX models to relate to speed and accuracy characteristics will also be covered.

6.2. Outline for a model-based approach

A model-based HPI computation for both computer-based and hardware-based systems aims to derive mathematical equations that describe human control actions in a form of linear parametric equation called *AutoRegressive with eXogeneous inputs* (ARX) model. This type of linear parametric model is one of a difference equation with a transfer function format of an autoregressive model family. That is, the ARX model is formulated by a pair of inputs and outputs from the system, where the least square

condition is used for minimisation yielding the best model orders. Effectively, this means a number of poles and zeros are selected in such a way that the actual and calculated data are maximally matched on the one hand. On the other hand, some of the model orders may be fixed so that the coefficients can be determined and this obviously results in lower percentage of matching. The latter rationale is used in this thesis due to a restriction to limit the model orders. Further details on ARX model structure and the least square condition will be given in the next section.

Regarding the steps for implementing the model-based HPI computation, it starts from executing system identification algorithms, computing an ARX model based on the data sets. The unknown system can be viewed as a black box, which is a human operator in this case, is the main target. This requires the right pair of input and output data otherwise extra elements in the system will be combined with the resultant model and need to be considered. However, the block separation can be done with ease if the system is simply a gain/position system as shown in Figure 6.1.

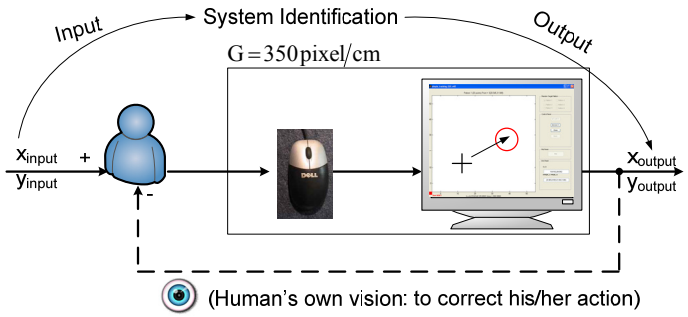

Figure 6.1. Input-output pair for system identification of a computer-based system

Figure 6.1 shows a pair of input and output positions in x-y coordinates for a use in system identification algorithms according to the setup. The input-output pairs are treated for the motion along x-axis and y-axis accordingly. The dotted line in Figure 6.1 represents a feedback of a current cursor position internally perceived with reference to the target position and this visual feedback can be considered imaginary. Hence, the dotted line is used in this context. The Human operator has to adjust or compensate his/her hand motion to minimise the difference between target and actual positions

based on this visual feedback. Practically, the experiment can be considered as an open-loop control scenario.

This is similar to the hardware-based system shown in Figure 6.2, except no gain block is involved. Only inverse mapping of a joystick voltage is required to obtain a deflection angle of a joystick, which will then be used in system identification algorithms.

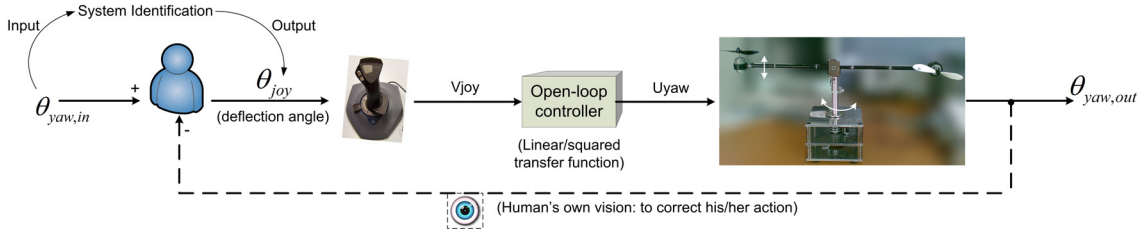

Figure 6.2. Input-output pair for system identification of a hardware-based system [A joystick-controlled helicopter test rig]

For the hardware-based system, the human operator needs to use not only his/her visual feedback but also to understand the helicopter dynamics to some extent, to estimate a relationship of a controller in order to overcome the static friction at a rotational bearing and to manoeuvre the helicopter test rig according to the target sequence successfully.

With regard to the main objective to verify the non-model HPI results by a model-based approach, this chapter emphasizes on examination of performance variables suitable from human mathematical models and investigation into discrepancies for both fixed and variable HPI forms (see details in Sections 5.5.1 and 5.5.2). Firstly, the performance variables associated with the model will be discussed under *performance variables* section and then a comparison on these values will be presented under *variable HPI*, following a *performance variables* section. The calculation of these performance variables will be done in a distributive manner as explained in Section 3.5.4, Chapter 3.

6.3. Background on System Identification Theory

6.3.1. Structure of a linear parametric model

System identification theory aims to derive a linear parametric model or a linear difference equation whose set of coefficients can be obtained by minimising the value of least square differences between measured and fitted data from a system. The linear difference equation used in this thesis is in a structure called *Autoregressive with eXogenous input* or *ARX* (Chapter 2). According to the standard structure, a mathematical equation of the ARX model with 1-sample delay and a least square condition are as presented in Equations (6-1) and (6-2) respectively (Ljung, 1999):

$$y(t) + a_1 \cdot y(t-1) + \ldots + a_n \cdot y(t-n) = b_1 \cdot u(t-1) + b_2 \cdot u(t-2) \ldots + b_m \cdot u(t-m) \tag{6-1}$$

Where *y(t)* is the output at time *t*, *u(t)* is the input at time *t*. *n* is a number of poles, *m* is a number of zeros.

$$V_N = \frac{1}{N} \cdot \sum_{t=1}^{N} (y(t) - \hat{y}(t))^2 \tag{6-2}$$

Where $\hat{y}(t)$ is the calculated output from coefficient $a_1,\ldots,a_n$ and $b_1,\ldots,b_m$. The resultant set of $a_1,\ldots,a_n$ and $b_1,\ldots,b_m$ from minimizing V_N therefore forms the mathematical model that best describes a system output or the model with minimum error.

With reference to the MATLAB® system identification toolbox, there are a number differences from Equation (6-1) in having *n* denoted as n_a, *m* denoted as n_b and n_k introduced as a time delay (rather than $n_k = 1$) as follows:

$$\begin{aligned} &y(t) + a_1 \cdot y(t-1) + \ldots + a_{n_a} \cdot y(t-n_a) \\ &= b_1 \cdot u(t-n_k) + b_2 \cdot u(t-n_k-1) \ldots + b_{n_b} \cdot u(t-n_k-n_b+1) \end{aligned} \tag{6-3}$$

Applying a z-transform to Equation (6-3) leads to the following equation:

$$\begin{aligned} &Y(z) + a_1 \cdot z^{-1} \cdot Y(z) + \ldots + a_{n_a} \cdot z^{-na} \cdot Y(z) \\ &= b_1 \cdot z^{-nk} \cdot U(z) + b_2 \cdot z^{-nk-1} \cdot U(z) \ldots + b_{n_b} \cdot z^{-n_k-n_b+1} \cdot U(z) \end{aligned} \tag{6-4}$$

$$Y(z) \cdot \left(1 + a_1 \cdot z^{-1} + \ldots + a_{n_a} \cdot z^{-na}\right) = U(z) \cdot z^{-nk} \cdot \left(b_1 + b_2 \cdot z^{-1} \ldots + b_{n_b} \cdot z^{-n_b+1}\right) \tag{6-5}$$

$$\therefore \frac{Y(z)}{U(z)} = \frac{z^{-nk} \cdot \left(b_1 + b_2 \cdot z^{-1} \ldots + b_{n_b} \cdot z^{-n_b+1}\right)}{\left(1 + a_1 \cdot z^{-1} + \ldots + a_{n_a} \cdot z^{-na}\right)} \tag{6-6}$$

Considering the main difference from the original definition, a number of zeros equals to n_b+1 rather than m or simply n_b. A general ARX model can be denoted as ARX[n_a:n_b:n_k] with a structure according to Equation (6-6) and the ARX model mentioned in this thesis will be based on this format. Now, in order to extract human performance variables, the order of ARX model needs to be determined first and then mapped with parameters of a human model in the z-domain.

A human model or controller selected for this thesis is basically a PD controller with a first-order lag as suggested by Suzuki (2006b) except an inclusion of a time delay as an extra parameter. This is due to the main objective of this research to analyse speed characteristics of each human subject in addition to accuracy characteristics. A time delay of the model is considered appropriate for that matter. In addition, the PD controller with first-order lag and time delay also complies with the *quasi-linear model*, which was proposed by Mcruer(1962) (a pioneer in manual or man-machine control research, well known for his proposed human model). The selected human model and the quasi-linear model are presented in order as the following:

PD controller with a time delay and a first-order lag (Ragazzini, 1948; Suzuki, Kurihara et al., 2006):

$$Y_H(s) = \frac{(K_d \cdot s + K_p)}{T_N \cdot s + 1} \cdot e^{-\varpi} \tag{6-7}$$

$$\text{Or } Y_H(s) = \frac{K_p \cdot e^{-\varpi}}{T_N \cdot s + 1} \cdot (K_d / K_p \cdot s + 1) \tag{6-8}$$

Quasi-linear model Mcruer and Krendel, 1962:

$$Y_H(s) = \frac{K \cdot e^{-\varpi}}{T_N \cdot s + 1} \cdot \left[\frac{T_L \cdot s + 1}{T_I \cdot s + 1} \right] \tag{6-9}$$

Based on Equations (6-8) and (6-9), these two equations are exactly the same excluding the lag compensator term ($T_I s+1$) in Equation (6-9). Therefore, a PD controller can be regarded as a simplified quasi-linear model. For simplicity, the time delay term will be treated separately after the main parameters K_p, K_d and T_N are derived.

Applying a bilinear transformation or Tustin's method to Equation (6-7), s is replaced

by $\frac{2}{T}\cdot\frac{1-z^{-1}}{1+z^{-1}}$ (T represents a sampling period) and the resultant equation in a discrete form.

Equation (6-7) without a time delay term can be transformed into z-domain as follows: (6-10)

$$Y_H(s)=\frac{(K_d\cdot s+K_p)}{T_N\cdot s+1}\xrightarrow{z-transfom}Y_H(z)=\frac{2\cdot K_d\cdot(1-z^{-1})+K_p\cdot T\cdot(1+z^{-1})}{2\cdot T_N\cdot(1-z^{-1})+T\cdot(1+z^{-1})}$$

Equation (6-10) can then be rearranged into

$$Y_H(z)=\frac{\frac{(T\cdot K_p+2\cdot K_d)}{2\cdot T_N+T}+\left(\frac{T\cdot K_p-2\cdot K_d}{2\cdot T_N+T}\right)\cdot z^{-1}}{1+\left(\frac{T-2\cdot T_N}{T+2\cdot T_N}\right)\cdot z^{-1}} \tag{6-11}$$

According to the ARX model structure in Equation (6-6), the suitable values for n_a and n_b are therefore 1 and 2 respectively. The ARX model structure in Equation (6-11) can then be represented in the following form:

$$Y_H(z)=\frac{b_1+b_2\cdot z^{-1}}{1+a_1\cdot z^{-1}} \tag{6-12}$$

From Equations (6-11) and (6-12), it can be observed that the coefficients can be mapped as follows:

$$a_1=\left(\frac{T-2\cdot T_N}{T+2\cdot T_N}\right),b_1=\frac{(T\cdot K_p+2\cdot K_d)}{2\cdot T_N+T},b_2=\left(\frac{T\cdot K_p-2\cdot K_d}{2\cdot T_N+T}\right)$$

Finally, the equations for K_p, K_d, and T_N can be computed based on the above relationships for a_1, b_0 and b_1:

$$T_N=\frac{T}{2}\cdot\left(\frac{1-a_1}{1+a_1}\right) \tag{6-13}$$

$$K_p=\left(\frac{T+2\cdot T_N}{2\cdot T}\right)\cdot(b_1+b_2) \tag{6-14}$$

$$K_d=\left(\frac{T+2\cdot T_N}{4}\right)\cdot(b_1-b_2) \tag{6-15}$$

Now that K_p, K_d and T_N have been derived from the model without a time delay, a consideration on the original definition of z-transform ($z=e^{Ts}$) and the delay term($e^{-\varpi}$) can be achieved as follows.

$$z = e^{Ts} \xrightarrow{\text{Re-arranging into}} s = \frac{1}{T}\left(\frac{\log z}{\log e}\right) = \frac{1}{T}\ln z \tag{6-16}$$

Substituting Equation (6-16) into $e^{-\tau s}$ results in:

$$e^{-\tau s} = e^{\frac{-\tau}{T}\cdot \ln z} = e^{\ln z \frac{-\tau}{T}}$$

$$\therefore e^{-\tau s} \xrightarrow{z-transform} z^{\frac{-\tau}{T}} \tag{6-17}$$

Therefore, Equation (6-7) can now be presented as

$$Y_H(s) = \frac{(K_d \cdot s + K_p)}{T_N \cdot s + 1} \cdot e^{-\tau s} \xrightarrow{z-transform} Y_H(z) = \left(\frac{b_1 + b_2 \cdot z^{-1}}{1 + a_1 \cdot z^{-1}}\right) \cdot z^{\frac{-\tau}{T}} \tag{6-18}$$

Now the time delay term τ in Equation (6-7) can be calculated in terms of n_k as follows:

$$z^{-n_k} = z^{\frac{-\tau}{T}} \longrightarrow \therefore \tau = n_k \cdot T \tag{6-19}$$

This result is consistent with the real translation theorem (Nise, 2006):

$$z\{f(t - n \cdot T)\} = z^{-n} \cdot F(z) \tag{6-20}$$

6.3.2. ARX model computation

Up to this point, only a general ARX model of a human operator according to Ragazzini (1948) has been presented. To apply this to the tracking operation of human operators, a segment of motion or a motion between a pair of target positions will be analysed instead of a complete motion (as in Ertugrul, 2008). This rationale complies with the assumption that human control strategy is adaptive by nature and inconsistent throughout the whole operation. Additionally, this will also help verifying the result of HPI values with the non-model approach presented in Chapter 5 (which was also based on a segment-by-segment motion) and gaining an insight into a variation of human performance at a segment level. As a result, this chapter concerns a derivation of human ARX models that best describes a control motion of every single segment and use them for human performance computation.

With reference to the previous section, each ARX model of human operators is defined to have a fixed order of n_a=1, n_b=2 and varied n_k from the model with highest fitting percentage (denoted as ARX_{12nk}). To ensure that the resultant ARX_{12nk} is the best achievable model, the process is essentially iterative and computed up to a maximum allowable order of delays for that segment. That is, the best value of n_k is obtained by executing system identification function one set of parameters at a time, computing the percentage of fit, validating each model and incrementing n_k up to a total number of samples minus five. This limit was found empirically by using the MATLAB® system identification GUI to compute and arrive at the model without failure. In case of a number of samples being larger than 300, it will be truncated to 300 and a maximum value of n_k will therefore be 295 to avoid excessive computational load. The best value of n_k is the one yielding the highest percentage of fit and satisfying stability and residual tests.

The flowchart presented in Figure 6.3 shows the steps for deriving the best achievable model of a human operator in both computer-based and hardware-based experiments. Segmentation according to a pair of target positions is required for both data sets. These segmented data are referred to as *.mat* and *.xls* files at the top of part (a) in Figure 6.3 respectively. Raw data in *.mat* file for the computer-based experiment can be obtained directly as all the programs were written in MATLAB® but this is not the case for the hardware-based experiment where the programs were written in Microsoft Visual Basic®. In addition to that, the readings of potentiometers voltage from all channels are not simultaneously available. Therefore, a time offset for each channel needs to be treated carefully so that these data can be paired with their corresponding time vector, which will then be used for generating a time series object. The order of channel also affects how the readings offset from one another. Further details on this can be found in Appendix A.

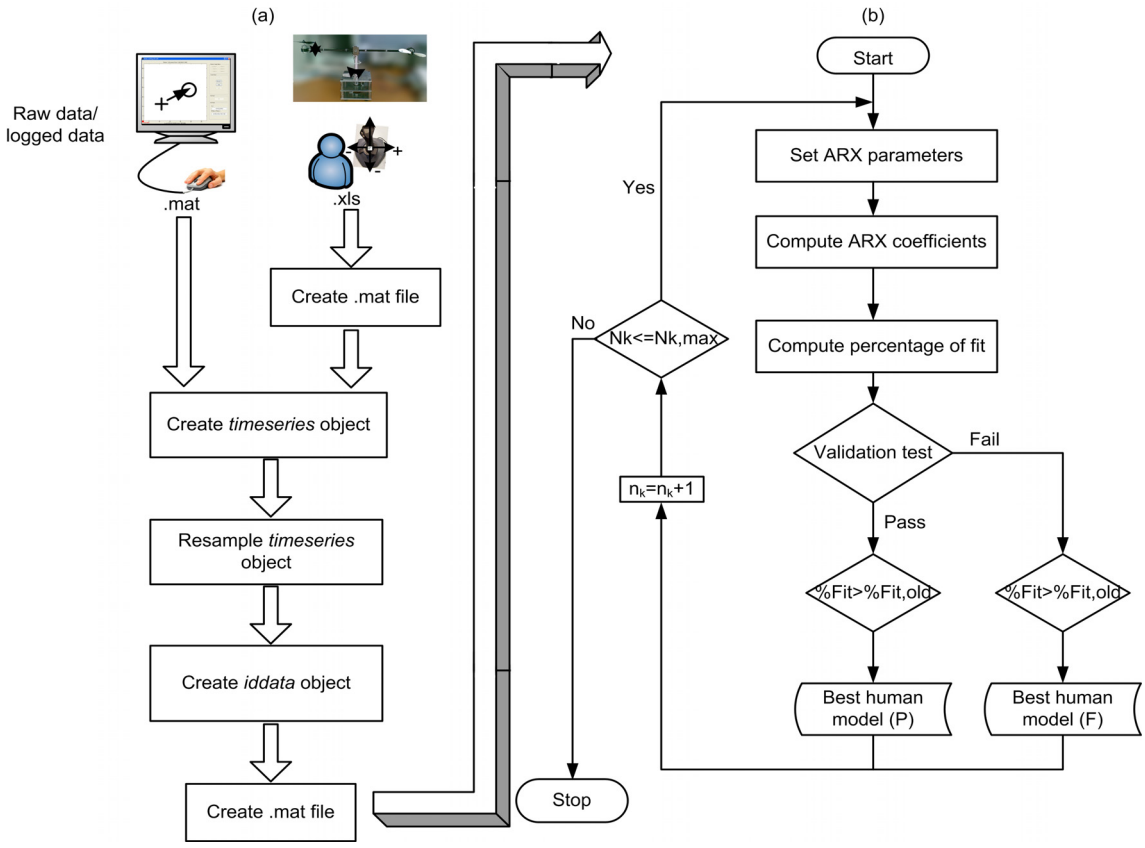

Figure 6.3. Flowchart of system identification steps based on segmented data (Note: Fail here means 99% Confidence Interval (CI) is used rather than the default 97% CI)

Once the data are in a suitable form and perfectly aligned with their corresponding time vectors, an object called *iddata* is created. *Iddata* is the MATLAB® timeseries object with fixed sampling time, input/output channel names, input/output units and starting time that is required for system identification. However, before an *iddata* object can be created, a *timeseries* object needs to be created first and then resampled to comply with *iddata* restriction to consist of only equally sampled data. For simplicity, all *iddata* objects for each segment are combined into a single .mat file. The collection of these *iddata* objects can then be imported into MATLAB® functions and processed with system identification algorithm directly and that concludes all the steps covered in part (a) of Figure 6.3. In short, this part deals with raw data preparation for system identification algorithm, which mainly includes data segmentation and re-sampling of the logged data.

For part (b) of Figure 6.3, the steps show how every *iddata* object is processed through a series of MATLAB functions with n_k or a number of time delay sample incremented iteratively up to a maximum limit ($n_{k,max}$). The process starts by assigning n_a, n_b and varied n_k value to the ARX model, computing the ARX coefficients, testing stability and residual conditions and storing a resultant model along with its percentage of fit. A percentage of fit for each ARX model is based on the difference between the output from a derived model and its validation data (actual output from the experiment) as follows.

$$fit = \left[1 - \frac{|y - \hat{y}|}{|y - \bar{y}|}\right] \times 100\% \tag{6-21}$$

Where y is the validation data, $\hat{y}$ is the predicted output from the model, $\bar{y}$ is the mean value of y. The definition of norm is as follows.

$$|x| = norm(x) = \sqrt{x_1^2 + x_2^2 + x_2^3 + \ldots + x_n^2} \tag{6-22}$$

A resultant model from the first iteration is regarded as the best human model for that particular segment. Its percentage of fit value is compared with the model of the next iteration to check which one is higher. If a model from the first iteration has higher percentage of fit, it will be kept as the best model otherwise a model from new iteration will be kept instead. That model remains the best model unless a model from the latest iteration has higher percentage of fit. This process continues until n_k value reaches its maximum limit and each model is ensured to satisfy the stability criterion.

Concerning these models being classified as *pass (P)* or *fail (F)*, they are justified based on its stability and residual test results. If there is no best passed model by the end of last iteration, the best failed model will be used instead. In all cases, the best-failed model passes an auto-correlation test but not a cross-correlation test due to a 97% confidence interval. The value of this confidence interval allows a model to sufficiently describe the human's action. The increased level of confidence on a larger range on the confidence interval is the key as long as the model output agrees with the actual data.

In order to compute an ARX model, there are two sets of data involved in this process, which are estimation and validation data. These sets of data are measured or logged from the experiments and in this thesis, two-thirds of the set is used for estimation and one-third of the set is used for validation. The following section covers a method to validate human models derived from the set of ARX parameters explained earlier.

6.3.3. Model validation

After the coefficients of each ARX model has been computed, a model validation process called a *residual analysis* is applied to determine a degree by which an actual system output is described by a model. The *residual* or the *leftover* ($\varepsilon(t)$) of a model refers to a difference between model output and measured data used in a modeling process with a mathematical equation as shown below.

$$\varepsilon(t) = y(t) - \hat{y}(t) \tag{6-23}$$

Where y(t) is the measured data at time t and $\hat{y}(t)$ is the model output based on the estimation data set at time t.

According to Ljung (1999), there are two standard residual tests: whiteness test and independence test. A whiteness test is based on a correlation of the residuals among themselves (auto-correlation) whereas an independence test is based on a correlation of the residuals with the inputs (cross-correlation) according to Equations (6-24) and (6-25) respectively.

$$\hat{R}_{\varepsilon}^{N}(\tau) = \frac{1}{N} \cdot \sum_{t=1}^{N} \left(\varepsilon(t) \cdot \varepsilon(t-\tau) \right) \tag{6-24}$$

$$\hat{R}_{\varepsilon u}^{N}(\tau) = \frac{1}{N} \cdot \sum_{t=1}^{N} \left(\varepsilon(t) \cdot u(t-\tau) \right) \tag{6-25}$$

Where $\hat{R}_{\varepsilon}^{N}$ is the autocorrelation of the residual (ε), $\hat{R}_{\varepsilon u}^{N}$ is the cross-correlation of the residual and input *(u)*.

In order for the model to pass both whiteness and independence tests, its correlation value has to fall within a confidence interval (*CI*). The confidence interval is defined statistically according to Equation (6-26).

$$CI = \bar{x} \pm Z_{\frac{\alpha}{2}} \cdot SD \tag{6-26}$$

Where $\bar{x}$ is an average value, *SD* is a standard deviation, $Z_{\frac{\alpha}{2}}$ is a probability at the confidence level under a normal distribution curve. The values of confidence interval, confidence level and standard deviation are tabulated for convenience in the table below.

Table 6-1. Confidence interval table

Confidence level / Variable	95%	97%	99%	99.9%	99.99%
$1-\alpha$	0.95	0.97	0.99	0.999	0.9999
α	0.05	0.03	0.01	0.001	0.0001
$\frac{\alpha}{2}$	0.025	0.015	0.005	0.0005	0.00005
$Z_{\frac{\alpha}{2}}$	1.96	2.17	2.58	3.29	3.89
CI	$\pm 1.96 \cdot SD$	$\pm 2.17 \cdot SD$	$\pm 2.58 \cdot SD$	$\pm 3.29 \cdot SD$	$\pm 3.89 \cdot SD$

From Table 6-1, it can be observed that a range of *CI* is larger at a higher confidence level due to the fact that a probability of any output residing within that range is higher. In other words, the wider the *CI* range, the higher the probability of that a model to have either auto-correlation or cross-correlation value within that range. 97% *CI* is regarded as *Pass* whereas 99% *CI* is regarded as *Fail* in this thesis. However, both of these models have to pass a stability test in order to represent a human model (according to Figure 6.3).

6.4. Performance Variables

This section is dedicated to a retrieval of performance variables with reference to human ARX models according to Sections 6.2 and 6.3. As described in Section 3.5.3.2, Chapter 3 regarding axes of motion, the computer-based human models consist of 2

SISO models (horizontal and vertical) whereas the hardware-based human models consist of only a single SISO model (horizontal or yaw). A number of human ARX models are mainly related to number of trials, system settings and axes of motions. System settings include sequence number and transfer function of the control device used in that experiment. For the computer-based system, only a single target sequence is used whereas three target sequences are used for the hardware-based system. Such difference is introduced to show an influence of target location and its order on human performance due to interaction with hardware and physical environment. Overall, a number of human models for computer-based and hardware-based systems in this thesis are summarised in Figure 6.4(a) and Figure 6.4(b) respectively.

(a) Computer-based system

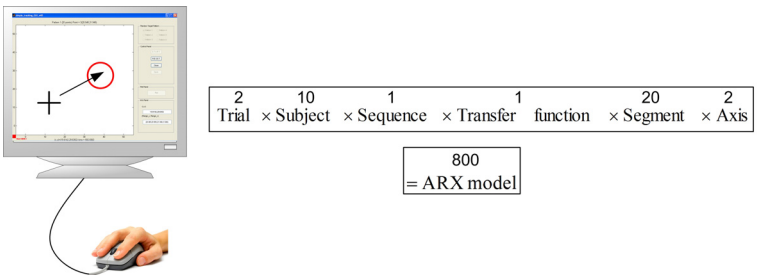

(b) Hardware-based system

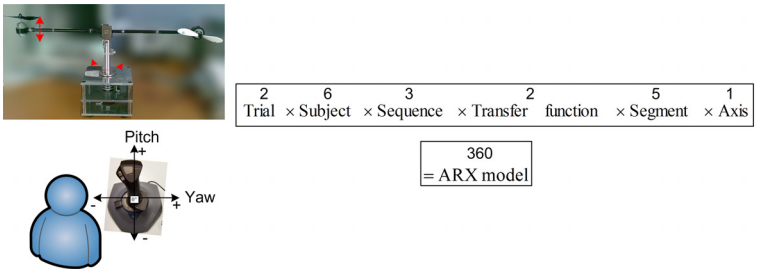

Figure 6.4. Overview of human models for computer-based and hardware-based systems

The major difference of this chapter from Chapter 5 is the focus on level of comparison (according to Figure 3.20, Chapter 3), which applies to both computer-based and hardware-based experiments. Particularly, this section emphasizes on choosing suitable performance variables for representing its corresponding performance criterion.

6.4.1. Speed criterion

Unlike the non-model approach, the speed characteristics are not readily available. Human models need to be computed first to allow ARX parameters to be extracted and analysed. These parameters will then be paired up with the speed variables from the non-model approach to compute differences and determine the best match.

6.4.1.1. Computer-based system

The simple tracking program is a platform for a computer-based experiment with all the codes written in MATLAB® and designed using MATLAB® GUIDE (as explained in Section 4.3.2, Chapter 4). Due to the MATLAB® architecture being matrix-based, the logged data are kept in a matrix form and the whole collection saved as .mat file. A computation of ARX parameters refers to each segment to yield one human model at a time. Then a set of parameters is stored and exported to Microsoft® Excel file for further computation according to Figure 6.5.

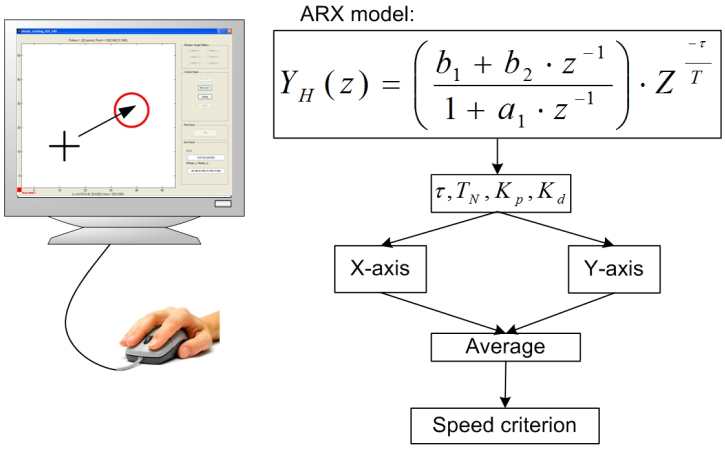

Figure 6.5. Human ARX model from a computer-based system (one segment)

Figure 6.5 presents ARX model of a human operator based on a single segment together with parameters for each axis. It is worth noting that a motion along each axis is considered independent from each other, which is also the case for the hardware-based system. Regarding the ARX parameters (τ or Tau, T_N, K_p and K_d) given in Figure 6.5,

they correspond to only one of 20 segments and the speed criterion is based on the average parameters of X and Y-models (Figure 6.4(a)). This is similar to the non-model approach explained in Chapter 5 with the differences in the format and data processing. In fact, Chapter 5 makes use of the logged data directly whereas Chapter 6 decomposes them into X- and Y-axis, applies system identification independently and calculates the ARX parameters for human performance computation.

The following table shows the ARX parameters in terms of τ, T_N, K_p and K_d with and without inclusion of abnormally high positive ($\geq 10^5$) and any negative entries. Based on these results, the values of ARX parameters vary drastically on every human operator except τ. This, in fact, hints a usability of τ as a speed variable. Moreover, those abnormally high ARX parameters are also found in the previous studies and they usually correspond to an irrespective response and complicated motion pattern (Suzuki, Kurihara et al., 2006).

Table 6-2. Computer-based system Trial 1: Average ARX parameters of human operators A to J

Subject	Tau (s)	TN (s)	Kp	Kd
A	2.792	2.281	0.004	0.000
B	1.609	0.548	0.003	0.002
C	1.683	0.159	0.003	0.001
D	1.596	0.412	0.003	0.001
E	1.903	0.789	0.003	0.002
F	1.729	0.764	0.003	0.001
G	1.594	0.495	0.003	0.002
H	1.569	0.256	0.003	0.001
I	2.019	1.398	0.003	0.025
J	1.615	0.429	0.003	0.003
Average	1.811	0.753	0.003	0.004
SD	0.375	0.640	0.000	0.007

a) with some segments dropped

Subject	Tau (s)	TN (s)	Kp	Kd
A	2.792	-3.73E+10	-2E+07	2083856
B	1.609	1.26E+10	-545323	-1E+07
C	1.683	9.86E+09	-1E+06	1.4E+07
D	1.596	4.08E+09	904453	-3E+06
E	1.903	2.84E+09	491613	-473493
F	1.729	1.11E+09	-1E+07	1.9E+07
G	1.594	-1.58E+09	-74710	1044967
H	1.569	-1.04E+09	-27879	-3E+06
I	2.019	-8.35E+09	4.7E+07	-5E+07
J	1.615	-1.64E+10	386602	-5E+07
Average	1.811	-3.41E+09	976078	-8E+06
SD	0.375	1.45E+10	1.8E+07	2.4E+07

b) without any segments dropped

Interestingly, there is still no variation among human operators even though the segments with unrealistically high or negative values are omitted. The results in Table 6-2(a) suggest that T_N, K_p and K_d cannot identify any difference among human and therefore, are not suitable for computing human performance. This observation is also true for Trial 2 (Table 6-3(a)).

Table 6-3. Computer-based system Trial 2: Average ARX parameters of human operators A to J

Subject	Tau (s)	TN (s)	Kp	Kd
A	2.119	0.728	0.003	0.001
B	1.689	0.268	0.003	0.001
C	1.844	0.857	0.003	0.003
D	1.966	2.265	0.012	0.003
E	2.972	0.104	0.003	0.001
F	1.974	0.231	0.003	0.000
G	2.047	1.257	0.004	0.001
H	1.619	2.508	0.003	0.006
I	2.437	0.186	0.003	0.001
J	2.256	0.355	0.003	0.001
Average	2.092	0.876	0.004	0.002
SD	0.394	0.875	0.003	0.002

a) with some segments dropped

Subject	Tau (s)	TN (s)	Kp	Kd
A	2.119	-3.81E+08	-111211	-1E+06
B	1.689	-7.84E+08	-60469	-2E+06
C	1.844	-6.02E+09	-39237	-9E+06
D	1.966	1.06E+10	-505956	4.3E+07
E	2.972	-1.1E+09	-552087	8241209
F	1.974	1.19E+09	-93963	2420883
G	2.047	-1.04E+09	12281.5	-1E+06
H	1.619	7.51E+10	1.6E+08	-4E+06
I	2.437	-5.93E+08	-11786	-2E+06
J	2.256	1.77E+09	86799.3	5076425
Average	2.092	7.87E+09	1.6E+07	3998541
SD	0.394	2.4E+10	5E+07	1.5E+07

b) without any segments dropped

In contrast to K_p and K_d, T_N values seem to reveal characteristics difference of human operators and may be reasonably used in combination with τ to compute human performance. However, the percentage of ARX parameters with normal values (Table 6-4(a) and (b) for both Trial 1 and 2 respectively) suggest that none of T_N, K_p and K_d are totally reliable even though their values are in the same range as Suzuki's experiment Suzuki, Kurihara et al., 2006 (K_p=0-2000 and K_d=0-1000).

Table 6-4. Computer-based system: percentage of normal parameters for subject A to J based on segments 1 to 20

Subject	Tau	TN	Kp	Kd
A	100%	60%	60%	55%
B	100%	75%	75%	75%
C	100%	75%	75%	70%
D	100%	75%	75%	65%
E	100%	90%	90%	90%
F	100%	50%	50%	50%
G	100%	70%	70%	70%
H	100%	80%	80%	80%
I	100%	75%	70%	75%
J	100%	70%	70%	70%
Average	100%	72%	72%	70%

a) Trial 1

Subject	Tau	TN	Kp	Kd
A	100%	85%	90%	85%
B	100%	85%	85%	80%
C	100%	65%	65%	55%
D	100%	65%	65%	65%
E	100%	40%	40%	40%
F	100%	45%	45%	30%
G	100%	65%	65%	60%
H	100%	80%	80%	80%
I	100%	65%	65%	60%
J	100%	85%	85%	80%
Average	100%	68%	69%	64%

b) Trial 2

Based on Table 6-4, it can be observed that the values of ARX parameter τ (time delay) for all human operators are 100% normal for both sets of experiments whereas other ARX parameters are only normal in most cases. This observation suggests that ARX human models are suitable for performance evaluation and τ, in particular, can be reliably derived from the experiments. A selection of speed variables and performance computation will be covered in details under a *variable HPI* section.

6.4.1.2. Hardware-based system

Similar analysis to the computer-based system is applied directly on resultant ARX models but with only a single axis treatment as presented in Figure 6.6.

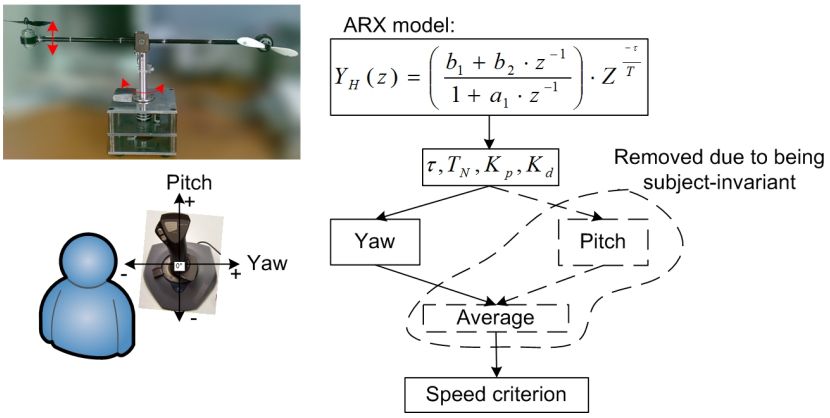

Figure 6.6. Human ARX model from a hardware-based system (one segment)

Before getting into details about speed variables, a proof for the successful derivation of only yaw-axis ARX models will be first given with reference to the observation on the actual logged data. The computation of the input excitation level will also be presented. The main reason for ignoring the pitch-axis ARX model is due to insufficient control actions to balance the helicopter test rig in a vertical direction based on data of all human operators. Theoretically, this is a consequence of deficiency on the input excitation level to produce ARX models. To prove this, the investigation into the experimental data will be made and then followed by a computation of excitation level.

First of all, Trial 1 sample of subject A based on sequence 1 (θ_{yaw}: 90°►270°►90°►270°► 90°►270° according to Figure 6.7(c)) with linear joystick transfer function is used for illustration. Figure 6.7(a)-(d) present a time-series of actual logged data in terms of pitch angle, pitch motor voltage, yaw angle and yaw motor voltage respectively. Points A to E in Figure 6.7 are marked according to the positions of targets defined in sequence 1. Undershoots (prior to settling at points A, C and E) and overshoots (prior to settling at points B and D) can be spotted at these locations and they are in response to correcting the motion either due to falling short or beyond the target location, which can be collectively considered as *correction points*.

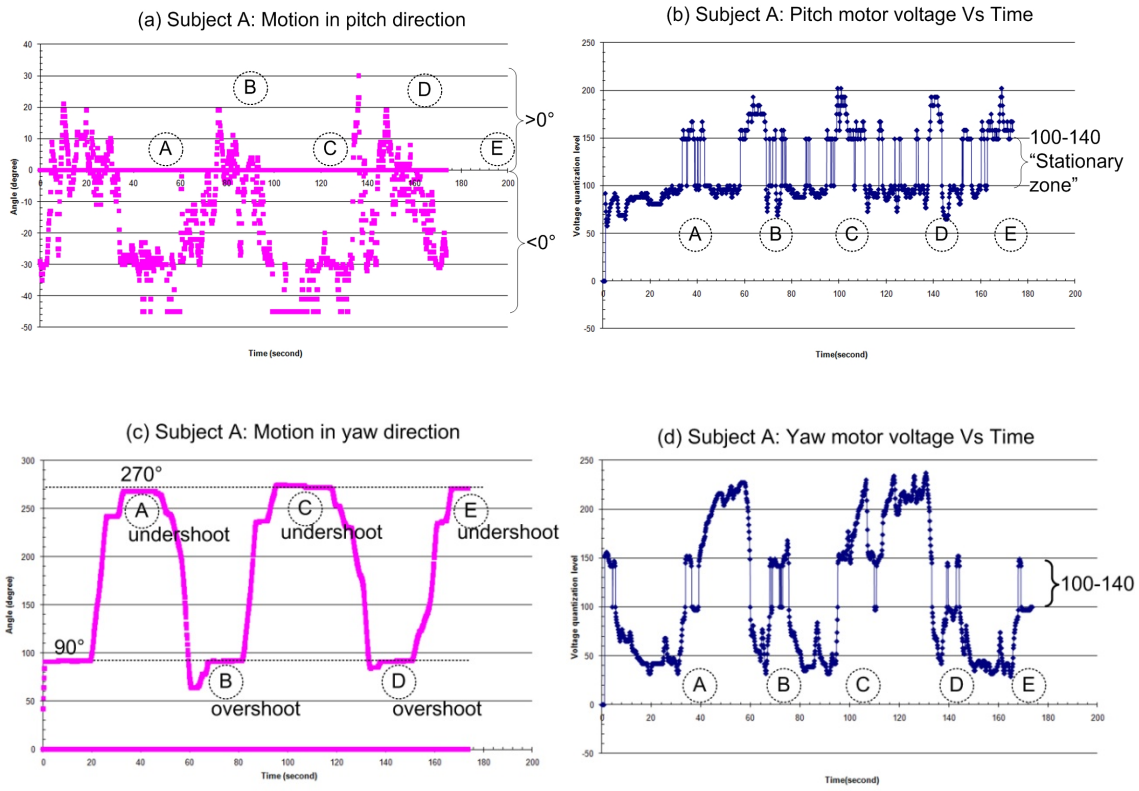

Figure 6.7. Time-series data of subject A for both pitch and yaw motions (Note: Stationary zone means no motion can be induced on the helicopter test rig.)

The corresponding U_{motor} or motor voltages, whose value ranges from 0 to 255 (Chapter 4), are reflective of how control actions of human are imposed onto the joystick or effectively onto two motors located on the helicopter test rig. From this perspective, $U_{motor,yaw}$ in Figure 6.7(d) can therefore be noticed to be outgoing at these correction points. In other words, $U_{motor,yaw}$ tends to move away from stationary zone to either carry on with the motion or reverse it as appropriate.

Regarding effort on making the helicopter test rig horizontal while traversing along a target sequence, motions of helicopter test rig in clockwise and counter-clockwise directions tend to move down and up respectively due to yaw and pitch thrust characteristics. By this statement, it means that the vertical angle or θ_{pitch} at those positions tends to wander around zero degree angles intrinsically if no compensation is applied to maintain its level. This implies that $U_{motor,pitch}$ values (with reference to Figure 5.20?) have to be lower than 127 and higher than 127 to decrease pitch angle by pulling and pushing respectively as shown in Figure 6.8.

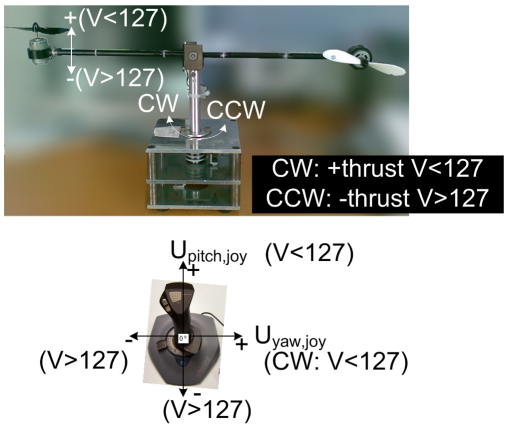

Figure 6.8. Detailed directions of motion with reference to joystick and helicopter test rig

Therefore, $U_{motor,pitch}$ must be higher than 127 for any clockwise motion (i.e. 90°►270°: Points A, C and E) to suppress thrust automatically generated by yaw motor in downward direction. Similarly, $U_{motor,pitch}$ must be lower than 127 to suppress thrust in downward direction for a counter-clockwise motion (i.e. 270°►90°: Points B and D). A magnitude of $U_{motor,pitch}$ depends not only on intrinsic thrust characteristics but also on deliberate hand motion on the joystick. Now with reference to points A, C and E in Figure 6.7(b), there is no reasonable period of time at which U_{pitch} is held at higher than 127 to pull θ_{pitch} up or maintaining it at nearly zero degree. This is similar for points B and D where Upitch of lower than 127 cannot be clearly observed. These behaviors are prior to the landing on positions of interest regardless of the type of corrections (undershoot or overshoot) and such behaviour can also be observed in control motions of other subjects as well (Appendix D.5).

To prove that the above observations are theoretically correct, the conditions of persistently exciting input are tested according to the following equations (*persistence of excitation* definition 13.13, page 412, Ljung, 1999):

$$\left|M_n(e^{j\omega})\right|^2 \cdot \Phi_u(\omega) \equiv 0 \tag{6-27}$$

$$M_n(e^{j\omega}) = 0 \tag{6-28}$$

$$\Phi_u(\omega) \neq 0 \tag{6-29}$$

Where

M_n is the system of interest in the form:

$$M_n(q) = m_1 \cdot q^{-1} + \ldots + m_n \cdot q^{-n} \tag{6-30}$$

$\Phi_u(\omega)$ is the spectrum or Fourier Transform of input signal *u(t)* with $R_u(\tau)$ or a covariance function of *u* in the following form:

$$\Phi_u(\omega) = \sum_{\tau=-\infty}^{\infty} R_u(\tau) \cdot e^{-i\tau\omega} \tag{6-31}$$

$$R_u(\tau) = E\left[u(t) \cdot u(t-\tau)\right] \tag{6-32}$$

To satisfy the condition specified in Equation (6-27), the excitation level condition requires the input spectrum with at least *n* points to lie within an interval $-\pi < \omega \leq \pi$ (or f=±0.5Hz) so as to estimate a system of order *n* without ambiguity. Figure 6.9 shows the input spectrum of yaw and pitch data based on Figure 6.7(a) and (b) presented earlier. It can be seen that the magnitude of spectrum in a frequency range of 0.1 and 1 Hz are positive for yaw data and both $\theta_{yaw,in}$ and $\theta_{yaw,joy,}$ appear to satisfy the persistently exciting condition. However, this is not the case for pitch data. According to Figure 6.9(b), the graph shows that $\theta_{pitch,in}$ is completely zero for all subjects and therefore, the input signal is not persistently exciting. As a result, Figure 6.9 agrees with the previous observation about marginal effort on pitch control actions and leads to a conclusion of why only yaw ARX models can be successfully derived by the system identification.

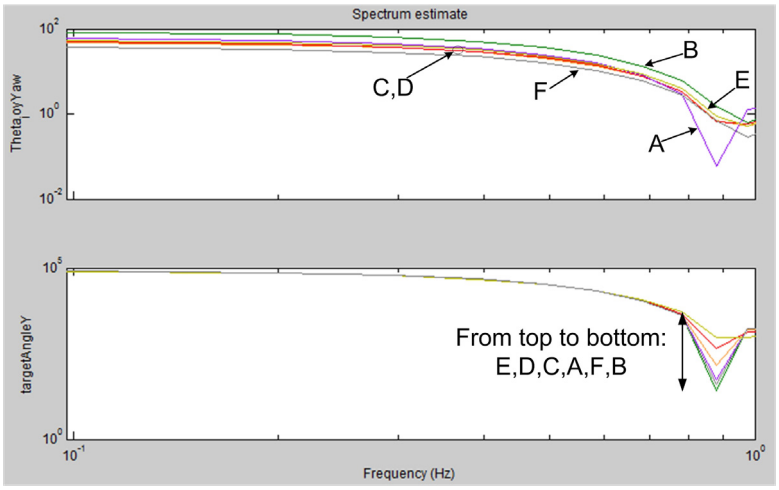

a) Spectral analysis of yaw data: targetAngleY and Theta_joy_yaw ($\theta_{yaw,in}$ and $\theta_{yaw,joy}$ according to Figure 6.2)

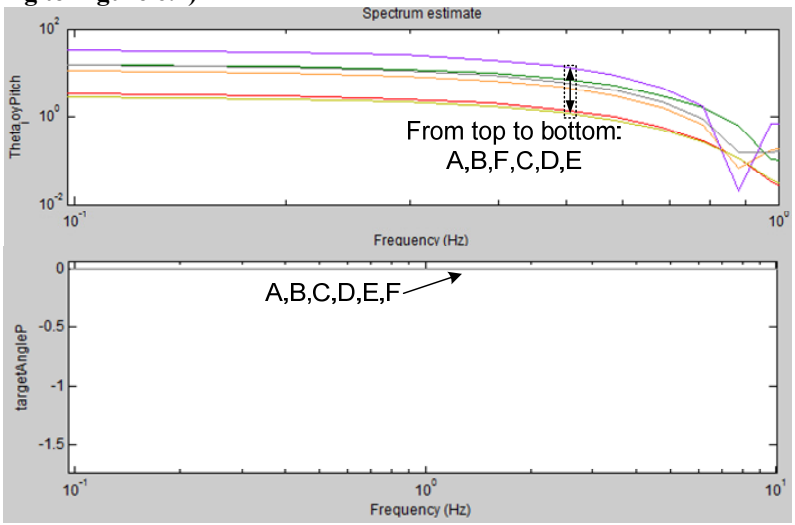

b) Spectral analysis of pitch data: targetAngleP and Theta_joy_pitch ($\theta_{pitch,in}$ and $\theta_{pitch,joy}$ according to Figure 6.2)

Figure 6.9. Input and output spectrum: Trial 1, sequence 1, linear transfer function (subjects A-F)

Referring back to the ARX parameters, the average values of τ ,T_N, K_p and K_d based on subjects A to F are tabulated in Table 6-5 with abnormally high or negative values excluded. In general, the average values of all parameters appear to be higher than those of computer-based system (Table 6-2 and Table 6-3), especially K_p and K_d by which the differences are approximately 100 times larger.

Table 6-5. Average ARX parameters for hardware-based experiments based on all subjects for target sequences 1, 2 and 3 (complete version can be found in Appendix D)

		T1				T2			
		τ (s)	T_N	K_p	K_d	τ (s)	T_N	K_p	K_d
Linear	Seq1	7.871	1.844	0.057	0.118	8.231	0.023	0.005	0.000
	Seq2	8.099	1.575	0.282	0.368	8.720	0.343	0.001	0.022
	Seq3	8.415	2.102	0.037	0.213	5.605	0.278	0.015	0.004
	Average	8.128	1.840	0.125	0.233	7.519	0.215	0.007	0.009
	SD	**0.2732**	0.2636	0.1358	0.1262	**1.6750**	0.1693	0.0069	0.0117
Squared	Seq1	8.469	0.865	0.077	0.062	8.169	0.020	0.001	0.000
	Seq2	9.029	6.917	0.052	0.140	7.267	0.512	0.121	0.000
	Seq3	7.128	0.268	0.034	0.013	8.017	0.235	0.004	0.009
	Average	8.209	2.683	0.055	0.072	7.818	0.256	0.042	0.003
	SD	**0.977**	3.679	0.022	0.064	**0.483**	0.247	0.068	0.005

Even though a variance of τ (time delay) were found to be approximately 0.4 and hence being neglected (Suzuki, Kurihara et al., 2006), it is of a major concern in this research as the values are varied across different settings and trials (Table 6-5: in bold). This is because the focus of this research is on classifying human characteristics in terms of performance difference. Therefore, a difference that reflects and indicates a human difference in controlling or performing a task is deemed important regardless of the scale. In addition to τ values, T_N values are also found to lie in the same range as the aforementioned article. A table of summary is now presented in Table 6-6.

Table 6-6. Hardware-based system: percentage of normal parameters for subject A to J on each target sequence (complete version can be found in Appendix D)

		T1				T2			
		τ(s)	T_N	K_p	K_d	τ(s)	T_N	K_p	K_d
Linear	Seq1	100%	100%	53%	50%	100%	100%	20%	33%
	Seq2	100%	100%	7%	13%	100%	100%	3%	13%
	Seq3	100%	100%	13%	33%	100%	100%	23%	30%
	Average	100%	100%	24%	32%	100%	100%	16%	26%
	SD	0%	0%	25%	18%	0%	0%	11%	11%
Squared	Seq1	100%	100%	30%	33%	100%	100%	17%	17%
	Seq2	100%	100%	27%	30%	100%	100%	7%	3%
	Seq3	100%	100%	30%	40%	100%	100%	37%	43%
	Average	100%	100%	29%	34%	100%	100%	20%	21%
	SD	0%	0%	2%	5%	0%	0%	15%	20%

The percentage of normal parameters presented in Table 6-6 gives an overview on how reliable these ARX parameters can be derived from the hardware-based system. Unlike the computer-based system, all values of τ and T_N are completely normal and they might be used to reflect a speed performance for each human subject. Further analysis

will be made in Section 6.5.1 to determine which ARX parameters are the best match with that of non-model approach.

Regarding a rise time effect imposed on the non-model approach to exclude hardware characteristics from human performance computation, the same rationale is not applicable to the model-based approach. This is indeed due to a pair of data involved in system identification for the hardware system. That is, the non-model approach purely relies on a system output and that output is apparently incorporated with hardware characteristics. Nevertheless, human ARX models in the hardware-based system are derived based on a pair of data involving just a joystick deflection angle and target angle before entering the helicopter test rig (Figure 6.2).

6.4.2. Accuracy criterion

As described in the proposed HPI concept in Section 3.4 (Chapter 3), the accuracy characteristic involves a deviation of actual output from a reference output. That is, the speed characteristic is based on human ARX model whereas the accuracy characteristic is based on a system output from that human ARX model. To fulfill this requirement, a step response to produce an output trajectory is required and a fixed target position is used instead of a predefined target sequence like that of non-model approach for simplicity and consistency. This is how the accuracy analysis differs from the accuracy analysis. Details for the computer-based and hardware-based systems will be covered correspondingly.

6.4.2.1. Computer-based system

According to Figure 6.10, human models that are derived from MATLAB® system identification algorithm are based on logged data or *iddata* objects from their corresponding axis. The only requirement for accuracy analysis is to use human ARX models to compute a step response or a system output in a trajectory/path format.

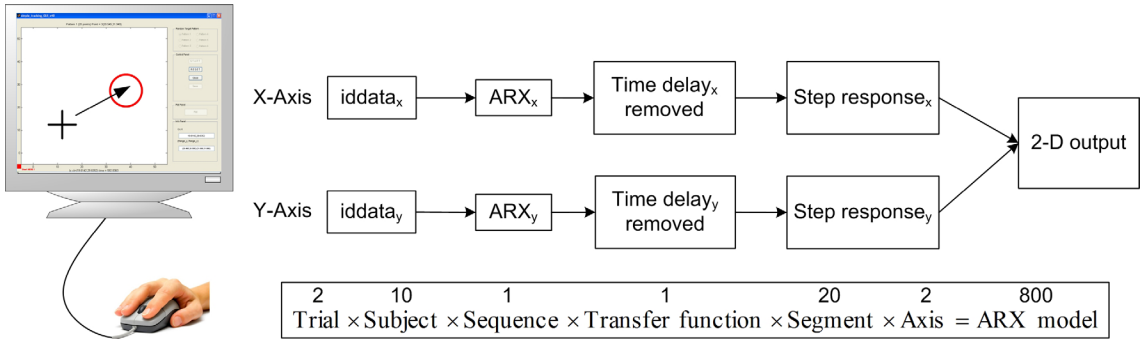

Figure 6.10. Overview of a computer-based HPI computation (accuracy criterion)

With regard to this process, it is straightforward to achieve a 2-dimensional output provided that a time delay for x and y-axes from human ARX models is treated correctly. This is because the resultant ARX models obtained according to a flowchart in Figure 6.3 are guaranteed to have a time delay that best describes or matches the input-output data of that human subject. Therefore, the associated time delay for each axis might differ and it has to be removed prior to a step response simulation to avoid a *time delay misalignment*, which is not the issue for the models with equal time delay.

In the computer-based system, a unit step response is used and applied to both x and y-axes. This is effectively a motion from a position (0,0) to a position (1,1) and a straight line connected between these two positions is regarded as a reference path. The effect of time delay on the output in terms of a *time delay misalignment* is illustrated in Figure 6.11(c) with Figure 6.11(a) and (b) showing a comparison of results from human ARX models with and without time delay respectively.

To compare user's path that is based on the actual logged data from the operating field with the step response produced from human ARX model (Figure 6.11), Figure 6.12 is presented.

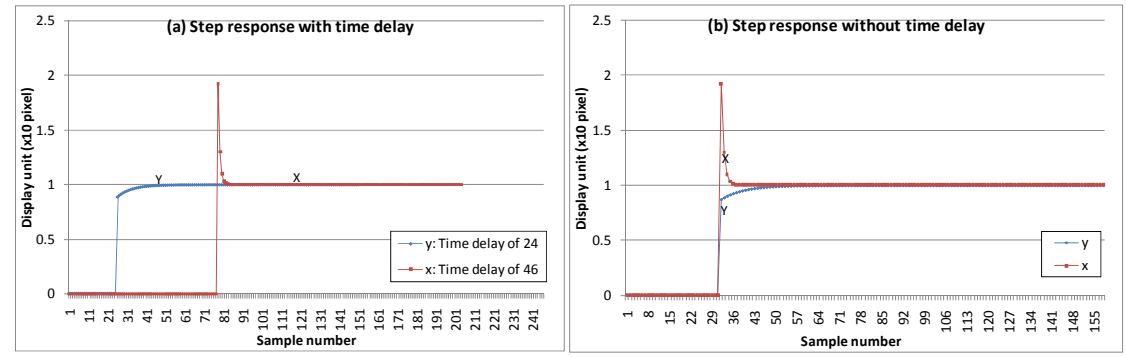

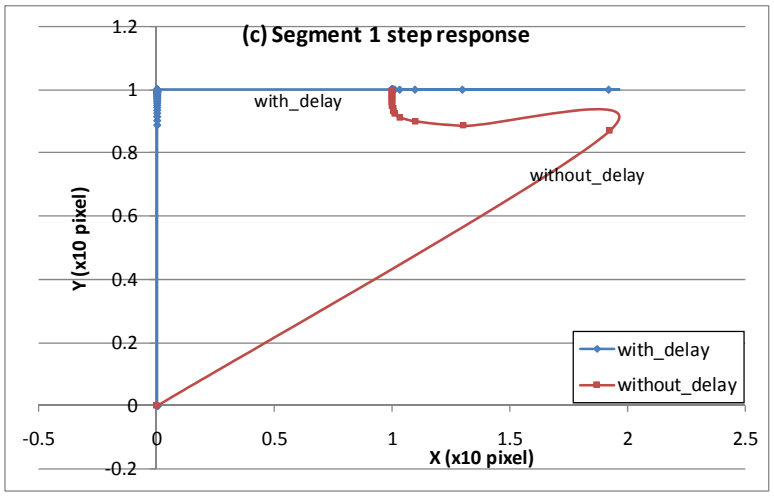

(d) Human ARX parameters for x and y-axes

	Y	X
Tau(nk)	24	46
TN	0.2936211	0.039136
Kp	0.002879	0.002885
Kd	0.0007293	0.00027

Figure 6.11. Computer-based experiment: 5-second 2-dimensional unit step response of subject B, segment 1 from (0,0) to (1,1) [Note: A multiplication factor of 10 is used to convert a display unit to pixel as described in Figure 4.7]

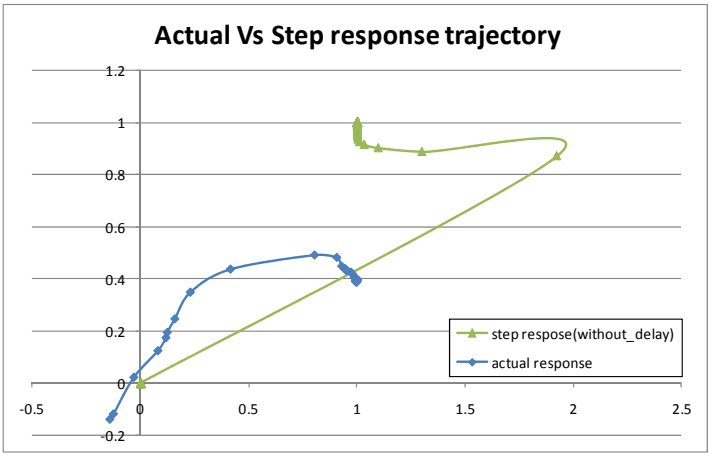

Figure 6.12. Computer-based experiment: comparison of actual and simulated response of subject B, segment 1 (x-axis: pixel, y-axis: pixel)

Regarding the target positions involved in this two scenarios, it can be observed that the actual response refers to initial red-box position (-5.9,-5.8) to target #1 (16.1,41.7)

(segment 1 according to Table 4-2, Chapter 4) whereas the step response refers to (0,0) to (1,1). Figure 6.12 shows that the shape of user's paths from these two different sources look similar in terms of R^2 quality showing closeness to the linear regression line or the line connecting between two target positions. On the contrary, *RMSE* quality is not apparent because the curvature pictured by these two sources look quite different and this requires further analysis.

6.4.2.2. Hardware-based system

Based on the previous remark on validity of only human ARX model on yaw axis, Figure 6.13 shows that a fixed pitch-axis model is required to produce a simulated output path according to the accuracy characteristics definitions (see Section 3.4.2, Chapter 3). A step response in yaw direction is computed from human ARX model whereas a step response in pitch direction is computed from a simple compensator without any time delay. According to these settings, the time delay is not an issue here because the response in pitch direction is constant regardless of an instant the simulation is executed.

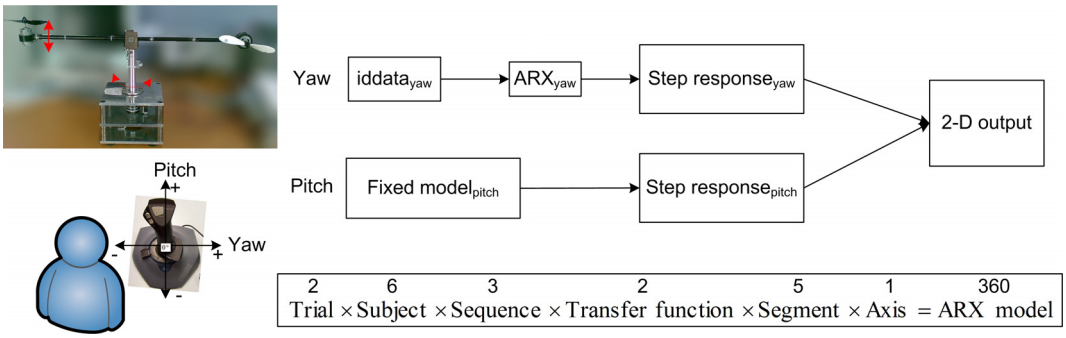

Figure 6.13. Overview of a hardware-based HPI computation (accuracy criterion)

With reference to the MATLAB Simulink® model presented in Figure 6.14(a), the model is mainly comprised of yaw components according to the Equation (4-11), Chapter 4 and pitch component as shown in Figure 6.14(b). In effect, a simple compensator increases or decreases pitch motor voltage in response to a vertical or pitch angle in response to the thrust generated from both pitch and yaw propellers. An

increment and decrement of pitch motor voltage is with reference to 102 (empirical value based on a stationary position of a joystick-see Section 4.4.1.3, Chapter 4).

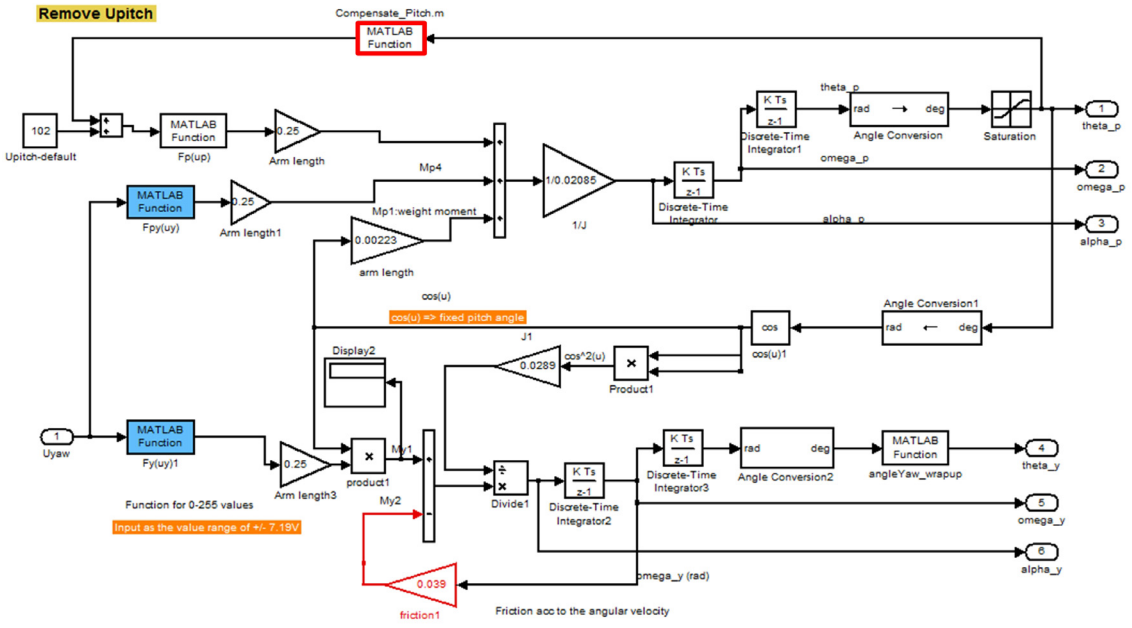

a) Helicopter test rig Simulink® model

```
if Pitch_angle >= 0 && Pitch angle <= 45
    Upitch = 117;
elseif Pitch_angle <= -44 && Pitch_angle >= -45
    Upitch = 5;
else
    Upitch = 20;
end
```

b) Compensate_Pitch function

Figure 6.14. Simulink® model of a hardware-based system

Regarding a consideration on step response, a unit step response is arbitrarily chosen for the computer-based system and the simulated results agree with the actual results without any issues. This is not the case for a hardware-based system because a 1° movement in yaw direction is considered unrealistic to perform on a physical system like the helicopter test rig. It is also irrespective of a physical setup where a destination angle is extremely small and not easy to visualise like the multiples of 45°. Therefore, a step response of 90° with an initial position of 0° is chosen to serve this purpose.

As described earlier that pitch motion is required to simulate user's path, the use of fixed pitch-axis model is applied to every human subject. Therefore, the compensation

mechanism is intentionally designed to be unbalanced to comply with the behavior illustrated in Figure 6.7. That is, a motor voltage is selected so that it tends to push a metal bar below its equilibrium level to simulate human's passive characteristics in a vertical direction. This unsurprisingly makes the simulated results more weighted in a negative region comparing to that of positive region. Now the actual and simulated output responses for a 90° to 270° in yaw direction are plotted in Figure 6.15 together with an ideal or horizontal trajectory.

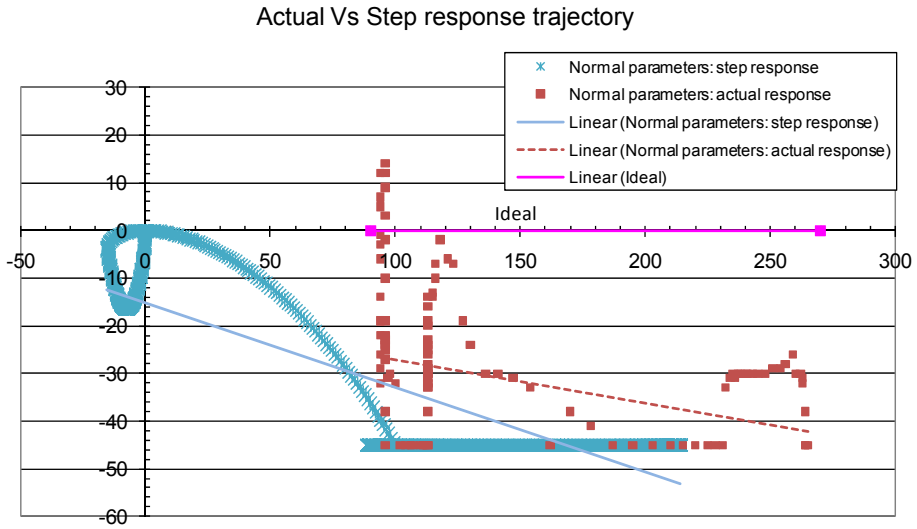

Figure 6.15. Hardware-based experiment: Comparison of actual and simulated response of subject C, segment 2, sequence 1, linear transfer function of Trial 1 (x-axis: yaw angle, y-axis: pitch angle).

As pointed out earlier, a proportion of pitch angle stays noticeably below horizontal level almost entirely showing agreement between the actual and simulated responses. Although the response shapes are not identical, they share similarities in terms of pitch angles and a linear regression path created by their corresponding data points, which potentially reflect similar behavior to that of actual human.

To conclude, the only requirement for accuracy analysis using the model-based approach is a step response. The reason for that is to simulate an output trajectory from human ARX models for each axis and use it to compute R^2 and *RMSE* the same way as that of non-model approach (refer to Section 5.4.2, Chapter 5). However, only ARX parameters from those human ARX models are required for speed analysis and this will become clearer in the following section.

6.5. Human Performance Index (HPI) forms

As mentioned earlier, the focus of this section is to verify the performance variables and from the model-based approach by comparing them with those of non-model approach. The monotonicity of performance variables is treated the same way as before (see Section 3.5.2.2, Chapter 3 for details). Such difference only concerns the case of speed variables, by which the ARX parameters are used instead of a V_{av} and T, because R^2 and *RMSE* are still used as accuracy variables in the same manner. Moreover, a consideration on monotonicity of ARX parameters does not cause much effect on the results and this will become clearer when the graphs are presented. The presentation of this section is similar to Section 5.5, Chapter 5 but with a comparison between the non-model and model-based approaches rather than that of Trials 1 and 2. This section will demonstrate the distribution of differences between the results from the non-model and model-based approaches (subject-level analysis) for each and every human subject and then followed by a summarized version in a tabular format to provide an overview for both Trials 1 and 2 (approach-level analysis). The objective is to illustrate suitable performance variables to represent a performance criterion in HPI computation and build awareness on the source of discrepancies in HPI values.

6.5.1. Variable HPI

Performance variables for speed criterion obtained earlier from human ARX models (τ ,T_N, K_p and K_d) are treated as monotonically decreasing to comply with their qualitative properties. For simplicity, the graphs illustrating the overview of all ARX parameters will be plotted against J_1 (from the non-model approach) first and then focused on the candidate variable(s).

6.5.1.1. Computer-based system

A discussion will be made with reference to all ARX parameters based on Table 6-2(a) and Table 6-3(a) for Trials 1 and 2 respectively starting from a speed score.

- *Speed score*

Based on Figure 6.16, the speed scores of subjects A to J computed by a non-model approach (J_1) are plotted against ARX parameters τ (Tau), T_N, K_p and K_d of the human ARX models. It can be observed from Trial 1 in Figure 6.16(a) that K_d largely differs from those of the non-model values whereas K_p are quite close to the non-model values. However, this is not the case for Trial 2 as shown in Figure 6.16(b). Therefore, these results reveal an inconsistency of T_N, K_p and K_d on top of a probability to be abnormally high or negative as shown in Table 6-4 except τ. Interestingly, re-considering T_N, K_p, and K_d as monotonically increasing that are the reflected versions with reference to 1.0 does not change the previously mentioned observations.

a) T1

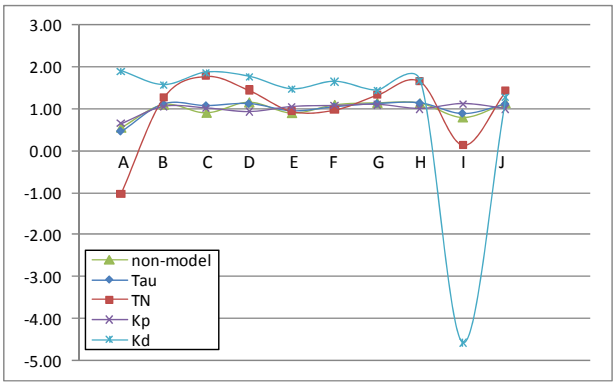

b) T2

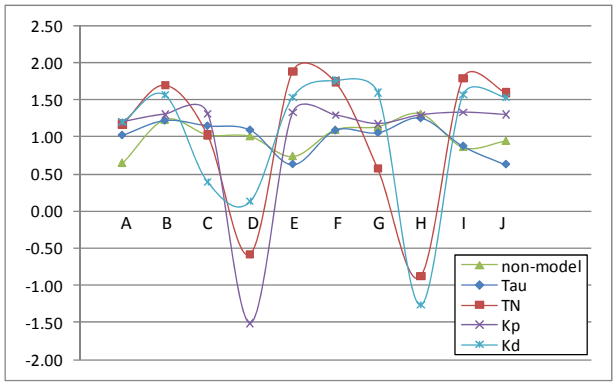

Figure 6.16. Computer-based experiment (subjects A to J): Speed score of non-model approach (J_1) vs. τ, T_N, K_p and K_d

With a closer look into only a time delay parameter (τ or Tau) in Figure 6.16, Figure 6.17(a) and Figure 6.17 (b) clearly reveal its closeness to the non-model counterpart J_1 or the weighted version of V_{av} and T (refer to the right-most columns of Table 5-4 and 5-5, Chapter 5). The agreement of these results suggests that τ can reasonably represent speed characteristic of human operator for the model-based approach as accurately as the time taken and average velocity variables for the non-model approach.

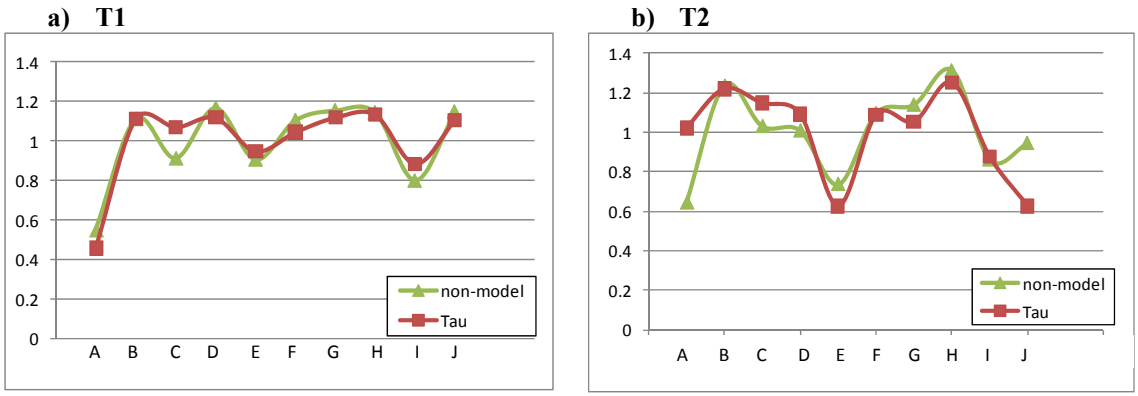

Figure 6.17. Computer-based experiment (subjects A to J): Speed score (J_1) vs. τ

Based on this analysis and the one presented in Section 6.4.1.1, it is reasonable to claim that τ can be reliably derived and best describes the speed score for the model-based approach (similar analysis will be completed for the hardware-based experiment as well). This consequently makes it the only speed variable that is suitable to represent a speed criterion.

In addition, it is important to stress that the sets of ARX parameters used in the computer-based system are the averaged version of parameters from X and Y models (according to Figure 6.5). However, it is obvious that there is different degree of discrepancies between the values from the non-model and model-based approaches for every human subject, which is likely caused by averaging the time delay from two axes. Other factors apart from this will be the cause of discrepancies for the hardware-based experiment because only yaw-axis model can be successfully derived.

- *Accuracy score*

Figure 6.18 shows a sample of a simulated response from the coordinated positions resulting from x and y-axis ARX models (derived from segment 1 of subject B). The ideal line or the line to be used as a reference in calculating *RMSE* and R^2 is also included along with the linear regression line based on the simulated response (dotted line).

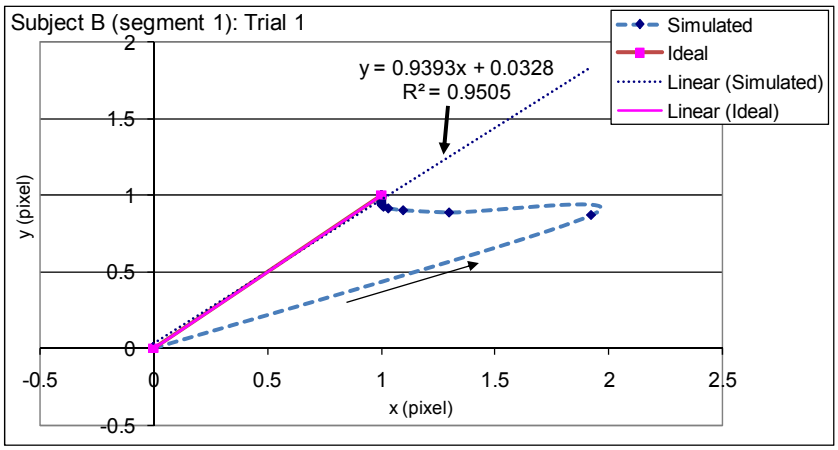

Figure 6.18. Computer-based experiment: 1-minute simulated trajectory used for accuracy analysis (from position (0,0) to (1,1))

In terms of accuracy characteristics, Figure 6.18 suggests that the *RMSE* value for subject B should be high due to a loophole pattern of his/her simulated response, which indicates a high degree of deviation. At the same time, its near-perfect alignment with the ideal trajectory also suggests that the R^2 value should be high indicating a high degree of closeness in terms of orientation between these two lines. Simulated trajectories for other segments, settings and subjects are created and used for accuracy analysis in the same fashion.

Now with reference to Figure 6.19, the individual R^2 and *RMSE* values from the model-based approach are plotted against J_2 from the non-model approach or the weighted version of R^2 and *RMSE* (refer to the right-most columns of Table 5-6 and 5-7, Chapter 5). It turns out that these results do not match very well like that of speed score scenario, whereby the speed criterion is well-represented by only a single variable τ. Therefore, a closer examination into each accuracy variable and difference among them will lead to

an understanding of the quality of actual and simulated trajectories. The smaller the difference, the higher degree of closeness for that accuracy variable is to its non-model counterpart. Further analysis into the entries with minimum or maximum difference will even lead to an understanding on the source and manner of influence on such outcome.

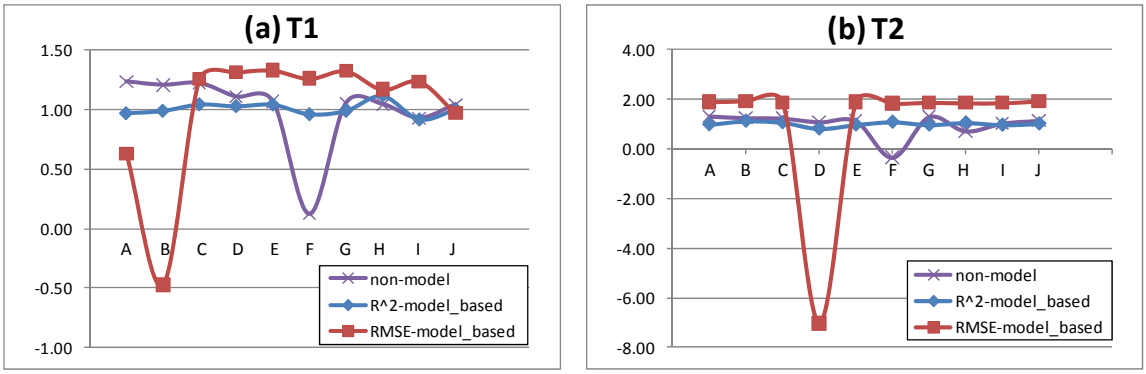

Figure 6.19. Computer-based experiment (subjects A to J): Accuracy score (J_2) vs. R^2 and *RMSE*

Based on the definitions of Step 2 comparison in Section 3.5.4, all accuracy variables (R^2, *RMSE* and J_2) computed from subjects A to F using the non-model and model-based approaches can be further processed and the results are as presented in Table 6-7.

Table 6-7. Computer-based experiment: Average difference for accuracy variables based on Trials 1 and 2 (Approach-level difference)

		T1: Non-model			T2: Non-model		
		R^2	RMSE	J_2	R^2	RMSE	J_2
Model-based	R^2	**0.04**	0.33	**0.18**	**0.09**	0.62	**0.35**
	RMSE	0.39	*0.59*	0.47	1.61	*1.65*	1.63
	J_2	0.20	0.43	0.30	0.82	0.93	0.84

With reference to Table 6-7, the smallest average differences can be observed to result from R^2-R^2 entries with the values of 0.04 and 0.09 respectively (in bold) whereas the results from R^2-J_2 entries seem to be the second smallest (in bold). On the other hand, the *RMSE-RMSE* entries appear to have the largest difference (in italics) and these observations are true for both Trials 1 and 2.

More importantly, an investigation into an individual average difference for each human or a subject-level difference reveals a slight difference on some subjects and a significantly larger difference on other subjects. This suggests that a discrepancy might be contributed by only few human subjects. To illustrate this, the distributions of accuracy scores for the entries with bold and italicised fonts, which are extreme cases, are presented in Figure 6.20 (notations according to Section 3.5.4, Chapter 3).

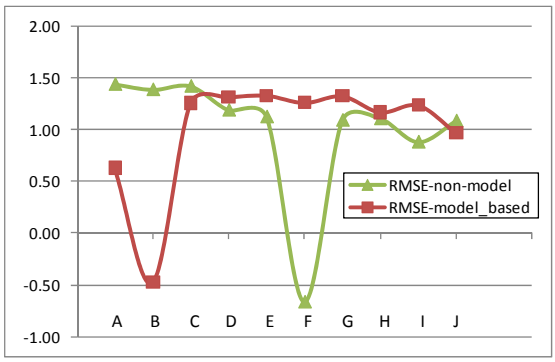

a) $(RMSE\text{-}RMSE)_{av}$ **= 0.59: Trial 1**
(a and b: largest)

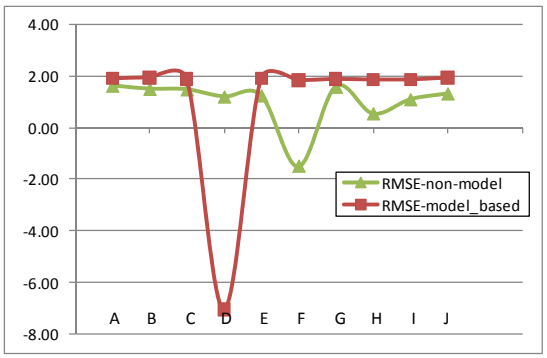

b) $(RMSE\text{-}RMSE)_{av}$ **=1.65: Trial 2**

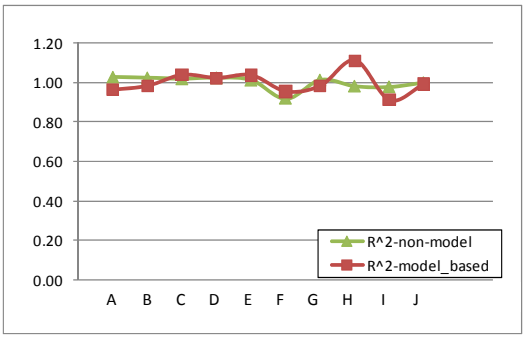

c) $(R^2\text{-}R^2)_{av}$ **= 0.04: Trial 1**
(c and d: smallest)

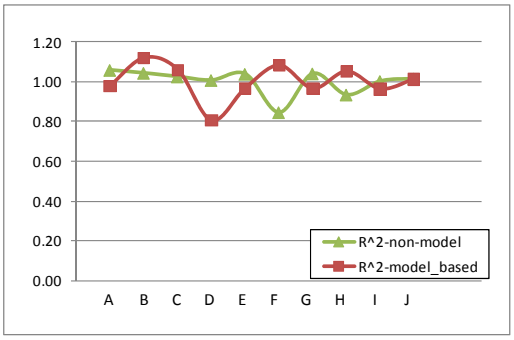

d) $(R^2\text{-}R^2)_{av}$ **= 0.09: Trial 2**

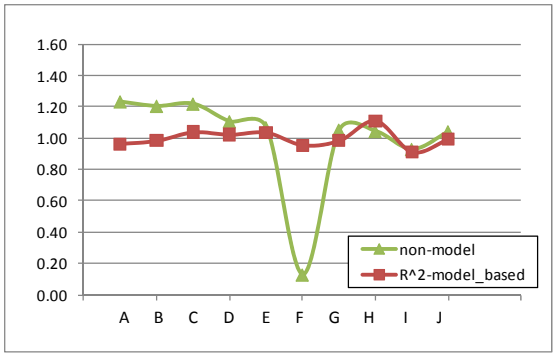

e) $(R^2\text{- }J_2)_{av}$ **= 0.18: Trial 1**
(e and f: second smallest)

f) $(R^2\text{- }J_2)_{av}$ **= 0.35: Trial 2**

Figure 6.20. Computer-based experiment (subjects A to J): Accuracy variables from model-based and non-model approaches with largest, smallest and second smallest average differences on each row (based on Table 6-7).

This set of figures is based on the entries with largest (Figure 6.20(a) and (b)), smallest (Figure 6.20(c) and (d)) and second smallest average differences (Figure 6.20(e) and (f)) according to Table 6-7. Starting from the entry with largest average differences, the first pair of graphs clearly shows that the average differences of *RMSE* values between model-based and non-model approaches for Trials 1 and 2 are mainly due to subjects B and F (Figure 6.20(a)) and subjects D and F (Figure 6.20(b)) respectively. The observation on subjects D and F being the main contributor also agrees with Figure 6.20(d) even though they are now in the entry with smallest average differences. The discrepancies incurred in Trial 2 can then be regarded to be mainly caused by subjects D and F.

Considering the smallest and second smallest average differences of Trial 1, subjects H and F appears to be the main contributors in R^2-R^2 and R^2-J_2 entries respectively (Figure 6.20(c) and (e)). Surprisingly for the R^2-J_2 entry in Figure 6.20(e) and (f), the results appear to suffer dramatically from their large *RMSE*-*RMSE* average differences but still remain at the second smallest entry thanks to the sharp drop in discrepancies of subjects B and D from Figure 6.20(a) and (b) respectively.

In general, there are higher discrepancies on results from Trial 2 than Trial 1 and it can also be observed that the average differences of Trial 2 are all higher. The average difference values of accuracy variables between model-based and non-model approaches are contributed by different human subjects rather than a common one. That is, one human subject may contribute to large average differences in one entry but contribute to small average differences in another one. Therefore, no conclusion can be made with regard to which accuracy variables precisely represent the quality of the model-based approach because there is a consistency issue among human subjects at different degree. This situation is not the same as that of speed criterion case, where τ can be precisely used as the only speed variable due to a strong agreement of the results from the two approaches. To spread the effect of inconsistency, R^2 and *RMSE* will be therefore averaged. Further detail will be explained under *fixed HPI* section. The hardware-based system will now be analysed.

6.5.1.2. Hardware-based system

Due to a number of settings involved in this experiment in terms of joystick transfer functions and target sequences, only selected sets of data will be used to illustrate the extreme cases. The analysis will be made in the same fashion as the computer-based system starting from speed score.

- *Speed score*

Similar to speed score section of the computer-based system, the values of J_1 from non-model approach are plotted against ARX parameters τ, T_N, K_p and K_d from all settings of Trial 1 (Figure 6.21, Figure 6.22 and Figure 6.23 for sequence 1, 2 and 3 respectively).

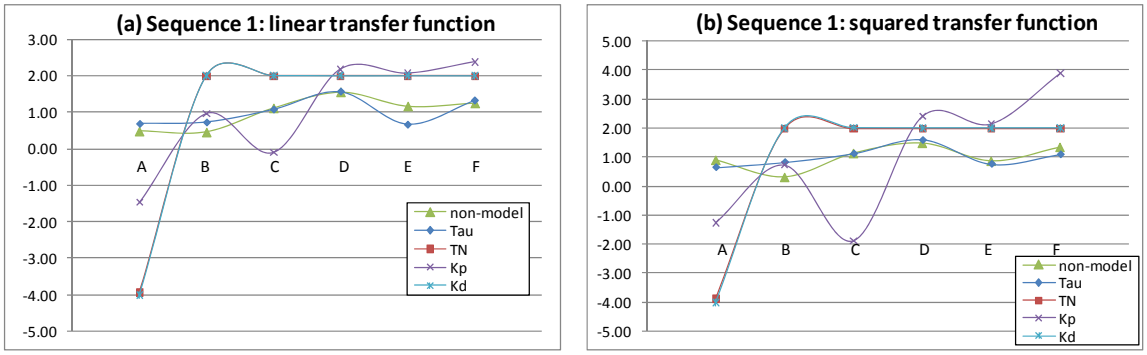

Figure 6.21. Hardware-based experiment (subjects A to J: sequence 1): Speed score of non-model approach (J_1) vs. τ, T_N, K_p and K_d

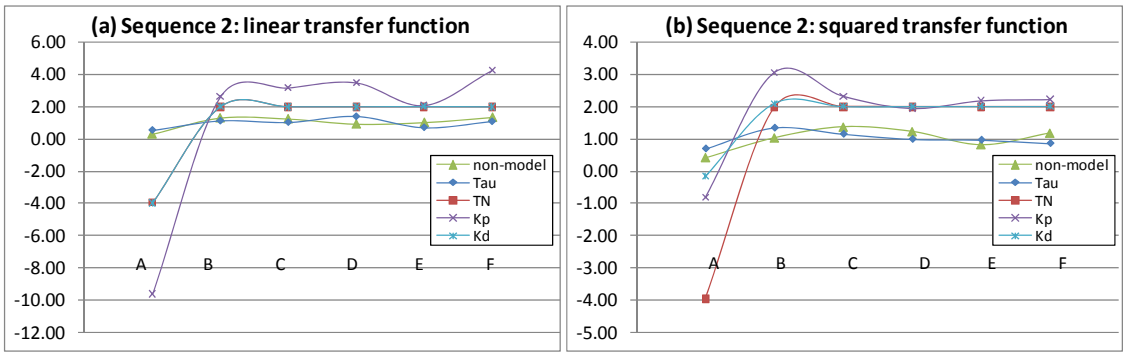

Figure 6.22. Hardware-based experiment (subjects A to J: sequence 2): Speed score of non-model approach (J_1) vs. τ, T_N, K_p and K_d

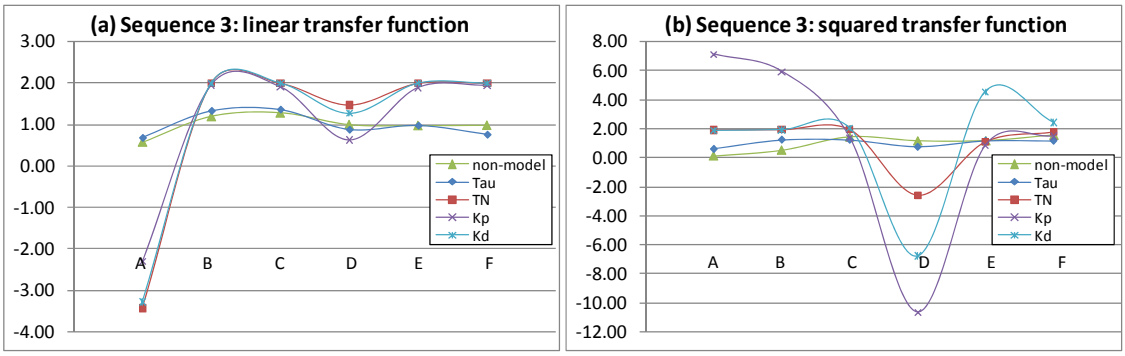

Figure 6.23. Hardware-based experiment (subjects A to J: sequence 3): Speed score of non-model approach (J_1) vs. τ, T_N, K_p and K_d

It can be observed that T_N appears to align perfectly with K_d in Figure 6.21 and Figure 6.22(a) along with K_p varying across a wide range and neither of these parameters are close to the non-model values like τ. Additionally, the variations of T_N, K_p and K_d also appear to have similar patterns with other graphs. In terms of extreme discrepancies, T_N and K_p values of subject A are noticeably large in all settings. Nevertheless, the closeness between J_1 and τ appears to be unaffected and once again, this is the reason why the time delay variable (τ) seems to be suitable as the only speed variable for the model-based approach.

Further analysis with a focus on just the non-model variable J_1 and time delay (τ) will help bring this hypothesis to conclusion. A closer look into Figure 6.21, Figure 6.22 and Figure 6.23 with the focus on only J_1 and τ are as presented in Figure 6.24, Figure 6.25 and Figure 6.26 respectively.

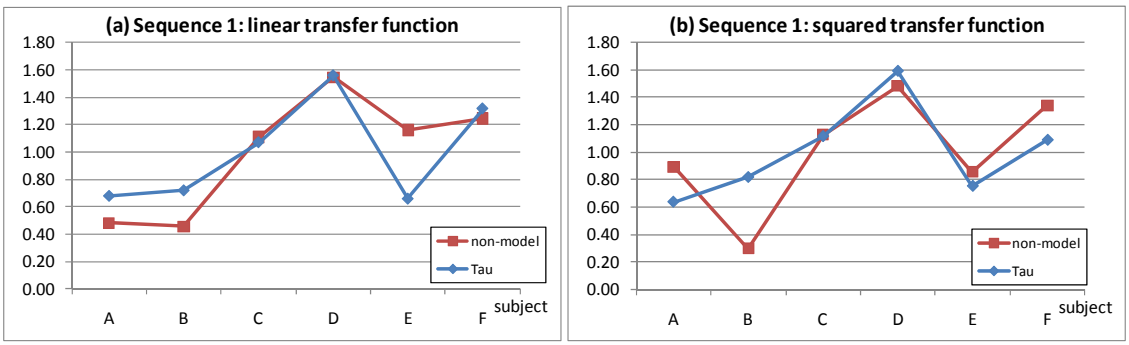

Figure 6.24. Hardware-based experiment (Sequence 1, Trial 1): Speed score (J_1) vs. τ

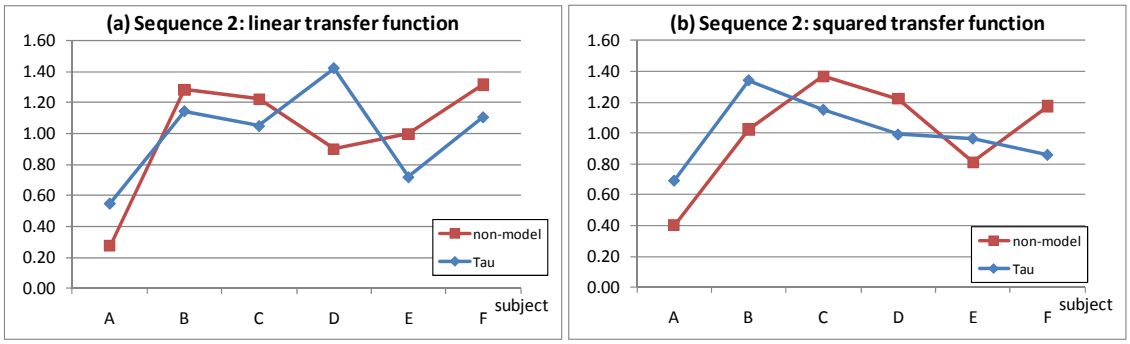

Figure 6.25. Hardware-based experiment (Sequence 2, Trial 1): Speed scores (J_1) vs. τ

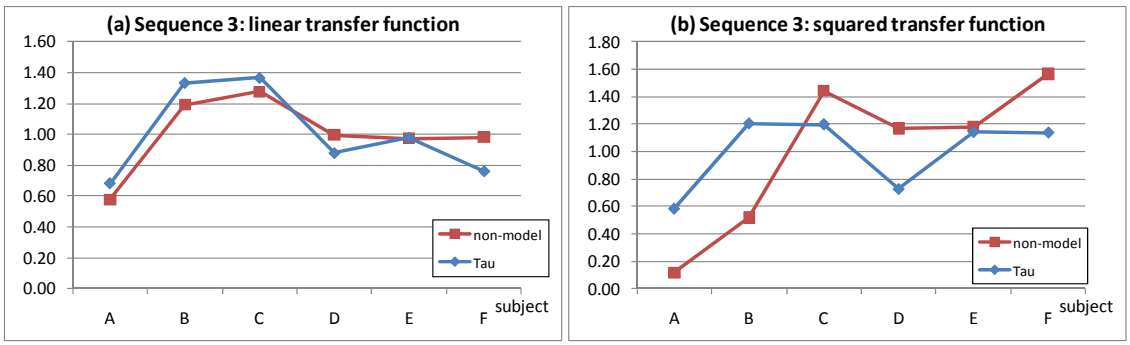

Figure 6.26. Hardware-based experiment (Sequence 3, Trial 1): Speed scores (J_1) vs. τ

In general, each graph shows that the degree of variation between the non-model variable (J_1) and the model-based variable (τ) differs randomly from subject to subject. This set of figures effectively illustrates the distribution of speed variables values for subjects A to F based on all sequences and settings in Trial 1. No particular subject obtains a constant value from these two approaches in all settings. The results also show that one human subject best described by the non-model approach in one setting may be worse described by the model-based approach in another setting. Subjects C and D are good examples for having rather consistent speed scores in sequence 1 (Figure 6.24(a) and (b)) but not in sequences 2 and 3. Similar observations are also true for other graphs and some subjects even have J_1 perfectly equal to τ.

With reference to Figure 6.26(a), the lines of τ and J_1 for all subjects can be seen to be almost aligned. The average difference between those two lines suggests that subject E even earns a perfect match whereas other subjects earn smaller difference comparing to other entries. In fact, this entry is the one with smallest average difference as hinted by the overall view of the graph itself comparing to others (see Table 6-8 for the numerical

values). To provide a summary of average differences for each entry, the results are as presented below.

Table 6-8. Hardware-based experiment: Average difference for speed variables based on Trial 1 (based on subjects A to F)

Seq1		Linear: Non-model	Squared: Non-model
		J_1	J_1
Model-based	τ	0.18	0.21
Seq2		Linear: Non-model	Squared: Non-model
		J_1	J_1
Model-based	τ	0.27	0.25
Seq3		Linear: Non-model	Squared: Non-model
		J_1	J_1
Model-based	τ	*0.11*	0.38

According to Table 6-8, the entry with smallest average differences is indeed sequence 3 linear transfer functions as suggested by Figure 6.26(a) (the entry in italics). It is interesting to see that the values of average differences vary from 0.11 to 0.38 based on different system settings. These values literally reflect how speed scores are affected on average for each setting, which may be proven useful for compensating the HPI values and making them more accurate. However, the focus of this research is not optimising the HPI values but rather offering a concrete structure for future developments on human performance analysis.

Apart from the experimental results based on Trial 1 presented earlier, the nature of graphs in terms of varied degree of agreement between J_1 and τ lines and inconsistency issues between subjects is similar in Trial 2. The set of comparison graphs for Trial 2 is then omitted and the summary will be presented in Table 6-9 instead. This table shows the average differences ranging from 0.23 to 0.73, which is larger comparing to Trial 1. Overall, this concludes that τ is the only suitable speed variable the same way as that of computer-based experiment.

Table 6-9. Hardware-based experiment: Average difference for speed variables based on Trial 2 (subjects A to F)

Seq1		Linear: Non-model	Squared: Non-model
		J_1	J_1
Model-based	τ	0.73	0.41
Seq2		Linear: Non-model	Squared: Non-model
		J_1	J_1
Model-based	τ	0.49	0.41
Seq3		Linear: Non-model	Squared: Non-model
		J_1	J_1
Model-based	τ	*0.23*	0.26

- *Accuracy score*

Due to the fact that a pitch-axis model cannot be derived from the hardware-based system, a fixed pitch-axis model together with a derived yaw-axis model is used to simulate a trajectory for accuracy score computation instead. As a result of this simulation, a resultant trajectory characterising pitch and yaw motions is examined with respect to a horizontal line connecting 0° to 90° along yaw axis or a reference line. As expected by the effect of the fixed pitch-axis model, Figure 6.27(a) and (b) show that the motion along vertical axis stays predominantly under the horizontal or 0° line for both linear and squared transfer functions respectively. The computation of *RMSE* and R^2 is carried out in the same fashion as that of computer-based system.

Figure 6.27(a) and (b) also show two samples of the simulated trajectory belonging to subjects A and C respectively along with the linear regression lines of the simulated response (dotted line). Although these two graphs are produced from different subjects based on different transfer functions, they have similar shapes in spite of the spike in Figure 6.27(a). This is also true for other segments and settings in the hardware-based experiment. Interestingly, the distance between the simulated and ideal lines in Figure 6.27(a) and (b) appears to be noticeably large. Such appearances suggest high RMSE values, which are not quite satisfactory. However, this effect will be reduced thanks to common appearances with other subjects and average-based HPI computation.

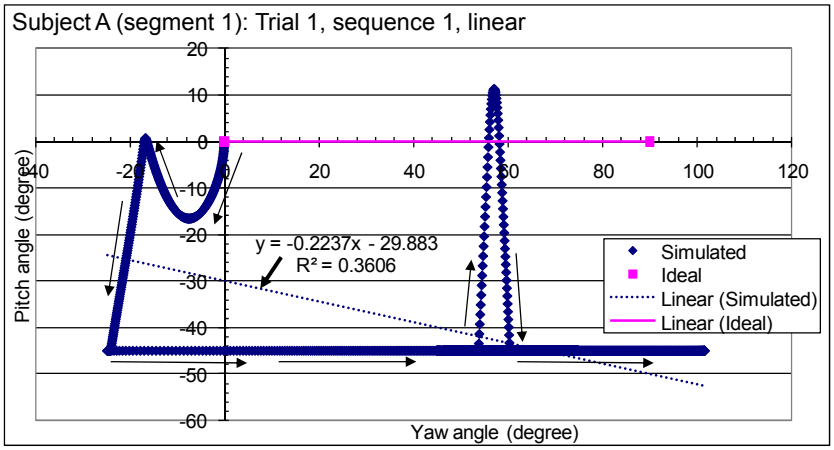

(a) Linear transfer function

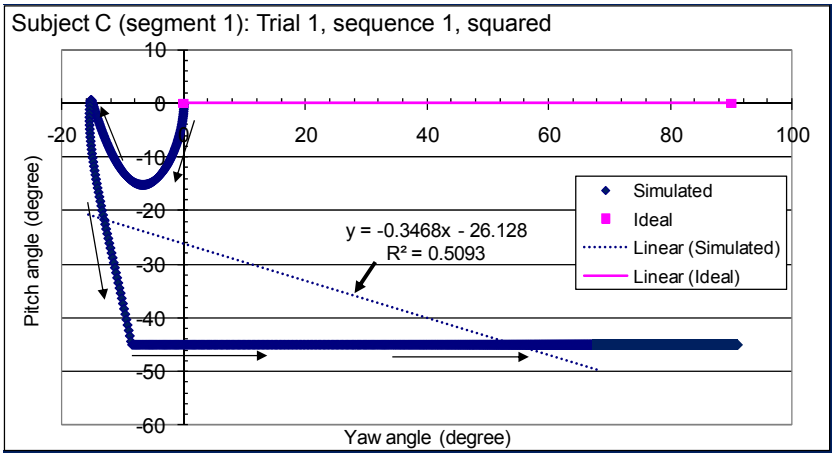

(b) Squared transfer function

Figure 6.27. Hardware-based experiment: 1-minute simulated trajectory used for accuracy analysis (from position (0°,0°) to (0°,90°))

To investigate the accuracy characteristics further and select the best accuracy variables, similar analysis to the computer-based system (Figure 6.19) will be now covered. Sequences 1, 2 and 3 of Trial 1 are chosen for this purpose and only J_2 (refer to Table 5-9, Chapter 5) will be plotted against the individual R^2 and *RMSE* values.

The results presented in Figure 6.28, Figure 6.29 and Figure 6.30 hint at different degrees of discrepancy for different settings despite similarities with the previous observations regarding non-matched patterns. The non-model accuracy score (J_2) does not seem to be well explained by either R^2 or *RMSE* of the model-based approach even though there are signs of good agreement in Figure 6.28(b) when *RSME* line follows the J_2 line closely. Even the values of some subjects almost coincide as of Figure 6.29(b),

Figure 6.30(a) and (b). However, the agreement is not clear-cut and universally true. In fact, the large difference revealed by subject B in Figure 6.28(a) suggests a closer investigation. Further analysis according to Step 2 comparison procedure will be made and the extreme cases from the two trials will be examined.

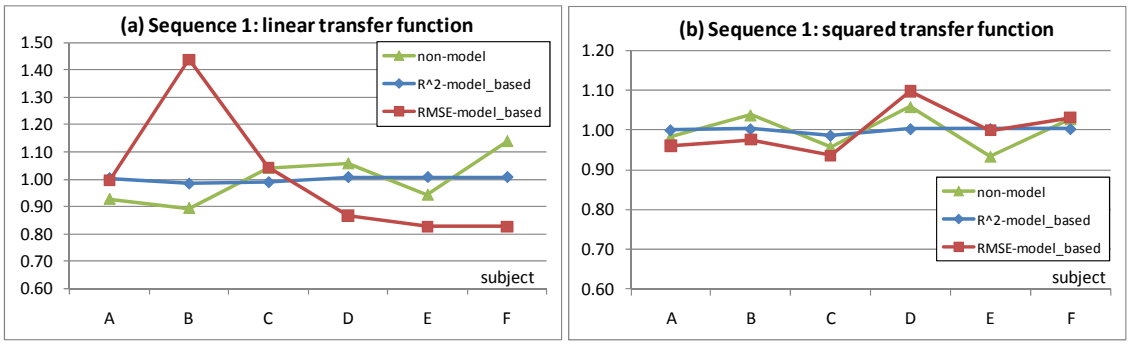

Figure 6.28. Hardware-based experiment (Trial 1 sequence 1): Accuracy score (J_2) vs. R^2 and *RMSE*

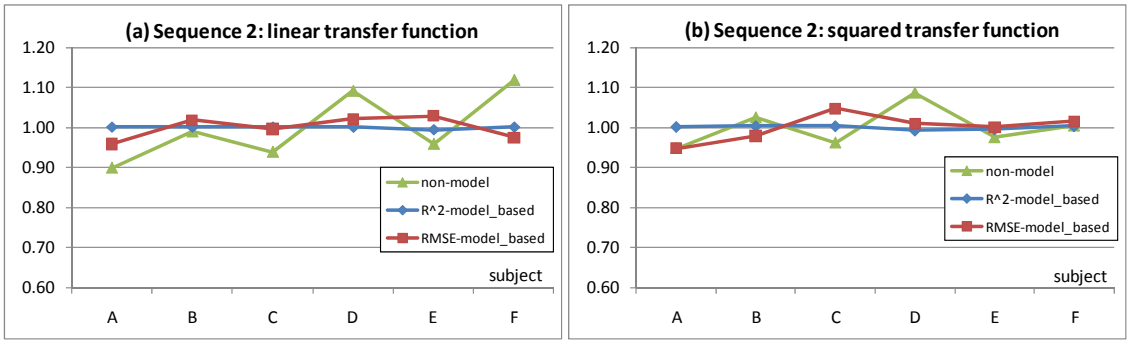

Figure 6.29. Hardware-based experiment (Trial 1 sequence 2): Accuracy score (J_2) vs. R^2 and *RMSE*

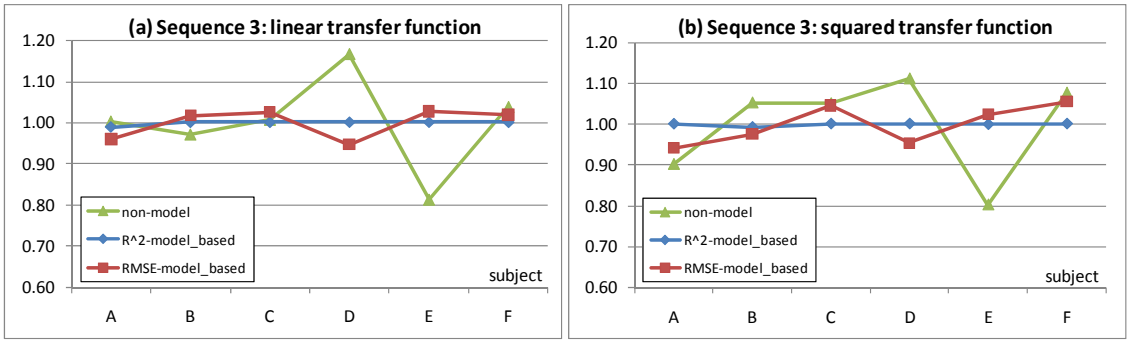

Figure 6.30. Hardware-based experiment (Trial 1 sequence 3): Accuracy score (J_2) vs. R^2 and *RMSE*

Before getting into detail, it is interesting to observe the pattern of R^2 lines in these figures and find that the R^2 values are noticeably constant regardless of the sequence numbers and transfer functions of the joystick. The values are particularly centred

around 1.0 or the average value and that indicates the majority of R^2 being relatively equal or slightly deviated from other subjects. In fact, this outcome is not very surprising since the pitch model is fixed and that mainly influences the pitch-axis motion for all subjects. The sign of R^2 deviation as in Figure 6.28 might be caused by the spike in the simulated response reminiscent of the one presented in Figure 6.27(a). However, determining the best-matched accuracy variables is of the focus rather than the source for such discrepancy.

Now considering the results from Step 2 comparison, the values of average differences based on subjects A to F for Trial 1 will be presented in Table 6-10 and then followed by that of Trial 2 in Table 6-11 For an overview on Table 6-10 for Trial 1 and Table 6-11 for Trial 2, the smallest and largest difference values for all settings can be found to be 0.02 and 0.26 respectively (bold italicized entries in Table 6-10). It can be observed that these values are comparatively smaller than that of the computer-based experiment for both trials (Table 6-7: 0.04 and 1.65) and this is considered satisfactory as the smaller the average difference values, the higher consistency between model-based and non-model approaches.

Table 6-10. Hardware-based experiment (Trial 1): Average difference for accuracy variables (Approach-level difference)

Seq1		Linear: Non-model			Squared: Non-model		
		R^2	RMSE	J_2	R^2	RMSE	J_2
Mode-based	R^2	0.10	0.17	0.08	0.02	0.09	0.04
	RMSE	0.21	***0.26***	0.21	0.04	0.06	0.04
	J_2	0.14	0.22	0.13	0.03	0.07	***0.02***
Seq2		Linear: Non-model			Squared: Non-model		
		R^2	RMSE	J_2	R^2	RMSE	J_2
Model -based	R^2	0.04	0.13	0.07	0.04	0.11	0.04
	RMSE	0.03	0.14	0.07	0.03	0.11	0.04
	J_2	0.03	0.14	0.07	0.03	0.11	0.04
Seq3		Linear: Non-model			Squared: Non-model		
		R^2	RMSE	J_2	R^2	RMSE	J_2
Model-based	R^2	0.03	0.17	0.07	0.08	0.23	0.10
	RMSE	0.04	0.19	0.09	0.10	0.22	0.09
	J_2	0.04	0.18	0.08	0.09	0.23	0.09

Table 6-11.Hardware-based experiment (Trial 2): Average difference for accuracy variables (Approach-level difference)

Seq1		Linear: Non-model			Squared: Non-model		
		R^2	RMSE	J_2	R^2	RMSE	J_2
Model-based	R^2	0.05	0.19	0.08	0.07	0.06	0.07
	RMSE	0.05	0.20	0.08	0.10	0.08	0.09
	J_2	0.05	0.20	0.08	0.08	0.07	0.08
Seq2		Linear: Non-model			Squared: Non-model		
		R^2	RMSE	J_2	R^2	RMSE	J_2
Model-based	R^2	0.10	0.11	0.06	0.03	0.10	0.05
	RMSE	0.12	0.13	0.09	0.05	0.12	0.07
	J_2	0.11	0.12	0.08	0.04	0.11	0.06
Seq3		Linear: Non-model			Squared: Non-model		
		R^2	RMSE	J_2	R^2	RMSE	J_2
Mode-based	R^2	0.02	0.15	0.07	0.06	0.12	0.06
	RMSE	0.04	0.15	0.08	0.08	0.13	0.07
	J_2	0.03	0.15	0.07	0.07	0.12	0.07

Regarding the R^2 values observed to be rather constant for all subjects discussed earlier, the results are also reflected in the average differences values of R^2-R^2 entries being extremely low in the range of 0.02 and 0.1. On the other hand, the *RMSE-RMSE* entries appear to have their values in the range of 0.06-0.26 that show a larger degree of deviation comparing to those of R^2-R^2. This consequently turns the results of the weighted version of R^2 and *RMSE* or J_2-J_2 entries to be more varied than R^2 alone in the range of 0.02-0.13 (refer to the diagonal entries for each box of settings in Table 6-10 and Table 6-11, i.e. R^2-R^2, *RMSE-RMSE* and J_2-J_2).

Based on the graphs and tables presented earlier, the level of discrepancy may be contributed by different subjects rather than one. To illustrate this, the following set of figures based on the entries with largest and smallest average differences are selected (bold italicised fonts in Table 6-10*)*. Figure 6.31 and Figure 6.32 present the whole set of these two entries with each figure containing its own subfigures, which are the ones with common accuracy variables or diagonal elements.

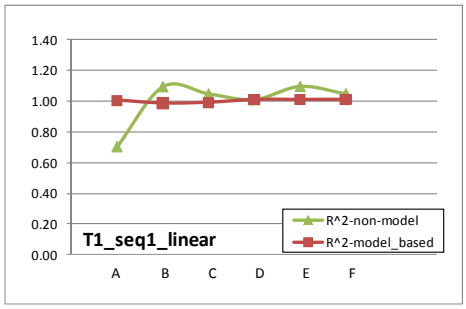

a) $(R^2\text{-}R^2)_{av}$ = 0.10

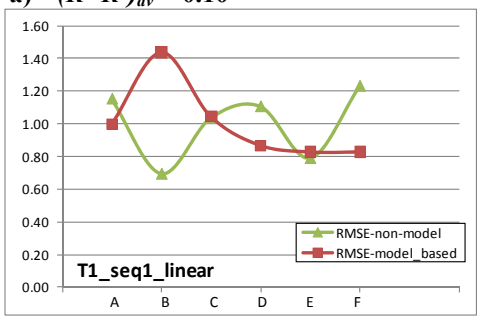

b) $(RMSE\text{-}RMSE)_{av}$ = 0.26 (largest)

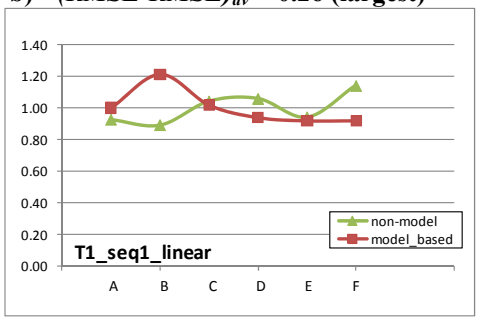

c) $(J_2\text{-}J_2)_{av}$ = 0.13
(Note: largest in J_2-J_2 category)

Figure 6.31. Hardware-based experiment (subjects A to F): the entry with largest average difference

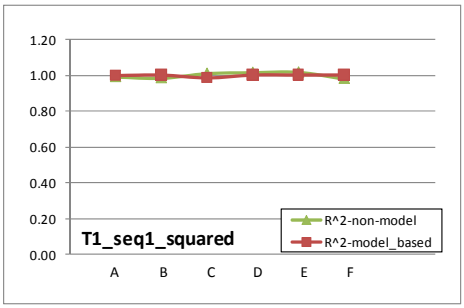

a) $(R^2\text{-}R^2)_{av}$ = 0.02

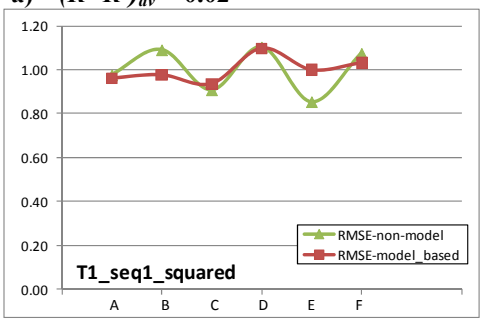

b) $(RMSE\text{-}RMSE)_{av}$ = 0.06

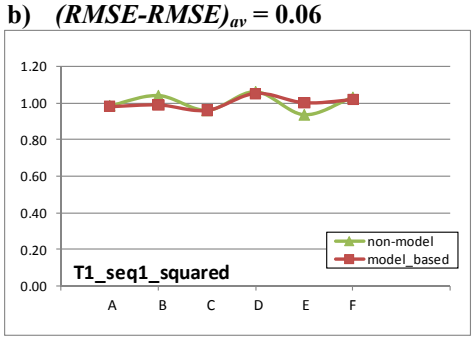

c) $(J_2\text{-}J_2)_{av}$ = 0.02 (smallest)
(Note: smallest in J_2-J_2 category as well)

Figure 6.32. Hardware-based experiment (subjects A to F): the entry with smallest average difference

Starting from the set with largest average difference entry (*RMSE-RMSE*), Figure 6.31(b) clearly shows that subjects B, D and F are the main contributors because the values from the remaining subjects are almost aligned and their difference values are significantly larger than other subjects. For the R^2-R^2 entry of the same set, subjects B and E along with subject A are spotted in Figure 6.31(a) as the main contributors. From these two entries, subject B appears to be the one with largest difference values or a noticeably outstanding contributor. As a result, the J_2-J_2 entry in Figure 6.31(c) can be observed to be the one with largest average differences in J_2-J_2 category with once again, subjects B, D and F as the main contributors. It turns out that J_2 value of subject B is largely compensated by smaller R^2 value and so are subjects D and F, whereas

subject A is compensated by smaller *RMSE* value instead. Similarly for the set with smallest average difference entry (J_2-J_2), the main contributors to the *RMSE-RMSE* entry in Figure 6.32(b) or subjects B and E appear to be drastically compensated by their smaller R^2 values (as in Figure 6.32(a)).

Based on these investigations, the situation of accuracy score for the hardware-based experiment turns out to be similar to that of computer-based experiment, where no conclusion can be drawn to completely rely on either R^2 or *RMSE* as the accuracy variable. The averaged value of these two accuracy variables will then be used to help compensate the discrepancy due to the flat R^2 and varied *RMSE* values. In fact, such decision is reasonable because R^2 and *RMSE* are not extracted directly from human ARX parameters like the case of speed score. More importantly, the source for calculating R^2 and *RMSE* or the simulated response is also the 2-dimensional trajectory, which is of the same nature as the actual response used in the non-model approach. It can then be concluded that several facts and proofs strongly support the use of both R^2 and *RSME* as accuracy variables for both computer-based and hardware-based experiments.

6.5.2. Fixed HPI

As discussed in Section 6.5.1, ARX parameters derived from the system identification algorithms raises a concern on how to use them as an alternative to the non-model approach. The requirements for speed and accuracy characteristics defined in Chapter 3 lead to a direct extraction and trajectory simulation of human ARX models before applying the HPI concept. The approach-level analyses on these performance variables based on both computer-based and hardware-based systems suggest that a time delay (τ) is suitable as a speed variable whereas both R^2 and *RMSE* are suitable as accuracy variables. A summary is presented in the HPI structure form as shown in Figure 6.33.

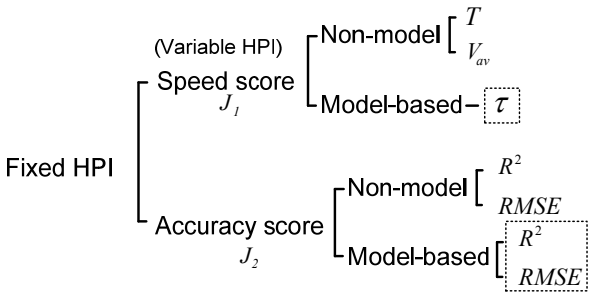

Figure 6.33. Fixed HPI computation summary (Note: Dotted rectangles represent the items to be used in computing the variable HPI. i.e. speed and accuracy scores)

To compute the fixed HPI using model-based approach, speed score and accuracy score will be computed according to the structure in Figure 6.33 and to be consistent, the fixed speed-accuracy ratios of 30:70, 40:60, 50:50, 60:40 and 70:30 will be used to allow easy comparison with the non-model results presented in Section 5.5.2, Chapter 5. Moreover, only Step 2 or approach-level comparison will be focused like the previous *variable HPI* section. The fixed HPI computation will be now started from the computer-based system and followed by the hardware-based system.

6.5.2.1. Computer-based system

The fixed HPI results for Trials 1 and 2 can be found in Figure 6.34 and Figure 6.35 respectively. The model-based results presented here correspond to those of non-model results in Figure 5.19 and Figure 5.21. The difference for each speed-accuracy ratio between these two approaches will be summarised in a tabular format shortly.

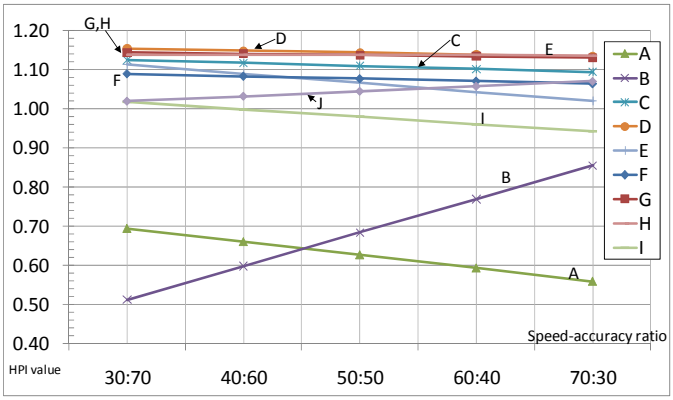

Figure 6.34. Trial 1: Fixed HPI with varied speed-accuracy ratio (hardware-based experiment)

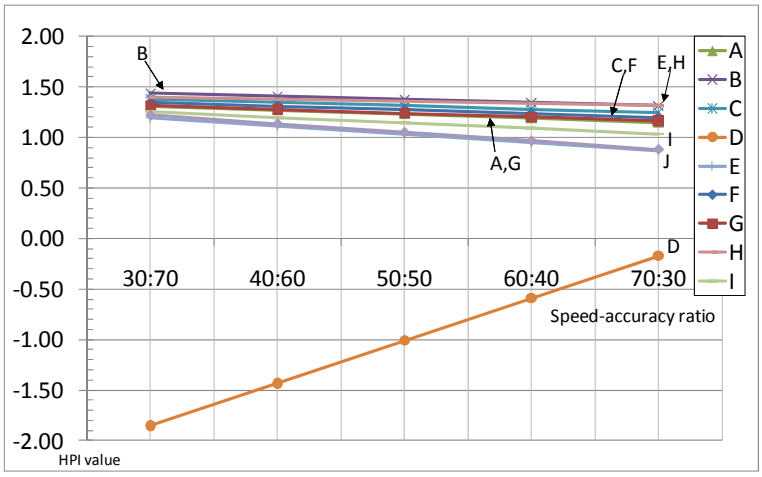

Figure 6.35. Trial 2: Fixed HPI with varied speed-accuracy ratio (hardware-based experiment)

Based on Figure 6.34 and Figure 6.35, the fixed HPI can be observed to vary at different rates (slopes) and directions as the speed-accuracy ratios increase from 30:70 to 70:30. More importantly, it is the interesting to see that not only the trend is reversed by the model-based approach but also the rate at which it is changed suggests the discrepancy between these two approaches. Some subjects that previously have positive slopes from the non-model approach now have negative slopes and *vice versa*. Similarly, some subjects that previously have higher slope values based on the non-model approach now have lower slope values and *vice versa*. Referring to Figure 6.34, the subjects that fall into the first category are B, D, F, G and H whereas the subjects that fall into the second category are A, C, E, I and J. It seems obvious that this comes as a result of high degree of discrepancy in performance score computation. Nevertheless, subjects A, E, I and J are the from the second category that have almost unchanged slope comparing to the non-model results in Figure 5.19 that shows a high degree of consistency as well even though it is quite different in Figure 6.35. To be specific, subject D seems to end up having only one value of the 30:70 speed-accuracy ratio in the positive region.

It is apparent from the discussion of accuracy score that accuracy variables contain higher average differences between results from model-based and non-model approaches in comparison to speed variable. This essentially affects the results of fixed HPI values as expected, which is presented in Table 6-12. This table shows that the average differences for Trial 2 are significantly higher than those of Trial 1 and

accuracy score seems to be the main contributor to such large magnitude of discrepancy as it corresponds to the highest difference in Table 6-7. The term *average difference* associated with individual human subject here refers to the average difference based on 5 speed-accuracy ratios (as defined in Equation (3-26)) whereas the average difference associated with a particular speed-accuracy ratio (HPI_{xx} in Table 6-12 and Table 6-14) refer to the average difference based on subjects A to J for that particular speed-accuracy ratio (ΔHPI_{av} in Table Table 6-13). Such context also applies to the case of the hardware-based system.

Table 6-12. Computer-based experiment: Summary of average difference of the fixed HPI based on subjects A to J for 5 speed-accuracy ratios

	Speed-accuracy ratios					HPI_{av}
	$HPI_{30:70}$	$HPI_{40:60}$	$HPI_{50:50}$	$HPI_{60:40}$	$HPI_{70:30}$	
T1	0.21	0.18	0.16	0.13	0.11	0.16
T2	*0.57*	*0.48*	*0.40*	*0.33*	*0.26*	0.41

Several other issues can be observed from Table 6-12, which are a larger magnitude of difference for ratio with higher weight on accuracy and significantly larger values in every speed-accuracy ratio for Trial 2 (in italics). Difference values for each speed-accuracy ratio of this trial are as presented in Table 6-13.

Table 6-13. Computer-based experiment: Fixed HPI differences for Trial 2

Subject	$\Delta HPI_{30:70}$	$\Delta HPI_{40:60}$	$\Delta HPI_{50:50}$	$\Delta HPI_{60:40}$	$\Delta HPI_{70:30}$	ΔHPI_{av}
A	0.21	0.25	0.28	0.32	0.35	0.28
B	0.18	0.15	0.12	0.09	0.06	0.12
C	0.19	0.18	0.17	0.16	0.15	0.17
D	2.93	2.50	2.07	1.64	1.21	**2.07**
E	0.17	0.13	0.09	0.05	0.01	0.09
F	1.25	1.07	0.89	0.71	0.53	**0.89**
G	0.05	0.03	0.01	0.01	0.03	**0.03**
H	0.49	0.41	0.33	0.25	0.17	0.33
I	0.26	0.22	0.19	0.15	0.12	0.19
J	0.12	0.06	0.01	0.07	0.14	0.08
Average	0.59	0.50	0.42	0.34	0.28	0.42
SD	0.89	0.76	0.63	0.50	0.36	0.63

Referring back to the issues mentioned earlier, the first issue is not surprising because there is a discrepancy in *RMSE*, which is one of the two accuracy variables used in a variable HPI computation. The focus will then be shifted to the second issue. To examine the second issue and illustrate how fixed HPI values from model-based and

non-model approaches compare based on Trial 2 data, some samples on human subjects with smallest and largest average differences (bold entries in Table 6-13) will be presented starting from the one with smallest difference.

Figure 6.36 shows the fixed HPI values of subject G. The closeness of model-based and non-model values suggest that his/her performance can be precisely determined by both model-based and non-model approaches. The HPI values have slightly higher difference from the left end and decrease towards the right end as the weight on speed increases. These values are even aligned at the 60:40 speed-accuracy ratio. On the contrary, the characteristics of subjects D and F seem to be totally different from the case of subject G as can be seen in Figure 6.37(a) and (b) respectively.

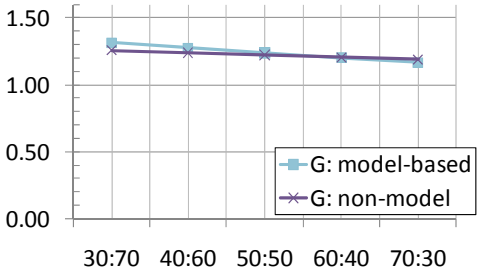

Figure 6.36. Fixed HPI value vs. speed-accuracy ratios: Subject G with smallest average difference of only 0.03 (Trial 2)

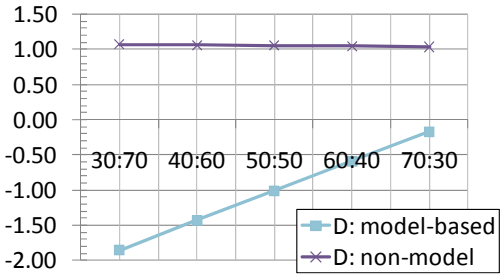

a) Subject D: Average difference of 2.07

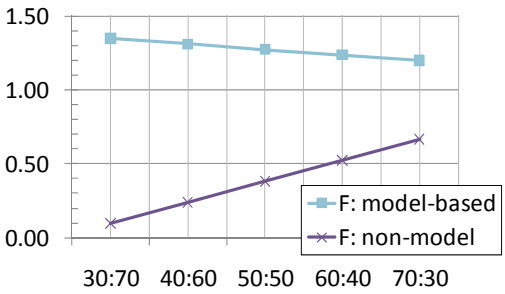

b) Subject F: Average difference of 0.9

Figure 6.37. Fixed HPI value vs. speed-accuracy ratios: Two main contributors to HPI discrepancies (Trial 2)

Subjects D and F are regarded as the main contributors to HPI discrepancies due to a large variation of their HPI values between model-based and non-model approaches. The average difference values of 2.07 (subject D) and 0.9 (subject F) are the two highest values of two trials in the computer-based experiment. It can also be observed that

higher weights on accuracy score inversely affect the average difference values comparing to that of subject G.

In other words, the difference seems to be less as the weight on accuracy score increases. Interestingly, subject D also obtains negative HPI values on all speed-accuracy ratios and that is due to his/her abnormally low *RMSE* values (Figure 6.20(b)) whereas subject F's *RMSE* values are high enough to be compensated and resulted in all positive although they are very small.

6.5.2.2. Hardware-based system

To show the model-based results of the hardware-based system, the fixed HPI results for Trial 1 on sequence 1, 2 and 3 are selected and will be presented in Figure 6.38, Figure 6.39 and Figure 6.40 respectively. Each figure also contains 2 subfigures for the linear and squared transfer functions of the joystick. All of these graphs correspond to the non-model results presented in subfigures (a) and (b) of Figure 5.22, Figure 5.23 and Figure 5.24.

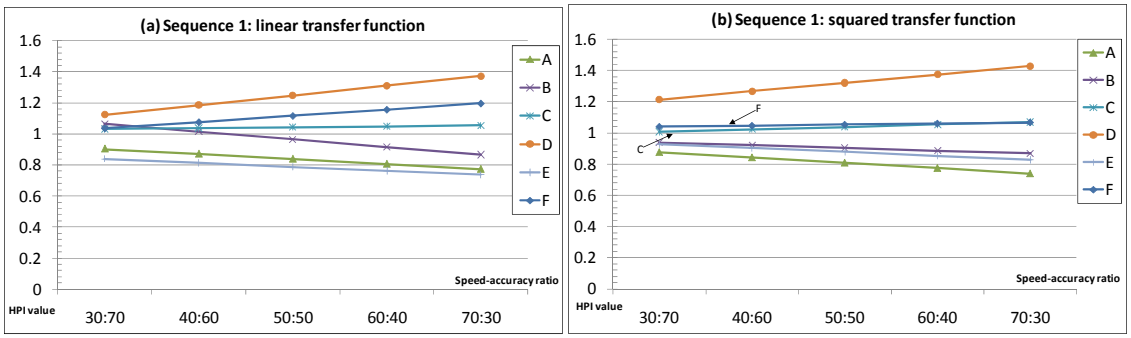

Figure 6.38. Hardware-based system (Trial 1): Fixed HPI based on sequence 1

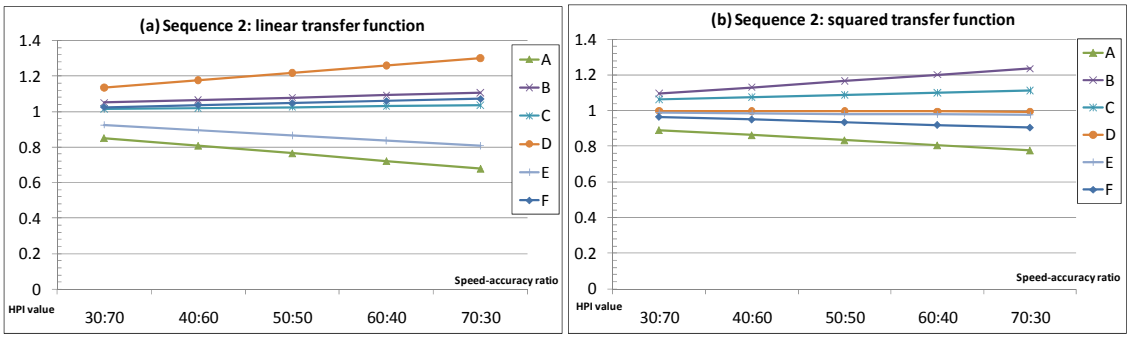

Figure 6.39. Hardware-based system (Trial 1): Fixed HPI based on sequence 2

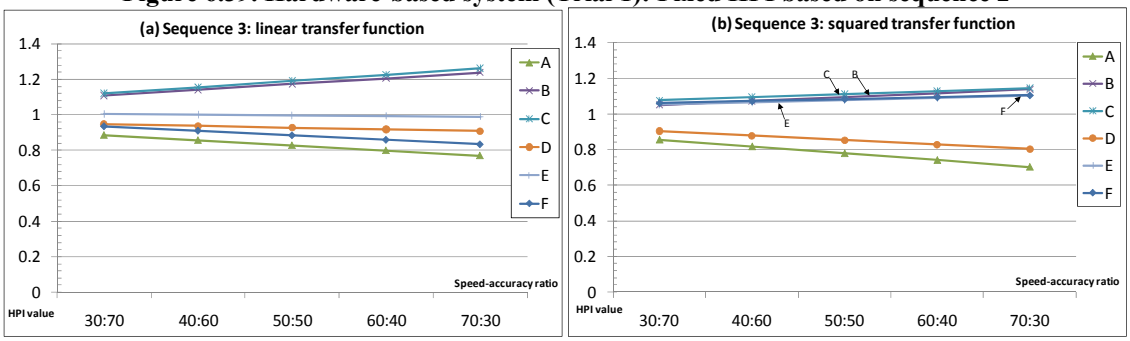

Figure 6.40. Hardware-based system (Trial 1): Fixed HPI based on sequence 3

Before getting into a summary on overall performance of the model-based approach for this system, the results above turn out to contain completely no outliers or extreme cases like that of subject D in the previous experiment. In fact, the graphs' orientation is preserved for almost all subjects or even the cases by which the orientation is not consistent, those changes are relatively slim. One good example is subject A as his/her results from both approaches are very constant in terms of slope and range of the values. Overall, the results for the hardware-based system are very similar to that of computer-based system but with significantly smaller discrepancies in all cases. The trend of increasing discrepancies with increasing weight on accuracy score is the opposite due to rather small average differences in general as presented in Table 6-10 and Table 6-11. Table 6-14 shows a summary on values of these differences from all settings and subjects in the experiment.

Table 6-14. Hardware-based experiment: Summary of average differences of the fixed HPI based on subjects A to F for 5 speed-accuracy ratios

			Speed-accuracy ratios					HPI_{av}
			$HPI_{30:70}$	$HPI_{40:60}$	$HPI_{50:50}$	$HPI_{60:40}$	$HPI_{70:30}$	
T1	Seq1	Linear	0.14	0.11	0.10	0.09	0.10	0.11
		Squared	0.05	0.07	0.08	0.10	0.12	0.08
	Seq2	Linear	*0.08*	*0.08*	*0.08*	*0.08*	*0.10*	*0.08*
		Squared	0.08	0.08	0.08	0.09	0.10	0.09
	Seq3	Linear	0.09	0.10	0.12	0.15	0.17	0.13
		Squared	0.16	0.16	0.16	0.16	0.16	0.16
T2	Seq1	Linear	*0.25*	*0.28*	*0.30*	*0.33*	*0.35*	*0.30*
		Squared	0.15	0.16	0.18	0.21	0.23	0.19
	Seq2	Linear	0.18	0.19	0.20	0.21	0.22	0.20
		Squared	0.14	0.16	0.17	0.18	0.20	0.17
	Seq3	Linear	0.08	0.09	0.10	0.11	0.12	0.10
		Squared	0.10	0.10	0.10	0.10	0.11	0.10

With regard to the entry with largest average differences as tabulated in Table 6-14, Trial 2 of sequence 1 based on a linear transfer function is the one with the average value of 0.30 whereas the entry with smallest average differences Trial 1 of sequence 2. The one with linear transfer function is preferred due to its consistency across the full range of speed-accuracy ratios. See Table 6-15(a) and (b) for the fixed HPI values for each human subject.

Table 6-15. Hardware-based experiment: Fixed HPI differences for italicized entries in Table 6-14

(a) Trial 2: sequence 1, linear (largest average differences)

Subject	$\Delta HPI_{30:70}$	$\Delta HPI_{40:60}$	$\Delta HPI_{50:50}$	$\Delta HPI_{60:40}$	$\Delta HPI_{70:30}$	ΔHPI_{av}
A	0.26	0.35	0.43	0.52	0.60	0.43
B	0.18	0.21	0.23	0.26	0.28	0.23
C	0.06	0.11	0.16	0.21	0.26	**0.16**
D	0.36	0.45	0.53	0.62	0.70	**0.53**
E	0.32	0.41	0.51	0.60	0.69	0.51
F	0.34	0.41	0.48	0.54	0.61	0.48
Average	0.25	0.32	0.39	0.46	0.53	0.39
SD	0.12	0.14	0.16	0.18	0.20	0.16

(b) Trial 1: sequence 2, linear (smallest average differences)

Subject	$\Delta HPI_{30:70}$	$\Delta HPI_{40:60}$	$\Delta HPI_{50:50}$	$\Delta HPI_{60:40}$	$\Delta HPI_{70:30}$	ΔHPI_{av}
A	0.14	0.16	0.18	0.20	0.22	0.18
B	0.03	0.04	0.06	0.07	0.09	0.06
C	0.01	0.03	0.06	0.08	0.10	**0.06**
D	0.10	0.16	0.22	0.28	0.34	**0.22**
E	0.05	0.08	0.11	0.15	0.18	0.11
F	0.15	0.16	0.17	0.18	0.19	0.17
Average	0.08	0.11	0.13	0.16	0.19	0.13
SD	0.06	0.06	0.07	0.08	0.09	0.07

To take a closer look into the entries with italicized fonts, the fixed HPI graphs from subjects with only the largest and smallest difference are selected for demonstration (entries in bold according to Table 6-15), which can be regarded as the worst-case and best-case scenario respectively. The results for other subjects appear to have a degree of variation for their model-based values from that of non-model between these two cases. Subject C is chosen to represent the best-case scenario whereas subject D is for the worst-case scenario and their graphs are as presented in Figure 6.41 and Figure 6.42 respectively.

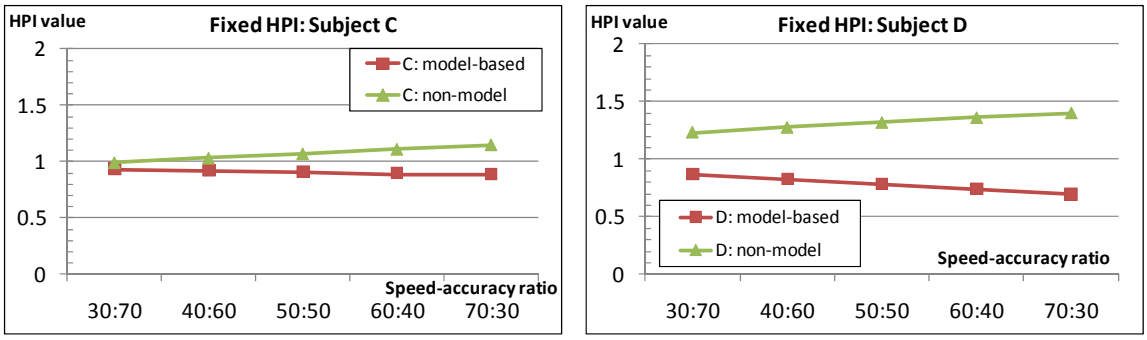

a) Average difference of 0.16 (smallest) **b) Average difference of 0.53 (largest)**

Figure 6.41. Hardware-based experiment: the entry with largest average difference (Trial 2, sequence 1, linear transfer function)

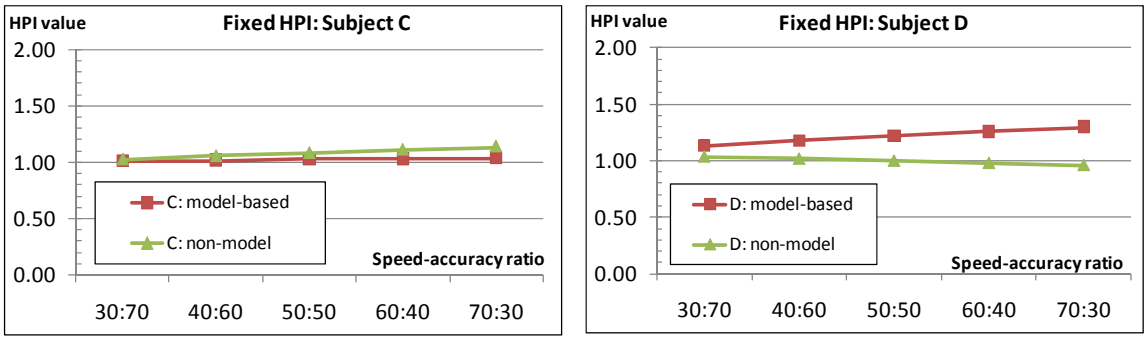

a) Average difference of 0.057 (smallest) **b) Average difference of 0.22 (largest)**

Figure 6.42. Hardware-based experiment: the entry with smallest average difference (Trial 1, sequence 2, linear transfer function)

The agreement of values based on these entries indicates that discrepancies for the fixed HPI vary from subject to subject. For the best-case scenario, subject C appears to have consistent HPI values regardless of the computation approaches even though the differences look higher in Figure 6.41(a). For the worst-case scenario, the patterns of

subject D's HPI graphs turn out to be quite different comparing to that of subject C in both Figure 6.42(a) and (b). However, it can be observed that the magnitude of such differences is not as drastic as the values from those of subjects D and F in the computer-based experiment (Figure 6.37).

Referring back to the graphs of accuracy variables for the hardware-based experiment given in Figure 6.31 and Figure 6.32, those results suggest that subjects B, D, F and subjects B, E are the main contributors to the accuracy variable differences based on the entry with largest and smallest average differences respectively. These observations are, in fact, consistent with the closed-from HPI results for every subject as noted in Figure 6.41 and Figure 6.42. Mainly, the fact on main contributors are found to be subjects D, E and F as expected except subject B having the second smallest average difference just after subject C. This one and only case suggests the existence of inconsistency between non-model and model-based approaches of human performance computation proposed in this thesis as results from other subjects agree with their counterparts as anticipated.

Possible source of error is a limitation on the order of human ARX model used in this thesis, which is not fully capable to describe a complex or repetitive pattern of control motion for that human subject. The value of *RMSE* difference between model-based and non-model approaches is a good indicator of how the output derived by the model-based approach deviates from that of non-model. It is also worth noting that the differences of model-based *RMSE* are generally varied across a number of subjects whereas that is not the case for R^2. This suggests that the model-based approach is able to precisely describe the orientation of the path taken by human subjects.

6.6. HPI Computation issues

With regard to the discrepancies induced as a result of the model-based approach, there are three big issues involved in the variable HPI computation and they are all related to the system identification algorithm. The first issue is the parameter definitions. This

issue links to the ARX parameters derived from the experimental data, which are analysed segment by segment to match with those of non-model approach. Such basis for deriving the ARX model leads to a successful computation and results in a set of 4 parameters, which are τ, T_N, K_p and K_d. Despite this success, the usefulness of these parameters is limited in a way that they are not exactly matched to those of non-model approach. Namely, the average velocity and the time taken variables to finish a single target position cannot be fully described by a simple parameter τ. In fact, this is apparent from the alignment of various graphs from the computer-based (Figure 6.17) and hardware-based experiments (Figure 6.21).

The second issue is about the axis separation. The discrepancy of results for the hardware-based system differs from the computer-based system because the pitch-axis models cannot be derived leaving only yaw-axis models to be used for ARX parameters extraction. Therefore, the discrepancy of speed scores is rooted from only yaw-axis models rather than both pitch and yaw-axis models like the case of the computer-based system.

The third issue concerns the complexity of the ARX model used to describe human control actions in this research. The model order is restricted to only 2 to comply with the PD controller structure as described in Section 6.3.1 and this can be considered a limitation on the accuracy of the resultant models. However, this is not necessarily the case for all ARX models as some simulated responses appear to be very close to the actual one. Further analysis on this issue will be elaborated in Chapter 7.

Apart from those three aforementioned issues, there are also issues about the fixed HPI due to its dependable structure and definitions on the variable HPI. Consequently, the effects on speed criterion and accuracy criterion are conveyed directly to the fixed HPI as it is essentially a weighted sum of the variable HPI. In addition to that, there is also a personal control strategy involved in causing a rate of change of HPI values to vary from subject to subject as suggested from the data in Table 6-14. This is the main reason why one subject is affected differently from others when the speed-accuracy ratio

increases. Human control strategy is therefore involved with this intrinsic weight in terms of focus on speed and accuracy characteristics.

From a practical point of view, the weights associated with speed and accuracy criteria or a speed-accuracy ratio is unknown at first and needs to be determined by achieving the statistical significance of the task or operation of interest. Five speed-accuracy ratios are selected for demonstration purposes in this research and they suggest how one human subject can possibly reach the same performance level or the same HPI value by a variation of speed-accuracy ratios. An example best suited for this implementation is the system that requires a certain level of performance and machine has to determine how to achieve it by measuring the performance of human operator first and fulfilling the difference. This is indeed reminiscent of a driving style, by which certain criteria like safety, fuel consumption, comfort, mileage and so on have to be satisfied and can be satisfied by many different ways. The implementation of an intelligent mechanism to measure and adjust itself according to a HPI of a driver allows this technology to be realized and that is what this research is ultimately aiming for.

6.7. Summary

This chapter mainly introduces a methodology used for a model-based approach in computing the HPI values. The use of human ARX model is presented along with a discussion on how to select and use suitable ARX parameters in computing speed and accuracy characteristics, which includes the direct extraction and simulated trajectory techniques. Both variable and fixed HPI computation have also been discussed in detail and compared with the results from the non-model approach given in Chapter 5. The distribution graphs of performance scores for each subject are presented and the sources of inconsistent values resulted from the model-based are discussed.

Chapter - 7.

Discussion and Conclusion

7.1. Introduction

This chapter discusses the merit of Human Performance Index (HPI) concept and its aspects regarding a real implementation on human-machine systems including complications of speed-accuracy ratios. Details about inconsistency issues are also provided.

7.2. HPI experiments

According to the HAM modules presented in Figure 3.1, Modules 1 and 2 (human skill quantification and human modeling) are two main targets of this research that have been fulfilled in several ways. First of all, human skill quantification is fulfilled by a human performance index instead of human skill to incorporate goodness of control action by means of the non-model approach to quantify its quality. Second of all, human modeling is fulfilled by a model-based approach with a non-model approach as part of the human skill quantification. In fact, the use of model-based approach enhances the coverage of the HPI concept by not only adding the ability to compute the human performance level but also a potential to compute future response based on that human model. However, the latter advantage of the model-based approach has not been exercised in this research.

Regarding the core content of Module 1, the HPI concept is considered fundamental and complementary to recent research in human skill evaluation (Tervo, 2010; Tervo, 2009; Masamune, 2005; Xu, 2002; Nechyba and Xu, 1997), of which the focus is on precision and certainty in accomplishing a task rather than the quality of execution (definitions of the words *performance* and *skill*, The Oxford English Dictionary (1989)). The distinctions of human performance and human skill, as also explained in Chapter 2, set their qualities apart and allow reasonable use of speed and accuracy to represent human control strategy. This means a set of speed and accuracy characteristics can be viewed as fundamentals to the way human performs a task. The manner in achieving that particular task along with consistency and/or adaptability suggests a skill developed on top of his/her performance.

Similar research involving human-machine systems requires human experts in their studies (Xu, Song et al., 2002; Katsura, Matsumoto et al., 2005; Suzuki, Harashima et al., 2005; Suzuki, Kurihara et al., 2006; Mori, Sakaguchi et al., 2007; Palmroth, Tervo et al., 2009). By doing so, a set of training and selection of human subjects to perform a task is compulsory. Sequence and smoothness of control motions are the main factors used to evaluate skill(s) of human operator. At the end of training, those with high skill will then be used as a reference for adaptive control design. This framework is generally appropriate for specialised operations but it is also important to note that relying on a general human operator is beneficial when the operation is truly innovative. That is, no human expert can be found to perform that operation just yet.

Moreover, the manner the operation is completed by human expert does not necessarily adhere to the level of performance of that person because a higher rate of error owing to negligence may be induced. Therefore, all the experiments in this thesis were not only conducted on general human subjects but also without intensive training neither during nor prior to the experiments. The main reason is to ensure the resultant human performance is unbiased as the HPI concept is designed to be scalable regardless of sample size and diversity. Skilled humans or human experts would likely cause

skewness to the distribution of human performance. Nevertheless, a statistically significant experimentation is required to address and conclude the aforementioned statements. This is simply because the scope and research work reported in this thesis is designed to only prove the HPI concept and apply it using two different approaches on two systems with different characteristics.

7.3. Inconsistency issues

Inconsistency between HPI values computed from model-based and non-model approaches is indeed unsurprising due to nature of implementation. To clarify, this occurs due to the ARX order of 2 being imposed on the System Identification algorithms to comply with the PD-controller structure of a human operator. As a result, human subjects with complicated motion patterns cannot be precisely modeled and this consequently leads to a high degree of difference between the actual and simulated responses, which in turn increases the *RMSE* values. By the term *complicated motion pattern* in this context, it refers to a choppy or jittery trajectory that a human subject follows in order to finish a tracking as quickly as possible. The possibilities are endless depending on one's control strategy but the results often contain noises and overshoots, which require a higher degree of model to cope with. For instance, the graphs in Figure 6.19 shows that subject B has the largest difference between values from the two approaches (J_2 and *RMSE*) and his/her trajectory really corresponds to this observation (see Figure 7.1).

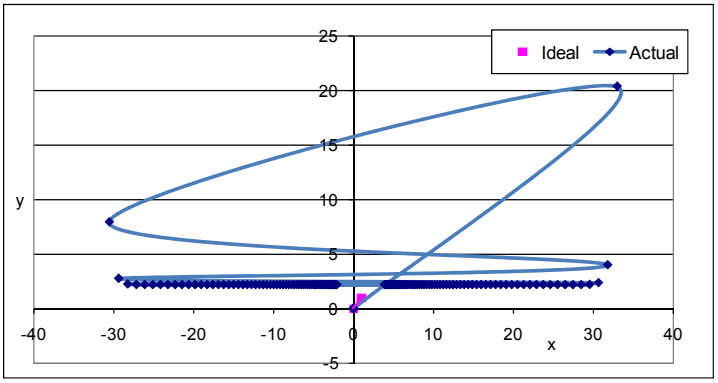

Figure 7.1. Example of a complicated motion pattern in a computer-based experiment (Trial 1, subject B, segment 8: with reference to data in Figure 6.19)

The inconsistency involved with human modeling can be observed from both computer-based and hardware-based systems as described in Chapter 6. In this thesis, two set of graphs from Trial 1 of the computer-based system will be used for demonstration purposes. The first set will be used to illustrate inconsistency in general (Figure 7.2) and the second sample will be used to present the entry with lowest inconsistency (Figure 7.3).

Figure 7.2(a) shows that the motion followed by subject F covers a significantly large area towards the inflection point around the origin position (0,0) before turning back to the target position at (5.3,0.1). In fact, there was a large overshoot on subject E's vertical action and therefore, required a correction in both directions to compensate and land successfully onto the target position. As a result, the simulated path is far too different from the ideal path plotted in the graph for comparison and that is how the inconsistency from the term *RMSE* takes place. The shape of motion pattern based on these two graphs appears to be noticeably different despite their spanned area and that is a consequence of human ARX model of only order 2.

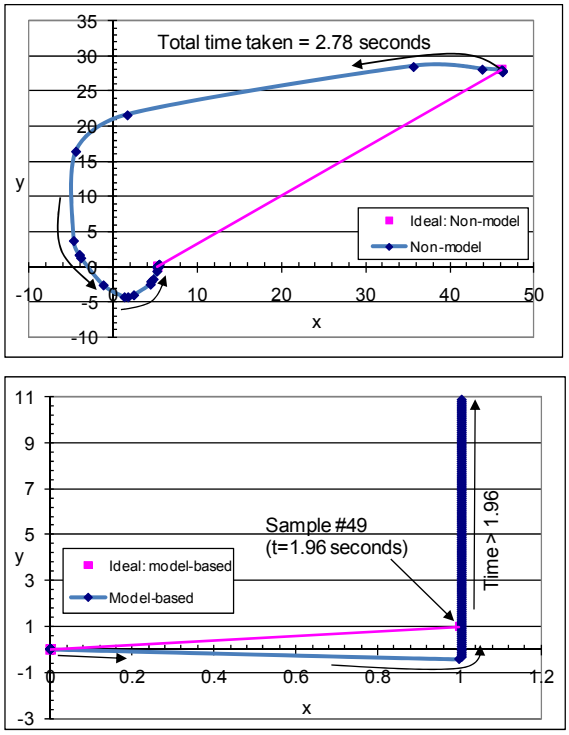

a) Actual response from position (46.1,28.1) to (5.3,0.1)

b) Simulated response from position (0,0) to (1,1)
[x-axis: ARX_{1249}, y-axis: ARX_{1253}]

Figure 7.2. Example of inconsistency: Computer-based experiment, Trial 1, segment 8, subject F
[Notes: ARX model subscripts are according to n_a, n_b and n_k]

Now according to observations on the subject with lowest *RMSE* values, his/her motion path appears to be slightly curvy towards a target position with only small deviation from a straight line connected between initial and final target positions. The simulated response and linear regression line appear to be close to each other. In fact, the experimental results suggest that the path whose linear regression line is very close to that of ideal path is likely to produce a very accurate ARX model as shown in Figure 7.3.

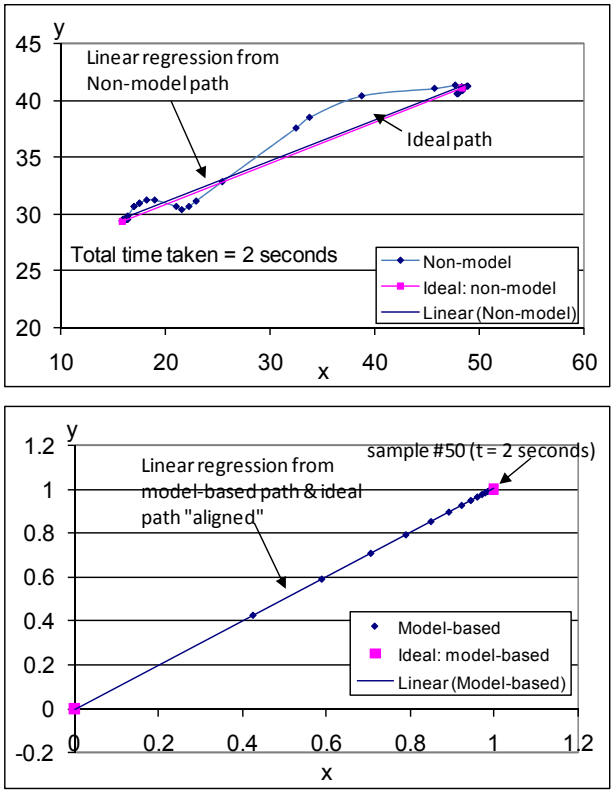

a) Actual response from position (48.3,41.1) to (15.9,29.4)

b) Simulated response from position (0,0) to (1,1) [x-axis: ARX_{1245}, y-axis: ARX_{1245}]

Figure 7.3. Example of lowest discrepancy: Computer-based experiment, Trial 1, segment 5, subject E [Notes: ARX model subscripts are according to n_a, n_b and n_k]

The example in Figure 7.3 is selected based on the segment and subject with smallest *RMSE* value from the computer-based experiment. It can be observed from Figure 7.3(a) that the path followed by subject E is in a simple fashion as it deviates from the ideal path slightly up and down without overshooting or undershooting. The graph in Figure 7.3(b) confirms that the human ARX model of order 2 is more than sufficient to describe tracking actions of human subjects in majority and this is also the case for the hardware-based experiment.

To conclude, the inconsistency between model-based and non-model approaches is only found in a minority of the experiments conducted in this research and it is of noticeably high probability due to the output pattern containing overshoots and undershoots. Regarding the hardware-based experiment, it is highly likely that there is also a hardware-related discrepancy on top of the algorithmic inconsistency as mentioned earlier. Trivial issues like friction at the rotational bearing on days with different weather conditions and drifting of operating voltage on both pitch and yaw motors may

contribute to such inconsistency as the experiments with all subjects were not completed within the same day.

7.4. HPI ratios

With reference to HPI concept formulation, this thesis targets at the way to classify human performance into speed and accuracy characteristics and quantify them numerically. The concept is novel in aiming to present individual characteristic of human in terms of speed and accuracy as an open form and determining the resultant performance value based on the weight of each characteristic as a closed form (the reported work is an article in press for the Special Issue on Human Adaptive Mechatronics (HAM)-Institute of Mechanical Engineers (IMechE) as provided in Appendix D). The weight on each performance criterion essentially depends on the application or system of interest as one may require a human operator to pay more attention on speed than that of accuracy and *vice versa.* A significance of speed-accuracy ratio can be viewed as a variable of which an adaptive control mechanism relies upon and uses to adjust in relation to human performance level.

Under the same working conditions and output requirements, the human operates on the task according to his/her own interpretation on limitations, evaluation of difficulty level and decision on a control strategy to achieve that task successfully. Based on this reasoning, there is a dependency issue of his/her control strategy due to the nature of speed-accuracy tradeoff. That is, the degree of dependency is subjective in such a way that it affects one's control strategy more than the other does.

To illustrate the dependency issue, the results presented in Chapters 6 under *closed-form HPI* section for the computer-based experiment (Figure 6.19) will be revisited and analysed by a piecewise linear relationship on the speed-accuracy ratio. For simplicity,

the weights on speed and accuracy criteria are denoted as variables *a* and *1-a* respectively so that a summation is 100% or 1.0. It is worth stressing that instead of each speed-accuracy ratio being treated categorically as earlier, it is now treated numerically according to its variable *a* value. That is, category 1 or 30:70 speed-accuracy ratio category is now presented as *a=0.3*, category 2 or 40:60 speed-accuracy ratio category is now presented as *a=0.4* and so on as shown in Figure 7.4. As an example, the segment connecting between 30:70 and 40:60 speed-accuracy ratios is used to observe the rate of change (m_{HPI}) with reference to the speed and accuracy scores difference (Δ or J_1-J_2). The slope for that piece of linear segment can be proved to be in the following form.

$$m_{HPI} = (J_1 - J_2) \cdot a \cdot (1 - a) \tag{7-1}$$

According to this equation, it means that the rate of change of HPI is faster for the subjects with large difference between speed and accuracy scores whereas it is slower for the ones with smaller difference. The sign of m_{HPI} indicates a direct or inverse effect of increasing speed-accuracy ratios on HPI values for positive and negative slopes respectively. These results also mean that HPI values increase for the former case and decrease for the latter case.

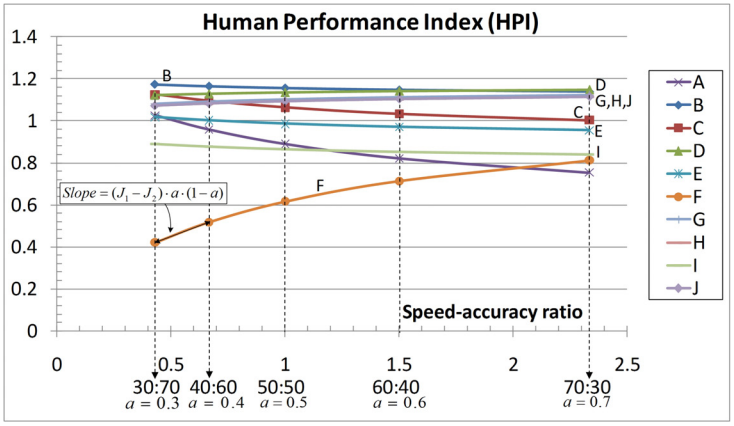

Subject	Speed score	Accuracy score	ΔJ
A	0.55	1.23	-0.68
B	1.11	1.20	-0.09
C	0.91	1.22	-0.30
D	1.17	1.10	0.06
E	0.91	1.07	-0.16
F	1.11	0.13	0.98
G	1.15	1.05	0.11
H	1.14	1.04	0.10
I	0.80	0.93	-0.13
J	1.15	1.04	0.11
Average	1.00	1.00	0.00
SD	0.20	0.32	0.42

Figure 7.4. Dependency of speed and accuracy for Trial 1 of computer-based experiment for human subjects A to J

The table in Figure 7.4 stresses the previous statement that larger values of ΔJ result in a steeper HPI change in either increasing (subject F) or decreasing directions (subjects A, C, E and I). This graph also suggests that it is possible to solve for associated weights

that yield the same HPI value for all subjects by considering the intersections of all HPI curves. These intersection points reflect possible and achievable human performance index with reference to a sample group. Suitable assistance or adaptive control mechanism can then be implemented based on these speed-accuracy characteristics.

In a real implementation, the larger the sample group, the better and higher accuracy of the results from the HPI concept would be. Therefore, extensive experiments are required prior to system integration.

7.5. HPI Applicability

With regard to the fundamentals of the HPI concept, it is defined to incorporate a number of performance variables, formulate a performance criterion from these variables and consequently use them to compute a performance value. The underlying structure to expand its applicability is essentially based on the well-renowned *speed-accuracy tradeoff* or *Fitts' Law* but with additional frameworks and definitions in order for qualities of speed and accuracy to be computed numerically. A *speed-accuracy ratio* in the fixed HPI is essentially related to a human control strategy and a derivation of suitable speed-accuracy characteristics for a particular human-machine system can potentially lead to a standardisation of human factor requirements.

The validation of HPI values from the non-model approach with those of the model-based approach has shown reasonable agreements but not without issues. It is worth stressing that such consistency is true not only for the computer-based system but also for the hardware-based system. The HPI concept can be reliably applied to any human-machine with and without hardware elements provided that required characteristics and performance variables processing are readily available prior to a computation.

Apart from the issue about inconsistency discussed earlier, there is also an issue about the accuracy characteristics that raises the concern about applicability. Considering the overview on average differences of HPI based on two sets of experiments, their values turn out to be 0.29 for the computer-based experiment and 0.14 for the hardware-based experiment, which are 0.15 and 0.13 for the linear and squared transfer functions respectively (see Table 7-1).

Table 7-1. Summary of average differences for fixed HPI values (based on Table 6.12 and 6.14, Chapter 6)

Computer-based		Hardware-based					
HPI_{av}		HPI_{av}					
T1	0.16	Linear	T1	0.11	Squared	T1	0.11
T2	0.41		T2	0.2		T2	0.15
Average	0.29		Average	0.15		Average	0.13

The results shown in the table suggest that the resultant HPI value computed from these two systems has a ± discrepancy attached to it and such discrepancy emerges from the imperfect algorithms of non-model and model-based approaches. It literally means a computed value X should be adjusted by ± average difference to represent the closer to the real values so that the value is simply X±HPI_{av}. It also reflects that the smaller the average difference, the better and more accurate their HPI values are. According to Table 7-1, this means people with average performance (the HPI value of 1.0 as described in Chapter 3) have approximately 10% discrepancy involved with his/her computed HPI value for the hardware-based system and approximately 30% discrepancy for the computer-based system. Considering the fact that the simulated response from human ARX models derived from the hardware-based system indicates high RMSE values, these results may seem surprising (consider the examples given in Figure 6.27, Chapter 6). However, looking into the root of these calculations help clarify what likely is the cause for this and it is related to the average-based algorithm.

Despite the advantages of average-based architecture being extensible and sample-based, the quality of a sample group and the accuracy of the algorithms play important roles in affecting the results as well. Similar and invariant behavior of human operator in performing the operation makes the human performance results less realistic and carries less meaning. This is the problem with the hardware-based system because it turns out that the balancing action of the helicopter test rig is minimal leading to the use of pitch-axis model for every subject (as discussed in Chapter 6). As a result from the model-based approach, almost all simulated response appears to stay below pitch axis with slight variation causing all *RMSE* values to be high and similar rationale applies to the R^2 values. By averaging these variables, it make their values lower and more centered but not necessarily reflective of the real goodness. In other words, the situation here is like having a good HPI when everyone else also has a good HPI even though his/her performance is bad in reality. In the worst-case scenario, the results can even be misleading if all subjects have extremely poor performance. Unlike the computer-based system, there is a genuine variation in the pattern of his/her control actions and the simulated responses associated with each axis can be successfully derived. Such diversity is reflected in their performance values causing the average difference value to be higher as presented inTable 7-1.

Due to these drawbacks on the average-based computation, extra features are required to mitigate the situation especially when dealing with the hardware-based system. For example, the improvements can be made by coordinating the results from the model-based approach with model-based approach to check the output anomalies in terms of performance diversity.

7.6. Conclusions

This thesis presents a structure of human characteristics to be used as a fundamental for incorporating a human into the control loop or to build awareness of human existence in machine understandable format. Two approaches of Human Performance Index (HPI)

computation have been proposed to implement and validate the HPI concept, which are non-model and model-based approaches respectively. The following main research novelties have been achieved to mark several aspects on research work in this thesis.

7.6.1. Human Performance Index (HPI) Concept

The HPI is proposed to be a hierarchy of performance criteria and performance variables with corresponding weight to reflect a significance of its associated physical quality. A collection of performance variables constitutes one performance criterion and a collection of performance criteria constitutes a Human Performance Index (HPI). With a focus on the well-renowned *speed-accuracy tradeoff* or *Fitts' Law*, speed and accuracy criteria are mainly considered in this thesis with their characteristics quantified computationally and numerically for the first time. It can be viewed as a low-level or crude performance computation. The HPI concept also incorporates a treatment of corresponding performance variables to suit their monotonicity prior to a computation. This is to ensure the resultant HPI value is of monotonically increasing regardless of performance variables' monotonicity in the hierarchy. Two forms of HPI are proposed with a condition of its corresponding performance criteria weight being unassigned (open-form) and assigned (closed-form).

Despite advantages of the HPI concept summarized here, it is restricted to the point-to-point operation at this stage mainly according to the current definitions of accuracy characteristics. Obvious manually-controlled applications requiring a point-to-point operation appear to be, but not limited to, robot manipulator, vehicle and sports training device. The actual interpretation of speed and accuracy characteristics might differ from application to application depending on their system characteristics. More importantly, a logical thinking and reasoning associated with human control actions are part of the higher-level performance evaluation, which are not addressed by the HPI.

7.6.2. Analysis of Human Performance

To illustrate the validity of HPI concept, two approaches have been proposed and applied to two different human-machine systems, which are computer-based and hardware-based. The HPI values computed from these two approaches turned out to have inconsistent issues and there are mainly from the limitations on the model complexity. Major concerns on implementing the HPI concept to systems with hardware elements or a number of connecting components have also been pointed out and discussed in details. Requirements on the pattern of inputs and outputs along with selection criteria on a suitable pair of data for System Identification have been covered. Model optimization with variation of time delay has been achieved along with axis consideration to yield reliable simulated results.

Even though the HPI concept is proposed to be implemented using both non-model and model-based approaches, the critical analysis on their strength and weaknesses are still incomplete in this research. These two approaches have been independently used suggesting a possibility to introduce coordination and optimisation between these two approaches to their full potential. The ability to compute future response based on the resultant human ARX model might move the development on a model-based approach forward with its predictability feature in reshaping human control action. Therefore, the analysis of human performance will not by simply at the very moment of measurement but rather involved in determining how the pattern of change is to be supported in case of too different response from the predicted one.

7.6.3. Human Control Strategy

For the first time, the derivation of human control strategy is based on his/her speed and accuracy characteristics and illustrated with reference to the results from systems

containing and not containing hardware elements. The ratio of speed and accuracy scores for each human operator indicates a weighting or focus on each his/her speed and accuracy characteristics respectively and this potentially reflects his/her control strategy. More importantly, the fixed HPI values vary according to that operator's own weight on speed and accuracy, which suggests how one operator pays attention to perform a particular task comparing to others.

It is interesting to see how human control strategy differs from different viewpoints. In fact, there are two speed-accuracy ratios involved in the HPI concept. The first one is an intrinsic speed-accuracy ratio and the second one is a system speed-accuracy ratio, which simply refers to a personal style of control motion and a suitable requirement for a particular system respectively. In the latter sense, only five fixed speed-accuracy ratios have been chosen to demonstrate this idea (30:70, 40:60, 50:50, 60:40 and 70:30) leaving a real optimal value to be determined by system designers. This scenario is very similar to a demand-supply relationship, by which one's performance needs to match system's requirement to allow a successful operation. The speed-accuracy ratio for particular system is likely to differ from other systems depending on their manual control system variables (Figure 2.2, Chapter 2).

7.7. Recommendations for Further Work

The current implementation of HPI concept relies on an offline facility to process the logged data, extract necessary parameters from either system output directly or human mathematical models depending on the computation approaches, and compute the corresponding human performance. Even though this is a successful implementation in proving the HPI validity in representing human performance in terms of speed and accuracy, a complete experiment on every human subject in a sample group is required prior to the performance evaluation and this can be viewed as a limitation. A use of real-

time computing system with designed set of algorithms and dedicated interface could therefore maximize its full potential in terms of scalability and dynamic architecture of the HPI concept. The convergence of results between those of non-model and model-based approaches can be possibly used to formulate the end condition of the real-time experimental processes. This hybrid mode of computation takes the HPI concept to the whole new level, whereby the performance values can be optimized and will always become available even in case of unreliable sources or high disturbances. Progressive mode of operation may be easier to implement and more practical at its early stage of development.

Another interesting issue that have not been fully explored in this research is the source of discrepancy between non-model and model-based approaches. Due to a lack of in-depth analysis, the study on the pattern of control actions may be useful to standardize the HPI concept and improve its reliability. More importantly, intensive set of experimentations is essential in order to prove a statistical significance of the HPI concept prior to a real implementation as this research only aims at proving its principle. Sample group diversity is also one of the important factors that will lead to realistic experimental results and performance values. Other case studies based on systems with different characteristics and setups are also crucial to ensure that the concept is still valid.

Apart from the implementation issue, a design of adaptive controller with reliance on human performance is the next step towards a complete HAM system. Artificial intelligence methods can be formulated to determine human's learning based on his/her speed-accuracy ratio shift and use it in designing suitable sets of assistant and adaptive mechanisms.

References

Institution of Ergonomics & Human Factors: What Is Ergonomics? , from http://www.ergonomics.org.uk/what-ergonomics, May 2011.

International Ergonomics Association: What Is Ergonomics? , from http://iea.cc/01_what/What%20is%20Ergonomics.html, May 2011.

(2004). Tokyu Denki University (Tdu), the 21st Century Coe Research Program. from http://www.ham.coe.dendai.ac.jp.

(2009). Reflection-Wolfram Mathworld. Retrieved March 13, 2009, from http://mathworld.wolfram.com/Reflection.html.

Accot, J. and Zhai, S. (1997). Beyond Fitts' Law: Models for Trajectory-Based Hci Tasks. *Proceedings of the SIGCHI Conference on Human Factors in Computing Systems*, Atlanta, Georgia, United States. pp: 295 - 302. ISBN: 0-89791-802-9

Agah, A. (2000). Human Interactions with Intelligent Systems: Research Taxonomy. *Computers & Electrical Engineering* 27(1), pp: 71-107. ISSN: 0045-7906

Andrade, G., Ramalho, G., Santana, H. and Corruble, V. (2005). Challenge-Sensitive Action Selection: An Application to Game Balancing. *Intelligent Agent Technology, IEEE/WIC/ACM International Conference on*, 19-22 Sept. 2005 pp: 194-200. ISBN:

Angel, E. S. and Bekey, G. A. (1968). Adaptive Finite-State Models of Manual Control Systems. *IEEE Transactions on Man-Machine Systems* 9(1), pp. ISSN: 0536-1540

Aseltine, J., Mancini, A. and Sarture, C. (1958). A Survey of Adaptive Control Systems. *Automatic Control, IRE Transactions on* 6(1), pp: 102-108. ISSN: 0096-199X

Ashkenas, I., Jex, H. and McRuer, D. (1964). Pilot-Induced Oscillations: Their Cause and Analysis, Defense Technical Information Center, Systems Technology Inc., Inglewood, California.

Åström, K. J. (1983). Theory and Applications of Adaptive Control--a Survey. *Automatica* 19(5), pp: 471-486. ISSN: 0005-1098

Auslander, A. M. (1996). What Is Mechatronics? *IEEE/ASME Transactions on Mechatronics* 1, pp: 5-9. ISSN: 1083-4435

Beamish, D., Scott MacKenzie, I. and Wu, J. (2006). Speed-Accuracy Trade-Off in Planned Arm Movements with Delayed Feedback. *Neural Networks* 19(5), pp: 582-599. ISSN: 08936080

Beardmore, R. (2010). Rolling Bearing Friction from http://www.roymech.co.uk/Useful_Tables/Tribology/Bearing%20Friction.html.

Birmingham, H. P. and Taylor, F. V. (1954). A Design Philosophy for Man-Machine Control Systems. *Proceedings of the IRE* 42(12), pp: 1748-1758. ISSN: 0096-8390

Bobál, V., Bohm, J., Fessl, J. and Machá ek, J. (2005). *Digital Self-Tuning Controllers: Algorithms, Implementation and Applications*: Springer Verlag. ISBN: 1852339802

Boer, E. R. and Kenyon, R. V. (1998). Estimation of Time-Varying Delay Time in Non-Stationary Linear Systems: An Approach to Monitor Human Operator

Adaptation in Manual Tracking Tasks. *IEEE Transactions on Systems, Man and Cybernetics-Part A: Systems and Humans* 28(1), pp: 89-99. ISSN: 1083-4427

Bradshaw, E. J. and Sparrow, W. A. (2000). The Speed-Accuracy Trade-Off in Human Gait Control When Running Towards Targets. *Journal of Applied Biomechanics* 16(4), pp: 331-341. ISSN: 10658483

Brockett, W. (1997). Minimum Attention Control. *Proceedings of the 36th IEEE Conference on Decision and Control, 10-12 December 1997,* , San Diego, California, USA. Piscataway (N.J.) : IEEE 1997. pp: 2628-2632. ISBN: 0-7803-4187-2

Cai, Z. (2009). *Iterative Learning Control: Algorithm Development and Experimental Benchmarking*. (Doctor of Philosophy). University of Southampton,

Card, S., Moran, T. and Newell, A. (1983). *The Psychology of Human-Computer Interaction*: Lawrence Erlbaum Associates. ISBN: 0898592437

Card, S. K., Moran, T. P. and Newell, A. (1980). The Keystroke-Level Model for User Performance Time with Interactive Systems. *Commun. ACM* 23(7), pp: 396-410. ISSN: 0001-0782

Centre, M. M. T. (2010). *Mtc: Manufacturing Technology Centre* http://www.the-mtc.org/. ISBN:

Cleary, K. and Nguyen, C. (2001). State of the Art in Surgical Robotics: Clinical Applications and Technology Challenges. *Computer Aided Surgery: Official Journal of the International Society for Computer Aided Surgery* 6(6), pp: 312-328. ISSN: 1341-0849

Cooper, R. A. (1991). System Identification of Human Performance Models. *IEEE Transactions on Systems, Man and Cybernetics* 21(1), pp: 244-252. ISSN: 0018-9472

Cooper, R. A., Jones, D. K., Fitzgerald, S. and Boninger, M. L. (2000). Analysis of Position and Isometric Joysticks for Powered Wheelchair Driving. *IEEE Transactions on Biomedical Engineering* 47(7), pp: 902-910. ISSN: 00189294

Corlett, E. N. and Stapleton, C. (2001). The Ergonomics Society: 50 Years of Growth. *Ergonomics* 44(14), pp: 1265-1277. ISSN: 00140139

Coxeter, H. S. M. and Greitzer, S. L. (1967). *Geometry Revisited (New Mathematical Library)* The Mathematical Association of America, Washington D.C., USA ISBN: 0883856190

Cusumano, M. (1992). Shifting Economies: From Craft Production to Flexible Systems and Software Factories. *Research Policy* 21(5), pp: 453-480. ISSN: 0048-7333

Dander, V. A. (1963). Predicting Pilot Ratings of Multi-Axis Control Tasks from Single-Axis Data. *IEEE Transactions on Human Factors in Electronics* 4(1), pp: 15-17. ISSN: 0096-249X

Davidson, J., Schmidt, D., Aeronautics, N., Administration, S., States, U., Scientific and Program, T. I. (1992). Modified Optimal Control Pilot Model for Computer-Aided Design and Analysis, National Aeronautics and Space Administration, Office of Management, Scientific and Technical Information Program; For sale by the National Technical Information Service.

Doman, D. B. and Anderson, M. R. (2000). A Fixed-Order Optimal Control Model of Human Operator Response. *Automatica, Journal* 36(3), pp: 409-418. ISSN: 0005-1098

Dornheim, M. (1992). Report Pinpoints Factors Leading to Yf-22 Crash. *Aviation Week and Space Technology* 137(19), pp: 53-54. ISSN: 0005-2175

Elkind, J. (1956). *Characteristics of Simple Manual Control Systems*. (Doctoral). Massachusetts Institute of Technology (MIT),

Ertugrul, S. (2008). Predictive Modeling of Human Operators Using Parametric and Neuro-Fuzzy Models by Means of Computer-Based Identification Experiment. *Engineering Applications of Artificial Intelligence, Journal* 21(2), pp: 259-268. ISSN: 0952-1976

Fitts, P. (1954). The Information Capacity of the Human Motor System in Controlling the Amplitude of Movement. *Journal of Experimental Psychology* 47(6), pp: 381-391. ISSN: 0096-3445

Fitts, P. and Peterson, J. (1964). Information Capacity of Discrete Motor Responses. *Journal of Experimental Psychology* 67(2), pp: 103-112. ISSN: 0096-3445

Förster, J., Higgins, E. T. and Bianco, A. T. (2003). Speed/Accuracy Decisions in Task Performance: Built-in Trade-Off or Separate Strategic Concerns? *Organizational Behavior and Human Decision Processes* 90(1), pp: 148-164. ISSN: 0749-5978

Furuta, K. (2003). Control of Pendulum: From Super Mechano-System to Human Adaptive Mechatronics. *Proceedings of IEEE Conference on Decision and Control, 9-12 December 2003.* , Mauli, Hawaii, USA. Piscataway, N.J : IEEE Service Center, 2003. pp: 1498-1507. ISBN: 0-7803-7924-1

Furuta, K. (2004). What Is Human Adaptive Mechatronics? *Proceedings of the 8th International Conference on Mechatronics Technology, 2004. ICMT2004. November 8-12, 2004*, Hanoi, Vietnam. pp: ISBN:

Furuta, K., Iwase, M. and Hatakeyama, S. (2005). Internal Model and Saturating Actuation in Human Operation from View of Human-Adaptive Mechatronics. *IEEE Transactions on Industrial Electronics, Journal* 52(5), pp: 1236-1245. ISSN: 0278-0046

Furuta, K., Kado, Y. and Shiratori, S. (2006). Assisting Control in Human Adaptive Mechatronics-Single Ball Juggling. *Proceedings of IEEE International Conference on Control Applications, 2006. CCA'06. October 4-6, 2006*, Munich, Germany. . pp: 545-550. ISBN: 0-7803-9795-5

Gaines, B. R. (1969). Linear and Nonlinear Models of the Human Controller. *International Journal of Man-Machine Studies* 1(4), pp: 333-360. ISSN: 0020-7373

Gingrich, C. G., Kuespert, D. R. and McAvoy, T. J. (1992). Modelling Human Operators Using Neural Networks. *ISA Transactions. The Instrumentation, Systems, and Automation Society* 31(3), pp: 81-90. ISSN: 0019-0578

Gittleman, B., Dwan, T. E. and Smiley, C. S. (1992). System Identification: Human Tracking Response. *IEEE Transactions on Education* 35(1), pp: 31-37. ISSN: 0018-9359

Greenstein, J. S. and Arnaut, L. Y. (1987). Human Factors Aspects of Manual Computer Input Devices. Handbook of human factors**:** 1450–1489.

Higgins, E., Shah, J. and Friedman, R. (1997). Emotional Responses to Goal Attainment: Strength of Regulatory Focus as Moderator. *JOURNAL OF PERSONALITY AND SOCIAL PSYCHOLOGY* 72(3), pp: 515-525. ISSN: 0022-3514

Higgins, E. T. (1997). Emotional Responses to Goal Attainment: Strength of Regulatory Focus as Moderator. *JOURNAL OF PERSONALITY AND SOCIAL PSYCHOLOGY* 72(3), pp: 515-525. ISSN: 0022-3514

Hirata, Y., Jr.Oscar, C., Hara, A. and Kosuge, K. (2005). Human-Adaptive Motion Control of Active and Passive Type Walking Support System. Proceedings of IEEE workshop on Advanced Robotics and its Social Impacts, 2005. ARSO2005. Nagoya, Japan. June 12-15, 2005**:** 139-144.

Hölttä, V. and Koivo, H. (2009). Quality Index Framework for Plant-Wide Performance Evaluation. *Journal of Process Control* 19(7), pp: 1143-1148. ISSN: 0959-1524

Hunicke, R. (2005). The Case for Dynamic Difficulty Adjustment in Games. *2005 ACM SIGCHI International Conference on Advances in Computer Entertainment Technology, ACE '05, June 15, 2005 - June 17, 2005*, Valencia, Spain. Association for Computing Machinery. pp: 429-433. ISBN:

Hunicke, R. and Chapman, V. (2004). Ai for Dynamic Difficulty Adjustment in Games. *19th National Conference on Artificial Intelligence, July 25, 2004 - July 26, 2004*, San Jose, CA, United states. American Association for Artificial Intelligence. pp: 91-96. ISBN:

Igarashi, H., Takeya, A., Shirasaka, S., Suzuki, S. and Kakikura, M. (2005). Adaptive Teleoperation System with Ham-Gui Control Based on Human Sensitivity Characteristics. *Proceedings of the 9th International Conference on Mechatronics Technology, 2005. ICMT2005. Kuala Lumpur, Malaysia. December 5-8, 2005*, pp: ISBN:

Imamizu, H., Miyauchi, S., Tamada, T., Sasaki, Y., Takino, R., Putz, B., Yoshioka, T. and Kawato, M. (2000). Human Cerebellar Activity Reflecting an Acquired Internal Model of a New Tool. *Nature, Journal* 403(6766), pp: 192-195. ISSN: 0028-0836

Iwase, M., Hatakeyama, S. and Furuta, K. (2006). Analysis of Intermittent Control Systems by Human Operations. *IEEE Industrial Electronics, IECON 2006 - 32nd Annual Conference on*, pp: 4516-4521. ISBN: 1553-572X

Iwase, M., Shoshiro, H. and Furuta, K. (2005). Analysis of Intermittent Control Systems by Human Operations. *Proceedings of the 31th Annual Conference of the IEEE Industrial Electronics Society, IECON2005. November 6-10, 2005*, pp: 56-60. ISSN: 0-7803-9252-3

Jagacinski, R. J. and Flach, J. M. (2002). *Control Theory for Humans: Quantitative Approaches to Modeling Performance*. Mahwah, New Jersey. ISBN: 0805822925

Jang, J. R. (1993). Anfis: Adaptive-Network-Based Fuzzy Inference System. *IEEE Transactions on Systems, Man and Cybernetics* 23(3), pp: 665 - 685. ISSN: 0018-9472

Jang, J. S. R. and Chuen-Tsai, S. (1995). Neuro-Fuzzy Modeling and Control. 83, pp: 378-406. ISSN: 0018-9219

Kado, Y., Pan, Y. and Furuta, K. (2006). Control System for Skill Acquisition-Balancing Pendulum Based on Human Adaptive Mechatronics. *IEEE International Conference on Systems, Man and Cybernetics. SMC2006. October 8-11, 2006.* , Taipei, Taiwan. pp: 4040-4045. ISBN: 1-4244-0100-3

Katsura, S., Matsumoto, Y. and Ohnishi, K. (2005). Realization Of "Law of Action and Reaction" By Multilateral Control. *IEEE Transactions on Industrial Electronics* 52(5), pp: 1196-1205. ISSN: 0278-0046

Kawato, M. (1999). Internal Models for Motor Control and Trajectory Planning. *Journal: Current Opinion in Neurobiology* 9(6), pp: 718-727. ISSN: 0959-4388

Kelley, C. R. (1968). *Manual and Automatic Control: A Theory of Manual Control and Its Application to Manual and to Automatic Systems*. New York: Wiley. ISBN:

Kleinman, D. (1969). Optimal Control of Linear Systems with Time-Delay and Observation Noise. *Automatic Control, IEEE Transactions on* 14(5), pp: 524-527. ISSN: 0018-9286

Kleinman, D. L., Baron, S. and Levison, W. H. (1970). An Optimal Control Model of Human Response-Part 2: Prediction of Human Performance in a Complex Task. *Automatica, Journal* 6(3), pp: 371- 383. ISSN: 0005-1098

Kleinman, D. L., Baron, S. and Levison, W. H. (1970). An Optimal Control Model of Human Response-Part I: Theory and Validation. *Automatica, Journal* 6(3), pp: 357-369. ISSN: 0005-1098

Kurihara, K., Suzuki, S., Harashima, F. and Furuta, K. (2004). Human Adaptive Mechatronics(Ham) for Haptic System. *Proceedings of the 30th Annual Conference of IEEE Industrial Electronics Society, 2004. IECON 2004. November 2-6, 2004*, Busan, Korea. pp: 647-652. ISBN: 0-7803-8730-9

Lee, S. and Chen, J. (1994). Skill Learning from Observations. *Proceedings of IEEE International Conference on Robotics and Automation, 1994. ICRA1994. May 8-13, 1994*, California, USA. pp: 3245-3250. ISBN: 0-8186-5330-2

Liao, M.-J., Jagacinski, R. J. and Greenberg, N. (1995). Quantifying the Performance Limitations of Older Adults in a Target Acquisition Task. Santa Monica, CA, USA. Human Factors and Ergonomics Society, Inc. pp: 961. ISBN: 0163-5182

Ljung, L. (1999). *System Identification: Theory for the User*: Prentice Hall PTR. ISBN: 0136566952

Marayong, P. and Okamura, A. M. (2004). Speed-Accuracy Characteristics of Human-Machine Cooperative Manipulation Using Virtual Fixtures with Variable Admittance. *Human Factors* 46(3), pp: 518-532. ISSN: 00187208

Masamune, K., Ohnuma, K., Yoshimitsu, K., Ohshima, K., Fukui, Y. and Miyawaki, F. (2005). Development of Ham Surgical Support System for Laparoscopic Surgery-Analysis of Intraoperative Motion of a Surgeon Scenario. *Proceedings of the 9th International Conference on Mechatronics Technology, 2005. ICMT2005. December 5-8, 2005*, Kuala Lumpur, Malaysia. . pp: ISBN:

Masamune, K., Takeda, T. and Ohshima, K. (2004). Evaluation of the Skill for Operating Minimally Invasive Spine Surgery Robot toward Ham Based Surgery System. *Proceedings of the 8th International Conference on Mechatronics Technology, 2004. ICMT2004. November 8-12, 2004*, Hanoi, Vietnam. Hanoi : Vietnam National Univ. Publ., 2004. pp: ISBN:

Mcruer, D. (1980). Human Dynamics in Man-Machine Systems. *Automatica, Journal* 16(3), pp: 237-253. ISSN: 0005-1098

Mcruer, D. T. (1967). A Review of Quasi-Linear Pilot Models. *IEEE Transactions on Human Factors in Electronics* 8(3), pp: 231-249. ISSN: 0096-249X

Mcruer, D. T. and Krendel, E. S. (1959). The Human Operator as a Servo System Element-Part I. *Journal of the Franklin Institute* 267, pp: 381-403. ISSN: 0016-0032

Mcruer, D. T. and Krendel, E. S. (1959). The Human Operator as a Servo System Element-Part Ii. *Journal of the Franklin Institute* 267, pp: 511-536. ISSN: 0016-0032

Mcruer, D. T. and Krendel, E. S. (1962). The Man-Machine System Concept. *Institute of Radio Engineers, Journal* 50(5), pp: 1117-1123. ISSN: 0096-8390

Mehr, M. H. (1973). Two-Axis Manual Positioning and Tracking Controls. *Applied Ergonomics* 4(3), pp: 154-157. ISSN: 00036870

Meyer, D. E., Abrams, R. A., Kornblum, S., Wright, C. E. and Smith, J. E. K. (1988). Optimality in Human Motor Performance: Ideal Control of Rapid Aimed Movements. *Psychological Review* 95(3), pp: 340-370. ISSN: 0033-295X

Meyer, D. E., Smith, J. E. K., Kornblum, S., Abrams, R. A. and Wright, C. E. (1990). Speed-Accuracy Tradeoffs in Aimed Movements - toward a Theory of Rapid Voluntary Action. *13th International Symp on Attention and Performance : Organization of Action*, Jun 27-Jul 02 Arc Et Senans, France. Mit Press. pp: 173-226. ISBN: 0262132842

Miall, R. C., Weir, D. J., Wolpert, D. M. and Stein, J. F. (1993). Is the Cerebellum a Smith Predictor? *Journal of Motor Behavior* 25(3), pp: 203-216. ISSN: 0022-2895

Miller, D. P. and Swain, A. D. (1986). Human Error and Human Reliability. Handbook of Human Factors**:** 219-252. ISBN: 0471116904

Montgomery , D. C., Runger, G. C. and Hubele, N. F. (2003). *Engineering Statistics*: Wiley. ISBN: 0471448540

Mori, S., Sakaguchi, A. and Yamamoto, T. (2007). Design and Experimental Evaluation of a Data-Driven Skill-Based Pid Controller. *Advanced intelligent mechatronics, 2007 ieee/asme international conference on*, pp: 1-5. ISBN: 978-1-4244-1263-1

Mottet, D., Bootsma, R. J., Guiard, Y. and Laurent, M. (1994). Fitts' Law in Two-Dimensional Task Space. *Experimental Brain Research* 100(1), pp: 144-148. ISSN: 0014-4819

Murata, A. and Iwase, H. (2001). Extending Fitts' Law to a Three-Dimensional Pointing Task. *Human Movement Science* 20(6), pp: 791-805. ISSN: 0167-9457

Nechyba, M. C. and Xu, Y. (1995). Human Skill Transfer: Neural Networks as Learners and Teachers. *Proceedings of IEEE/RSJ International on Intelligent Robots and Systems (Human Robot Interaction and Cooperative Robots), 1995. IROS1995. August 5-9, 1995*, Pittsburgh, Pennsylvania, USA. . Piscataway, NJ : IEEE Service Center, 1995. pp: 314-319. ISBN: 0-8186-7108-4

Nechyba, M. C. and Xu, Y. (1996). On the Fidelity of Human Skill Models. *Proceedings of the 1996 IEEE International Conference on Robotics and Automation, 1996. ICRA1996. April 1996*, Minnesota, USA. . pp: 2688-2693. ISBN: 0-7803-2988-0

Nechyba, M. C. and Xu, Y. (1997). Human Control Strategy: Abstraction, Verification, and Replication. *IEEE Control Systems Magazine, Journal* 17(5), pp: 48-61. ISSN: 0272-1708

Nise, N. (2006). *Control Systems Engineering*: John Wiley & Sons. ISBN: 978-0471-44577-7

Ollero, A. and Garcia-cerezo, A. J. (1989). Direct Digital Control, Auto-Tuning and Supervision Using Fuzzy Logic. *Fuzzy Sets and System, Journal* 30(2), pp: 135-153. ISSN: 0165-0114

Pachter, M. and Miller, R. B. (1998). Manual Flight Control with Saturating Actuators. *Control Systems Magazine, IEEE* 18(1), pp: 10-20. ISSN: 0272-1708

Palmroth, L., Tervo, K. and Putkonen, A. (2009). Intelligent Coaching of Mobile Working Machine Operators. *Intelligent Engineering Systems, 2009. INES 2009. International Conference on*, 16-18 April 2009 Barbados, 16-18 April 2009. Piscataway, N.J.: IEEE, 2009. pp: 149-154. ISBN: 978-1-4244-7650-3

Parasuraman, R. (1997). Humans and Automation: Use, Misuse, Disuse, Abuse. *Human factors : the journal of the Human Factors Society.* 39(24), pp: 230-253. ISSN: 0018-7208

Parasuraman, R. (2008). Humans: Still Vital after All These Years of Automation. *Human factors : the journal of the Human Factors Society.* 50(10), pp: 511-520. ISSN: 0018-7208

Parasuraman, R., Sheridan, T. and Wickens, C. (2000). A Model for Types and Levels of Human Interaction with Automation. *IEEE Transactions on Systems, Man and Cybernetics, Part A: Systems and Humans* 30(3), pp: 286-297. ISSN: 1083-4427

Pemberton, M. and Rau, N. (2007). Mathematics for Economists: An Introductory Textbook. pp: 712. ISSN: 0719075394

Perry, B. L. and Birmingham, H. P. (1968). Joystick Dynamics. *Human Factors* 10(4), pp: 413-418. ISSN: 0018-7208

Pew, R. W. (2008). More Than 50 Years of History and Accomplishments in Human Performance Model Development. *Human Factors* 50(3), pp: 489-496. ISSN: 00187208

Preyss, A. E. and Meiry, J. L. (1968). Stochastic Modeling of Human Learning Behavior. *IEEE Transactions on Man-Machine Systems* 9(2), pp: 36-46. ISSN: 0018-9472

Ragazzini, J. R. (1948). Engineering Aspects of the Human Being as a Servo-Mechanism. *American Psychological Association* 3, pp: 219-314. ISSN:

Rao, R. S., Seliktar, R. and Rahman, T. (2000). Evaluation of an Isometric and a Position Joystick in a Target Acquisition Task for Individuals with Cerebral Palsy. *Rehabilitation Engineering, IEEE Transactions on* 8(1), pp: 118-125. ISSN: 1063-6528

Rasmussen, J. (1983). Skills, Rules and Knowledge; Signals, Signs and Symbols and Other Distinctions. *Human Performance Models. IEEE Transactions on Man, Systems and Cybernetics* 13(3), pp: 257-266. ISSN: 0018-9472

Rasmussen, J. (1986). *Information Processing and Human-Machine Interaction: An Approach to Cognitive Engineering*: Elsevier Science Inc. ISBN: 0444009876

Rasmussen, J., Pejtersen, A. and Goodstein, L. (1994). *Cognitive Systems Engineering*. ISBN: 0471011983

S.Tzafestas and Papanikolopoulos, N. P. (1990). Incremental Fuzzy Expert Pid Control. *Industrial Electronics, IEEE Transactions on* 37, pp: 365-371. ISSN: 0278-0046

Santos, M., Lopez, R. and Cruz, J. M. d.-l. (2005). Fuzzy Control of the Vertical Acceleration of Fast Ferries. 13, pp: 305-313. ISSN: 0967-0661

Sasaki, T., Takeya, A., Igarashi, H. and Suzuki, S. (2007). Operation Skill Quantification for Mobile Vehicle Operation. *SICE(Society of Instrument and Control Engineers)Annual Conference, SICE 2007, September 17, 2007 - September 20, 2007*, Takamatsu, Japan. Society of Instrument and Control Engineers (SICE). pp: 274-279. ISBN: 4907764286

Schirner, G. and Domer, R. (2008). Quantitative Analysis of the Speed/Accuracy Trade-Off in Transaction Level Modeling. *Transactions on Embedded Computing Systems* 8(1), pp. ISSN: 15399087

Schweitzer, S. (1996). Mechatronics for the Design of Human-Oriented Machines. *IEEE/ASME Transactions on Mechatronics* 1(2), pp: 120-126. ISSN: 1083-4435

Scott MacKenzie, I. (1992). Fitts' Law as a Research and Design Tool in Human-Computer Interaction. *Journal of Human-Computer Interaction* 7(1), pp: 91-139. ISSN: 0737-0024

Scott MacKenzie, I. and Buxton, W. (1992). Extending Fitts' Law to Two-Dimensional Tasks. *Proceedings of the SIGCHI Conference on Human Factors in Computing*

Systems, Monterey, California, United States, pp: 219 -226. ISBN: 0-89791-513-5

Shaw, I. S. (1993). Fuzzy Model of a Human Control Operator in a Compensatory Tracking Loop. *International Journal on Man-Machine Studies* 39(2), pp: 305-332. ISSN: 0020-7373

Sheridan, T. B. and Ferrel, W. R. (1974). *Man-Machine Systems: Information, Control, and Decision Models of Human Performance*. Cambridge, MA. ISBN: 0262191180

Skolnick, A. (1966). Stability and Performance of Manned Control System. *IEEE Transactions on Human Factor in Electronics* 7(3), pp: 115-124. ISSN: 0096-249X

Spronck, P., Sprinkhuizen-Kuyper, I. and Postma, E. (2004). Difficulty Scaling of Game Ai. *Proceedings of the 5th International Conference on Intelligent Games and Simulation (GAME-ON 2004)* pp: 33–37. ISBN:

Sribunruangrit, N., Marque, C. K., Lenay, C., Hanneton, S., Gapenne, O. and Vanhoutte, C. (2004). Speed-Accuracy Tradeoff During Performance of a Tracking Task without Visual Feedback. *IEEE Transactions on Neural Systems and Rehabilitation Engineering* 12(1), pp: 131-139. ISSN: 15344320

Suzuki, S., Furuta, K. and Harashima, F. (2005). Overview of Human Adaptive Mechatronics and Assist-Control to Enhance Human's Proficiency. *Proceedings of the International Conference on Control, Automation, and Systems, 2005. ICCAS2005. June 2-5, 2005*, Gyeong Gi, Korea. . Bucheon City : ICCAS, 2005. pp: 1759-1765. ISBN: 978-988-98671-4-0

Suzuki, S. and Harashima, F. (2005). Human Adaptive Mechatronics. *Proceedings of IEEE International Conference on Intelligent Engineering Systems, 2005. INES '05. September 16-19, 2005*, cruising on Mediterranean Sea. pp: 11-16. ISBN: 0-7803-9474-7

Suzuki, S. and Harashima, F. (2006). Assist Control and Its Tuning Method for Haptic System. *Proceedings of the 9th IEEE International Workshop on Advanced Motion Control, 2006. AMC06.* , Istanbul, Turkey. pp: 374-379. ISBN: 0-7803-9511-1

Suzuki, S., Harashima, F., Pan, Y. and Furuta, K. (2005). Skill Analysis of Human in Machine Operation. *Proceedings of International Conference on Neural Networks and Brain, 2005. ICNNB'05. October 13-15, 2005*, Beijing, China. . pp: 1556-1561. ISBN: 0-7803-9422-4

Suzuki, S., Kurihara, K., Furuta, K. and Harashima, F. (2005). Variable Dynamic Assist Control on Haptic System for Human Adaptive Mechatronics. *Proceedings of the 44th IEEE Conference on Decision and Control and European Control Conference, 2005, CDC-ECC'05. December 12-15, 2005*, Seville, Spain. . pp: 4596-4601. ISBN: 0-7803-9567-0

Suzuki, S., Kurihara, K., Furuta, K. and Harashima, F. (2006). Assistance Control on a Haptic System for Human Adaptive Mechatronics. *Advanced Robotics* 20(3), pp: 323-348. ISSN: 0169-1864

Suzuki, S., Pan, Y. and Kurihara, K. (2004). Voluntary Operation Assistance Based on Human Adaptive Mechatronics (Ham) Concept. *Proceedings of the 8th International Conference on Mechatronics Technology, 2004. ICMT2004. November 8-12, 2004*, Hanoi, Vietnam. . pp: ISBN:

Suzuki, S., Tomomatsu, N., Harashima, F. and Furuta, K. (2004). Skill Evaluation Based on State-Transition Model for Human Adaptive Mechatronics.

Proceedings of the 30th Annual Conference of the IEEE Industrial Electronics Society. November 2-6, 2004, Busan, Korea. Piscataway, N.J. : IEEE, 2004. pp: 641-646. ISBN: 0-7803-8730-9

Suzuki, S., Watanabe, Y., Igarashi, H. and Hidaka, K. (2007). Human Skill Elucidation Based on Gaze Analysis for Dynamic Manipulation. *IEEE International Conference on Systems, Man and Cybernetics. SMC'07. October 7-10, 2007.*, pp: 2989-2994. ISBN: 978-1-4244-0991-4

Suzuki, Y., Pan, Y., Suzuki, S., Kurihara, K. and Furuta, K. (2006). Human Operation with Xy-Stages - Human Adaptive Mechatronics. *IEEE International Conference on Systems, Man and Cybernetics. SMC 2006. October 8-11, 2006.*, Taipei, Taiwan. pp: 4034-4039. ISBN: 1-4244-0100-3

Takeuchi, S., Suzuki, S., Kakikura, M. and Kobayashi, H. (2006). Development of Vision-Based Measurement System for Hand Motion. *International Joint Conference, Society of Instrument and Control Engineers and Institute of Control, Automation and System Engineers (SICE-ICCAS 2006), 18-21 October 2006*, Bexco, Busan, Korea. Bucheon-City, Korea : Institute of Control, Automation and Systems Engineers, 2006. pp: 5770-5775. ISBN: 89-950038-5-5

Tervo, K. and Koivo, H. (2010). Towards Human Skill Adaptive Manual Control. *International Journal of Advanced Mechatronic Systems* 2(1), pp: 46-58. ISSN: 1756-8412

Tervo, K., Palmroth, L. and Koivo, H. (2010). Skill Evaluation of Human Operators in Partly Automated Mobile Working Machines. *IEEE Transactions on Automation Science and Engineering* 7(Compendex), pp: 133-142. ISSN: 15455955

Tervo, K., Palmroth, L. and Putkonen, A. (2009). A Hierarchical Fuzzy Inference Method for Skill Evaluation of Machine Operators. *Advanced Intelligent Mechatronics, 2009. AIM 2009. IEEE/ASME International Conference on*, 14-17 July 2009 Suntec Convention and Exhibition Center, Singapore, 14-17 July. Piscataway, N.J. : IEEE, 2009. pp: 136-141. ISBN: 978-1-4244-2852-6

Tustin, A. (1947). The Nature of the Operator's Response in Manual Control, and Its Implications for Controller Design. *Journal of the Institution of Electrical Engineers* 94(2), pp: 190-201. ISSN:

Ueno, A., Manabe, S. and Uchikawa, Y. (2005). A Real-Time Sound Feedback System with Dsp for Maintaining Alertness and Analysis of Arousal Reaction Induced by the Sound. *Proceedings of the 9th International Conference on Mechatronics Technology, 2005. ICMT2005. December 5-8, 2005*, Kuala Lumpur, Malaysia. pp: ISBN:

Ueno, A. and Uchikawa, Y. (2004). An Approach to Quantification of Human Alertness Using Dynamics of Saccadic Eye Movement-for an Application to Human Adaptive Mechatronics. *Proceedings of the 8th International Conference on Mechatronics Technology, 2004. ICMT2004. November 8-12, 2004*, Hanoi, Vietnam. . pp: ISBN:

Walpert, D. M. and M.~Kawato (1998). *Multiple Paired Forward and Inverse Models for Motor Control*. ISBN:

Wang, Y., Gao, F. and Doyle Iii, F. J. (2009). Survey on Iterative Learning Control, Repetitive Control, and Run-to-Run Control. *Journal of Process Control* In Press, Corrected Proof, pp. ISSN: 0959-1524

Wickens, C. D. and Hollands, J. (1999). *Engineering Psychology and Human Performance*: Prentice Hall. ISBN: 0321047117

Wikander, J., Törngren, M. and Hanson, M. (2001). The Science and Education of Mechatronics Engineering. *Robotics & Automation Magazine, IEEE* 14, pp: 20-26. ISSN: 1070-9932

Won, K., Tendick, F., Ellis, S. and Stark, L. (1987). A Comparison of Position and Rate Control for Telemanipulations with Consideration of Manipulator System Dynamics. *IEEE Journal of Robotics and Automation* 3(5), pp: 426-436. ISSN: 0882-4967

Xu, Y., Song, J., Nechyba, M. C. and Yam, Y. (2002). Performance Evaluation and Optimization of Human Control Strategy. *Robotics and Autonomous Systems* 39(1), pp: 19 -36. ISSN: 0921-8890

Yannakakis, G. N. and Hallam, J. (2004). Evolving Opponents for Interesting Interactive Computer Games. *From animals to animats* 8, pp: 499-508. ISSN:

Yoneda, M., Arai, F., Fukuda, T., Miyata, K. and Naito, T. (1997). Assistance System for Crane Operation Using Multimodal Display. *Proceedings of IEEE International Conference on Robotics and Automation 1997. Albuquerque, New Mexico. April 20-25, 1997.*, pp: 40-45. ISBN: 0-7803-3612-7

Yoneda, M., Arai, F., Fukuda, T., Miyata, K. and Niato, T. (1999). Assistance System for Crane Operation with Haptic Display Operational Assistance to Suppress Round Payload Swing. *Proceedings of IEEE International Conference on Robotics and Automation, 1999. May 10-15, 1999.*, Detroit, Michigan. . pp: 2924-2929. ISBN: 0-7803-5180-0

Yoshimitsu, K., Tanaka, T., Ohnuma, K., Miyawaki, F., Hashimoto, D. and Masamune, K. (2005). Prototype Development of Scrub Nurse Robot for Laparoscopic Surgery. *Internation Congress Series, Journal* 2005(1281), pp: 845-850. ISSN:

Young, L. R. and Meiry, J. L. (1965). Bang-Bang Aspects of Manual Control in High-Order Systems. *IEEE Transactions on Automatic Control* 10(3), pp: 336-341. ISSN: 0018-9286

Zapata, G., Kawakami, R., Galvao, H. and Yoneyama, T. (1999). Extracting Fuzzy Control Rules from Experimental Human Operator Data. *Systems, Man and Cybernetics, Part B, IEEE Transactions on* 29(3), pp: 398-406. ISSN: 1083-4419

Zhai, S., Kong, J. and Ren, X. (2004). Speed-Accuracy Tradeoff in Fitts' Law Tasks: On the Equivalency of Actual and Nominal Pointing Precision. *International Journal of Human-Computer Studies* 61(6), pp: 823-856. ISSN: 1071-5819

Zhang, T. and Nakamura, M. (2006). Neural Network-Based Hybrid Human-in-the-Loop Control for Meal Assistance Orthosis. *IEEE Transactions on Neural Systems and Rehabilitation Engineering, Journal.* 14(1), pp: 64-75. ISSN: 1534-4320

Appendix A: Hardware details

1. PCIO card (DAQ card | Amplicon PCI236)

Amplicon PCI236 is a digital Input/Output board with Intel 82C55(Complementary High Performance Metal Oxide Semiconductor (CHMOS) version of an Intel 8255A Programmable Peripheral Interface (PPI) chip). 24 digital I/O lines are arranged as three 8-bit ports (A, B and C) that supports PCI bus version 2.1. Ports A and B can be configured for input or outputs whereas Port C provides two 4-bit ports, each of which can be input or output. The board and connector layout are as presented in Figure A.1(a) and (b) respectively.

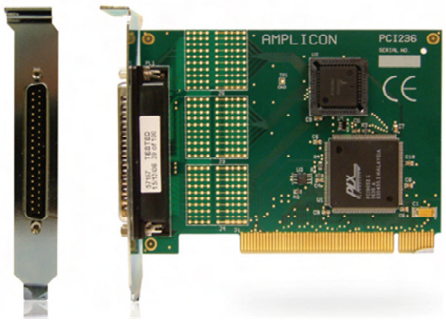

(a) Amplicon PCI236 board

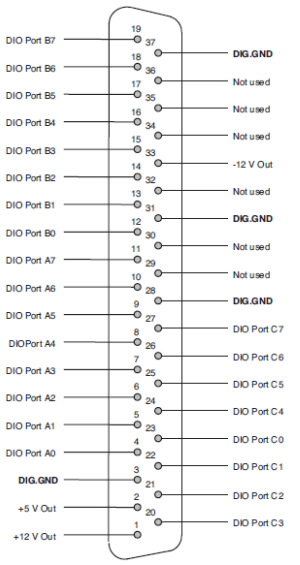

(b) 37-way connector layout

Figure A.1. PCIO card

In this research, the operation **Mode 0** with **control word #5 (89H)** is used to configure port A and B to work as an output and port C to work as an input (Refer to http://www.intersil.com/data/fn/fn2969.pdf for full details). This control word has to be set in an initialization stage, practically along with port address definitions.

2. PC adapter board

A PC adapter board is an interface between the PCIO card and the helicopter test rig containing Analog-to-Digital Converter (ADC), Digital-to-Analog Converter (DAC), 16-channel Multiplexer-Demultiplexer (MUX-DEMUX) chips and a 37-way ribbon connector as shown in Figure A.2.

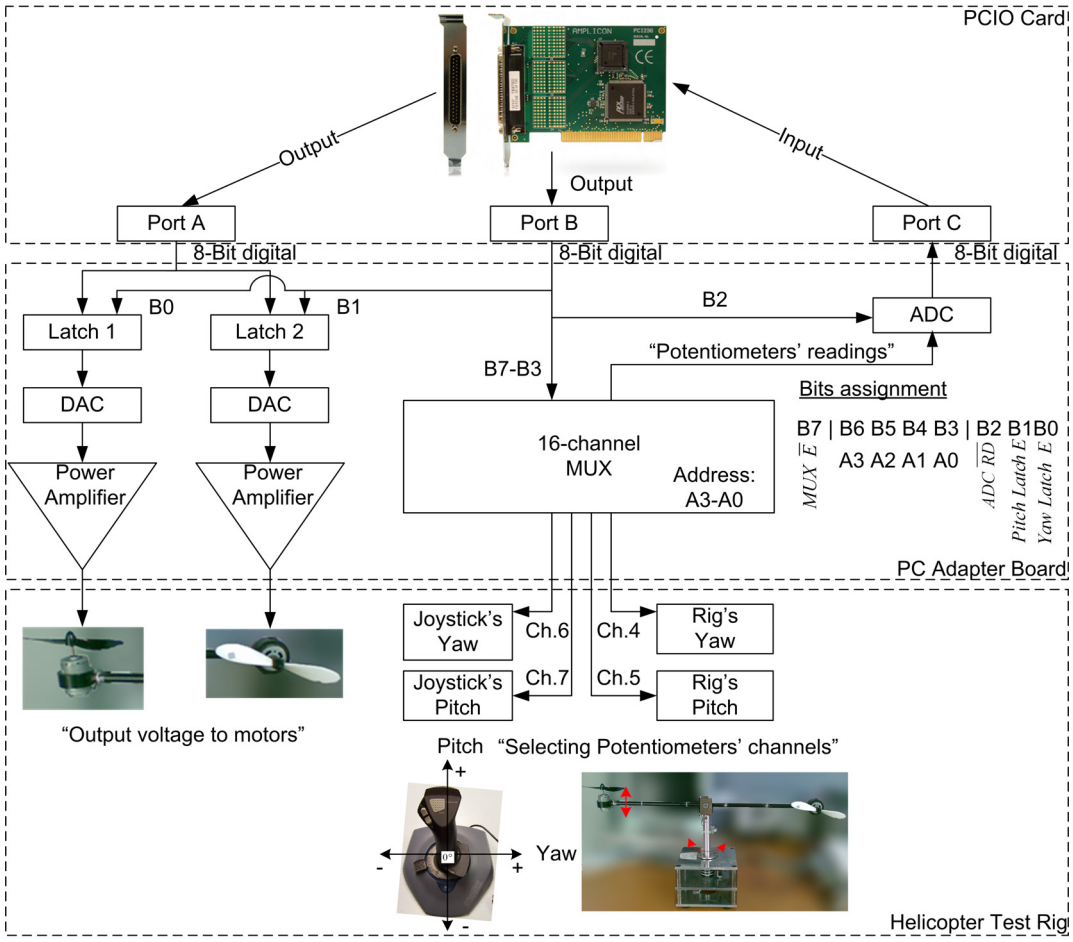

Figure A.2. Schematic diagram of PCIO card, PC adapter board and helicopter test rig (Note: B7=MSB, B0=LSB)

3. Position sensors/Potentiometers (Vishay Spectrol 157)

Two servo mount potentiometers with maximum resistance of 5kΩ and 10kΩ are installed to measure pitch and yaw angles respectively at the positions as shown in Figure A.3.

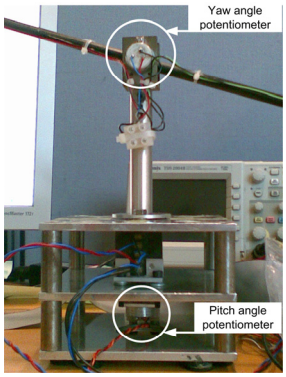

a) Pitch and yaw angle potentiometers

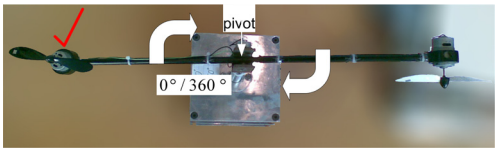

b) Yaw angle orientation

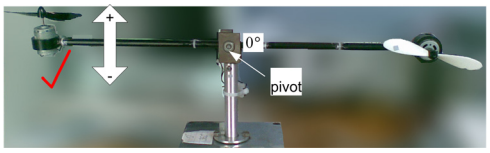

c) Pitch angle orientation

Figure A.3. Potentiometers and angles orientation [Note: The red ticks represent a reference position for measuring angles]

The following sets of figures consist of yaw and pitch angles measured against potentiometer's voltage and quantized voltage levels for yaw and pitch potentiometers in Figure A.4(a) and (b) respectively (0.03s sampling time).

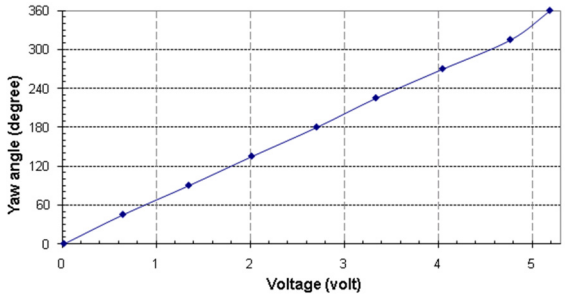

a) Yaw angle Vs potentiometer's voltage

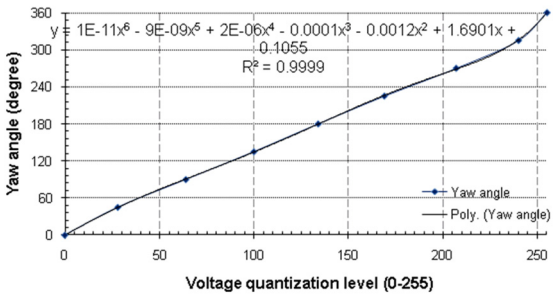

b) Yaw angle Vs potentiometer's voltage quantization level

Figure A.4. Yaw potentiometer characteristics

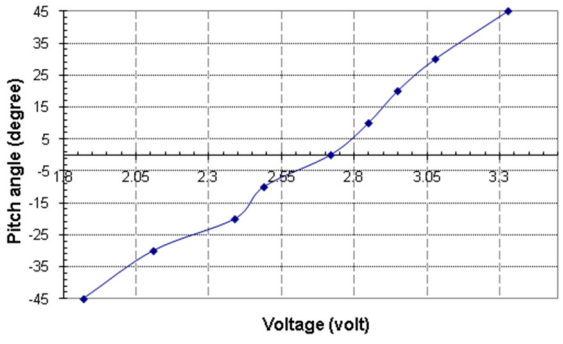

a) Pitch angle Vs potentiometer's voltage

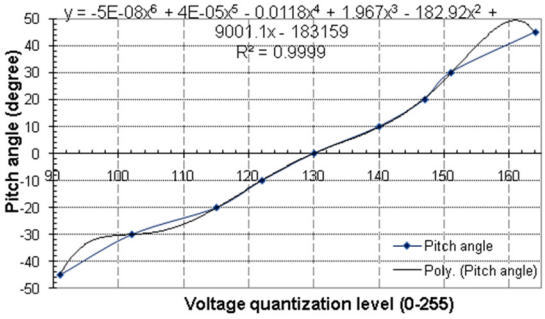

b) Pitch angle Vs potentiometer's voltage quantization level

Figure A.5. Pitch potentiometer characteristics

It is worth noting that, due to hardware limitations, potentiometers have to be programmed to read only one multiplexer channel at a time to avoid failure. As a result, 4 sampling interval is required to retrieve 4 readings for all channels (according to Figure A.2).

4. Motors (Mabuchi Motor RS-385PH)

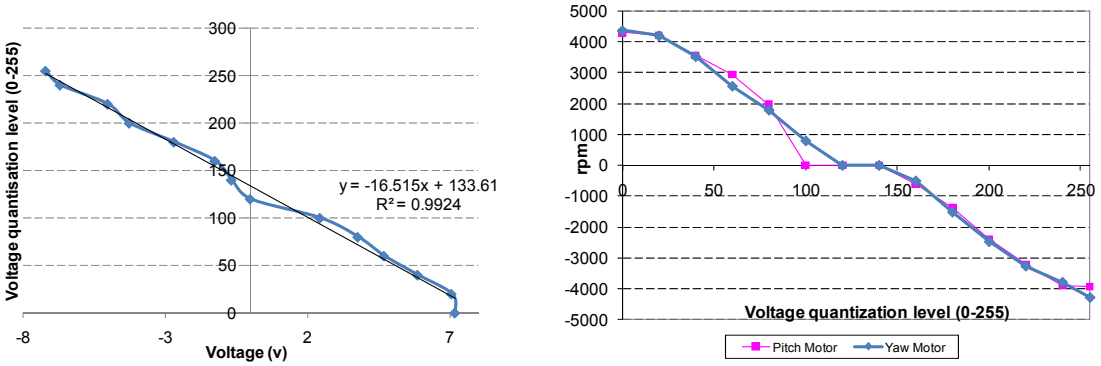

a) ADC outputs: voltage range of ±7.19V **b) Rotational speed for yaw and pitch motors**

Figure A.6. Motors characteristics: (+ for CCW/- for CW)

Almost identical characteristics for both yaw and pitch motors leads to a reasonable claim that the same thrust magnitude can be assumed from these two propellers.

5. Joystick (Logitech Wingman DA15 game controller)

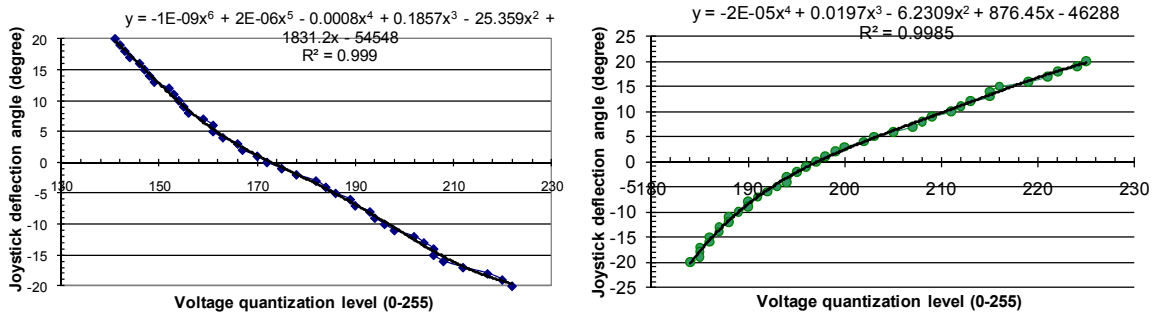

a) Yaw **b) Pitch**

Figure A.7. Joystick characteristics: Deflection angle (±20°) Vs Voltage quantization level

6. Other parameters

Mass of each motor clip = 75 g, each motor = 40 g, a metal beam = 0.3 kg

Effective mass of a motor and propeller (yaw/horizontal) = 41.66 g

Effective mass of a motor and propeller (pitch/vertical) = 42.57 g*
(Different values due to a motor's alignment, measured in equilibrium)
Minimum force to balance the metal beam = 0.008 N

Appendix B: Step responses of a helicopter test rig

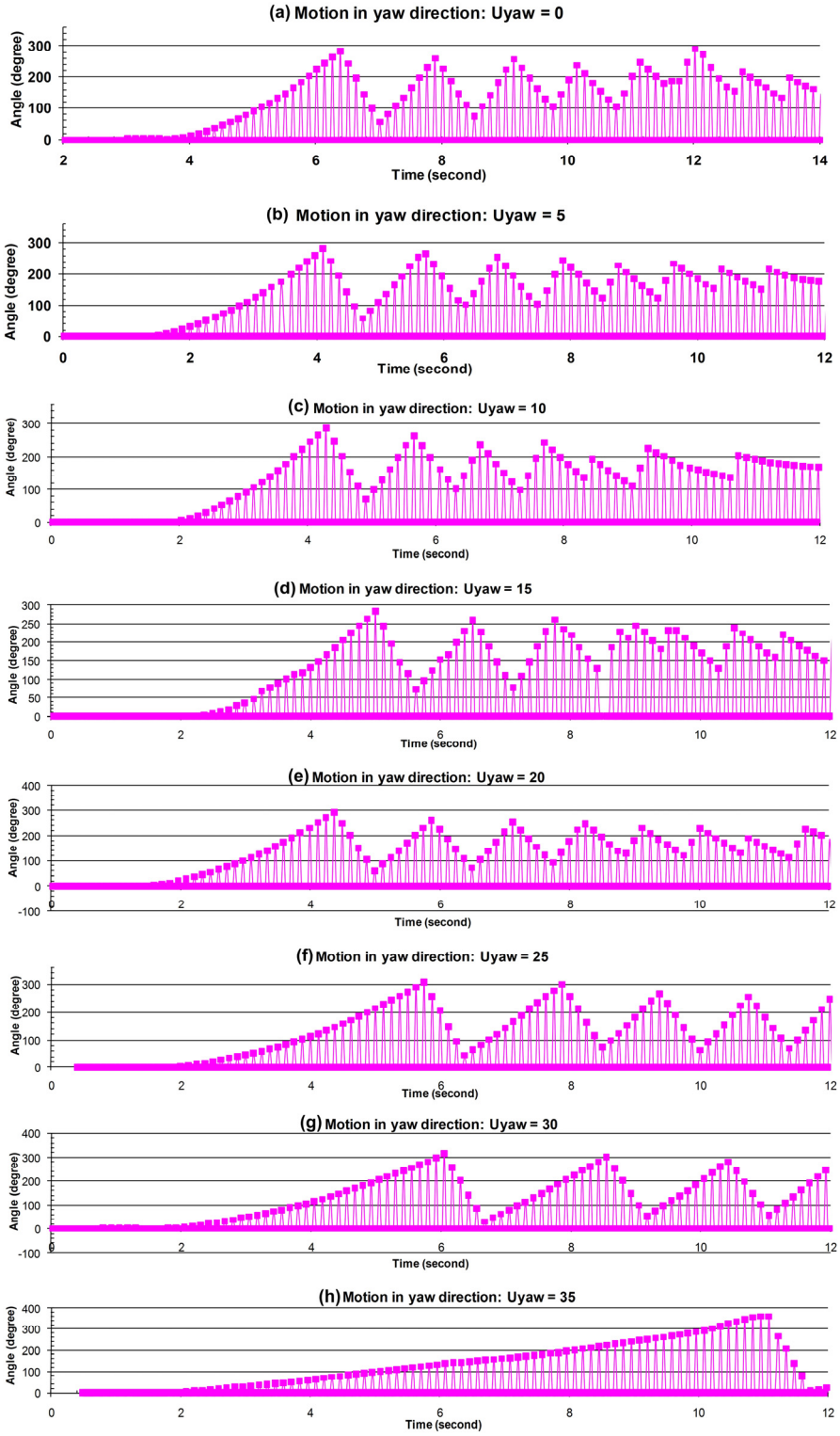

A yaw step response for a clockwise rotation starting from fastest to slowest (Uyaw<127)

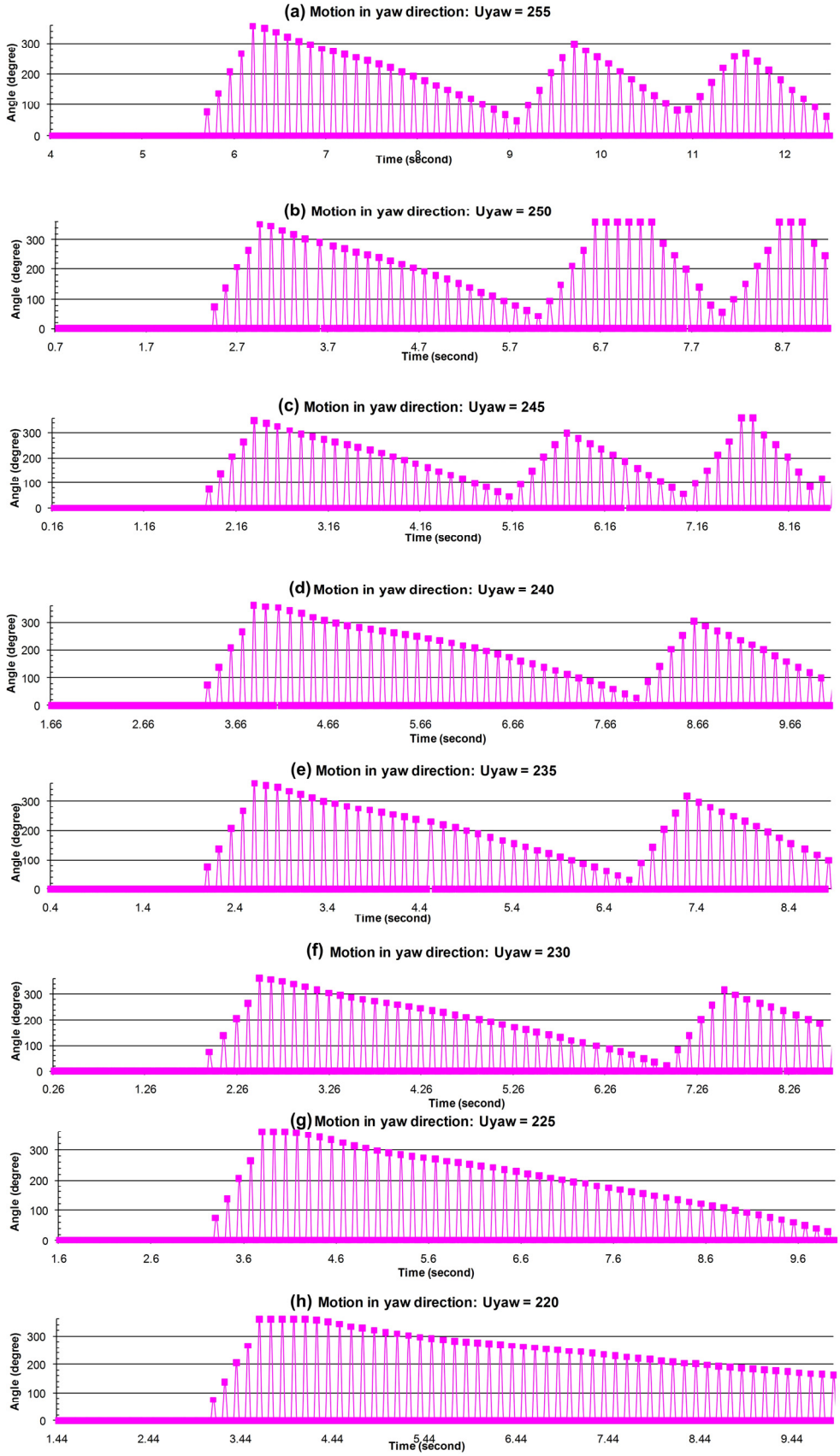

A yaw step response for a counter-clockwise motion starting from fastest to slowest (Uyaw>127)

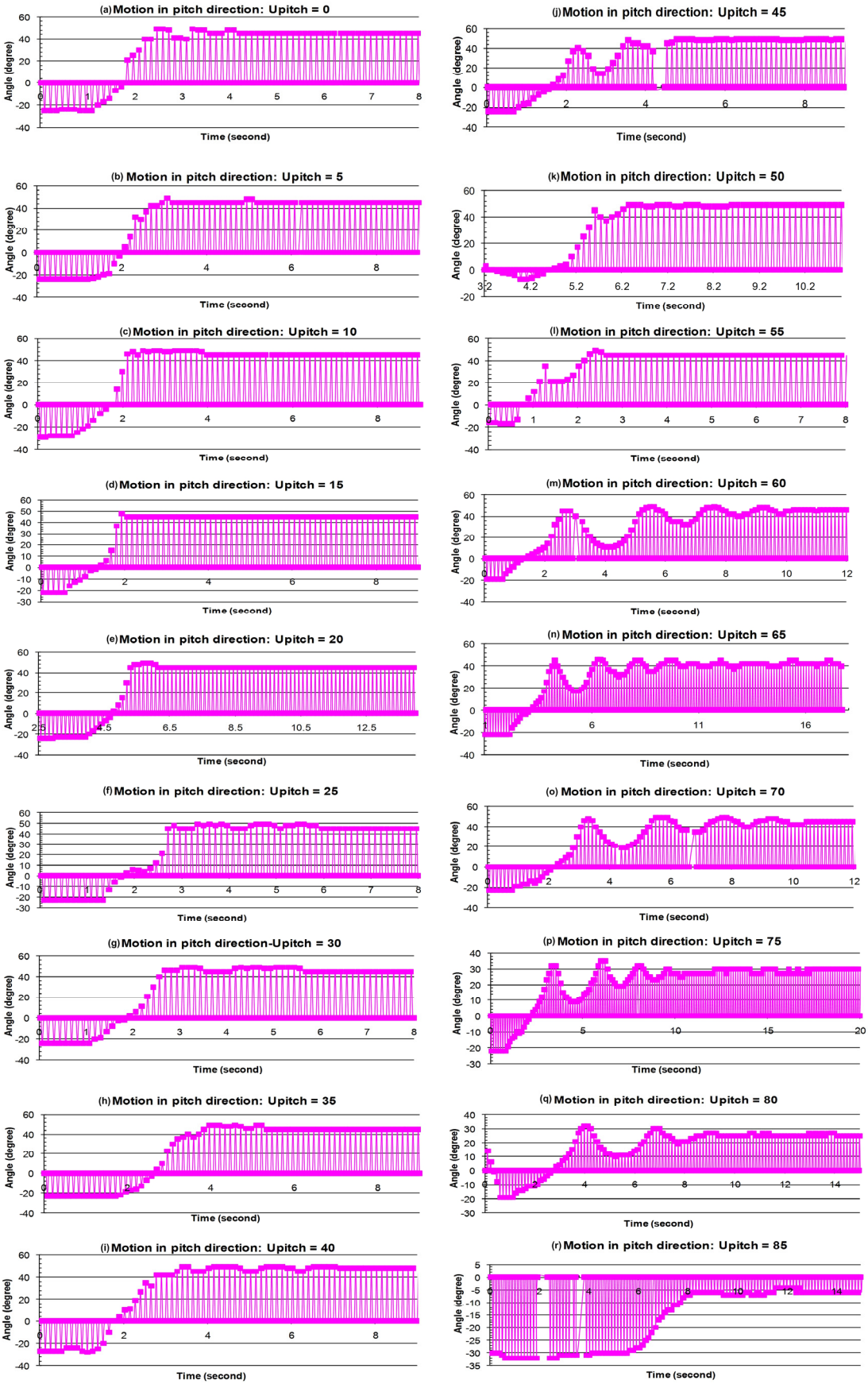

A pitch step response in an upward direction ($0<U_{pitch}<85$) [Note: a step response in a downward direction is not included as it is free-falling]

Appendix C: Additional results

C.1. Sample of Logged data from a hardware-based experiment

This section is a compilation of segment 1 data from all human subjects based on both linear and squared joystick transfer functions and target sequences 1 and 2 for Trial 1. **The order of these time-series graphs (a), (b), (c) and (d) is Pitch angle, Pitch motor voltage, Yaw angle and Yaw angle voltage respectively.** The order is consistent for every set of graphs presented under this section. The observation that the effort on controlling a helicopter test rig in the pitch direction being minimal is also true for sequences 3 and all sequences in Trial 2.

C.1.1 Linear transfer function

- **Sequence 1** (only larger versions for Subject B to F as Subject A has already been presented in details in Chapter 7.)

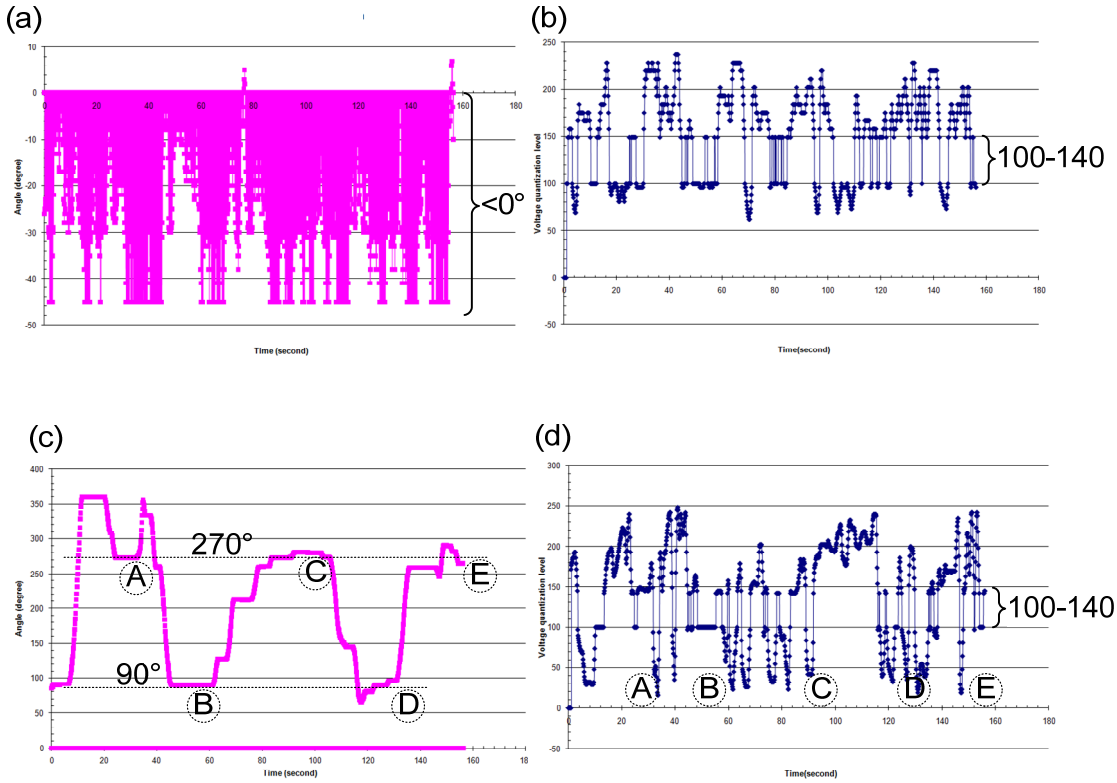

Figure C.1. Subject B: Linear, sequence 1

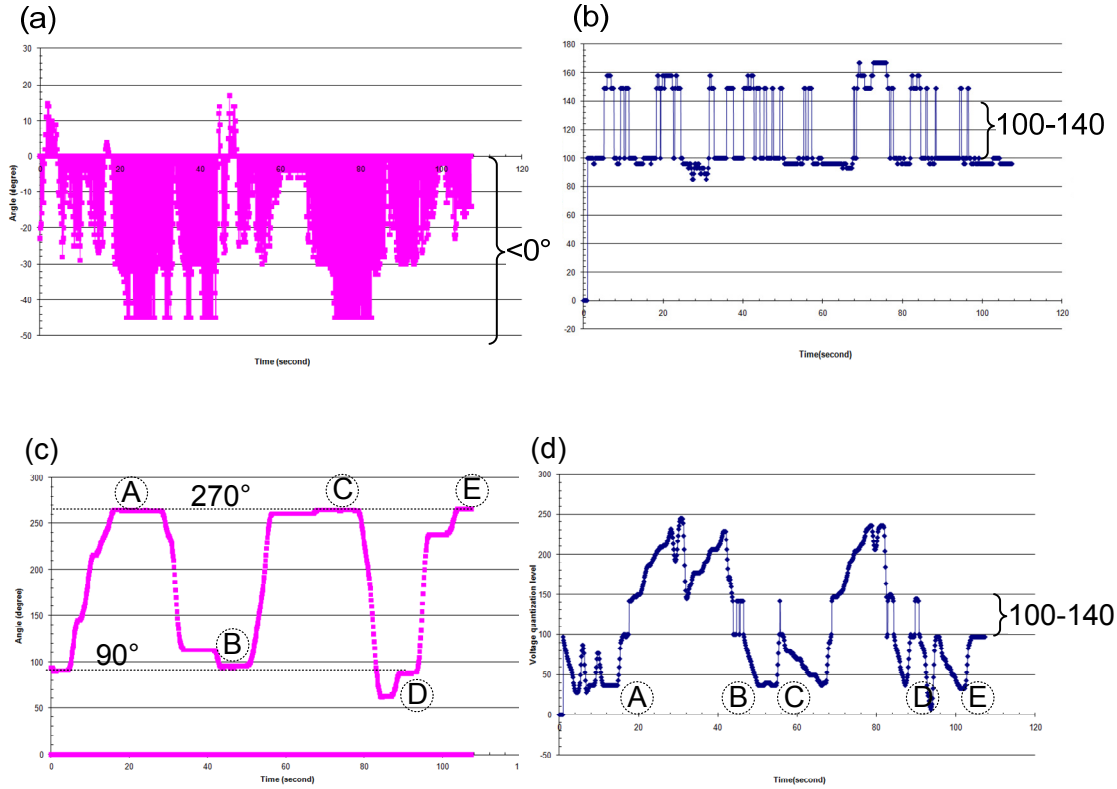

Figure C.2. Subject C: Linear, sequence 1

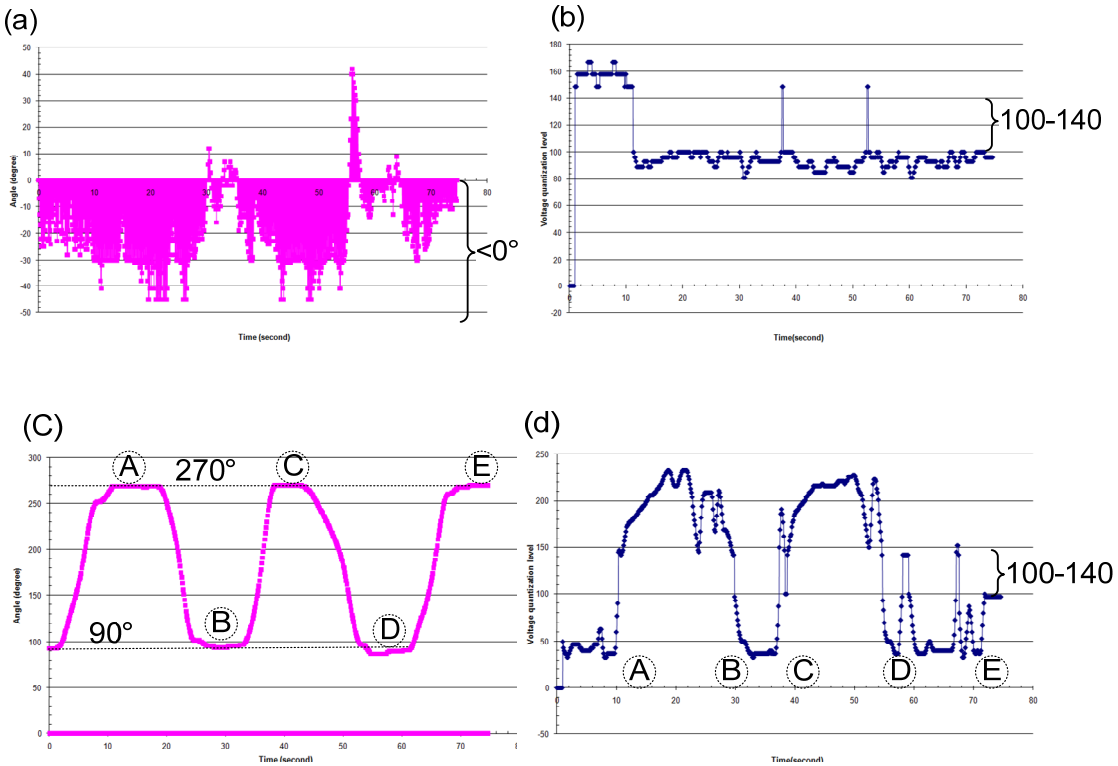

Figure C.3. Subject D: Linear, sequence 1

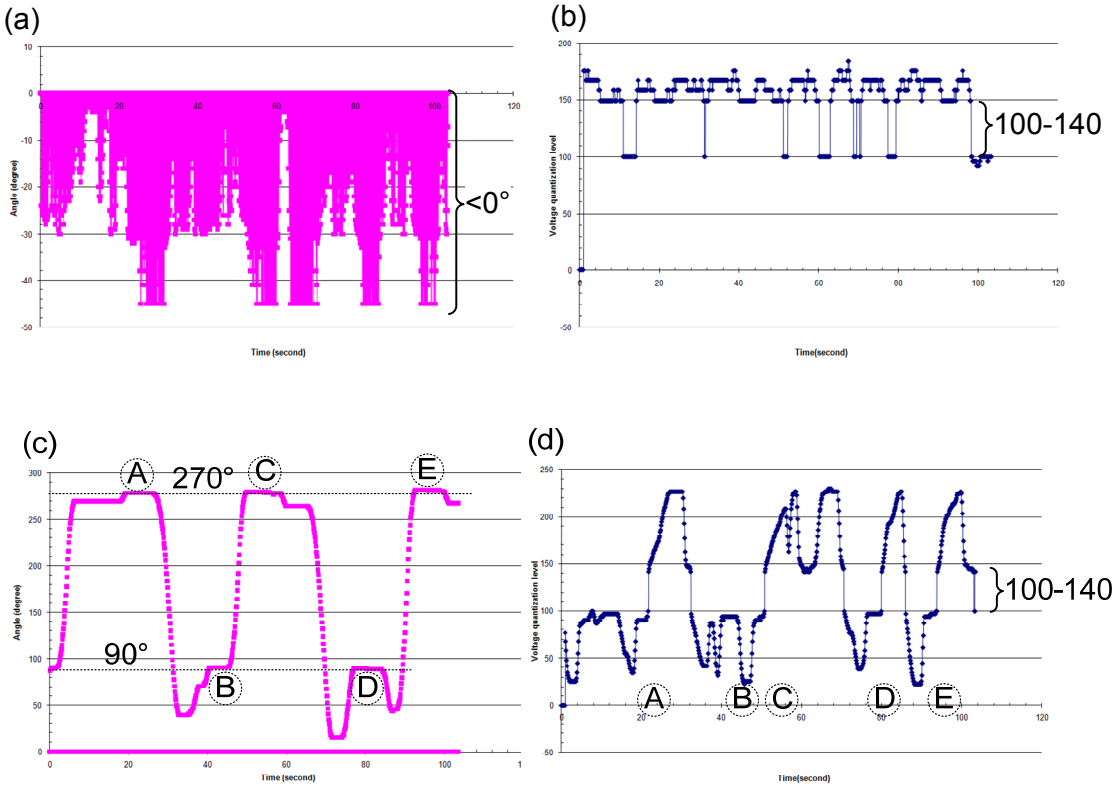

Figure C.4. Subject E: Linear, sequence 1

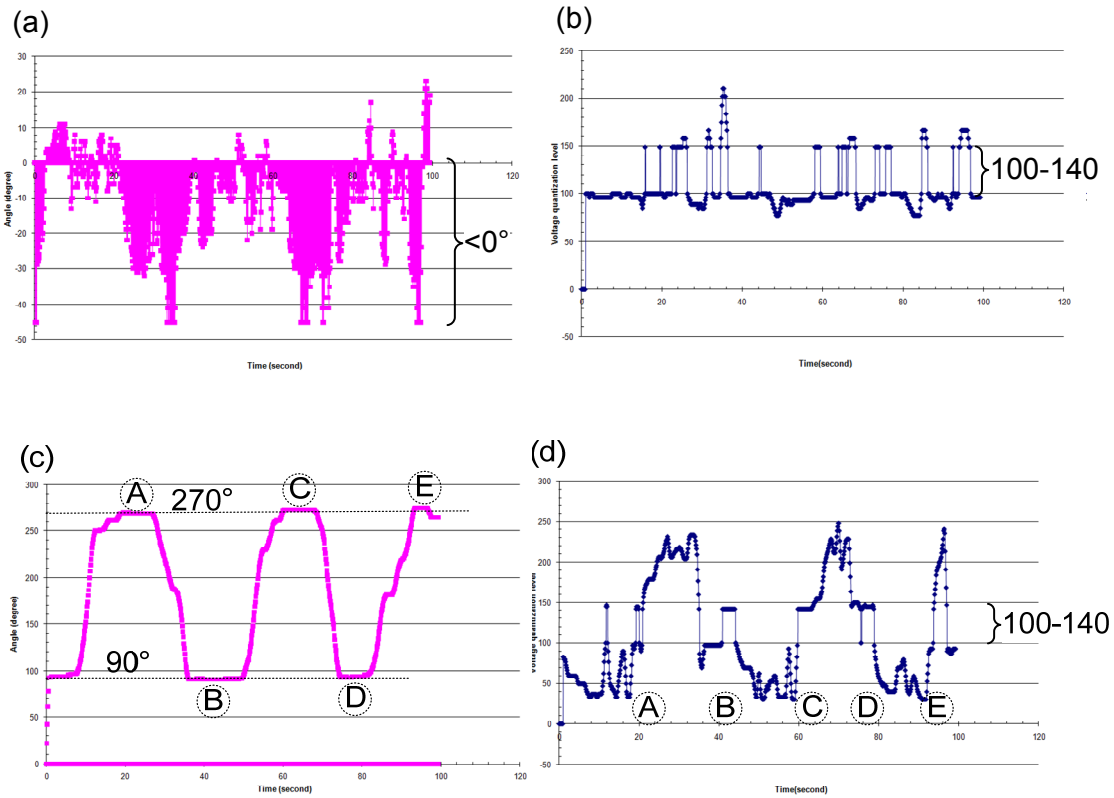

Figure C.5. Subject F: Linear, sequence 1

- **Sequence 2**

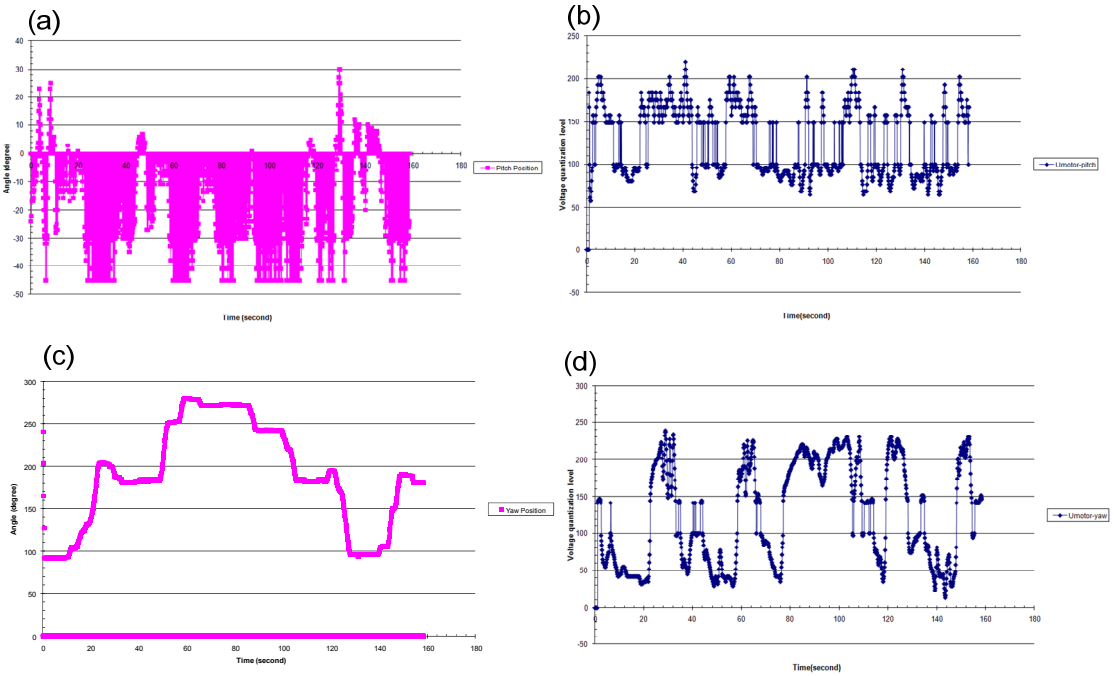

Figure C.6. Subject A: Linear, sequence 2

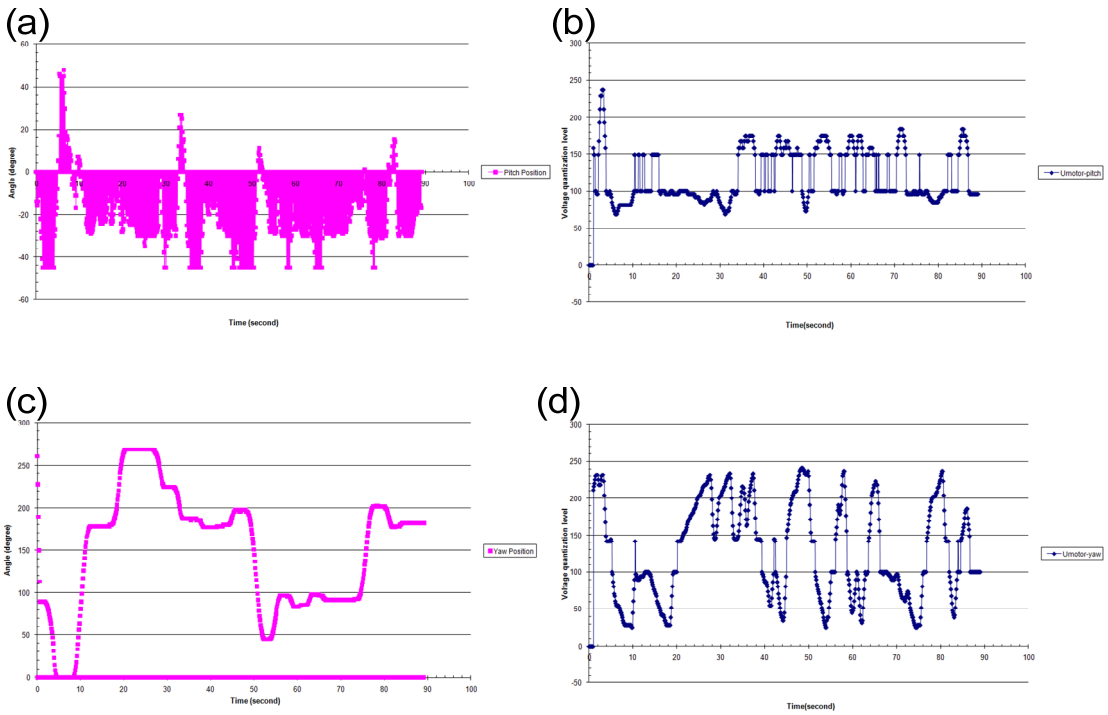

Figure C.7. Subject B: Linear, sequence 2

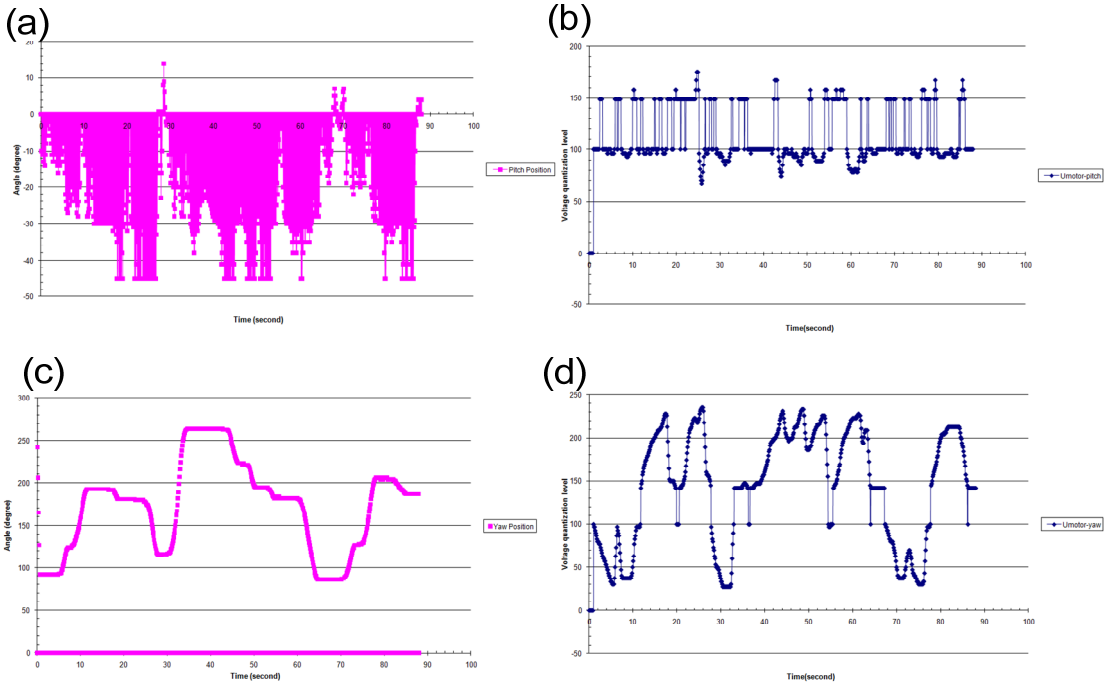

Figure C.8. Subject C: Linear, sequence 2

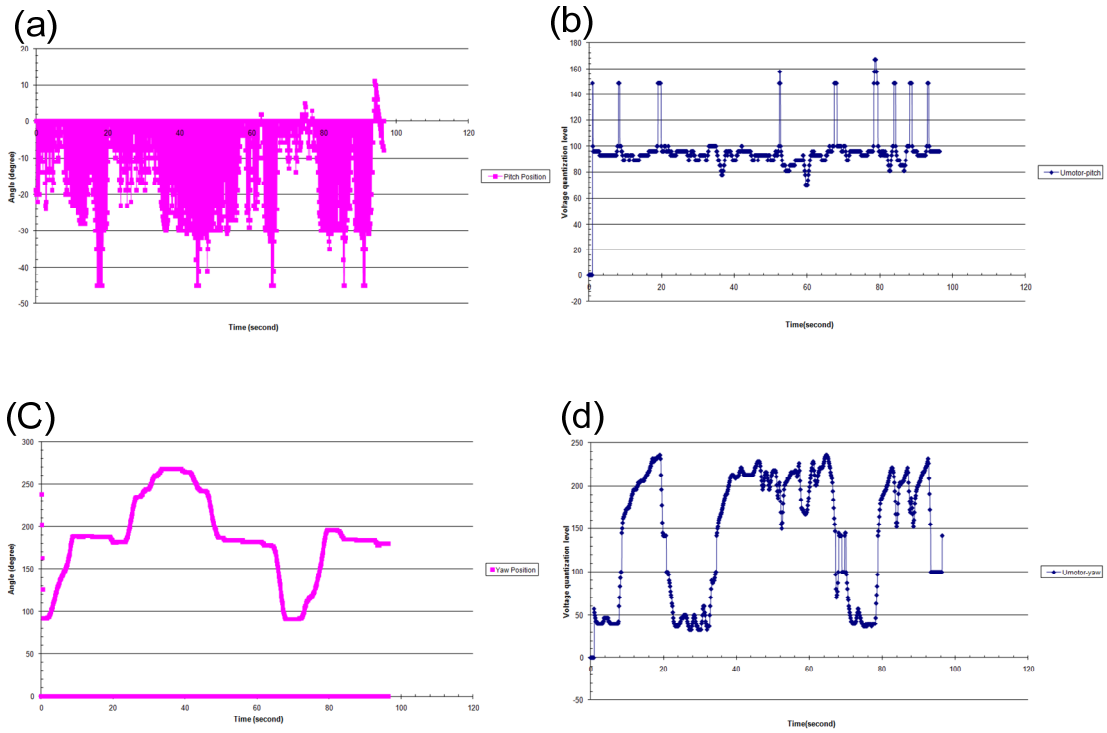

Figure C.9. Subject D: Linear, sequence 2

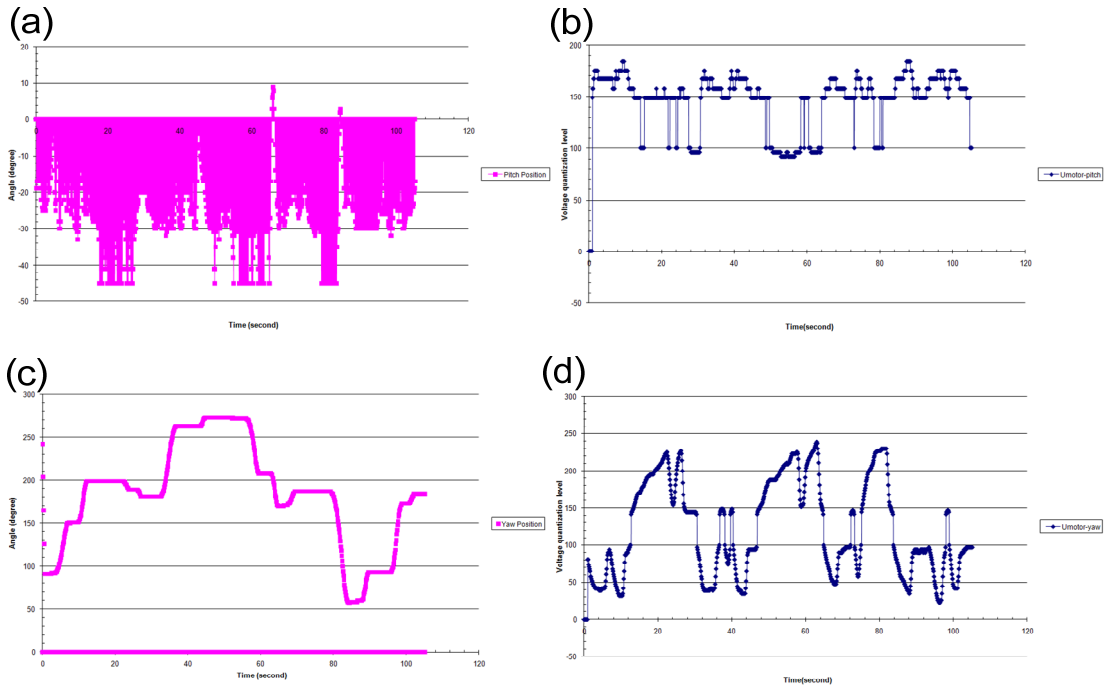

Figure C.10. Subject E: Linear, sequence 2

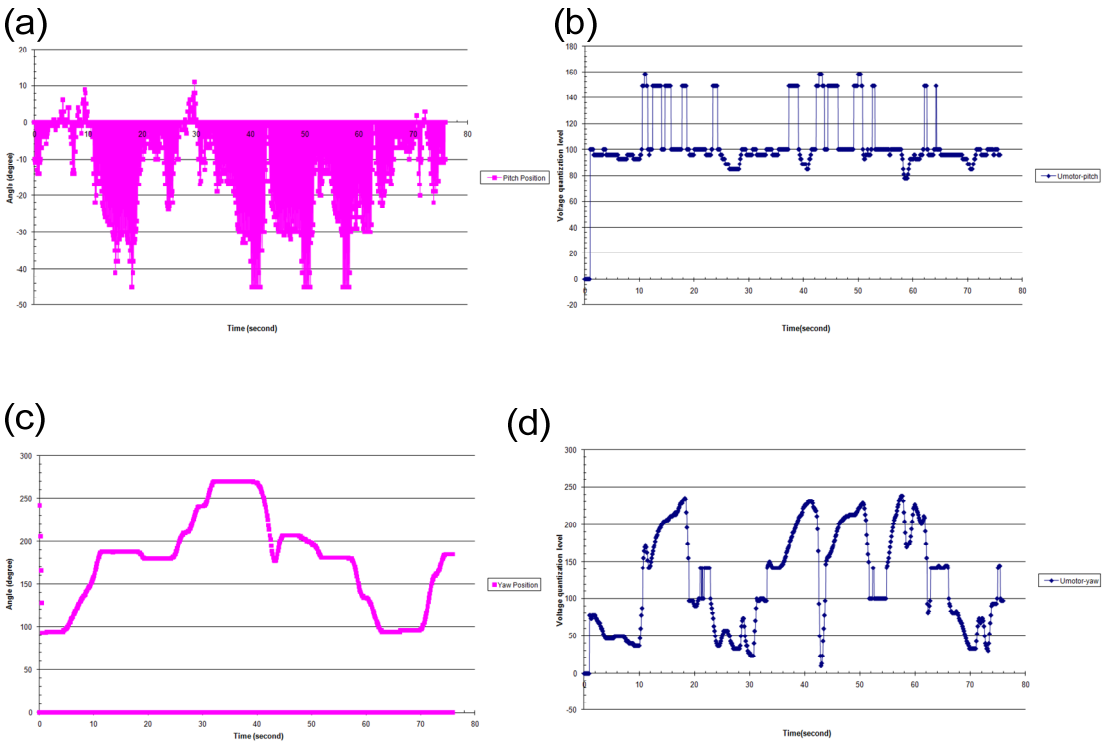

Figure C.11. Subject F: Linear, sequence 2

C.1.2 Squared transfer function

- Sequence 1

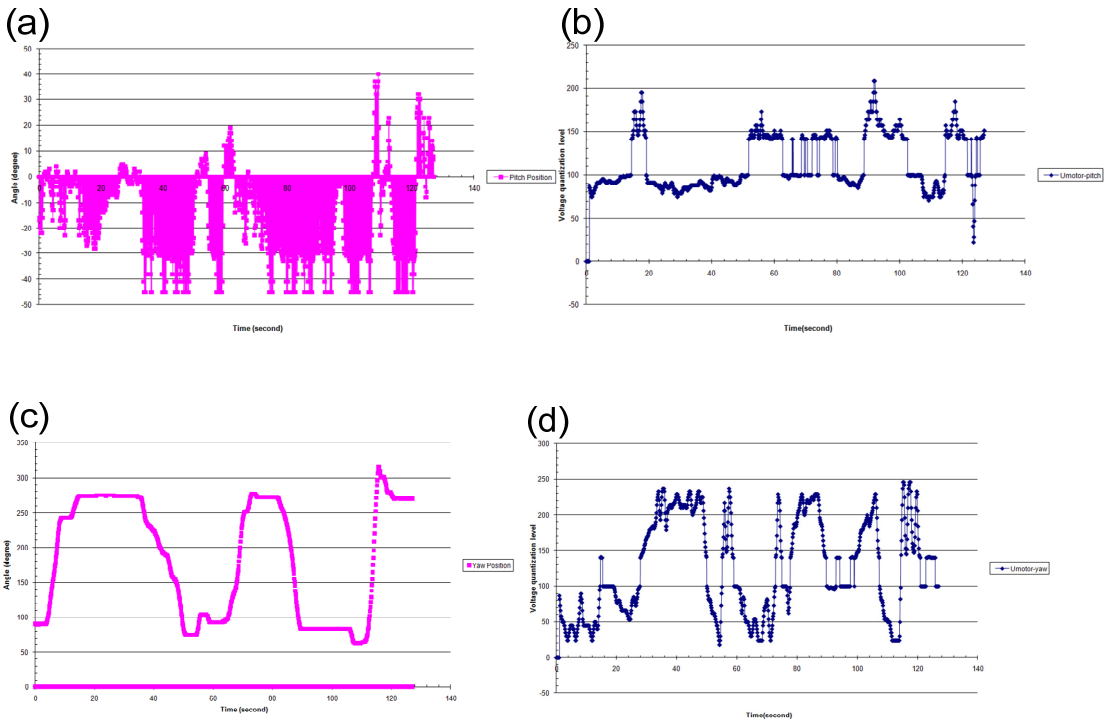

Figure C.12. Subject A: Squared, sequence 1

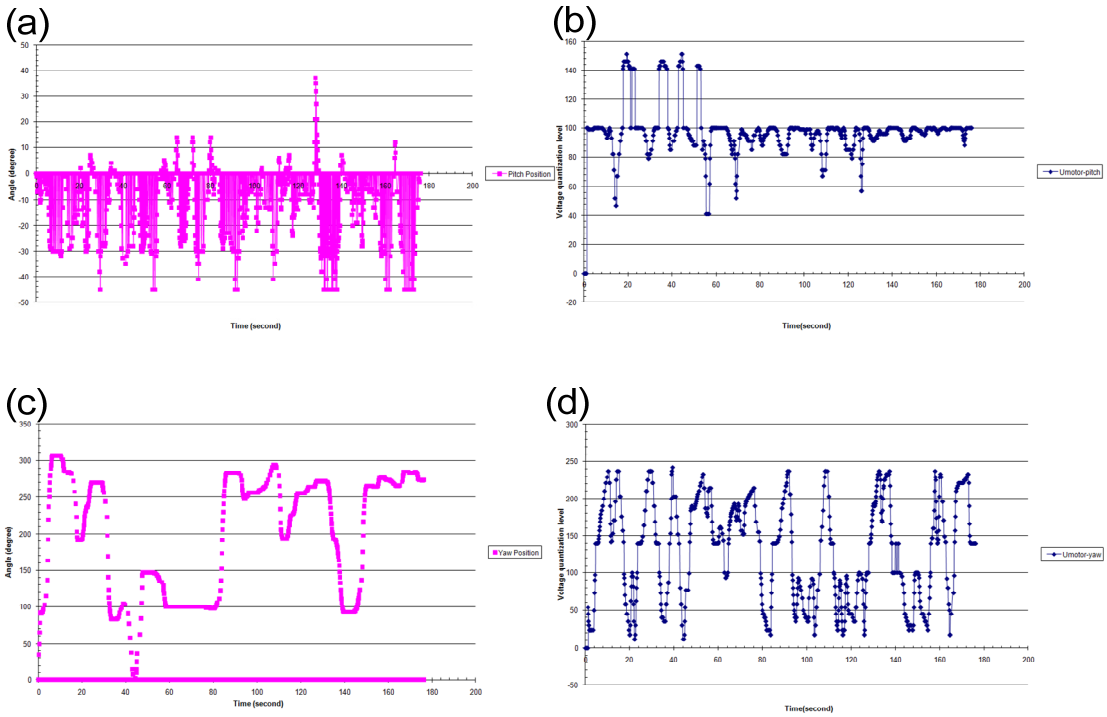

Figure C.13. Subject B: Squared, sequence 1

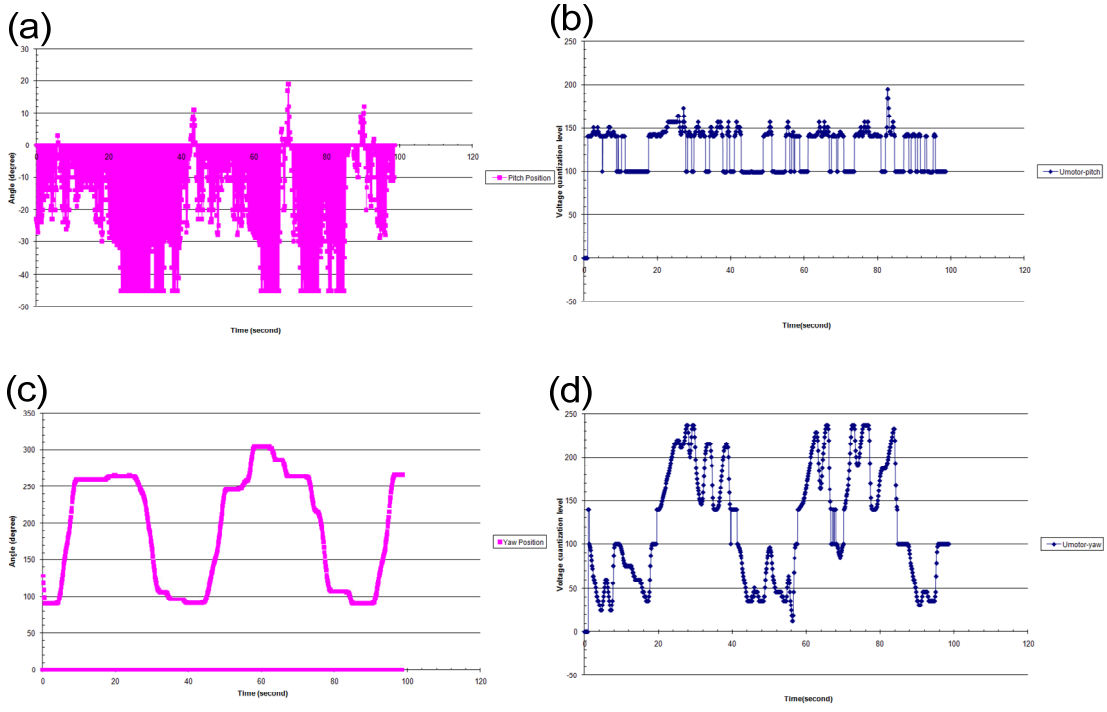

Figure C.14. Subject C: Squared, sequence 1

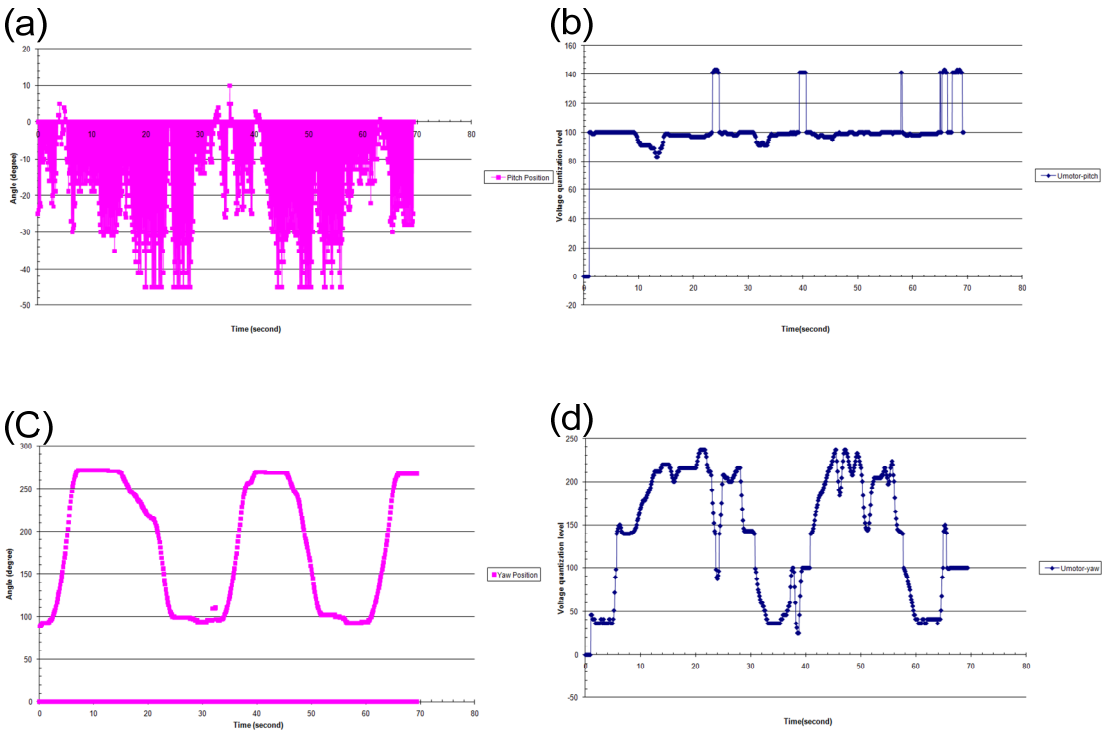

Figure C.15. Subject D: Squared, sequence 1

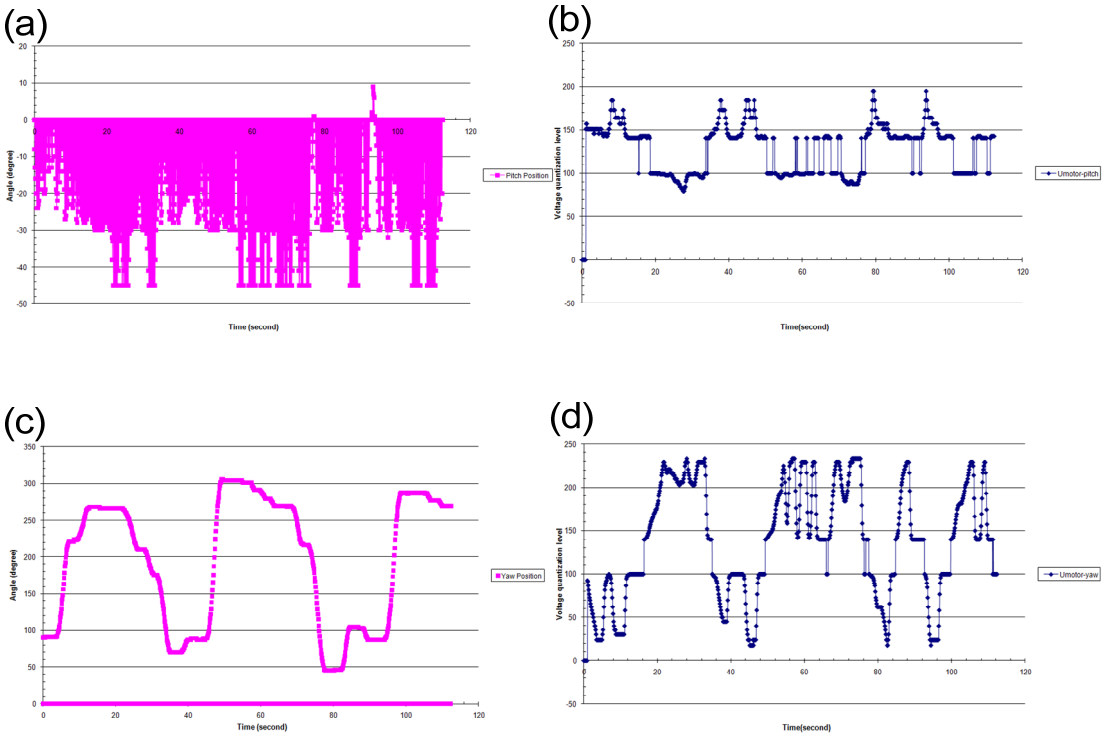

Figure C.16. Subject E: Squared, sequence 1

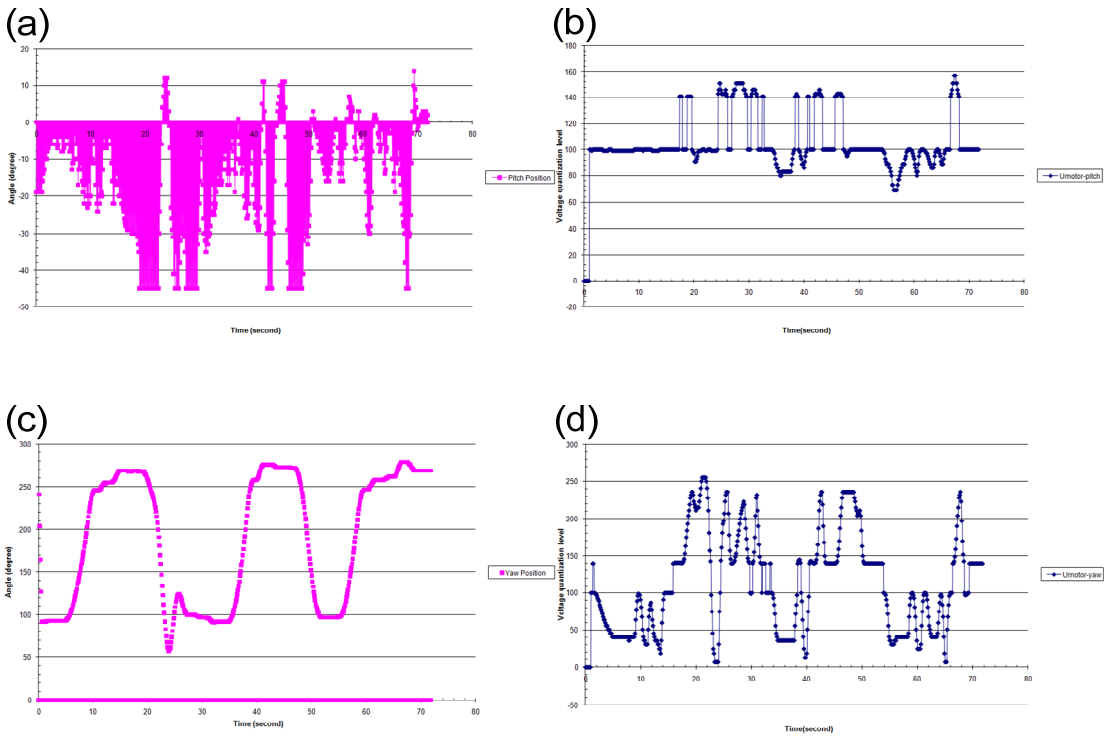

Figure C.17. Subject F: Squared, sequence 1

- Sequence 2

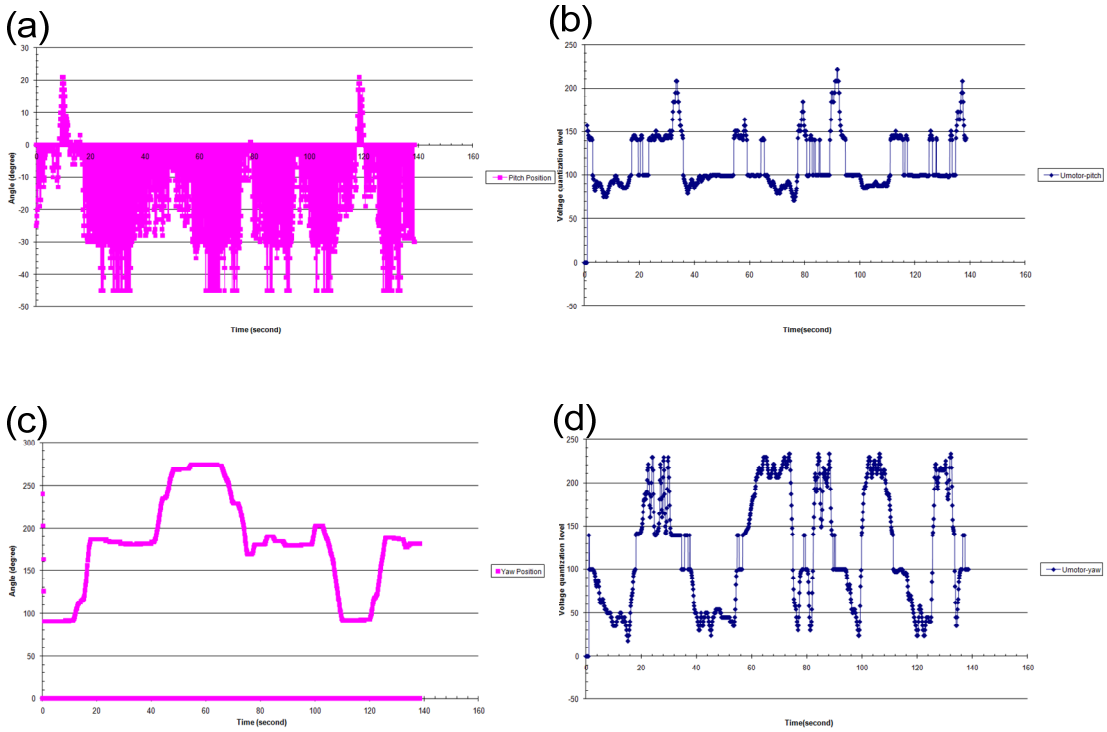

Figure C.18. Subject A: Squared, sequence 2

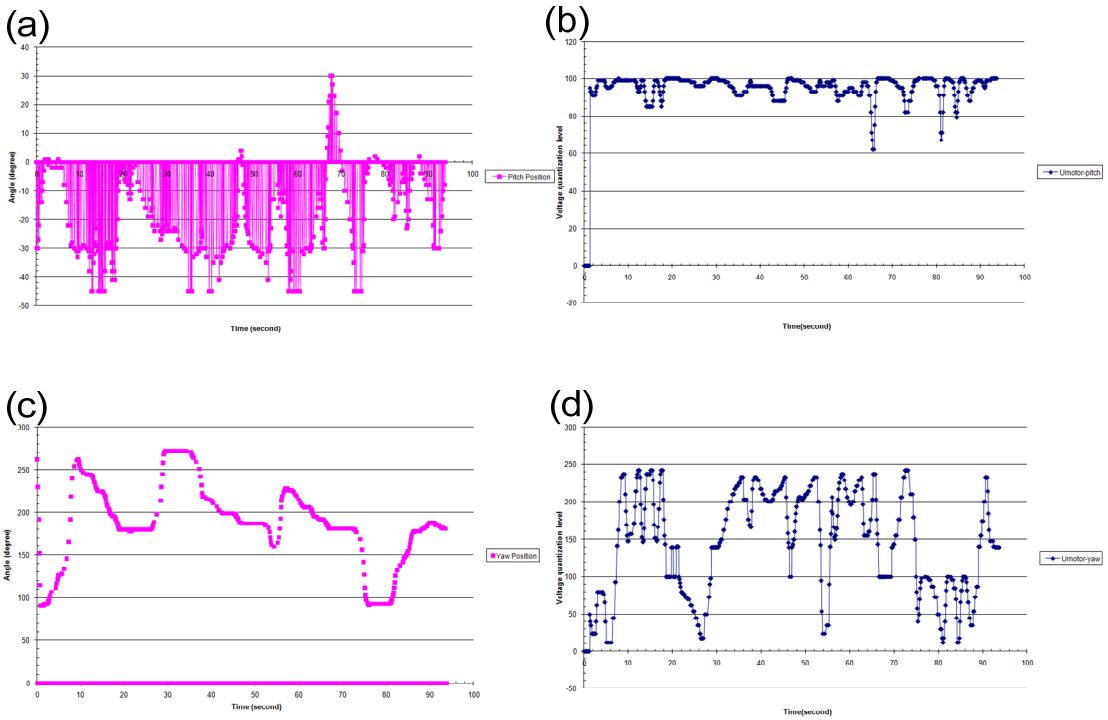

Figure C.19. Subject B: Squared, sequence 2

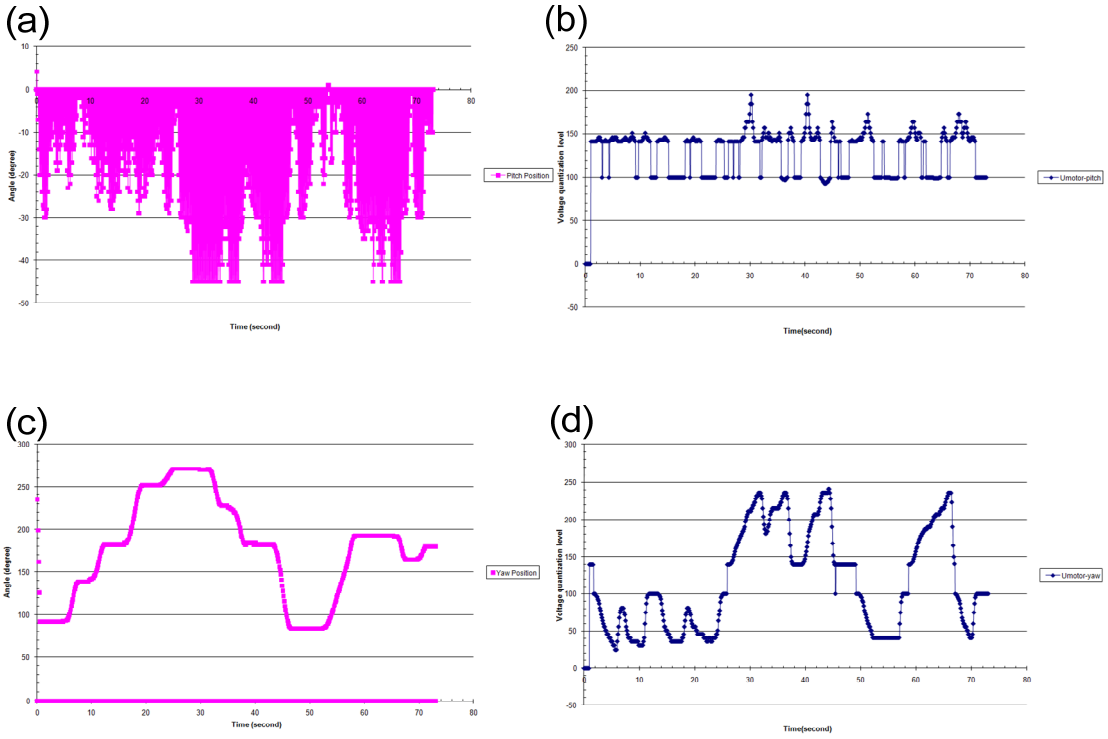

Figure C.20. Subject C: Squared, sequence 2

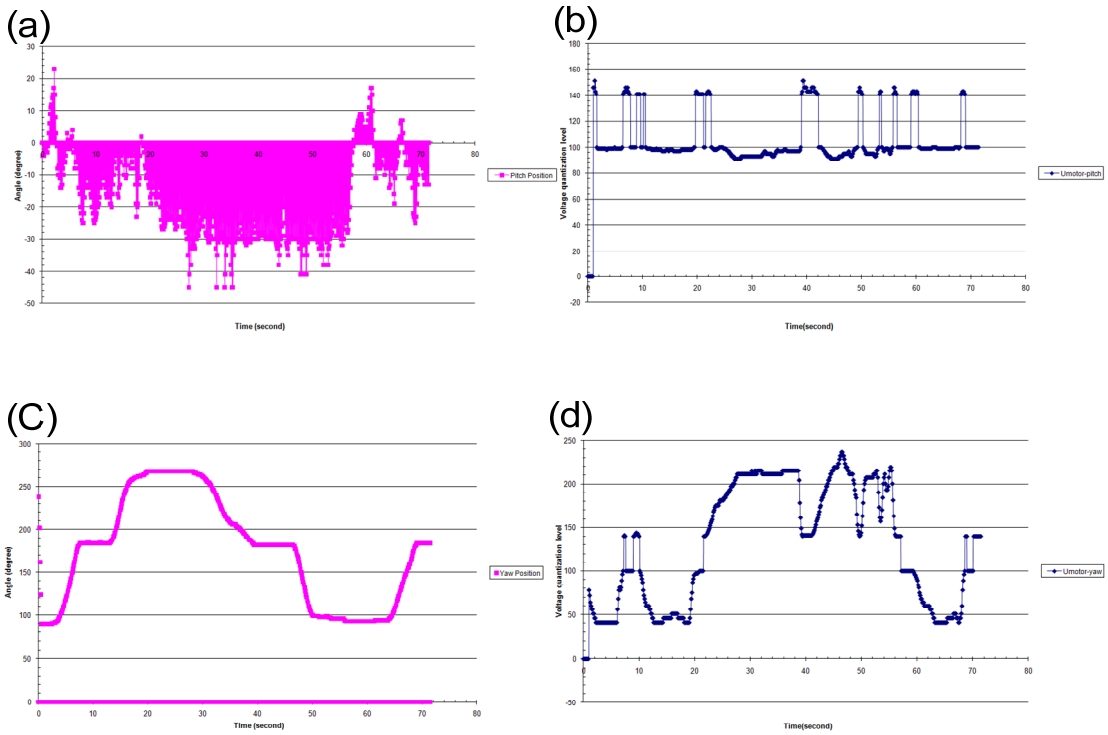

Figure C.21. Subject D: Squared, sequence 2

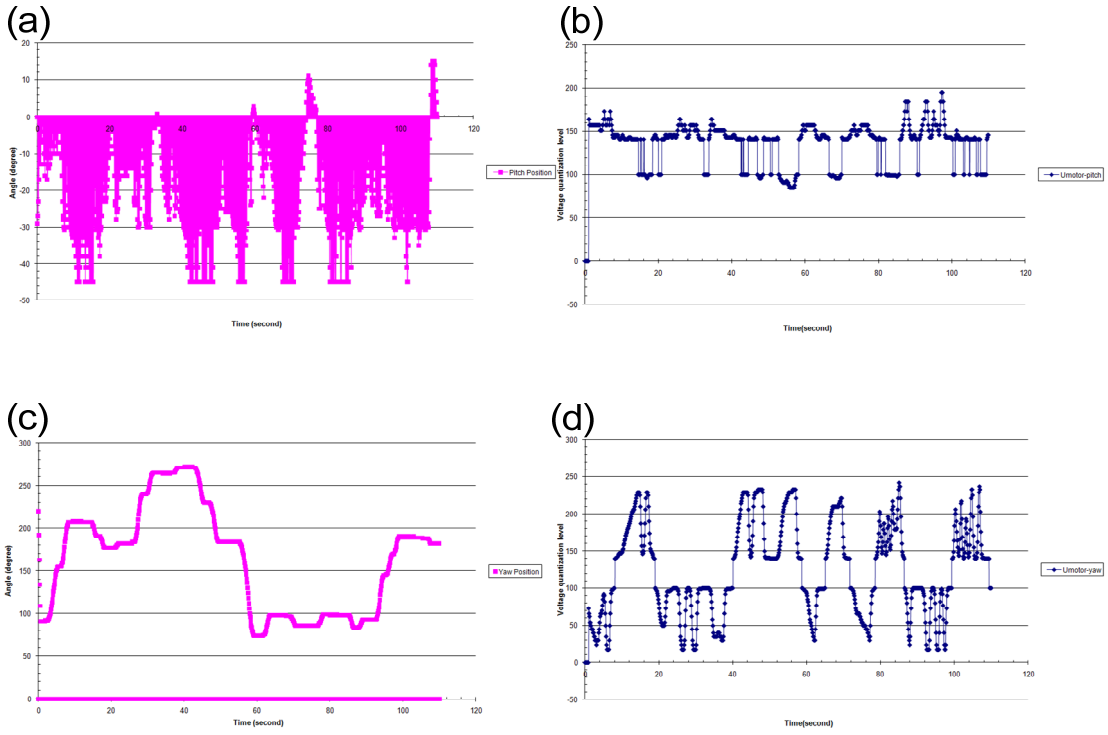

Figure C.22. Subject E: Squared, sequence 2

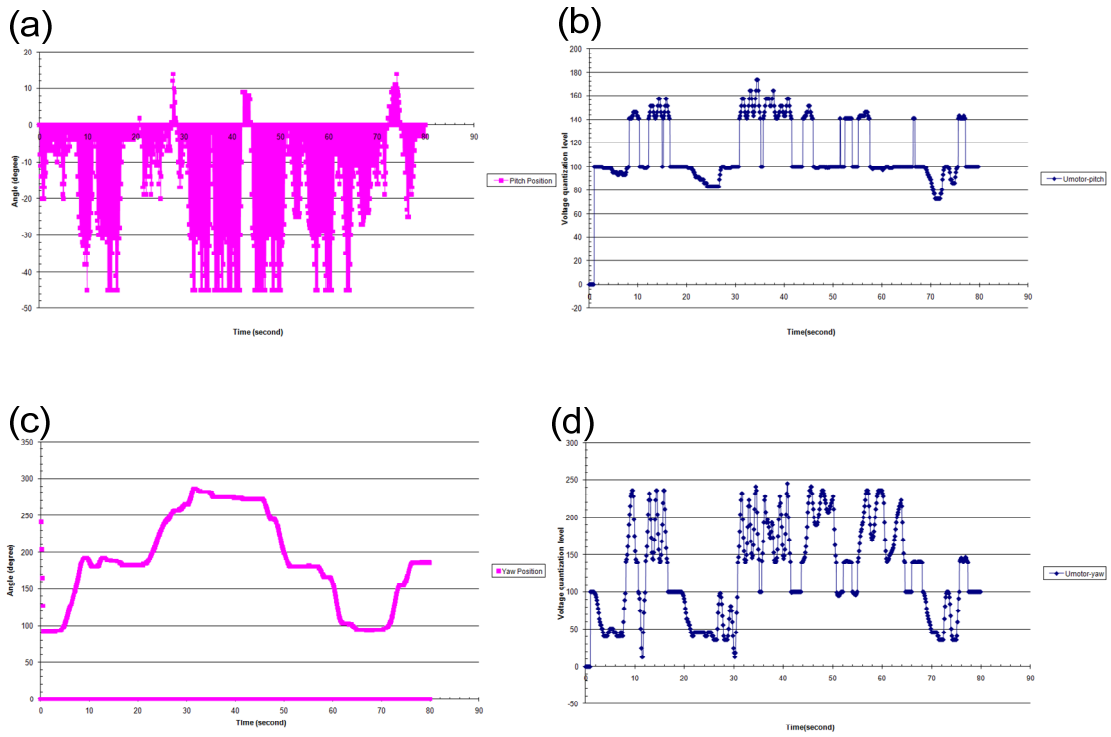

Figure C.23. Subject F: Squared, sequence 2

C.2. A complete set of ARX parameters from all settings in hardware-based experiments

			Average values without drops								Average values with drops							
			T1				T2				T1				T2			
		Subject	Tau(s)	TN	Kp	Kd	Tau(s)	TN	Kp	Kd	Tau(s)	TN	Kp	Kd	Tau(s)	TN	Kp	Kd
Linear	Seq1	A	10.4	10.9566	0.08804	-2.1952	4.8	0.02	-0.0015	-3E-05	10.4	10.9566	0.14759	0.46898	4.8	0.02	N/A	N/A
		B	10.08	0.02438	0.02636	0.00068	8.2	0.02	0.0013	2.6E-05	10.08	0.02438	0.02636	0.00068	8.2	0.02	0.0013	2.6E-05
		C	7.32	0.02011	0.0533	0.00107	9.432	0.02007	-0.0283	-0.0006	7.32	0.02011	0.0533	0.00107	9.432	0.02007	0.00825	0.00016
		D	3.48	0.02	-0.0043	-9E-05	11.8	0.02	-0.0043	-9E-05	3.48	0.02	N/A	N/A	11.8	0.02	N/A	N/A
		E	10.56	0.02	-0.0015	-3E-05	5.44	0.02	-0.0029	-6E-05	10.56	0.02	N/A	N/A	5.44	0.02	N/A	N/A
		F	5.384	0.02001	-0.0094	-0.0002	9.712	0.03706	-0.0016	0.00015	5.384	0.02001	0.0013	2.6E-05	9.712	0.03706	N/A	0.0002
	Seq2	A	11.736	9.34999	0.06081	-0.1246	4.8	0.02	-0.0015	-3E-05	11.736	9.34999	0.55895	0.73539	4.8	0.02	N/A	N/A
		B	6.912	0.02	-0.0033	-7E-05	9.784	0.02	-0.0022	-4E-05	6.912	0.02	N/A	N/A	9.784	0.02	0.0013	2.6E-05
		C	7.688	0.02	-0.0061	-0.0001	10.8	0.02001	-0.0172	-0.0003	7.688	0.02	N/A	N/A	10.8	0.02001	N/A	N/A
		D	4.664	0.02	-0.0078	-0.0002	9.144	1.95882	-0.0255	0.02655	4.664	0.02	N/A	N/A	9.144	1.95882	N/A	0.04442
		E	10.36	0.02	-0.0004	-8E-06	10	0.02	-0.0001	-3E-06	10.36	0.02	0.00412	8.2E-05	10	0.02	N/A	N/A
		F	7.232	0.02198	-0.0117	-0.0002	7.792	0.02	-0.0039	-8E-05	7.232	0.02198	N/A	N/A	7.792	0.02	N/A	N/A
	Seq3	A	11.096	11.4102	-0.3417	0.37473	5.48	0.02	-0.001	-2E-05	11.096	11.4102	0.03681	0.37473	5.48	0.02	0.0013	2.6E-05
		B	5.592	0.02	-0.004	-8E-05	5.424	0.31918	-0.0498	-0.0089	5.592	0.02	N/A	N/A	5.424	0.31918	N/A	N/A
		C	5.32	0.02403	-0.0075	-0.0002	7.592	1.26839	-0.0084	0.00693	5.32	0.02403	N/A	N/A	7.592	1.26839	0.04786	0.01751
		D	9.44	1.12018	-0.109	0.05176	5.192	0.02	-0.0041	-8E-05	9.44	1.12018	N/A	0.05176	5.192	0.02	N/A	N/A
		E	8.6	0.02	-0.0089	-0.0002	4.536	0.02	0.00198	4.6E-05	8.6	0.02	N/A	N/A	4.536	0.02	0.0034	5.8E-05
		F	10.44	0.02	-0.0046	-9E-05	5.408	0.02	-0.002	-4E-05	10.44	0.02	N/A	N/A	5.408	0.02	0.0055	0.00011
Squared	Seq1	A	11.536	5.08629	0.03562	-1.0144	4.8	0.02	-0.0015	-3E-05	11.536	5.08629	0.15248	0.18498	4.8	0.02	N/A	N/A
		B	10.016	0.02263	0.01396	0.00037	8.2	0.02	0.0013	2.6E-05	10.016	0.02263	0.02636	0.00068	8.2	0.02	0.0013	2.6E-05
		C	7.496	0.02009	0.04233	0.00085	10.6	0.02001	-0.0155	-0.0003	7.496	0.02009	0.0533	0.00107	10.6	0.02001	N/A	N/A
		D	3.48	0.02	-0.0043	-9E-05	11.8	0.02	-0.0043	-9E-05	3.48	0.02	N/A	N/A	11.8	0.02	N/A	N/A
		E	10.56	0.02	-0.0015	-3E-05	8.256	0.02	-0.0001	-3E-06	10.56	0.02	N/A	N/A	8.256	0.02	N/A	N/A
		F	7.728	0.02002	-0.0205	-0.0004	5.36	0.02	-0.0015	-3E-05	7.728	0.02002	N/A	N/A	5.36	0.02	N/A	N/A
	Seq2	A	11.8	41.1626	0.07136	-0.7901	4.8	0.02	-0.0015	-3E-05	11.8	41.1626	0.14746	0.47401	4.8	0.02	N/A	N/A
		B	5.952	0.25221	-0.0269	0.03369	7.384	0.02	-0.0032	-6E-05	5.952	0.25221	N/A	0.08434	7.384	0.02	N/A	N/A
		C	7.672	0.02	-0.0084	-0.0002	9.552	0.02001	-0.0122	-0.0002	7.672	0.02	N/A	N/A	9.552	0.02001	N/A	N/A
		D	9.112	0.02	0.00119	2.4E-05	7.32	0.02001	-0.013	-0.0003	9.112	0.02	0.00423	8.5E-05	7.32	0.02001	N/A	N/A
		E	9.344	0.02	-0.0048	-1E-04	5.264	2.97491	0.04822	-0.045	9.344	0.02	0.00412	8.2E-05	5.264	2.97491	0.12074	8.2E-05
		F	10.296	0.02591	-0.0058	-0.0001	9.28	0.02	-0.0002	-4E-06	10.296	0.02591	N/A	N/A	9.28	0.02	N/A	N/A
	Seq3	A	10.08	0.02438	0.02636	0.00068	8.2	0.02	0.0013	2.6E-05	10.08	0.02438	0.02636	0.00068	8.2	0.02	0.0013	2.6E-05
		B	5.664	0.02005	0.02021	0.00041	10.28	0.02	0.00825	0.00016	5.664	0.02005	0.0533	0.00107	10.28	0.02	0.00825	0.00016
		C	5.712	0.02	-0.0034	-7E-05	7.824	1.26632	-0.0174	0.00675	5.712	0.02	N/A	N/A	7.824	1.26632	N/A	0.03407
		D	9.064	1.23292	-0.0654	0.04161	8.736	0.02	-0.0018	-4E-05	9.064	1.23292	N/A	0.05203	8.736	0.02	N/A	N/A
		E	6.112	0.24639	-0.0061	-0.0121	5.024	0.06083	-0.0034	-0.0034	6.112	0.24639	0.02319	2.6E-05	5.024	0.06083	0.00194	3.4E-05
		F	6.136	0.06425	-0.0028	-0.002	8.04	0.0209	-0.0028	-5E-05	6.136	0.06425	N/A	N/A	8.04	0.0209	N/A	N/A
		Average	8.16844	2.26181	-0.0064	-0.101	7.66822	0.23518	-0.0047	-0.0005	8.16844	2.26181	N/A	N/A	7.66822	0.23518	N/A	N/A
		SD	2.39619	7.32244	0.06713	0.42315	2.23262	0.63306	0.01403	0.00911	2.39619	7.32244	N/A	N/A	2.23262	0.63306	N/A	N/A

C.3 Percentage of normal parameters for a hardware-based experiment.

			T1				T2			
		Subject	Tau(s)	TN	Kp	Kd	Tau(s)	TN	Kp	Kd
Linear	Seq1	A	100%	100%	60%	40%	100%	100%	0%	0%
		B	100%	100%	100%	100%	100%	100%	100%	100%
		C	100%	100%	100%	100%	100%	100%	20%	20%
		D	100%	100%	0%	0%	100%	100%	0%	0%
		E	100%	100%	0%	0%	100%	100%	0%	0%
		F	100%	100%	60%	60%	100%	100%	0%	80%
	Seq2	A	100%	100%	20%	60%	100%	100%	0%	0%
		B	100%	100%	0%	0%	100%	100%	20%	20%
		C	100%	100%	0%	0%	100%	100%	0%	0%
		D	100%	100%	0%	0%	100%	100%	0%	60%
		E	100%	100%	20%	20%	100%	100%	0%	0%
		F	100%	100%	0%	0%	100%	100%	0%	0%
	Seq3	A	100%	100%	80%	100%	100%	100%	20%	20%
		B	100%	100%	0%	0%	100%	100%	0%	0%
		C	100%	100%	0%	0%	100%	100%	20%	40%
		D	100%	100%	0%	100%	100%	100%	0%	0%
		E	100%	100%	0%	0%	100%	100%	60%	80%
		F	100%	100%	0%	0%	100%	100%	40%	40%
Squared	Seq1	A	100%	100%	40%	60%	100%	100%	0%	0%
		B	100%	100%	60%	60%	100%	100%	100%	100%
		C	100%	100%	80%	80%	100%	100%	0%	0%
		D	100%	100%	0%	0%	100%	100%	0%	0%
		E	100%	100%	0%	0%	100%	100%	0%	0%
		F	100%	100%	0%	0%	100%	100%	0%	0%
	Seq2	A	100%	100%	60%	40%	100%	100%	0%	0%
		B	100%	100%	0%	40%	100%	100%	0%	0%
		C	100%	100%	0%	0%	100%	100%	0%	0%
		D	100%	100%	60%	60%	100%	100%	0%	0%
		E	100%	100%	40%	40%	100%	100%	40%	20%
		F	100%	100%	0%	0%	100%	100%	0%	0%
	Seq3	A	100%	100%	100%	100%	100%	100%	100%	100%
		B	100%	100%	40%	40%	100%	100%	100%	100%
		C	100%	100%	0%	0%	100%	100%	0%	20%
		D	100%	100%	0%	80%	100%	100%	0%	0%
		E	100%	100%	40%	20%	100%	100%	20%	40%
		F	100%	100%	0%	0%	100%	100%	0%	0%
		Average	100%	100%	27%	33%	100%	100%	18%	23%
		SD	0%	0%	35%	38%	0%	0%	33%	35%

C.4. Sample of residual test for a computer-based experiment

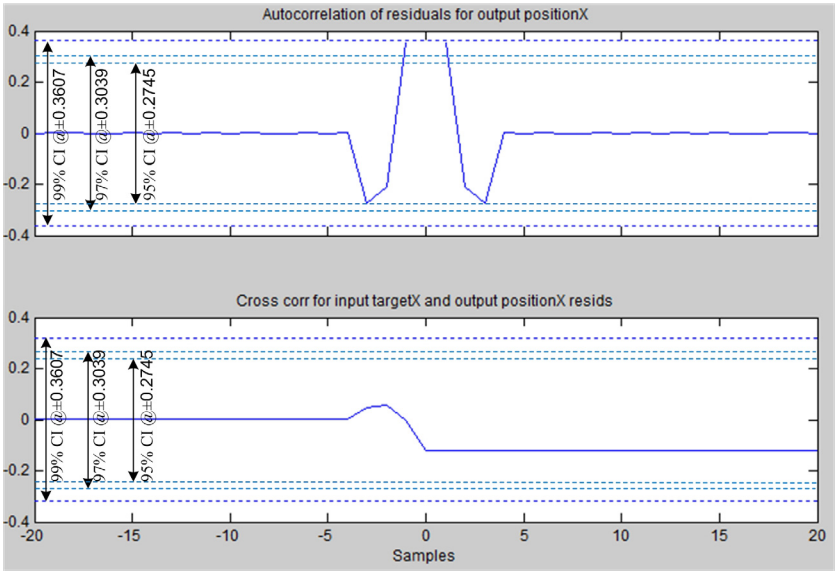

Figure C.24. Correlation graphs for x-axis model: segment 1, subject B

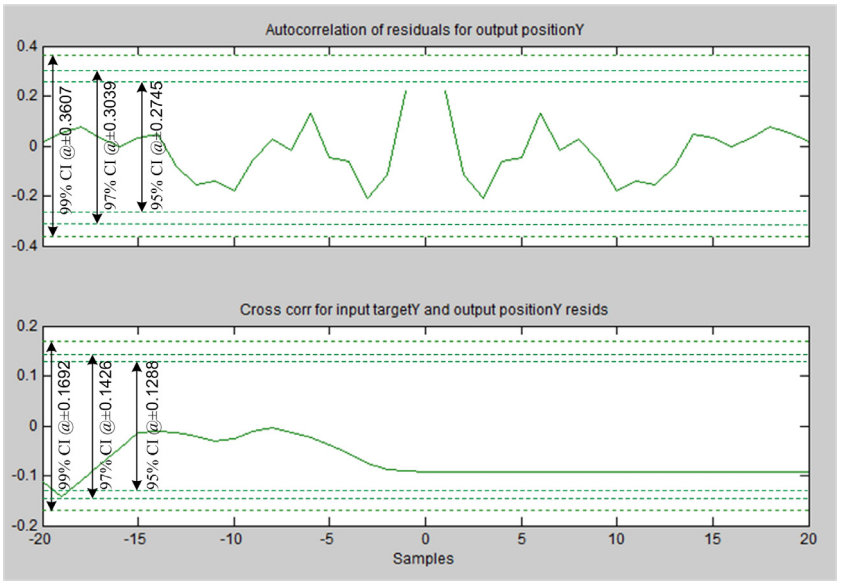

Figure C.25. Correlation graphs for y-axis model: segment 1, subject B

An example on x and y ARX models based on segment 1 of subject B is illustrated. Residual tests for both ARX models for x and y-axes are satisfactory with 99% confidence interval (CI) in both cases and this is really what happens to other models.

Appendix D: Journal paper

Parthornratt, T., Parkin, R. M., and Jackson M.R., Human Performance Index (HPI)-A generic performance indicator, Article in press, a Special Issue on Human Adaptive Mechatronics, Proceedings of the Institution of Mechanical Engineers (IMechE), Vol.225 Part I, Journal of Systems and Control Engineering.

Human Performance Index (HPI)-A generic performance indicator

T Parthornratt*, R M Parkin, and **M Jackson**
Intelligent Automation Research Centre, Holywell building, Holywell way, Loughborough University, Leicestershire, LE11 3UZ, UK

The manuscript was received on xx xx and was accepted after revision for publication on xx xx

DOI: 10.1177/0959651811407598

Abstract: Human skill evaluation or human skill quantification in the original definition of a human adaptive mechatronics system is the main concern of this paper. However, a deficiency in terms of consistency and subjectivity makes human skill not fully indicative of actual human performance. That is, the term human skill can mean repeatability, adaptability, or learning capability depending on the aspects and systems of interest. This paper proposes a human performance index (HPI) concept to focus on human performance instead. The main contributions are the quantification of speed–accuracy characteristics based on Fitts' classical speed–accuracy trade-off and determination of human control strategy involved in completing a task. The experiment in this paper was conducted on a computer-based simple tracking system by using a computer mouse to follow a set of random circles on a display. Human operators were told to complete the task as quickly as possible. HPI values were then calculated with and without weightings on speed and accuracy criteria. Different human performance values reflect how human operators accomplish the same task under the same working conditions. These control strategies are associated with a degree of emphasis on the speed and accuracy characteristics of the operators' control actions.

1 INTRODUCTION

The term mechatronics is used to describe a machine system or device that contains actuation and control mechanisms [**1**]. Following its inception in the 1940s [**2**] there has been continuous interest in improving the man–machine interface in these systems [**3**, **4**]. The latest development in this area is the creation of human adaptive mechatronics (HAM) which can be viewed as an intelligent human–machine system which changes the classical man–machine interaction so that it has an assistive and adaptive nature that ultimately improves human skill. It is important under these circumstances to minimize errors and other problems created by a negligent human operator [**5**]. One technique that has been proposed to resolve this issue and yield a constant quality of product regardless of the human operator is the use of a human performance index (HPI) [**6**]. In a fully fledged implementation, a man–machine system with HPI functionalities features computing, reading, and processing of the human operators' HPI data and then it assists/adapts accordingly in order to produce the constant system throughput. Further details on this will be discussed in section 2. Background information on HAM will now be given, followed by a discussion of human skill evaluation.

**Corresponding author: Intelligent Automation Research Centre, Holywell building, Holywell way, Loughborough University, Leicestershire, LE11 3UZ, UK*
email: T.Parthornratt@lboro.ac.uk

1.1 The background to HAM

Based on the original definition of HAM [**7**, **8**] there are four essential features of a HAM system implementation [**9**]

HAM must quantify human skill-level of the manipulation. HAM has to assist an operator by giving useful supports and by changing its own functions and structures. For the realization, the following items are needed.

1. Definition and quantification of human skill,
2. Cognition of a human model from the machine-side,
3. Assistance method for human by the machine,
4. Change of machine's function.

Based on this structure, it is worth noting that modules 3 and 4 (assistance mechanism and adaptive control mechanism, respectively) are dependent on modules 1 and 2 (human skill evaluation and human modelling, respectively) since the assistive or adaptive mechanisms have to relate to human characteristics. Further details will be given in the following section.

In fact, HAM can be viewed as an evolution of a conventional manual control system, which is sometimes used interchangeably with the term man–machine system, such as vehicles, weapons, and joystick-controlled manipulators. These systems require a degree of flexibility and human intelligence in order to operate successfully, maximize efficiency, and avoid system failures [**10**]. The HAM concept implementation allows a system to be integrated with assistance or adaptive control mechanisms to work in conjunction with a human according to his/her abilities. Initially, a machine may need to change or adjust its characteristics drastically to suit that individual. Usually, the degree of change will decrease with time as the human learns and the machine converges to its optimal state. This kind of machine system characterizes the intelligence along with the adaptive and training capabilities.

1.2 Related work on human skill evaluation

According to the literature, it is apparent that there is a wide range of contributions to human skill evaluation and human modelling that is modules 1 and 2, respectively. However, only module 1 will be covered in this paper due to its relevance to the proposed HPI concept. In the engineering field, skill is defined as the ability to quickly perform a task, at a low error rate, using a problem-solving strategy if required [**11**]. According to the literature, characteristics that contribute to human skill can be classified into attention, similarity measurement, and model-based analysis.

1.2.1 Attention

The concept of a minimum attention level for human control actions has been proposed and linked to the skill of that individual [**12**]. This is similar to a term called intermittency, as stated by [**13**], which connects to a human's concentration or attention to a stimulus in an intermittent fashion. Initially, a human tends to have a shorter intermittent period or longer attention, which gets lower as time progresses due to his/her skill or expertise being developed during the operation.

1.2.2 Similarity measure

A number of researchers have proposed the concept of a similarity measure, as inspired by expert control behaviours. The autoregressive with exogeneous inputs model has been widely used to obtain human control parameters [**11**, **14**]. The difference between normal human parameters and expert human parameters can be used to represent a skill index [**15**]. Similarly, a method to abstract human skills based on a cascaded neural network learning method has also been proposed [**16**]. The resulting learned model is used to compare similarity among different human and other learned models.

1.2.3 Model-based analysis

This technique relies on the sequence of a task execution with movement smoothness or dexterity which is regarded as a major characteristic of the human expert. A state-transition model or a statistical human model such as the hidden Markov model (HMM) is commonly used in this process. An example of the use of a state-transition model is the investigation of remotely controlling surgical equipment during a medical procedure with the human skill level being computed based on the surgeon's body motions [**17**] or line of sight [**9**, **18**]. The concept of a microslip or jerky action from cognitive science has been used to confirm that the smoothness of control actions is one of the main characteristics of an expert [**9**, **19**].

For a HMM, this type of statistical model has been used widely to quantify human skill and determine a human's intent for a pattern of movement. Other approaches proposed to evaluate human skill levels include a neural network [**16**] and fuzzy logic [**20**, **21**]. Skill metrics consisting of task efficiency, complexity of task sequence, ability to plan and make decisions, and task difficulty have also been proposed and implemented in operating mobile machines [**22**, **23**].

In summary, all of these human skill evaluation techniques are based on a flow of states in an operation and the model has to be trained to represent the skill level of a particular person. This implies that information on *a posteriori* probability or expert characteristics has to be readily available.

Applying this technique to a newly invented or unseen machine system without the existence of a human expert would be a challenging task. This paper addresses this drawback and proposes a generalized framework that does not need an expert human but rather focuses on performance evaluation based on a sample group. This paper is divided into four main sections. The first section, skill versus performance (section 2) discusses the difference between these terms and how they can be implemented. The second section, HPI concept (section 3) provides a background on a representation of human performance based on speed and accuracy characteristics. The third section, HPI computation (section 4) describes the characteristics of performance variables and data processing. Experimental results on HPI computation are presented and discussed in section 5 and conclusions are drawn in section 6.

2 SKILL VERSUS PERFORMANCE

According to the Oxford English Dictionary (1989), performance is defined as 'the quality of execution of such an action, operation, or process' whereas skill is defined as 'the capability of accomplishing something with precision and certainty'. It is apparent that human performance is more general and reliant on output quality whereas human skill is specific to the manner of completion. Skill can also be acquired or learnt by practice and in effect, increases the performance.

Therefore, the concept of an HPI is proposed with reference to the fact that a human is indispensable in craft-based manufacturing but can be replaced in pure mass production environments [**24**]. To maximize productivity and efficiency, product quality has to be controlled and one of the key challenges is to optimize interactions between humans of any skill level and intelligent machines. The advantage of relying on human performance instead of human skill is that the complacency or negligence in performing a task can be properly treated [**5**, **25**, **26**]. In other words, overall productivity is of higher priority than the manner of completion.

3 THE HPI CONCEPT

A generalized structure of human performance is preferable for the design of a controller that can work effectively with a plant without dominating a human operator. The rationale for using human performance instead of human skill is based on

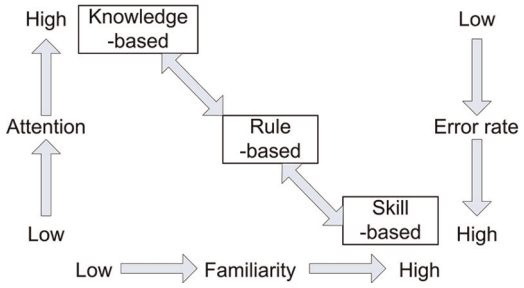

Fig. 1 A human performance diagram summarized from Rasmussen's model

Rasmussen's model [**27**]. Human performance, consisting of skill, rules, and knowledge, is intuitively chosen and it is highly dependent on the degree of training (Fig. 1). In addition, human performance can also be varied by intention and the requirements/constraints imposed by an operation, according to the Regulatory Focus Theory [**28**], by adjusting the operators' speed and accuracy characteristics (Fig. 2). The HPI is proposed based on these theories. This concept is not only supported by the validity of the speed–accuracy trade-off based on Fitts' law but also the fact that it is a strategy-related approach [**29**]. The relationship between movement time (MT) and index of difficulty ($\log_2(2A/W)$) has the following form (W and A are target width and distance between targets respectively)

$$MT = a + b\log_2\left(\frac{2A}{W}\right) \tag{1}$$

Despite awareness of the speed–accuracy trade-off, it is worth stressing that these implications are considered to exist in various man–machine operations but without rigorous methods for quantification [**30**–**33**]. It is obvious from Fitts' law that only a movement time or speed characteristic is considered. That is, there is no explicit representation of the speed–accuracy relationship. The HPI concept is defined to resolve this issue by quantifying the speed and accuracy characteristics of a human and representing them numerically. From this

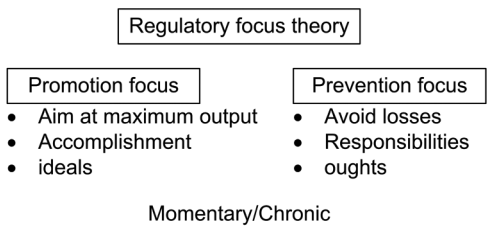

Fig. 2 Regulatory focus theory

perspective, HPI can potentially lead to the formulation of human factor requirements.

3.1 Overview

HPI is proposed to consist of three levels of hierarchy as shown in Fig. 3. HPI is essentially a weighted sum of criteria based on a number of variables that are attributed to a human performance classified as the performance criterion and the performance variable. The concept of representing a performance criterion based on a characteristic of interest is similar to Xu *et al.* [**34**] and Hölttä, and Koivo [**35**]. The only difference from the former case is the way an overall performance value from a number of performance criteria is represented rather than a single performance value on its own. For the latter case, HPI is similar to the Quality Index Framework, which was originally defined with reference to industrial processes and based on human skill rather than human performance. Although the low-level, second-level, and high-level indices are very similar to the performance variables, performance criteria, and the HPI, the number of levels is defined to be flexible rather than fixed to only two performance criteria like that of HPI.

According to the proposed HPI structure in Fig. 3, the lowest hierarchy consists of a number of physical quantities or variables that contribute to a cumulative quality of a higher hierarchy. The physical quantities classified into the lowest hierarchy are literally contributing factors to the same characteristic. These contributing factors in the lowest hierarchy are defined as human performance variables or simply performance variables. For the higher hierarchy, a group of physical quantities or variables sharing the same characteristic is cumulatively referred to as a human performance criterion or simply a performance criterion. Each criterion effectively represents a single characteristic of the human performance. The weighted sum of these criteria is defined as the HPI.

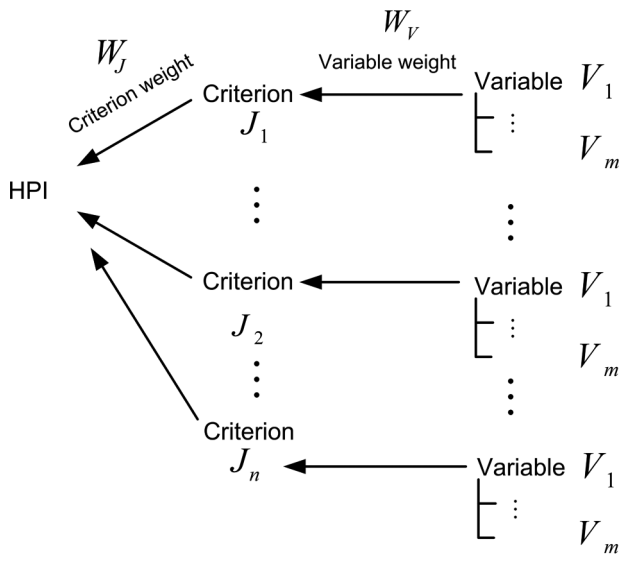

Fig. 3 Proposed HPI structure containing speed and accuracy variables

To illustrate the applicability of the HPI concept, non-model and model-based performance computation approaches are proposed and applied to systems with and without hardware elements, which are referred to as computer-based and hardware-based systems, respectively. The difference between the two performance computation approaches is mainly the integration of human models into the performance evaluation. As the name suggests, a non-model approach relies purely on the 'goodness' of the system output pattern whereas a model-based approach requires a human model from the System Identification algorithms. The work reported in this article is only from a computer-based experiment with the HPIs computed by the non-model approach (Fig. 4). The HPI computation using other approaches and systems will be presented in a follow-up paper.

3.2 Definitions

The HPI is proposed to be a generic performance indicator based on a sample group and can be visualized as a relative performance value. In effect, a person with an HPI value greater than one is considered to be above average whereas a person with a value smaller than one is considered to be below average. Processing of the performance variables is obviously required to yield this specified numerical meaning and format.

Defining an HPI as a relative quantity is advantageous in its scalability and reasonability. An expansion of a sample group is always possible to reflect a wider range of human abilities and characteristics. In effect, the larger and wider the range of the sample group, the less subjective will be the computed HPI.

A performance variable (*Vi*) is defined as a basic element of an HPI, which is literally a physical quantity extracted from a human operator's control action. A group of performance variables with the same characteristic is defined as a performance criterion (*Ji*) and each variable of the same criterion is associated with a performance variable weight (*Wv*) or degree of significance of the physical quantity it represents. In general, the conditions for equal weights for all variables can be safely assumed. For

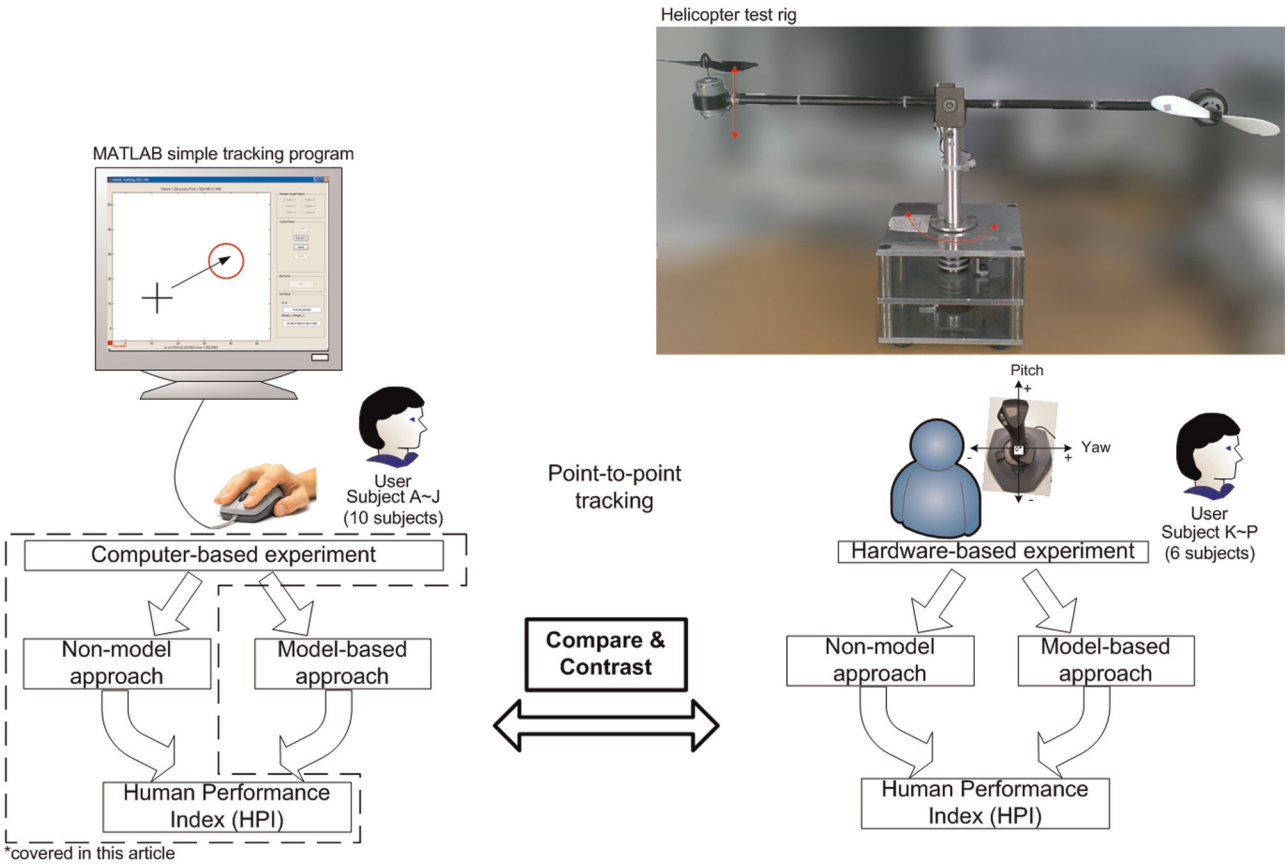

Fig. 4 Outline for the coverage of HPI computation in this article

each performance criterion, its associated performance criterion weight (Wj) is connected to a human control strategy according to the Regulatory Focus Theory [**28**].

In brief, there are two weighted sums involved in the HPI computation, which are the weighted sum of the performance variables (Vi) and the weighted sum of the performance criteria (Ji). The first weighted sum is defined as a performance criterion score or simply a criterion score and the latter weighted sum is defined as an HPI. Equations for computing a performance criterion score (J_i) with m number of performance variables and an HPI with n number of performance criteria are as follows

$$J_i = J_i(V_1, V_2, \ldots, V_k) = \frac{\sum_{k=1}^{m} W_{V_k} \times V_k}{\sum_{k=1}^{m} W_{V_k}} \tag{2}$$

$$HPI = HPI(J_1, J_2, \ldots, J_n) = \frac{\sum_{i=1}^{n} W_{J_i} \times J_i}{\sum_{i=1}^{n} W_{J_i}} \tag{3}$$

3.3 Forms of the HPI

In order to use an HPI as a performance indicator, two forms of HPI are proposed for use in two different conditions. These conditions are based on the availability of the application requirements on particular human characteristics, which is effectively the performance criterion weights (W_j). An HPI structure containing both open-form and closed-form HPI can be found in Fig. 5.

3.3.1 *Open-form HPI*

An open-form HPI is a raw HPI consisting of only a set of performance criterion scores (J_i) based on each criterion. This form of HPI represents only one

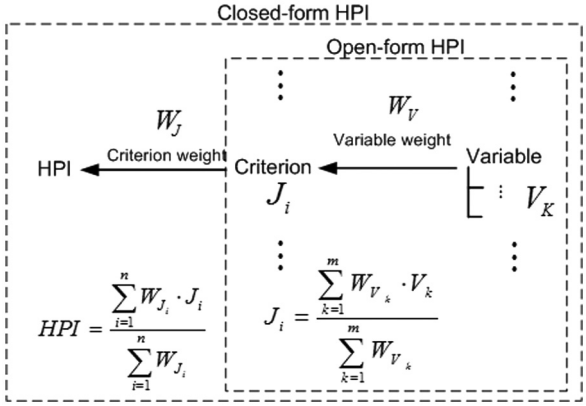

Fig. 5 HPI forms

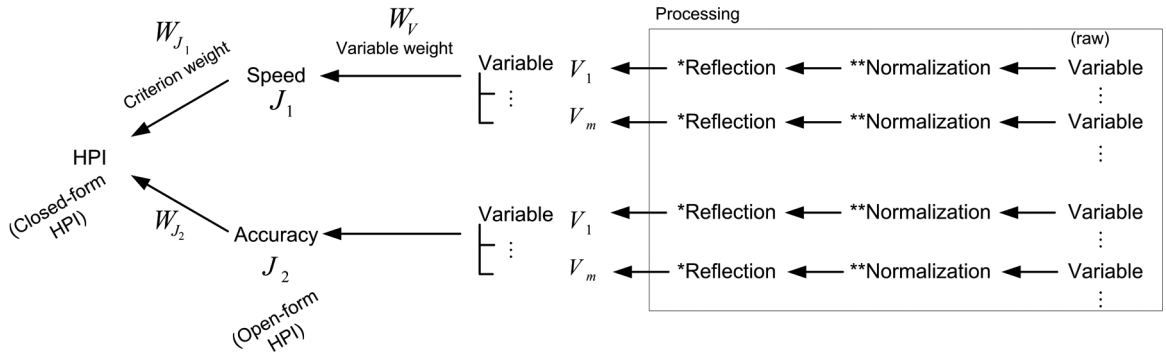

Fig. 6 Average-based HPI computation overview (note: * denotes a reflection operation, ** denotes a normalization by an average value)

particular human characteristic and is open for a performance criterion weight, hence the name of this HPI form. Only speed and accuracy characteristics are used as the performance criteria and, from the application point of view, the open-form HPI serves as a performance indicator of a human operator in one particular characteristic. This might be useful in a system design process to optimize a man–machine system performance affected by either the speed or accuracy characteristic of a human operator.

3.3.2 Closed-form HPI

A closed-form HPI or simply HPI is a summation of a product of all performance criterion scores and their associated performance criterion weights. A closed-form HPI literally reflects an overall human performance level. Considering the difference between an open-form HPI and closed-form HPI as an analogy to a grade point average (GPA) grading system ensures the meaning of the HPI concept. That is, an open-form HPI can be viewed as a grade assessed for one particular subject whereas a closed-form HPI can be viewed as a GPA.

In essence, an open-form HPI is a raw HPI without weighting of the performance criterion whereas a closed-form HPI is an HPI with all weightings derived empirically from a specific operation in a specific system. The use of the same weightings in different systems would induce discrepancies, hence the name of the HPI form.

3.4 HPI based on only speed and accuracy criteria

With speed and accuracy chosen to be the performance criteria of an HPI, a performance criterion score can be simply referred to as either a speed score or an accuracy score. The numerical value of the speed score reflects the 'goodness' of time-efficiency characteristics whereas the numerical value of the accuracy score reflects the 'goodness' of error-related characteristics. Due to the fact that there are only two performance criteria, the relationship between these two performance criterion weights can be easily perceived as a ratio or a speed : accuracy ratio. Variation of this speed : accuracy ratio results in different HPI values and a degree of variation can interestingly lead to a selected control strategy.

4 HPI COMPUTATION

In order to comply with the HPI definitions, an average-based method for HPI computation is proposed. An average value of the raw performance variables extracted from the logged data is used as a normalization factor instead of a maximum value. Resulting variables are therefore greater than, equal to, or less than the average value. That is, these variables are now centred about the average value, hence the name of the proposed method. An overview of how the average-based HPI computation method links to the HPI structure is presented in Fig. 6 and it aims to make all variables monotonically consistent.

4.1 Monotonicity of the performance variables

A monotonic function is mathematically defined as a strictly increasing (monotonically increasing) or strictly decreasing (monotonically decreasing) function, whose value either increases or decreases as a magnitude of an independent variable increases [**36**]. Conditions for a strictly increasing function and strictly decreasing function are as follows

$$f(x_2) > f(x_1), \quad \text{if } x_2 > x_1 \tag{4}$$

$$f(x_2) < f(x_1), \quad \text{if } x_2 > x_1 \tag{5}$$

Monotonicity or magnitude interpretation is the main issue for HPI computation as the performance variables may not have a common monotonicity. HPI itself, by definition, is a strictly increasing function. This means the greater the value, the higher the performance level. Every performance variable is therefore required to be strictly increasing to comply with the HPI definition. The extra processing for the strictly decreasing performance variables is called reflection.

4.2 Processing of the performance variables

There are two main processing methods for the performance variables: average normalization and reflection, with further details as follows.

4.2.1 Average normalization

An average normalization process is applied to all performance variables regardless of their monotonicity. Given $x_1, x_2 \ldots x_i \ldots x_N$ is a series of raw performance variables logged from N human operators in a sample group, i represents the ith human operator. The average value and average normalized value of the performance variables are denoted as $x?$ and $\hat{x}_i$ respectively, as follows

$$\hat{x}_i = \frac{x_i}{\bar{x}} \tag{6}$$

Regarding the statistical properties of the performance variables after average normalization, it can be proved that the average and variance values of the average normalized performance variables have become an integer value of one and scaled by the average value squared respectively.

4.2.2 Reflection

A reflection is a process required for only a strictly decreasing performance variable by translating a point on one side to the opposite side of a mirror (axis of reflection) while preserving its distance [**37**]. It can be proved that a reflected variable ($\hat{x}'$) can be calculated by using the average value of a normalized variable ($\bar{\hat{x}}$) and average-normalized variable ($\hat{x}$) as follows

$$\hat{x}' = -\hat{x} + 2\bar{\hat{x}} \tag{7}$$

A strictly decreasing performance variable has now been converted to a strictly increasing variable with its original 'goodness' preserved.

5 EXPERIMENTAL RESULTS

A simple form of man–machine system based on a tracking operation is used to illustrate the use of the HPI concept.

5.1 Experimental setup

Ten human subjects at the Intelligent Automation Research Centre, aged from 18 to 35, and with familiarity in using a computer on a daily basis, participated in this experiment. It is worth noting that there was neither intensive training nor selection of subjects prior to the experiment because the objective was to evaluate human performance in general rather than studying expert control actions. A MATLAB® program was designed and written by the GUIDE (Graphical User Interface Design Environment) toolbox, including data logging and analysing features for a point-to-point tracking operation. Each human operator was instructed to move a crosshair cursor on a 12.1 inch laptop computer screen with an optical computer mouse to align at the centre of the circle as quickly as possible (Fig. 7). The same target sequence containing 20

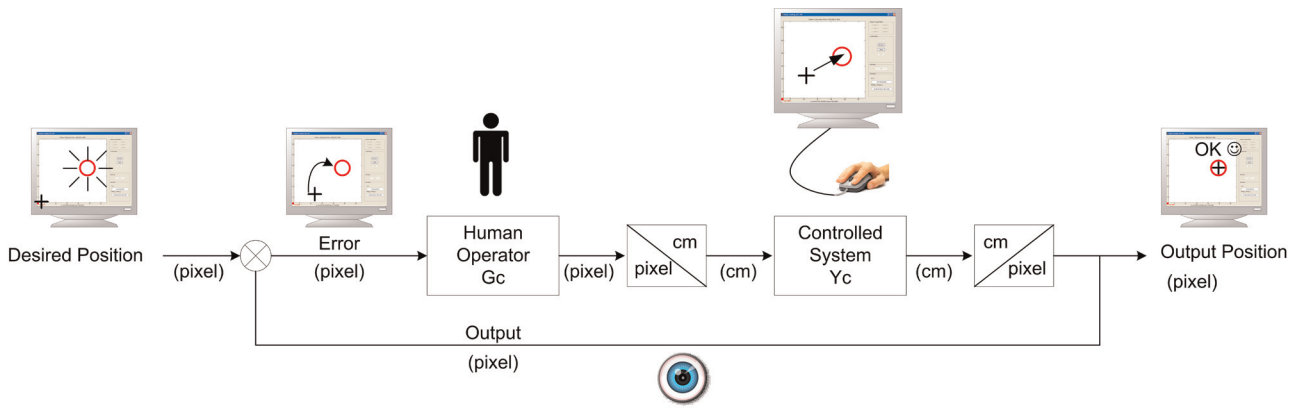

Fig. 7 Simple tracking task block diagram

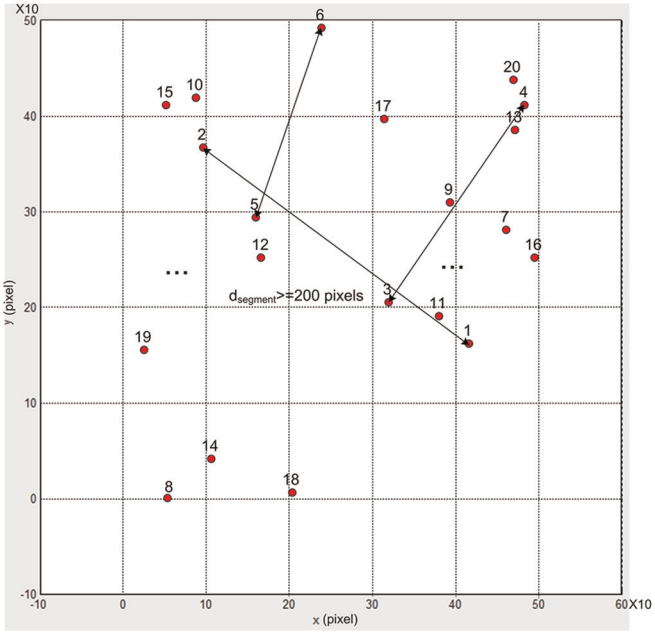

Fig. 8 Target sequence 1 and its segment distance

targets was repeated five times for every human subject, which is referred to as five trials.

In order to analyse the human control action and compute an HPI value, the cursor's trajectory was analysed segment by segment. The target sequence was randomized with a minimum of 200 pixels distance to ensure intentional success. The sequence used in this experiment and information on segment distance can be found in Fig. 8. In this scenario, a segment distance is the distance of a straight line connected between a pair of targets, starting from an initial position to target number 1 (segment1), from target number 1 to target number 2 (segment 2), and so on.

5.2 HPI computation

In this paper, only the best trial or the one with minimum time taken for each subject was used for the HPI computation. A non-model approach was applied to extract performance variables of interest directly from the experimental/logged data. These extracted performance variables were classified into speed and accuracy criteria according to the proposed HPI definition. Regarding performance variables of interest in this experiment, average speed (V_{av}) and time taken (T) were selected as speed variables; a redefined coefficient of determination (R^2) and root mean squared error (*RMSE*) were selected as accuracy variables. Each variable and its parameters are illustrated in Fig. 9.

5.2.1 *Speed criterion*

Performance variables that reflect or contribute to time-efficiency characteristics can be reasonably classified as a speed criterion. In this case, an average speed and time taken were chosen. Time taken (T) was defined as the time stamp at the beginning (T_{start}) subtracted from the time stamp at the final target position (T_{stop}) i.e. $T = T_{stop} - T_{start}$. Average speed (V_{av}) was defined as the summation of linear segments distance (L_i) between a pair of target positions divided by time taken (T)

$$V_{av} = \frac{\sum_{i=1}^{\text{no.of segments}} L_i}{T} \tag{8}$$

5.2.2 *Accuracy criterion*

For the accuracy variables, the *RMSE* and a redefined coefficient of determination (R^2) were chosen. *RMSE* was defined as the error between a cursor position and a target position on a straight line connected from one target to another. With the total number of samples in a corresponding segment denoted as N, *RMSE* can be written as follows

$$e = \sqrt{(x_{target} - x_{cursor})^2 + (y_{target} - y_{cursor})^2} \tag{9}$$

$$RMSE = \sqrt{\frac{\sum_{i=1}^{N} e_i^2}{N}} \tag{10}$$

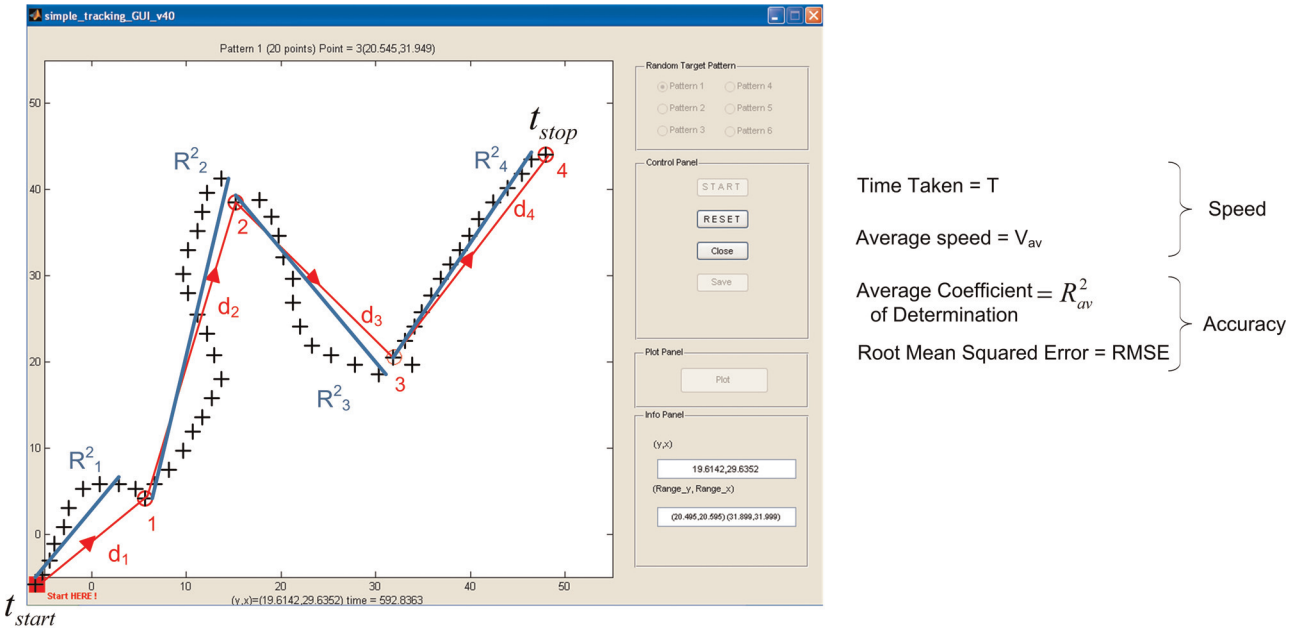

Fig. 9 Control action of one human subject (target 1 to 4) with speed and accuracy criteria definitions. + represent actual user's cursor position, O represents target positions. Straight lines with arrows represent a straight line connected from one target to another. The plain straight lines represent a linear regression line based on user's trajectory

An average coefficient of determination (R^2_{av}) was defined to be the quantity that represents the average goodness of fit across all target-to-target segments. This variable aims to quantify the closeness between the path taken by a human subject (actual path) and that of the ideal path. Such a quantity is based on a linear regression concept with a coefficient of determination (R^2) value to indicate the goodness of fit. The original coefficient of determination is defined as follows [**38**]

$$R^2 = 1 - \frac{SS_E}{SS_T} \tag{11}$$

$$SS_E = \sum_{i=1}^{n} (Y_i - \hat{Y}_i)^2 = \text{sum of a squared error} \tag{12}$$

$$(Y_i = \text{actual data}, \hat{Y}_i = \text{fitted data})$$

$$SS_T = \sum_{i=1}^{n} (\hat{Y}_i - \bar{Y})^2 = \text{sum of a squared total} \tag{13}$$

$$(\bar{Y} = \text{average value of actual data})$$

In this article, Y_i is redefined as projected actual data and $\hat{Y}_i$ is redefined as fitted ideal data, as illustrated in Fig. 10, to comply with the R_{av} definition. In effect, a redefined coefficient of determination can now be calculated directly from equation (11) with substitution of the original variables by redefined variables. To determine 'goodness' for all segments, a redefined coefficient of determination is averaged over a number of segments as follows

$$R^2_{\text{av}} = \frac{\sum_{i=1}^{\text{no.of segments}} R_i^2}{\text{no .of segments}} \tag{14}$$

All of these raw performance variables are now ready for an average normalization and reflection for open-form and closed-form HPI computation. However, before proceeding, the following section discusses the experimental results in relation to Fitts' law in order to observe the speed–accuracy trade-off.

5.3 Fitts' law validation

To determine the existence of a speed and accuracy trade-off in the computer-based experiment covered in this article, a user's motion path or trajectory of a cursor in the Cartesian coordinate systems was analysed and 20 segments based on 20 target positions were examined according to Fitts' Law presented in equation (1). It is worth noting that this validation involved only one performance variable of the speed criterion in the HPI, which is the time taken (T), with the values of I_{d} ranging from 4.4 to 5.7. Figure 11 shows the time taken for each target position of human subject A, with the summary of Fitts'

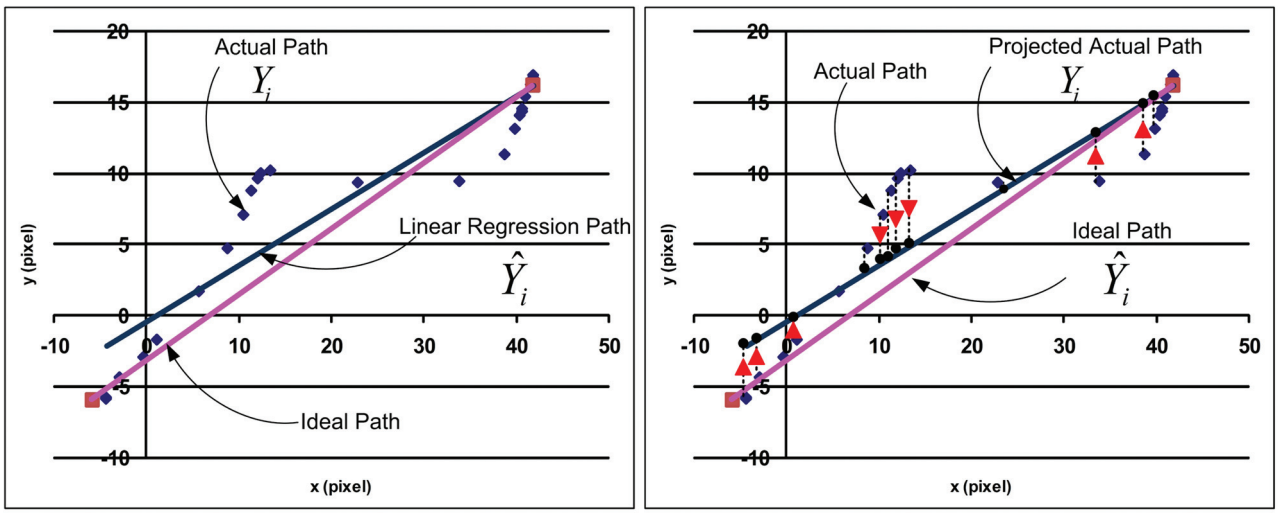

Fig. 10 Comparison of the original (left) and redefined (right) coefficient of determination parameters on one segment sample

parameters for all subjects in Table 1. Based on these results, only subjects A, E, and H gain a positive information-processing rate whereas the rest gain a negative information-processing rate. This means that one group uses more time to track a target with the higher level of difficulty whereas another group 0075ses uses less. Therefore, these results clearly classify human subjects into two groups based on their control strategies and suggest their decision to compromise accuracy for higher speed. Even though a degree of compromise depends on the location and distance of the operating points, due to the fact that the HPI concept relies on a sample group, every member of the group is theoretically affected by the same operating point conditions and this is reflected in their performance values.

Apart from the human control strategy characteristic, it can be observed that the coefficients of determination (R^2) are relatively low in the range between zero and 0.2, which means these experimental results loosely obey Fitts' law. The reason for that is based on the difference between the instructions given to the human subjects in the original Fitts' experiments and the ones in this experiment. That is, human subjects were explicitly instructed to either emphasize accuracy rather than speed or perform without errors at all in the original Fitts' experiments [**39**, **40**] whereas human subjects were explicitly instructed to emphasize speed rather than accuracy in this experiment. Such instructions directly affect human control actions in the original Fitts' experiments by forcing human subjects to spend more time as the index of difficulty increases in order to avoid error. Therefore, the low R^2 values are not surprising because human subjects are free to choose their control strategies accordingly. The next section will discuss the HPI in both open and closed forms, including their interpretation and limitations.

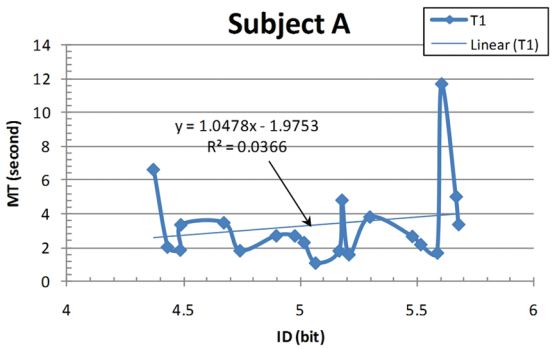

Fig. 11 Trial 1-subject A: movement time (MT) versus index of difficulty (I_d) for the computer-based experiment ($W = 20.6$ pixels and $A =$ Euclidean distance)

5.4 Discussion

5.4.1 Open-form HPI

The associated performance scores are referred to as speed and accuracy scores with reference to the speed and accuracy variables. Regarding the monotonicity of the chosen speed variables, V_{av} is strictly increasing whereas T is strictly decreasing. Similarly, for the chosen accuracy variables, R^2_{av} is strictly increasing whereas $RMSE$ is strictly decreasing. This means a reflection process is required for T and $RMSE$ following the average normalization process.

Table 1 Summary of Fitts' law parameters

Subject	Slope	*Y*-intercept	Information-processingrate rate (bits/s)	R^2
A	1.05	-1.98	0.95	0.040
B	-0.46	4.24	-2.18	0.100
C	-1.01	7.37	-0.99	0.150
D	-0.05	2.08	-21.4	0.000
E	0.31	1.06	3.26	0.010
F	-0.25	3.33	-4.08	0.050
G	-0.41	3.95	-2.42	0.090
H	0.29	0.31	3.46	0.050
I	-0.12	3.08	-8.33	0.000
J	-0.4	3.90	-2.53	0.120

Table 2 Speed score table (J_1) based on the average speed (V_{av}) and time taken (T)

Subject	V_{av} (cm/s)	$V_{av\text{-}norm}$	T (s)	$T_{av\text{-}norm}$	T_{refl}	Speed score
A	0.31	0.60	67.19	1.50	0.50	0.55
B	0.58	1.10	39.53	0.88	1.12	1.11
C	0.44	0.84	45.57	1.02	0.98	0.91
D	0.61	1.17	37.47	0.84	1.16	1.17
E	0.52	0.99	52.70	1.17	0.83	0.91
F	0.60	1.16	42.40	0.95	1.05	1.11
G	0.60	1.15	37.50	0.84	1.16	1.15
H	0.57	1.10	36.23	0.81	1.19	1.14
I	0.40	0.76	51.85	1.16	0.84	0.80
J	0.60	1.15	38.11	0.85	1.15	1.15
Average	0.52	1.00	44.85	1.00	1.00	1.00
SD	0.10	0.20	9.85	0.22	0.22	0.20

Table 3 Accuracy score (J_2) based on the redefined coefficient of determination (R^2) and path *RMSE* value

Subject	R^2	$R^2_{avg-norm}$	*RSME* (cm)	$RSME_{avg\text{-}norm}$	$RSME_{refl}$	Accuracy score
A	0.98	1.03	0.44	0.57	1.43	1.23
B	0.98	1.02	0.48	0.62	1.38	1.20
C	0.97	1.02	0.46	0.59	1.41	1.22
D	0.98	1.02	0.64	0.82	1.18	1.10
E	0.97	1.01	0.69	0.88	1.12	1.07
F	0.88	0.92	2.07	2.67	-0.67	0.13
G	0.97	1.01	0.71	0.91	1.09	1.05
H	0.94	0.98	0.87	1.12	0.88	0.93
I	0.93	0.98	0.87	1.12	0.88	0.93
J	0.96	1.00	0.72	0.92	1.08	1.04
Average	0.96	1.00	0.78	1.00	1.00	1.00
SD	0.03	0.03	0.48	0.61	0.61	0.32

Each column of Table 2 and Table 3 presents processed variables with abbreviations of avg for average, avg-norm for normalization by an average value, and refl for reflection. Speed scores and accuracy scores are now centred around an integer value of one and strictly increasing. These performance variables are ready to be used for a closed-form HPI computation.

Interestingly, the difference between the standard deviation values of speed and accuracy scores, which are 0.20 and 0.32, respectively, reflects how human operators interpret the statement 'completing the task as quickly as possible'. This indicates that, based on the sample group, different control strategies were used by different human operators with a greater degree of interpretation on accuracy characteristics. By the term control strategy, this article refers to a technique of handling or completing the task in terms of speed and accuracy characteristics. To achieve a particular task of interest, the significance of speed and accuracy strongly depends on its nature and output requirements. For instance, controlling a construction crane via a control joystick apparently requires higher accuracy

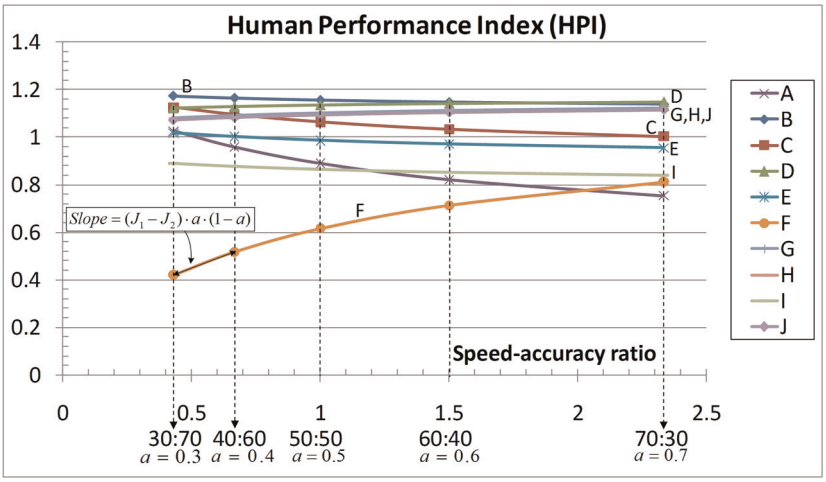

Subject	Speed score	Accuracy score	ΔJ
A	0.55	1.23	-0.68
B	1.11	1.20	-0.09
C	0.91	1.22	-0.30
D	1.17	1.10	0.06
E	0.91	1.07	-0.16
F	1.11	0.13	0.98
G	1.15	1.05	0.11
H	1.14	1.04	0.10
I	0.80	0.93	-0.13
J	1.15	1.04	0.11
Average	1.00	1.00	0.00
SD	0.20	0.32	0.42

Fig. 12 HPI value versus speed-accuracy ratio for human operators A to J

than driving a car as safety is of the highest priority in the operation. Now that the individual performance scores or the open-form HPI have been obtained, the closed-from HPI will be discussed.

5.4.2 Closed-form HPI

With all performance variables in a ready-to-use format, a closed-form HPI could be computed with varied speed : accuracy ratio to illustrate overall human performance. The result presented in Fig. 12 shows the HPI graphs alongside the table for speed scores (J_1), accuracy scores (J_2), and performance score differences (J_1 - J_2) for each human subject. For demonstration, the graph shows only a variation of HPI values with speed : accuracy ratios ranging from 30:70 to 70:30 with a step increment of ten. In other words, the weights on speed criterion ranging from 30 to 70 per cent with 10 per cent increment are considered. For simplicity, the weights on speed and accuracy criteria are denoted as variables a and 1 - a respectively so that a summation is 100 per cent or unity. In a real implementation, the speed : accuracy ratio has to be determined empirically prior to HPI computation and it has to be specific to the system and operation of interest.

Interestingly, it can be observed that some human operators obtain higher HPI values for an increasing value of speed criterion weight whereas some human operators obtain lower HPI values. This is a result of the control strategy selected by each individual. It is also obvious that the HPI values of human operators A, B, C, E, and I are higher when the speed criterion weight increases, but the opposite is true for human operators D, F, G, H, and J. The results suggest an emphasis on speed for human operators A, B, C, E, and I whereas the emphasis is shifted to accuracy instead for human operators D, F, G, H, and J. The slopes in these graphs reflect how strong the emphasis is for each particular person. Based on these observations, it is reasonable to claim that there is a high dependency of HPI values on speed : accuracy ratios or weights for each performance criterion.

To investigate the dependency issue, the piecewise linear relationship in Fig. 12 was considered. The segment connecting between 30:70 and 40:60 speed : accuracy ratios was used to observe the rate of change (m_{HPI}) with reference to the speed and accuracy scores difference (ΔJ or J_1 - J_2). The slope for that piece of linear segment could be written in the following form

$$m_{\mathrm{HPI}} = (J_1 - J_2) \times a \times (1 - a) \tag{15}$$

According to this equation, the rate of change of HPI is faster for the subjects with a large difference between speed and accuracy scores whereas it is slower for the ones with a smaller difference. The sign of m_{HPI} indicates a direct or inverse affect of increasing speed : accuracy ratios on HPI values for positive and negative slopes, respectively. This also means that HPI values increase for the former case and decrease for the latter case, respectively. The table in Fig. 12 stresses that larger values of ΔJ result in a steeper HPI change in either increasing (subject F) or decreasing directions (subjects A, C, E, and I) and that indeed agrees with the previous observations.

These results demonstrate how the HPI concept can be applied and that it strongly relies on the fact that a suitable speed and accuracy ratio is obtainable. From a practical point of view, this is possible through a series of extensive experimentations to

repetitively determine suitable speed : accuracy ratios that match constant output quality. However, that is beyond the scope of this research.

6 CONCLUSIONS

The value of an open-form HPI can represent the goodness of one characteristic in operating a man–machine system whereas a closed-form HPI is an overall performance value. The approach presented in this paper is based only on a non-model approach with analysis of human performance drawn directly from a control action in the time domain. A speed : accuracy ratio variation suggests a characteristic of the human operator in performing a simple tracking task, which links directly to the control strategy of that person. The result suggests that a higher performance can be obtained from a person with emphasis on speed rather than a person with emphasis on accuracy if a time-efficiency characteristic is required. A similar rationale applies for a person with emphasis on speed. More specific output requirements are essential to determine the speed : accuracy ratio precisely. The HPI graphs can potentially provide either a performance profile or a human factors profile for a man–machine operation. A possible way to determine the associated weights for speed and accuracy is to consider the intersections of HPI curves from all subjects as those points reflect the possible HPI that is achievable by a sample group. A suitable assistance or adaptive control mechanism can then be implemented based on these speed–accuracy characteristics. In practice, speed and accuracy requirements may be independently derived in order for a system designer to determine how associated system characteristics can be altered to improve system performance in that aspect. A simple example could be the design of an adaptive acceleration controller for an automobile relying on the driver's speed performance to maximize his/her full potential.

REFERENCES

1 **Auslander, A. M.** What is mechatronics? *IEEE/ASME Trans. Mechatron.*, 1996, **1**, 5–9.
2 **Tustin, A.** The nature of the operator's response in manual control, and its implications for controller design. *J. Instn Elect. Engrs*, 1947, **94**, 190–201.
3 **Wikander, J.** *et al.* The science and education of mechatronics engineering. *IEEE Robot. Autom. Mag.*, 2001, **14**, 20–26.
4 **Schweitzer, S.** Mechatronics for the design of human-oriented machines. *IEEE/ASME Trans. Mechatron.*, 1996, **1**, 120–126.
5 **Parasuraman, R.** Humans and automation: use, misuse, disuse, abuse. *Human Fact. : J. Human Fact. Soc.*, 1997, **39**, 230.
6 MTC. Manufacturing technology centre, 2010 available from http://www.the-mtc.org/ (access date).
7 **Furuta, K.**. What is human adaptive mechatronics? In Proceedings of the Eighth International Conference on *Mechatronics technology*, Hanoi, Vietnam, 8–12 November 2004.
8 **Furuta, K.**. Control of pendulum: from super mechano-system to human adaptive mechatronics. In *Proceedings of the IEEE Conference on Decision and control*, Mauli, Hawaii, 2003, pp. 1498–1507.
9 **Suzuki, S.** *et al.* Skill evaluation based on state-transition model for human adaptive mechatronics. In Proceedings of the 30th Annual Conference of the IEEE Industrial Electronics Society, Busan, Korea, 2–6 November 2004, pp. 641–646.
10 **Elkind, J.** *Characteristics of simple manual control systems*. PhD Thesis, Lincoln Laboratory, Department of Electrical Engineering, Massachusetts Institute of Technology, 1956.
11 **Suzuki, S.** *et al.* Overview of human adaptive mechatronics and assist-control to enhance human's proficiency. In Proceeding of the International Conference on *Control, automation, and systems*, Gyeong Gi, Korea, 2–5 June 2005, pp. 1759–1765.
12 **Brockett, W.** Minimum attention control. In Proceedings of the 36th IEEE Conference on *Decision and control*, San Diego, California, 1997, pp. 2628–2632.
13 **Birmingham, H. P.** and **Taylor, F. V.** A design philosophy for man-machine control systems. *Proc. IRE*, 1954, **42**, 1748–1758.
14 **Ertugrul, S.** Predictive modeling of human operators using parametric and neuro-fuzzy models by means of computer-based identification experiment. *Engng Appl. Artif. Intell.*, 2008, **21**, 259–268.
15 **Suzuki, S.** *et al.* Assistance control on a haptic system for human adaptive mechatronics. *Adv. Robot.*, 2006, **20**, 323–348.
16 **Nechyba, M. C.** and **Xu, Y.** Human skill transfer: neural networks as learners and teachers. In Proceedings of the IEEE/RSJ International Conference on *Intelligent robots and systems (human robot interaction and cooperative robots*), Pennsylvania, 5–9 August 1995, pp. 314–319.
17 **Masamune, K.** *et al.* Evaluation of the skill for operating minimally invasive spine surgery robot toward HAM based surgery system. In Proceedings of the Eighth International Conference on *Mechatronics technology*, Hanoi, Vietnam, 8–12 November 2004.
18 **Igarashi, H.** *et al.* Adaptive teleoperation system with HAM-GUI control based on human sensitivity characteristics. The Ninth International Conference on Mechatronics Technology, Kuala Lumpur, Malaysia. 5–8 December 2005.

19 **Takeuchi, S.** *et al.* Development of vision-based measurement system for hand motion. In Proceedings of the *International Joint Conference of the Society of Instrument and Control Engineers and Institute of Control, Automation and System Engineers*, 2006, pp. 5770–5775.

20 **Tervo, K.** *et al.* A hierarchical fuzzy inference method for skill evaluation of machine operators. In Proceedings of the IEEE/ASME International Conference on *Advanced intelligent mechatronics*, 2009, pp. 136–141.

21 **Palmroth, L.** *et al.* Intelligent coaching of mobile working machine operators. In Proceedings of the International Conference on *Intelligent engineering systems*, 2009, pp. 149–154.

22 **Tervo, K.** *et al.* Skill evaluation of human operators in partly automated mobile working machines. *IEEE Trans. Autom. Sci. Engng*, 2010, **7**, 133–142.

23 **Tervo, K.** and **Koivo, H.** Towards human skill adaptive manual control. *Int. J. Adv. Mechatron. Syst.*, 2010, **2**, 46–58.

24 **Cusumano, M.** Shifting economies: from craft production to flexible systems and software factories. *Res. Policy*, 1992, **21**, 453–480.

25 **Parasuraman, R.** Humans: still vital after all these years of automation. *Human Fact. : J. Human Fact. Soc.*, 2008, **50**, 511.

26 **Parasuraman, R.** *et al.* A model for types and levels of human interaction with automation. *IEEE Trans. Syst. Man Cybern., Part A: Syst. Humans*, 2000, **30**, 286–297.

27 **Rasmussen, J.** Skills, rules and knowledge; signals, signs and symbols and other distinctions. *IEEE Trans. Syst. Man Cybern.*, 1983, **13**, 257–266.

28 **Higgins, E.** *et al.* Emotional responses to goal attainment: strength of regulatory focus as moderator. *J. Personality Social Psychol.*, 1997, **72**, 515–525.

29 **Förster, J.** *et al.* Speed/accuracy decisions in task performance: built-in trade-off or separate strategic concerns?. *Organ. Behavior Human Decis. Process.*, 2003, **90**, 148–164.

30 **Cooper, R. A.** *et al.* Analysis of position and isometric joysticks for powered wheelchair driving. *IEEE Trans. Biomed. Engng*, 2000, **47**, 902–910.

31 **Meyer, D. E.** *et al.* Optimality in human motor performance: ideal control of rapid aimed movements. *Psychol. Rev.*, 1988, **95**, 340–370.

32 **Scott MacKenzie, I.** Fitts' law as a research and design tool in human-computer interaction. *J. Human–Comput. Interact.*, 1992, **7**, 91–139.

33 **Zhai, S.** *et al.* Speed-accuracy tradeoff in Fitts' law tasks: on the equivalency of actual and nominal pointing precision. *Int. J. Human–Comput. Stud.*, 2004, **61**, 823–856.

34 **Xu, Y.** *et al.* Performance evaluation and optimization of human control strategy. *Robot. Auton. Syst.*, 2002, **39**, 19–36.

35 **Hölttä, V.** and **Koivo, H.** Quality index framework for plant-wide performance evaluation. *J. Process Control*, 2009, **19**, 1143–1148.

36 **Pemberton, M.** and **Rau, N.** *Mathematics for economists: an introductory textbook*, 2007, p. 712.

37 **Coxeter, H. S. M.** and **Greitzer, S. L.** *Geometry revisited*, 1967 (The Mathematical Association of America,).

38 **Montgomery, D. C.** *et al. Engineering statistics*, third edition, 2003 (Wiley,).

39 **Fitts, P.** The information capacity of the human motor system in controlling the amplitude of movement. *J. Exp. Psychol.*, 1954, **47**, 381–391.

40 **Fitts, P.** and **Peterson, J.** Information capacity of discrete motor responses. *J. Exp. Psychol.*, 1964, **67**, 103–112.